Regulation of microtubular dynamics in response to pheromone in *Schizosaccharomyces pombe*

Thesis presented for the degree of
Doctor of Philosophy
University of London

by Teresa Niccoli

Cell Cycle Laboratory
Cancer Research UK
44 Lincoln's Inn Fields, London

Supervisor: Dr. Paul Nurse
August, 2002

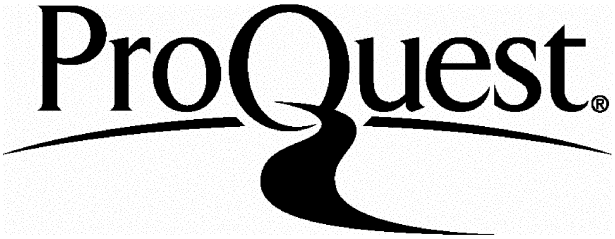

Abstract

Schizosaccharomyces pombe cells have two polarised growth modes: an intrinsic vegetative growth mode, determined by an internal positioning mechanism and an extrinsic shmooing growth mode, activated by external pheromone. I have analysed the role of the cell end marker Tea1p, the CLIP170 like protein Tip1p, the kinesin like protein Tea2p and the Dyrk like kinase Pom1p, during the switch between the two growth patterns, with the intention of studying the switch away from the vegetative growth mode. In vegetative growth these morphological factors are concentrated at cell ends, whereas during shmooing growth they are delocalised from the cell ends. In the absence of Tea1p, Tip1p and Tea2p, vegetative cells display microtubule and cell polarisation defects, but shmooing cells are indistinguishable from wild type and shmoo more readily. These results suggest that Tea1p, Tip1p and Tea2p are not required for polarised growth during shmooing, but form part of the intrinsic vegetative growth mode which needs to be dismantled before cells can generate an extrinsic growth pattern. In contrast, Pom1p appears to have a role in the initial stages of the switch to the shmooing growth mode.

I then went on to analyse factors which do play a role during growth in response to pheromone . During shmooing the nucleus oscillates back and forth in a characteristic horsetail movement. This movement is driven by microtubules. I analysed the role of Dhc1p, dynein heavy chain and Ssm4p, a dynactin homologue, in the regulation of this oscillatory movement. These two factors are specifically induced in response to pheromone and they interact with each other. Together with Tip1p they co-ordinate the

dynamics of microtubules at opposite ends of the cell to generate the oscillations which drive the nuclear movement.

Acknowledgements

I would like to thank my supervisor Paul Nurse for his help and guidance throughout my PhD, especially for his unlimited optimism and encouragement in the face of my gloominess.

Many thanks also go to all members of the Cell Cycle lab, for all their help and support in getting me started and getting my through my last four years. In particular I would like to thank Damian Brunner who initiated me to the "wonders" of microscopy and photoshop and Heidi Browning who took over his role and has always been there to help me out at all hours of the day and night. Zoi Lygerou got me started on the basics of fission yeast genetics and molecular biology and Satoko Yamaguchi kept me up to date on the secrets of trade. I would finally like to thank Jacky Hayles, Mercedes Pardo and Rafael Carazo-Salas for reading this thesis.

A big thank you to my sister and my parents for trying to understand what my PhD was all about, for their encouragement, and for bringing over from Italy vital supplies of good food and wine. Special thanks to Demis for his continuing support and interest in my shmoos and Ts.

This PhD was funded by the Imperial Cancer Research Fund.

Table of Contents

List of Figures and Tables

Chapter 1 ***Introduction to cell polarity in Fission Yeast***

Chapter 2 ***Role of Tea1p, Tea3p and Pom1p in the determination of cell ends during vegetative growth***

Chapter 3 ***Analysis of the response to pheromone***

***Chapter 4* Regulation of extrinsic cell growth**

***Chapter 5* Regulation of microtubular dynamics during shmooing**

List of Abbreviations

Adenomatous Polyposis Coli (APC)

Caenorhabditis elegans (C.elegans)

Carbendazim (MBC)

Cyan Fluorescent Protein (CFP)

Deoxyribonucleic acid (DNA)

Dimethyl Sulfoxide (DMSO)

Edinburgh minimal medium (EMM)

Ezrin/moesin/radixin (ERM)

Fluorescence Activated Cell Sorter (FACS)

Gap1, phase of the cell cycle between mitosis and S phase (G1)

Gap 2, phase of the cell cycle between S phase and mitosis (G2)

Green Fluorescent Protein (GFP)

Guanine TriPhosphatases (GTPases)

GTPase Activating Protein (GAP)

Guanosine Exchange Factor (GEF)

Hydroxyurea (HU)

Kilo Dalton (kDa)

Latrunculin A (LatA)

Messenger RNA (mRNA)

Microtubule Organising Centre (MTOC)

Mitogen Activated Protein Kinase (MAPK)

Mitosis (M)

New End Take Off (NETO)

Old End Take Off (OETO)

p21 Activated Kinase (PAK)

PhosphoInositol (PI)

Polyacrylamide Gel Electrophoresis (PAGE)

Polymerase Chain Reaction (PCR)

Schizosaccharomyces pombe (S. pombe)

Saccharomyces cerevisiae (S.cerevisiae)

Sodium Dodecyl Sulphate (SDS)

Spindle Pole Body (SPB)

Ribonucleic Acid (RNA)

Thiabendazole (TBZ)

Wiskott-Aldrich Syndrome Protein (WASP)

Yellow Fluorescent Protein (YFP)

Yeast Extract supplemented with amino acids (YE5S)

Publications Arising From This Thesis

Teresa Niccoli and Paul Nurse, Different mechanisms of cell polarisation in vegetative and shmooing growth in fission yeast, J Cell Sci. 2002 Apr 15;115(Pt 8):1651-62

Manuel Arellano, **Teresa Niccoli** and Paul Nurse, *Tea3p is a cell end marker activating polarised growth in Schizosaccharomyces pombe*, Curr Biol. 2002 Apr 30;12(9):751-6

Teresa Niccoli, Manuel Arellano and Paul Nurse, *Role of Tea1p, Tea3p and Pom1p in the determination of cell ends Schizosaccharomyces pombe,* (Submitted)

Teresa Niccoli, Akira Yamashita, Paul Nurse and Masayuki Yamamoto, *Fission yeast ssm4 encoding a homologue of the dynactin component Glued which regulates microtubular dynamics during mating*, (Manuscript in preparation)

Notes on Collaborative Work

My contribution to the work published by Arellano et al., (2002) consists of experiments showing the localisation of Tea3p in a *tea2Δ* strain and in the analysis of the genetic interaction between *tea3Δ*, and *ssp1Δ, orb2Δ* and *wee1Δ*. These results have not been presented in this thesis.

The paper submitted for publication with the title "*Role of Tea1p, Tea3p and Pom1p in the determination of cell ends Schizosaccharomyces pombe*" describes the work presented in chapter 2. The analysis of the mutants' growth patterns was work of Manuel Arellano while the rest of the paper consists of my own work.

The paper in preparation with the title "*Fission yeast ssm4 encoding a homologue of the dynactin component Glued which regulates microtubular dynamics during mating*" is a joint collaboration between me and Akira Yamashita, and we are co-authors on the paper. I carried out the analysis of Ssm4p in shmooing cells and Akira Yamashita analysed the role of Ssm4p in zygotes. Only my part of the work has been presented in this thesis.

Chapter 1

Introduction to cell polarity in Fission Yeast

1.1 Introduction

1.1.1 Intrinsic and extrinsic polarity

Eukaryotic cells, from yeast to mammals, display a wide range of polarised morphologies, important for cellular function and development. A polarised shape is generated via the organisation of cytoskeletal elements, usually leading to actin becoming located at sites of growth and to microtubule arrangement reflecting the cell shape. Eukaryotic cells can become polarised in response to signals of two types: intrinsic and extrinsic signals. Intrinsic signals are generated within a particular cell, for example nuclear movement in the Drosophila oocyte establishes the Dorso-Ventral axis (Micklem et al., 1997), or internal landmarks determine the bud site in budding yeast (Hartwell, 1971). Extrinsic signals are provided by sources external to the cell such as mating pheromones in budding and fission yeast, which direct the shmooing projection during mating (Chenevert, 1994; Fukui et al., 1986), or sperm entry in the *Caenorhabditis elegans* zygote, which determines the Anterior-Posterior axis (Goldstein and Hird, 1996). In both types of polarisation, cells have to be able to select growth sites, reorganise their cytoskeleton accordingly, and direct polarised secretion of growth components (Drubin and Nelson, 1996). Cells responding to an internal program either generate polarised cell growth *de-novo* or they use inherited landmarks to direct growth. The latter is the case for budding yeast, where the site of bud emergence is marked by a cortical tag set down in the previous cell cycle (Casamayor and Snyder, 2002). Another example is found in *Drosophila melanogaster* neuroblasts, whose asymmetric cell division is directed by the

localisation of Bazooka inherited from their epithelial progenitors (Shulman and St Johnston, 1999). When polarisation is externally directed, the site and direction of cell growth are dictated by the position of the external signal (Chenevert, 1994). In this case, a cell needs to be able to detect the signal's location and directionality, relay this information to its interior, and then redirect its cytoskeleton to generate polarised growth or directionalised movement. Individual cells can switch between the intrinsic and extrinsic polarisation modes (Shulman and St Johnston, 1999), but how this transition occurs is not well understood.

Some of the molecules involved in the selection and maintenance of sites for polarised growth are conserved from yeast to mammals. Rho small GTPases (Guanine TriPhosphatases), WASP-like proteins (Wiskott-Aldrich Syndrome Protein) and PAKs (P21 Activated Kinase) have been implicated in growth and movement in many organisms like *Saccharomyces cerevisiae*, *Drosophila*, mammals as well as fission yeast (Daniels and Bokoch, 1999; Mullins, 2000). Lipid products of phosphoinositol-3-kinase (PI3K) exhibit strong asymmetries in response to external signals and play a role in chemotaxis and polarity in *Dictyostelium discoideum* and many cell types such as neutrophils and fibroblasts (Insall and Weiner, 2001; Takenawa and Itoh, 2001). All these polarisation factors converge on a highly conserved set of proteins involved in actin polymerisation, which also become polarised to the site of growth (Daniels and Bokoch, 1999; Mullins, 2000; Takenawa and Itoh, 2001), suggesting that the basic mechanisms involved may have been maintained throughout evolution.

Components of the signalling cascades responding to external stimuli are also highly conserved. G-protein coupled receptors are often responsible for detecting the signal on the outside of the cell and relay it to the interior, and Mitogen Activated Protein Kinase (MAPK) cascades amplify and transmit the signal to the nucleus to alter transcription patterns (Widmann et al., 1999).

Signals inducing differentiation also alter microtubular dynamics, suggesting that this might be an essential step in the regulation of cell shape during this process (Chausovsky et al., 2000; Spencer et al., 2000). Pheromone signalling in *S. cerevisiae* induces the Microtubule organising centre (MTOC) to move to the edge of the nucleus facing the shmooing projection and a stable array of microtubules is generated by capturing and stabilising microtubule ends at the shmooing tip (Maddox et al., 1999). A similar rearrangement of microtubules is observed in fibroblasts stimulated by lysophosphatidic acid (LPA) (Palazzo et al., 2001), and cadherin signalling has been found to stabilise microtubular ends (Chausovsky et al., 2000). Recent work has started to shed some light as to how these microtubule rearrangements take place. The fibroblasts' polarised microtubular array is induced through the activation of two distinct Rho pathways: RHOA and CDC42. RHOA acts via mDIA (a member of the *DIAphanous* formin family) to stabilise microtubule ends, and CDC42 induces the MTOC to move to a position between the nucleus and the leading edge (Palazzo et al., 2001).

1.1.2 Intrinsic and extrinsic growth in *Schizosaccharomyces pombe*

The genetically amenable fission yeast (*Schizosaccharomyces pombe*) is a useful model system to study how cell polarity is established. Its well-determined cell shape has made it straightforward to carry out mutant screens for altered cell morphologies to identify novel components regulating cell polarity. Fission yeast's facile genetics and the sequencing of its whole genome has now made the cloning of these mutants relatively straightforward too. It is also as divergent from *S. cerevisiae* as it is from man, making it a very useful complementary system to the studies carried out in *S. cerevisiae*. *S. pombe* also displays two modes of polarised cell growth: one intrinsically established during vegetative growth and one extrinsically determined during mating, making it a good model system to investigate how the two modes of polarity are regulated and how the switch between the two modes of growth takes place. Many of the factors involved in cell polarity described so far in *S. pombe* are conserved throughout evolution, demonstrating that the analysis of fission yeast cell polarity should help our understanding of how cell polarity is established in higher eukaryotes. In this introduction I will describe the current understanding of how *S. pombe* actin and microtubule cytoskeletons are regulated to establish cell polarity during intrinsic and extrinsic growth, drawing parallels with other organisms when appropriate.

1.1.2.1 Intrinsic growth in *Schizosaccharomyces pombe*

During vegetative growth fission yeast is a cylindrical rod shaped cell, extending mostly in a bipolar fashion from its ends. When the cell reaches a critical cell size it undergoes cytokinesis by medial fission to generate two equal sized daughter cells, each with a new end at the site of cell division and an old end inherited from the mother cell (Mitchison and Nurse, 1985). Critical cell size is coupled to mitosis (Rupes et al., 2001) and mitosis is required to undergo cytokinesis (Nurse et al., 1976). This ensures that the cells generated at cytokinesis have a similar size and that each daughter cell inherits one nucleus. After cytokinesis cells begin to grow monopolarly from the old end. Once the cell has replicated its DNA and reached a particular length it undergoes NETO (new end take off), when growth at the new end is activated to generate a bipolar growing cell (Mitchison and Nurse, 1985) (Fig 1.1).

Filamentous actin is organised in patches and cables, with the majority of patches associated with a cable (Pelham and Chang, 2001). Patches are found at actively growing ends during interphase and relocate to the cell middle during cell division. On the other hand cables run along the length of the cell during interphase and form a medial ring at the site of cell division at cytokinesis (Arai and Mabuchi, 2002; Marks et al., 1986; Pelham and Chang, 2001). Patches move mostly randomly in the cell and this movement requires actin cables and active actin polymerisation (Pelham and Chang, 2001).

Interphase microtubules are arranged as 3-5 antiparallel bundles with overlapping minus ends located at the cell centre, at sites adjacent to the nuclear membrane. Each microtubule bundle probably contains 2-4 individual microtubules (C. Antony, personal

communication) and appears to behave as a single, highly dynamic structure. It nucleates from the cell centre, growing along the length of the cell and stalling at the cell ends, and then undergoes catastrophe back to the cell centre (Drummond and Cross, 2000; Hagan, 1998; Hagan and Hyams, 1988; Tran et al., 2001). This ensures that microtubules align with the long axis of the cell, with their minus ends in the cell middle, linked to the nucleus at their central overlap regions, and their plus ends reaching opposite cell ends. These bundles push on the cell ends before undergoing catastrophy and the transient pushing forces from opposite cell ends are thought to keep the nucleus in the cell middle (Tran et al., 2001) (Fig 1.2). The position of the nucleus directs the cytokinesis site (Chang and Nurse, 1996), it is therefore crucial that the nucleus is located in the cell middle at mitosis to ensure septation generates two equally sized daughter cells.

To maintain its shape in successive generations a vegetative fission yeast cell has to maintain growth along the long axis and has to generate two equal size daughters. To do this fission yeast cell growth undergoes three major transitions: 1- after cytokinesis growth is activated at the old end, 2- at NETO growth is activated at precisely the opposing end to guarantee growth along a single axis and 3- at cytokinesis the cell finds its middle to generate two equal size daughters.

The cell has therefore to be able to identify its ends and mark them as sites for growth. Once these sites have been selected growth has to be re-directed and restricted to those sites so as to generate a rod-shaped cell of uniform diameter. Both the actin and the microtubule cytoskeletons play a crucial role in the establishment and maintenance of appropriate growth zones essential for fission yeast cell polarity.

1.1.2.2 Role of the actin cytoskeleton in the determination of *Schizosaccharomyces pombe*'s cell shape

Actin is essential for growth. Cells treated with Latrunculin A (LatA), an inhibitor of actin polymerisation (Spector et al., 1983), are unable to elongate. Actin is known to be essential for secretion, which is a prerequisite for growth and may protect the plasma membrane from osmotic pressure (Mulholland et al., 1994; Novick and Botstein, 1985). To generate polarised growth therefore actin polymerisation has to be re-directed to the appropriate location at cytokinesis and NETO. The main questions therefore are: 1. How is actin localisation translated into active cell growth, 2. How is actin polymerisation activated, 3. How is actin polymerisation concentrated to a limited area, 4. How is actin positioned and 5. How is actin relocalisation triggered.

These issues are not unique to fission yeast, but apply to any polarised cellular projection.

How is actin localisation translates into active cell growth

Not much is understood about this process. *Orb5+*, which encodes a Casein Kinase II beta, is the only factor involved in this process identified so far. At the restrictive temperature *orb5* mutant cells undergo a couple of divisions without growth, leading to small round cells with delocalised actin. The same mutant cells, arrested in G1 at the restrictive temperature, maintain actin localisation to the ends but do not elongate, suggesting that Orb5p is required to translate actin localisation into active growth (Snell and Nurse, 1994).

How is its polymerisation activated

The core components of the actin polymerisation machinery are highly conserved from yeast to man. Experiments *in vitro* with purified components paralleled with *in vivo* mammalian studies have shown that actin polymerisation can be initiated by the Arp2/3 complex activated by WASP or SCAR. Actin monomers bound to profilin are added to extend the actin filament, and various actin binding proteins regulate the polymerisation network, either by directly influencing the dynamics of filament assembly or by generating higher order structures. Cofilin severs and depolymerises actin filaments. Gelsolin, villin and capping proteins bind and stabilise filament ends, whereas tropomyosin binds along actin filaments to stabilise them. Other factors, like fimbrin or α-actinin can cross-link actin filaments to generate more complex structures (Blanchoin et al., 2000; Machesky and Insall, 1999). Rho proteins, such as Cdc42 or Rac (Mullins, 2000) can regulate these polymerisation events by regulating the actin polymerisation machinery. For example Cdc42 binds WASP to induce actin polymerisation (Mullins, 2000), and Cdc42 or Rac can activate Pak1, which then phosphorylates and activates LIM kinase, an inhibitor of cofilin, thus stabilising actin filaments (Daniels and Bokoch, 1999) (Fig 1.3).

Homologues of many of these components have been found in fission yeast and are likely to be involved in similar processes as their mammalian counterparts. Arp2p and Arp3p localise to actin patches, their deletions are lethal and temperature sensitive mutants display delocalised actin patches and aberrant cytokinesis, with cells becoming swollen and eventually lysing (McCollum et al., 1996; Morrell et al., 1999). Actin cross-

linking proteins, like fimbrin (Fim1p), are also involved in assembly of actin structures in fission yeast. Fim1p localises and is involved in the formation of the F-actin ring and patches, counteracting the actin–depolymerising factor Adf1p, which also localises to patches (Nakano et al., 2001; Wu et al., 2001). Fim1p acts in collaboration with an F-actin capping protein, Acp1p (Nakano et al., 2001). Other proteins appear to be involved in F-actin cable formation. These include the tropomyosin Cdc8p which localises to actin cables and the cytokinetic ring and is involved in cable formation and cytokinesis (Balasubramanian et al., 1992). The profilin Cdc3p, and the α-actinin Ain1p, are also localised to the actin ring and are involved in cytokinesis (Balasubramanian et al., 1994; Wu et al., 2001). Overexpression of Cdc3p abolishes any actin staining, probably because it sequesters all actin monomers (Balasubramanian et al., 1994). Interestingly an *arp2-1* mutant can rescue the cytokinesis defect of a *cdc3-124* mutant, probably because actin patch mobility is delayed in *arp2-1* and the slow actin ring formation of *cdc3-124* can catch up (Morrell et al., 1999). This suggests that in fission yeast cables and patches are polymerised slightly differently, since some components appear to be primarily involved in patch formation and others in cable formation. An analogous situation has been found in *S. cerevisiae* where cables and patches appear to be polymerised by different mechanisms (Evangelista et al., 2002). Bni1 and Bnr1, two formins, have been shown to play a role in assembly of actin cables, independently of Arp2/3 (Evangelista et al., 2002), which are involved in the assembly of actin patches. The closest *S. pombe* Bni1 homologue, For3p, might also be involved in regulating actin cable polymerisation. It is

localised to the cell ends and the septum and in *for3Δ* cells no cables are formed, patches are delocalised and cells present aberrant cell morphology (Feierbach and Chang, 2001b). Deletion of *cdc42+* and *pak1/shk1/orb2+* are also lethal in fission yeast. Their temperature sensitive mutants (ts mutants) at the restrictive temperature give rise to small round cells with delocalised actin (Marcus et al., 1995; Miller and Johnson, 1994; Verde et al., 1995). Genetic and two-hybrid evidence suggests that Cdc42p interacts and activates Pak1p (Marcus et al., 1995; Ottilie et al., 1995; Tu and Wigler, 1999). Regulators of this interaction have been identified, none of which are essential, suggesting there might be multiple partially redundant regulators. Their mutant phenotype also suggests that they are mostly involved in localising actin polymerisation rather than in polymerisation *per se*, and therefore will be discussed in the next section.

Recently it has been shown that Myo1p, a type I myosin, localises to actin patches and acts in parallel to Wsp1p, a WASP homologue, to promote Arp2/3 mediated actin assembly (Lee et al., 2000). This is similar to the situation in *S. cerevisiae* where type I myosins, activated by the PAK homologue, also interact with Arp2/3 to promote actin polymerisation (Lechler et al., 2000). A downstream effector of Pak1p might be Orb6p, an essential serine/threonine kinase which localises to growing ends and plays a role in the maintenance of cell polarity. An *orb6* mutant at the restrictive temperature generates round cells with delocalised actin (Verde et al., 1998).

How actin polymerisation is concentrated to a limited area

Mutants which can not concentrate actin polymerisation will give rise to round cells, which can grow but are unable to focus actin localisation in one discrete area. This is the

case for deletion mutants of regulators of Cdc42p and Pak1p. Cells lacking Scd1/Ral1p, the GEF for Cdc42p, Scd2/Ral3p, an SH3 domain containing protein, and Skb1p, a positive regulator of Pak1p, all exhibit a similar phenotype. Scd1p is homologous to *S. cerevisiae*'s Cdc24, a Cdc42 activator which localises to growth sites (Nern and Arkowitz, 2000; Zheng et al., 1994). Scd1p localises to spindles and to cell ends when overexpressed (Li et al., 2000), and interacts with Cdc42p (Chang et al., 1994). Scd2p is localised to sites of active growth (Sawin and Nurse, 1998), where it acts as a scaffold protein, binding Pak1p, Cdc42p and Scd1p, and facilitating the interactions between these proteins (Chang et al., 1999; Chang et al., 1994). Scd2p is phosphorylated by Pak1p *in vitro* and stimulates Pak1p autophosphorylation activity when overexpressed (Chang et al., 1999), suggesting it might be regulating Pak1p activity in the cell. Bem1, the *S. cerevisiae* homologue of Scd2, also functions as a scaffold, interacting with Ste20, the PAK homologue (Leeuw et al., 1995), Cdc42 (Butty et al., 1998) and Cdc24 (Peterson et al., 1994) at sites of growth. Bem1 is thought to stabilise the activated Cdc24-Cdc42 complex at the bud tip thus allowing bud emergence (Gulli and Peter, 2001). The fission yeast Scd2p might be playing a similar role, stabilising the interaction between Cdc42p-Scd1p and Pak1p at the cell ends.

Another regulator of this interaction is Skb1p, which can form a complex with Pak1p and Cdc42p in a yeast two-hybrid assayand appears to act upstream of Pak1p and at the same level of Cdc42p (Gilbreth et al., 1996). A novel negative regulator of Cdc42p was recently identified: Nrf1p is a membrane protein which localises to vacuolar membranes

in a Scd1p-dependent fashion and appears to be involved in endocytosis (Murray and Johnson, 2001).

Ras1p also appears to regulate this pathway. Genetic data suggests it acts upstream of Cdc42p and Pak1p (Chang et al., 1994; Marcus et al., 1995) and it has been found to interact with Scd1p to promote the interaction between Scd1p and Cdc42p (Chang et al., 1994; Fukui and Yamamoto, 1988). During vegetative growth Efc25p is the guanine nucleotide exchange factor (GEF) which activates Ras1p (Papadaki et al., 2002) (Fig 1.4). A different set of activators and inhibitors appear to regulate Ras1p activity during mating, but these will be discussed later.

Fission yeast has another PAK, Shk2p/Pak2p, which is not essential and seems to interact with the Ras1-Cdc42-Pak1 morphological pathway, although its role is not clear (Sells et al., 1998).

This actin polymerisation network can also interact with the cell cycle machinery since overexpression of either Skb1p or Orb6p delays mitosis in a Wee1-dependent manner (Gilbreth et al., 1998; Verde et al., 1998). These components might play an important role in co-ordinating cell growth and cell cycle transitions.

Membrane dynamics and cell wall integrity also appear to influence actin localisation and therefore cell polarity. Growing evidence in other systems is implicating PhosphoInositol (PI) and its derivatives in the establishment of cell polarity (Takenawa and Itoh, 2001). PI(3,4,5)P3 is localised to the leading edge of neutrophils and *Dictyostelium* and together with PI(4,5)P2 is involved in actin polymerisation (Insall and Weiner, 2001; Takenawa and Itoh, 2001). Recently a positive feedback between RAC,

Cdc42, Rho and PI3kinase has been implicated in neutrophil polarity and motility (Wang et al., 2002; Weiner et al., 2002). In fission yeast PI kinases play a role in membrane fusion and the maintenace of cell morphology. They are especially required for cytokinesis and for maintaining cell polarity in response to stressful conditions (Colussi and Orlean, 1997; Morishita et al., 2002; Takegawa et al., 1995; Zhang et al., 2000). Myosins playing a role in vacuole mobility and membrane fusion, like Myp2p and Myo52p, are also involved in cell polarity, especially in response to stress (Bezanilla et al., 1997; Motegi et al., 2001), and Cdc4p, an essential myosin light chain, interacts with both Myo2p and PI4 kinase (Desautels et al., 2001). This suggests that membrane dynamics has to be properly regulated to ensure appropriate cell growth, possibly to guarantee the delivery of essential growth components to the sites of polarised cell growth. Alternatively membrane components could be directly effecting actin polymerisation.

Cell wall intergrity is also crucial to maintain cell polarity. Digestion of the cell wall with enzymes leads to total delocalisation of the actin cytoskeleton(Kobori et al., 1989), indicating that the cell can not polarise growth components in the absence of a cell wall. The cell wall might have a similar role to the extracellular matrix in higher eukaryotes, providing a substrate along which the cell can organise its polarity. Consistent with this view, mutants in cell wall components or its regulators lead to actin delocalisation and abnormal morphology as well as cell wall defects (Arellano et al., 1999; Katayama et al., 1999; Ribas et al., 1991). The small GTPases Rho1p and Rho2p regulate cell wall formation and actin localisation *via* Pck1p and Pck2p (Calonge et al.,

2000; Sayers et al., 2000). They both localise to the septum and Rho1p also localises to the cell periphery (Arellano et al., 1996; Sayers et al., 2000). Rho1p and Rho2p might also regulate actin more directly: Rng2p, an IQGAP protein and a downstream effector of Rho1p, binds actin and regulates assembly of actin cables at cytokinesis (Eng et al., 1998), and Rho2p effects on actin appear to be mediated specifically by Rkp1p, a RACK1 homologue (Won et al., 2001).

How is actin positioned and how its relocalisation triggered

The core actin polymerisation machinery and its regulators will ensure that actin polymerisation is restricted to a particular area, resulting in the formation of a polarised projection. However, in fission yeast this growth has to be positioned correctly to the cell ends. Failure to do so will result in polarised growth but in the wrong direction generating monopolar, bent or T-shaped cells.

As discussed above, fission yeast cells undergo three major growth transitions: 1. Initiation of growth at the Old End, 2.NETO, when growth is activated at the New End , 3.cytokinesis, when growth is redirected to the cell middle to form a septum. Probably the best understood of these transitions is cytokinesis. Many factors involved have been identified and recently reviewed (Feierbach and Chang, 2001a) .

Mutants that can not localise the growth machinery correctly after cell division will generate bent or branched cells. Many genes have been identified which are required to position the growth zone correctly after cell division: *tea1+, tip1+, pom1+, mal3+,* the *alp* proteins, the kinesins *tea2+, klp5+* and *klp6+*. Often bent and branched mutants cannot undergo NETO, thus generating monopolar cells. But mutants specific for NETO

have also been identified, these include mutants in *tea3, ssp1* and *bud6* genes. Sometimes mutations in factors involved in unrelated functions, like Wee1p or Orb2p mutants, also display a NETO defect. Tea2p, Tip1p, Klp5p, Klp6p and the Alp proteins are all factors regulating microtubular dynamics, indicating that microtubule defects can influence the positioning of the actin polymerisation machinery and they will be discussed separately.

Tea1p is a Kelch-repeat containing protein which localises to microtubules, the cell ends and the septum (Behrens and Nurse, 2002; Mata and Nurse, 1997). Although it does influence microtubular dynamics, it also plays a more direct role in positioning growth zones, since a *tea1* truncation mutant which does not cause a microtubule defect but is unable to localise to the cell ends, has the same polarity defects as a complete deletion (Behrens and Nurse, 2002). It is thought that Tea1p acts as a scaffold targeting other cell polarity factors, like Tea2p, Tip1p, Pom1p and Tea3p to the cell ends (Arellano et al., 2002; Behrens and Nurse, 2002; Browning et al., 2000; Brunner and Nurse, 2000). Pom1p is a Dyrk protein kinase involved in NETO, septation and marking cell ends (Bahler and Pringle, 1998). In the absence of Pom1p, cells are bent or T-shaped, monopolar, have misplaced septa (Bahler and Pringle, 1998), and slightly longer microtubules (Bahler and Nurse, 2001). Its kinase activity fluctuates in the cell cycle, being higher at times of bipolar growth and lower during monopolar growth and cytokinesis. Since both its kinase activity and its localisation are essential to its function, Pom1p at cell ends might phosphorylate a factor responsible for these growth transitions (Bahler and Nurse, 2001). Bud6p is also localised to cell ends and the septum, and is required for NETO. Its localisation to growing ends requires actin but not Tea1p,

although it does physically interact with Tea1p (Glynn et al., 2001). A cytokinesis mutant, *cdc11-119*, undergoes multiple rounds of nuclear division and repeated cycles between bipolar growth marked by actin at both cell ends, and a non-growing state with an actin ring in the middle of the cell. After each nuclear division the cell needs to re-identify the two ends of the cell to reactivate bipolar cell growth. When *cdc11-119* is combined with either *pom1Δ*, *tea1Δ* or *bud6Δ*, highly branched cells are produced, indicating a role for Pom1p, Tea1p and even Bud6p as markers identifying the cell ends (Bahler and Pringle, 1998; Glynn et al., 2001; Mata and Nurse, 1997).

In contrast, *Cdc 11-119* does not generate branched cells in combination with *tea3Δ*, suggesting that Tea3p might play a role as a specific trigger for NETO rather than a cell end identifier. Tea3p displays some homology to Tea1p and a weak homology to the Ezrin-Moesin-Radexin (ERM) family of proteins. It has been found to interact with Tea1p in a yeast two-hybrid assay, although this interaction could not be confirmed by immunoprecipitation (IP) (Arellano et al., 2002). Tea3p localises to non-growing ends during monopolar growth and to both ends during bipolar growth. *Tea3Δ* is synthetically lethal with *pom1Δ* at high temperatures, suggesting it might act in a parallel pathway (Arellano et al., 2002). A role for the actin cytoskeleton itself at NETO was demonstrated in experiments in which an increase of the actin monomer pool induced by LatA treatment resulted in premature activation of growth at the new end in monopolar cells. This LatA pulse could also rescue the NETO defect of *ssp1Δ* cells, suggesting that the Ssp1p phosphatase acts as a trigger for actin depolymerisation at NETO (Rupes et al., 1999); consistent with this explanation *ssp1Δ* cells displayed less dynamic actin. Cells

lacking the Ppe1p and Sts5p kinases become round as do cells overexpressing Ssp1p, and *ssp1* mutants can rescue *sts5* or *ppe1* defective cell shape (Matsusaka et al., 1995). This suggests that Ssp1p and Sts5p and Ppe1p might act antagonistically on the same substrate to regulate polarisation and actin localisation (Matsusaka et al., 1995).

Overall these controls ensure that actin polymerisation is targeted to the cell ends, where it is restricted to a limited area thus maintaining a limited cell diameter and directed cell growth. They also guarantee that actin is relocalised to the appropriate growth sites at particular stages of the cell cycle. This will ensure directed secretion of growth components and protection of the membrane at sites where the cell wall is weak. Plasma membrane and cell wall dynamics have to be co-ordinated with the actin polymerisation machinery to result in appropriate cell polarity.

1.1.2.3 Role of the microtubule cytoskeleton in the determination of *S. pombe*'s cell shape

Microtubules are arranged along the long axis of the cell, growing from the cell middle and terminating at the cell ends. The parallel arrangement of microtubules is designed to read the rod-shape of the fission yeast cell and maintain cell ends opposed to each other. Several lines of evidence suggest that microtubules play an important role in positioning growth zones. Mutants in the tubulin genes, as well as their folding cofactors and regulators of microtubular dynamics, often display bent or branched cells (Hirata et al., 1998; Radcliffe et al., 1998; Radcliffe et al., 2000a; Radcliffe et al., 1999; Radcliffe and Toda, 2000; Radcliffe et al., 2000b). Inducing short microtubules with Thiabendazole (TBZ, a microtubule depolymerising drug) leads to the formation of branched cells,

suggesting that growth can be re-directed to where the microtubule ends are located (Sawin and Nurse, 1998). Microtubules might be involved in delivering markers for growth or components of the growth machinery to the appropriate location.

Screens for mutants displaying altered cell polarity have identified many factors effecting microtubular dynamics. These factors are located in two main areas: the Spindle Pole Body (SPB) or the microtubule tips. Gamma-tubulin and components of the gamma-tubulin complex play an important role in establishing a wild type microtubular array, maybe through the regulation of their nucleation (Paluh et al., 2000; Vardy and Toda, 2000). Mutations in Alp4p, Alp6p and Alp16p, three SPB components, lead to the formation of fewer, longer microtubules which are still associated with the SPB (Fujita et al., 2002; Vardy and Toda, 2000). Another factor that might regulate microtubule dynamics from the SPB is Alp14p, a XMAP215 homologue, which localises along microtubules and to the SPB, and stabilises microtubules (Garcia et al., 2001). XMAP215 homologues stabilise microtubules (Gard and Kirschner, 1987) through an interaction with a TACC, a highly conserved centrosomal protein (Lee et al., 2001b).

Tea1p, which as I mentioned earlier plays a role in marking cell ends, travels with the microtubular tips to the cell ends where it is unloaded and accumulates (Behrens and Nurse, 2002). Tea1p plays a role in triggering microtubule depolymerisation once these have reached the cell ends (Mata and Nurse, 1997). To do this its localisation at microtubule tip and not at cell ends is important, suggesting there might be another microtubule depolymerising factor at the cell end that unloads Tea1p from the tips of microtubules and triggers microtubule depolymerisation (Behrens and Nurse, 2002).

Three further factors, Tea2p, Tip1p and Mal3p, which act upstream in the Tea1 pathway also play a role in microtubular dynamics (Beinhauer et al., 1997; Browning et al., 2000; Brunner and Nurse, 2000). In the absence of either of these factors microtubules are short and rarely reach the cell ends. Tip1p, a CLIP 170-like protein has been shown to stabilise microtubules when they reach the cell periphery, allowing them to grow just beneath the cell cortex until they have reached the cell ends. This enables microtubules to align along the long axis of the cell (Brunner and Nurse, 2000). Tip1p forms a complex with Tea2p (D. Brunner and P. Nurse, unpublished data), a kinesin-like protein, and both are found at the tips of microtubules and at the ends of cells (Browning et al., 2000; Brunner and Nurse, 2000). Mal3p is an EB1 homologue, which localises along as well as at the tips of microtubules and is important for both interphase microtubules and spindle stability (Beinhauer et al., 1997). EB1 binds APC (Adenomatous Polyposis Coli) and delivers it to the appropriate location. It has also been shown to localise to microtubule tips and to play a role in stabilising microtubular dynamics (Bu and Su, 2001; Tirnauer and Bierer, 2000). The KIP3 kinesins Klp5p and Klp6p on the other hand, play a role in destabilising microtubules. They are located along microtubules, and in their absence interphase microtubules and spindles are longer (West et al., 2001).

The Ras-Pak-Cdc42 pathway also plays some role in regulating microtubular dynamics. In *Pak1* mutant cells microtubules bend round the cell end, Pak1p localises to microtubules when overexpressed, and its kinase activity rises after microtubules have been depolymerised with TBZ (Qyang et al., 2002). Skb15p, a negative regulator of Pak1p, also plays a role in microtubule dynamics. A *skb15* mutant displays spindle and

interphase microtubule defects as well as actin localisation defects, all of which appear to require Pak1p activity (Kim et al., 2001). Moe1p, a highly conserved protein of unknown function identified as a Scd1p-binding protein, plays a role in organising microtubules and spindles. It localises to the nucleus in a Scd1p-dependent fashion, and in its absence microtubule bundles are more abundant and more stable, spindles are defective and cells are bent (Chen et al., 1999). *Moe1Δ* rescues *nda2-M52*, a tubulin mutant, suggesting Moe1p might play a role in microtubule assembly (Chen et al., 1999). *Moe1Δ* also displays synthetic lethal interactions with mutations in *ras1, scd1, scd2* and *cdc42,* mostly because of defects in spindle formation (Chen et al., 1999). It is difficult to establish if this is because the latter play a parallel role in regulating spindle formation, or if the combination of a severe microtubule defect with a severe actin defect results in lethality, since actin does play a role in spindle orientation and elongation (Gachet et al., 2001). Double deletion of *moe1* and *mal3* also displays a synthetic negative interaction, with a high number of short microtubules. This indicates that Moe1p plays two roles, one downstream of Mal3p in the regulation of microtubular dynamics, and one upstream of Mal3p in determining the number of microtubules nucleated (Chen et al., 1999). Cross-talk between actin and microtubule regulators has been recently described in mammalian cells, where microtubules are captured at the leading edge through binding of CLIP-170 at the microtubule tips to RAC and CDC42 at the leading edge, *via* IQGAP (Fukata et al., 2002). For3p, another protein involved in actin polymerisation, also determines the number of microtubule bundles in the cell. Since *for3Δ* cells display many more microtubules than wild type (Feierbach and Chang, 2001b).

This set of microtubule-binding proteins and regulators ensures that an appropriate array of microtubules extends from the cell centre to the cell ends, aligned with the long axis of the cell. This array delivers markers and growth factors to cell ends ensuring growth along a single axis (Brunner and Nurse, 2000; Hayles and Nurse, 2001). Computer models have shown that the semi-rigid linear microtubular structure, in collaboration with a destabilising cell end marker, could generate a rod shape from a round spore with no polarity. A slight imbalance of a particular cell end marker, which could randomly occur, would feed back into the microtubule system, which would amplify this initial difference and identify the opposite end, directing the growth machinery to these two opposite points thus generating a rod-shaped cell (Bela Novak, personal communication). This model is supported by the strong polarity defects shown by mutants with defective microtubules, but does not account for the polarity defects of cells with apparently normal microtubular arrays. This model is also challenged by the finding that the polarity defects seen in *tea1Δ* cells are not due to the microtubular defects of this mutant but to the lack of Tea1p at the cell ends, suggesting a role for cell end markers in directing growth machinery. It would be interesting to establish if in fission yeast landmarks are set down at the previous cell cycle which direct the polarisation machinery at the subsequent cell cycle, in a manner similar to *S. cerevisiae* and *Drosophila* neuroblasts.

1.1.2.4 Extrinsic growth in *S. pombe*

In response to external conditions such as osmotic stress, heat shock, altered nutrient conditions, or pheromones of the opposite mating type, the cell has to be able to

respond quickly and relocalise its cytoskeleton appropriately. This becomes particularly important during mating, where all stress and nutrient response pathways, as well as those specific for mating, appear to be required (Hughes, 1995; Kato et al., 1996; Loewith et al., 2000; Mochizuki and Yamamoto, 1992). This is probably because mating is brought about in response to multiple stimuli: lack of nitrogen, which is also a stressful condition and will therefore elicit both the stress response pathway and the nutritional pathway, and presence of pheromone of opposite mating type, which will stimulate the formation of a shmooing projection.

Five main signalling pathways have been identified, which are responsible for organising the cells' response to different external stimuli. Three of these are MAPK cascades. They are required for the mating response to pheromones, for the maintenace of cell wall integrity in response to high anion concentrations and for protecting the cell in conditions of high osmolarity and heat shock. The high osmolarity pathway (Fig 1.5) results in the production of glycerol, which protects the cell from the external osmotic pressure (Ohmiya et al., 1995). The cell wall integrity pathway (Fig 1.6) regulates cell wall composition, and collaborates with the stress pathway to allow vacuole fusion in response to stress (Bone et al., 1998). The pheromone pathway stimulates expression of mating genes and leads to the formation of a shmooing projection (Hughes, 1995) (Fig 1.7), this pathway will be discussed in more detail separately. All these pathways also induce actin relocalisation. The other two pathways respond to nitrogen and glucose, or calcium levels in the external medium. Lack of nitrogen inhibits the nutritional pathway, reducing the levels of cAMP in the cell, and leading to cell cycle arrest in the G1 phase of

the cell cycle, a prerequisite for mating (Mochizuki and Yamamoto, 1992). Glucose, on the other hand, stimulates c-AMP production, keeping the cell cycle active. Calcium stimulates Ppb1p, a Ca2+ dependent protein kinase, which is required for cell wall integrity and morphogenesis (Yoshida et al., 1994). Imbalances in Ca2+ in the cell lead to cell wall and shape defects (Carnero et al., 2000; Facanha et al., 2002).

Mutants in many components of these pathways show loss of viability in response to stress conditions or nutrient limitations. They also display morphological defects, from short and dumpy cells (c-AMP pathway) to long and multiseptated (cell integrity or Ca2+ response pathways), suggesting that cytoskeletal re-arrangements play an important part in protecting the cell from changing enviromental conditions. Defects in most of these pathways also lead to sterility because of failure to induce expression of *ste11+*, the main transcription factor for mating genes (Kato et al., 1996; Loewith et al., 2000; Yoshida et al., 1994). Overexpression of Ste11p can rescue the mating defect of *sty1Δ*, the osmotic pathway MAPK, but not the osmotic defect, suggesting that the pathway plays two distinct roles in osmoregulation and mating (Kato et al., 1996). Actin relocalisation in response to stress is mediated by Ssp1p. Upon Sty1p activation Ssp1p is relocalised from the cytoplasm to the whole cell membrane where it promotes actin relocalisation, maybe to reinforce the membrane (Rupes et al., 1999). Sty1p also stimulates glycerol production (Degols et al., 1996) and, as the cell adapts to the new conditions, actin relocalisation to the cell ends and Ssp1p membrane localisation is lost (Rupes et al., 1999).

Although fission yeast cells can respond to many environmental signals and relocalise actin accordingly, the only external signal which can induce a dramatic alteration in cell shape is the mating response. Since this is a main focus of this thesis I will describe this response in more detail.

1.1.2.5 Mating response

Fission yeast cells have two mating types, h^+ and h^-, and can only conjugate with a cell of an opposite mating type (Egel, 1971; Egel, 1989; Gutz and Doe, 1975). When fission cells are nitrogen-starved in the presence of a mating partner they activate a new pattern of cell growth that allows them to bend towards a mating partner (Fig 1.1). This extrinsic growth mode is induced by pheromones secreted from cells of opposite mating type and is, therefore, extrinsically determined (Fukui et al., 1986; Leupold, 1987). Cells are capable of detecting the directionality of the pheromone gradient, and orient their mating projection, called shmoo, towards the pheromone source (Fukui et al., 1986; Leupold, 1987). Cells then touch and undergo cellular and nuclear fusion, which is followed by meiosis and the formation of four haploid spores (Nielsen and Davey, 1995). Mating occurs only at temperatures below 32°C (Petersen et al., 1998), but cells can activate mating specific genes above that temperature (Stern and Nurse, 1998). It is therefore not clear why mating is inhibited at high temperatures.

Shmooing cells are characteristically bent, with one pointed and one rounded end, and extend in a monopolar fashion from the pointed end, where actin is localised (Petersen et al., 1998). Microtubules curve round the non-growing end and terminate at the shmooing end (Petersen et al., 1998). They also display a dramatic switch in

dynamics. Microtubules are mostly polymerised from the SPB and, instead of growing and shrinking from the cell middle as in vegetative cells, they drive the SPB back and forth in the cell in a characteristic oscillatory movement (Ding et al., 1998; Svoboda et al., 1995). The nucleus is linked to the SPB and therefore also oscillates back and forth in what is known as "horsetail movement".

This switch in cell growth is brought about in response to two main different signals: nitrogen starvation and presence of pheromone. Nitrogen starvation, as I discussed above, regulates the levels of c-AMP in the cell mainly through the inhibiton of the enzyme responsible for its production, adenyly cyclase, *cyr1+* (Kawamukai et al., 1991). C-AMP activates the protein kinase A Pka1p (Maeda et al., 1994) and targets Cdc25p for degradation to delay mitosis (Kishimoto and Yamashita, 2000). This appears to be a conserved mechanism to regulate cell cycle progression, since in *Xenopus* c-AMP also promotes degradation of Cdc25 (Grieco et al., 1994) and in macrophages c-AMP can control G1 and G2 arrest (Kato et al., 1994). In the absence of nitrogen Cyr1p is downregulated, c-AMP levels fall and Cdc25p is stabilised thus accelerating mitosis (Kishimoto and Yamashita, 2000), and transcription of *ste11+* is induced *via* Rst2p (Kunitomo et al., 2000). Levels of c-AMP are therefore a direct measure of nitrogen availability and might couple cell size to nutrient availability. Deletion of components of this pathway, including *cyr1+* abolish the requirement for nitrogen starvation in mating, and allow cells to arrest and mate solely in response to pheromone (Kawamukai et al., 1991; Nocero et al., 1994).

Pheromones are secreted into the medium via ABC transporters. Seven transmembrane-domains G-protein coupled receptors then bind specifically to the opposite mating type pheromone and transmit the signal to the interior of the cell. G-alpha dissociates from G-beta-gamma to activate the downstream MAPK cascade: Byr1p MAPKKK, Byr2 MAPKK and Spk1p MAPK, which activates, *via* an unknown factor, transcription of *ste11+* to induce the expression of mating-specific genes (Banuett, 1998) (Fig 1.7). This MAPK cascade can induce G1 arrest even in the absence of nitrogen starvation, probably via Rum1p, a cyclin-dependent kinase inhibitor, which binds the B-cyclins Cdc13p and Cig2p and specifically targets Cdc13p for cyclosome-mediated degradation (Stern and Nurse, 1998). The same MAPK cascade is activated in *S. cerevisiae* in response to pheromone binding (Banuett, 1998). In this case G-beta binds Ste20, a Pak1 homologue, which activates Ste11, the MAPKKK at the beginning of the cascade (Elion, 2000) (Fig 1.7). G-alpha, on the other hand is involved in binding the last component of the MAPK cascade, Fus3, to bring it to the cell tip and downregulate pheromone signalling (Metodiev et al., 2002). This MAPK cascade is important to induce G1 arrest and expression of mating type genes but it is not required for mating partner discrimination. Cells can still direct its shmooing projection along the highest pheromone concentration even in the absence of MAPK components (Schrick et al., 1997).

The main difference in fission yeast is that the cascade is activated by G-alpha, and that Ras1p is also required to activate Byr2p at the top of the MAPK cascade and to set up a shmooing projection (Nielsen et al., 1992). During mating Ras1p activity is

controlled by a different GEF and GAP that during vegetative growth, Ste6p activates Ras1p and Gap1p inhibits it (Hughes et al., 1990; Imai et al., 1991).

1.1.2.6 Actin relocalisation

Whereas in vegetative fission yeast cells, growth is concerned with maintaining cell shape, during mating cell shape has to be altered for a cell to meet its mating partner. To generate a shmooing projection actin has to relocate to a single end and growth has to be re-directed along a pheromone gradient. The transition from vegetative to shmooing growth is achieved via an intermediate bipolar step. Vegetative cells arrested in the G1 phase of the cell cycle are monopolar, but G1 arrested cells which switch to a mating pathway relocate actin to both ends before committing to a single end (Petersen et al., 1998). Maybe this step allows the cell to choose either end depending on which one is experiencing the highest pheromone concentration.

Not much is known about the establishment of a shmooing projection during mating in fission yeast. Ras1p is required for shmooing and a hyperactive *ras1* allele generates abnormally long shmoos, suggesting that Ras1p regulates shmooing cell polarity (Hughes, 1995). Screens for Ras Like proteins (Rals) have identified *ral1/scd1* and *ral3/scd2* as genes required for mating (Fukui and Yamamoto, 1988), and some mutant alleles of *pak1* and *cdc42* are sterile. This suggests that the Cdc42-Pak1 actin polymerisation cascade is important for setting up polarity in response to pheromone, but no factors specifically involved in shmooing polarisation have been identified.

After fission yeast mating cells have touched, they have to undergo membrane and then nuclear fusion. Fus1p is induced by the pheromone response pathway, it is

located at the shmooing projection tip and is required for cell wall degradation after cells have made contact (Petersen et al., 1995). Components of the osmotic stress and cell wall integrity pathways are also essential for mating. These components are needed for the membrane and cell wall remodelling steps involved in setting up a shmooing projection and in the subsequent fusion events. In *S. cerevisiae* the mating MAPK cascade also activates the protein kinase C pathway, that regulates cell wall integrity (Roberts et al., 2000).

Much is known about shmooing cell polarity regulation in *S. cerevisiae* . The pheromone receptor, G-beta and gamma, and components of the polarisation machinery are all crucial for directing the shmooing projection (Elion, 2000). This suggests that the pheromone receptor activates two pathways: the MAPK cascade to induce transcription of mating genes and the polarisation machinery to form a mating projection towards the mating partner. Recent papers have elucidated how the growth machinery can switch from a vegetative to a shmooing morphology. Far1p binds Cdc24, the GEF for Cdc42p, sequestering it to the nucleus. During vegetative growth Far1p is degraded at the G1/S boundary and Cdc24 exits the nucleus to bind bud site landmarks thus activating actin polymerisation and bud emergence. In response to pheromone the Far1-Cdc24 complex is exported via Msn5 to the cytoplasm. Far1 then targets Cdc24 to the activated G-beta at the surface, Cdc24 binds and activates Cdc42, which will induce the downstream effectors Ste20 and Bni1 to remodel the actin cytoskeleton, generating a shmooing projection (Gulli and Peter, 2001).

1.1.2.7 Microtubule cytoskeleton

As I mentioned above, the microtubule cytoskeleton undergoes dramatic rearrangements in response to pheromone, generating an oscillating array which drives the nucleus back and forth. The movement continues after nuclear fusion in the zygote and is thought to facilitate pairing of homologous chromosomes (Yamamoto et al., 1999) (Chikashige et al., 1994; Niwa et al., 2000) and the following meiotic nuclear divisions. Mutants defective in horsetail nuclear movements have defects in karyogamy, reduced recombination, and nuclear segregation defects leading to the formation of asci with less than four spores (Yamamoto et al., 2001; Yamamoto et al., 1999). The oscillations are probably generated by pulling forces on the microtubule ahead of the nucleus rather than pushing forces behind the nucleus and components of the dynein complex have been shown to be required for this movement (Yamamoto et al., 2001; Yamamoto et al., 1999).

Cytoplasmic dynein was first identified as a microtubular motor transporting vesicles towards the minus ends (Lye et al., 1987; Paschal et al., 1987; Paschal and Vallee, 1987). It has been implicated in multiple functions including maintenance of the Golgi apparatus (Harada et al., 1998), trafficking of vesicles (Lye et al., 1987), nuclear movement (DeZwaan et al., 1997) and microtubular dynamics (Han et al., 2001). It is a 1-2 MDa multisubunit complex composed of two heavy chains (500kDa), responsible for the motor activity, and multiple intermediate (70-74 kDa), intermediate light (53-59kDa) and light chains (8-22 kDa), regulating the motor activity of the heavy chains (King and Schroer, 2000).

Dynein heavy chain (Dhc1p) and two dynein light chains (Dlc1p and Dlc2p) have been identified in fission yeast. In mating cells Dhc1p and Dlc1p localise to the SPB, to microtubules and accumulate at the point where microtubules touch the cortex (Miki et al., 2002; Yamamoto et al., 1999). Dlc2p localises to the nuclear periphery and is not required for horsetail nuclear movement (Miki et al., 2002). Dhc1p and Dlc1p are both required for horsetail nuclear movement and play some role in karyogamy. These defects are probably due to altered microtubular dynamics. In the absence of Dhc1p, microtubules are less stable, rarely reach the cell ends and the nucleus does not display any oscillatory movement. It has been proposed that Dhc1p at the cortex is responsible for pulling on microtubules at the cortex, to generate the oscillations that drive the nucleus back and forth. This lack of nuclear movement leads to reduced recombination efficiency and meiotic segregation defects, resulting in the formation of asci carrying less than four spores. Dhc1p is only visible in the cell during mating and not during vegetative growth and a *dhc1* deletion has no phenotype during vegetative growth (Yamamoto et al., 1999), suggesting that, unlike most other organisms, the nucleus is positioned in a dynein-independent fashion during interphase (Tran et al., 2001). Dlc1p, on the other hand, is also expressed during vegetative growth, and localises to the SPB. In the absence of Dlc1p vegetatively growing cells have a shorter cell cycle, but the main defects appear during mating and meiosis. Nuclear movement does not span the length of the cell and appears more random; this is because forward-extending microtubules, normally resposible for the nuclear movement, are absent in *dlc1Δ* cells. Rearward extending microtubules are common and the nuclear movement observed seems to be due to

pushing rather than pulling forces. Recombination, too, is reduced. Dhc1p is no longer localised at the cortex, maybe also explaining the lack of pulling forces, but *dlc1Δ dhc1Δ* cells display more severe recombination defects than either of the single deletions alone, suggesting that Dlc1p might also play a role independently of Dhc1p (Miki et al., 2002). Genetic evidence suggests that Klp2p and Pkl1p, two kinesins required for spindle assembly during vegetative growth, also play some role during mating. *Klp2Δ dhc1Δ* cells fail to undergo karyogamy and *pkl1 Δdhc1Δ* fail to undergo meiosis (Troxell et al., 2001). Microtubule defects were not investigated in these cells but they appear likely.

Dynein is involved in nuclear orientation or movement in many organisms like *S. cerevisiae*, the fungi *Aspergillus Nidulas* and *Neurospora Crassa, Drosophila, C. elegans* and mammalian cells. During mitosis in *S. cerevisiae* the nuclear spindle has to align with the mother-daughter neck and then elongate through the neck. The latter requires microtubule sliding along the cortex and dynein is required for this movement (Adames and Cooper, 2000). Dynein localises to the hyphal tips in *A. nidulans* and *N. crassa* and is required for appropriate nuclear distribution in the hyphae (Minke et al., 1999; Xiang et al., 2000; Xiang et al., 1995). In *Drosophila, C. elegans* and MDCK cells, dynein has also been implicated in spindle rotation (reviewed in (Dujardin and Vallee, 2002)). In many of these organisms disruption of dynein function has been associated with microtubular defects, suggesting that, like in *S.pombe*, dynein plays a role in regulating microtubular dynamics (Gaglio et al., 1997; Han et al., 2001; Merdes et al., 1996; Shaw et al., 1997).

Most, if not all, of dynein's functions require dynactin, an 11 subunit complex, first identified as a component co-purifying with dynein preparations from rat's liver and testis (Collins and Vallee, 1989). Dynactin comprises eight or nine Arp1 (actin related protein) which bind together to form a short filament (Schafer et al., 1994), four or five dynamitin, two p150-Glued and a series of proteins capping the Arp filament, p62, p27, p25 and Arp11. The complex also contains one conventional actin and two p24 (Allan, 2000). Components of the dynactin complex often colocalise and co-immunoprecipitate with dynein (Busson et al., 1998; Karki and Holzbaur, 1995; Vaughan and Vallee, 1995), and they appear to regulate dynein's binding to cargoes (Kamal and Goldstein, 2002) as well as dynein's motor activity (Farshori and Holzbaur, 1997; Gill et al., 1991; King and Schroer, 2000). Different dynactin subunits appear to regulate dynein's binding to different cargoes: Arp1 to the Golgi (Holleran et al., 1996), p150-Glued to microtubules (Farkasovsky and Kuntzel, 2001; Kumar et al., 2000) and p50 to Golgi, microtubules (Echeverri et al., 1996) and the kinetochores (Starr et al., 1998). The capping proteins play a role in vesicle transport, although only p62 and Arp11 are involved in nuclear positioning (Lee et al., 2001a). These differential binding properties of different dynactin subunits might mediate the specificity of dynein for different cargoes.

No components of the dynactin complex have been extensively characterised in *S. pombe* and only one component has been cloned so far, Ssm4p, a p150-Glued. P150-Glued was first identified as a factor involved in *Drosophila* eye development (Meyerowitz and Kankel, 1978; Swaroop et al., 1987), and later shown to be associated with dynein (Holzbaur et al., 1991). It links dynein to dynactin by directly binding dynein

intermediate chain (Vaughan and Vallee, 1995). It also interacts with microtubules (Waterman-Storer et al., 1995) and it is thought to facilitate dynein's interaction with microtubules (King and Schroer, 2000). Ssm4p was identified as a multicopy suppressor of a *sme2Δ* mutant. *Sme2* encodes a RNA molecule which binds Mei2p to promote the first meiotic division (Watanabe and Yamamoto, 1994). Ssm4p is only expressed during mating, it localises to microtubules and spindles when overexpressed and mating between *ssm4Δ* cells generates asci carrying less than four spores. This suggests that Ssm4p is required for accurate nuclear segregation during meiosis (Yamashita et al., 1997). These defects are consistent with a role for this protein in dynein-mediated functions, but nothing is known about its relationship to dynein or its role in regulating microtubular dynamics.

Whereas during vegetative growth microtubules are responsible for maintaining the nucleus fixed in a particular position, microtubular dynamics during shmooing growth and mating are responsible for actively altering nuclear localisation. This is achieved through a completely altered microtubular array, suggesting that microtubular dynamics are regulated differently during externally determined shmooing growth relative to the internally regulated vegetative growth.

1.2 Objectives of this work

The main objective of this work is to further understand how intrinsic and extrinsic cell polarity are regulated. In particular:

1. To understand the role of cell end markers in identifying cell ends as sites for growth and for microtubule termination.
2. To understand how the switch between vegetative growth, directed by an intrinsic mechanism, and shmooing growth, directed by extrinsic pheromones, takes place.
3. To analyse how the switch to shmooing microtubular dynamics takes place and how the shmooing microtubular dynamics leads to oscillatory nuclear movement.

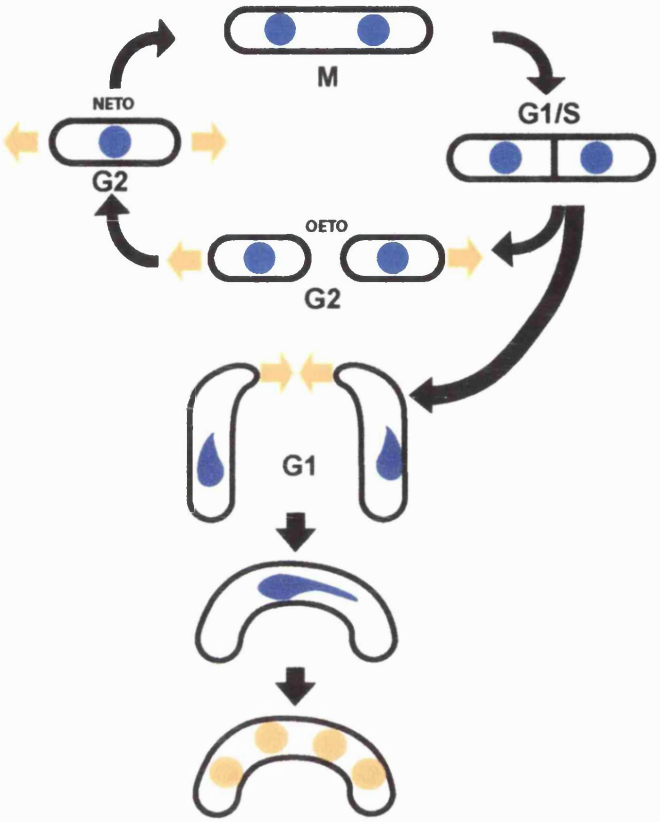

Figure 1.1 Fission yeast growth patterns.
During vegetative growth fission yeast is a cylindrical rod shaped cell, extending mostly in a bipolar fashion from its ends. When the cell reaches a critical cell size, it undergoes mitosis followed by cytokinesis, generating two equal sized daughter cells, each with a new end at the site of cell division and an old end inherited from the mother cell. After division the newly formed daughter cell resumes growth from the Old End in what is know as Old End Take Off (OETO), at a specified point in time the cell undergoes NETO, New End Take Off, when growth is activated at the second end.
When cells are starved in the presence of a mating partner they arrest in the G1 phase of the cell cycle and initiate to shmooing growth. During shmooing growth, cells are capable of detecting the directionality of the pheromone secreted by their mating partner, and they orient their mating projection towards the pheromone source. Cells then touch and undergo cellular and nuclear fusion, which is followed by meiosis and the formation of four haploid spores

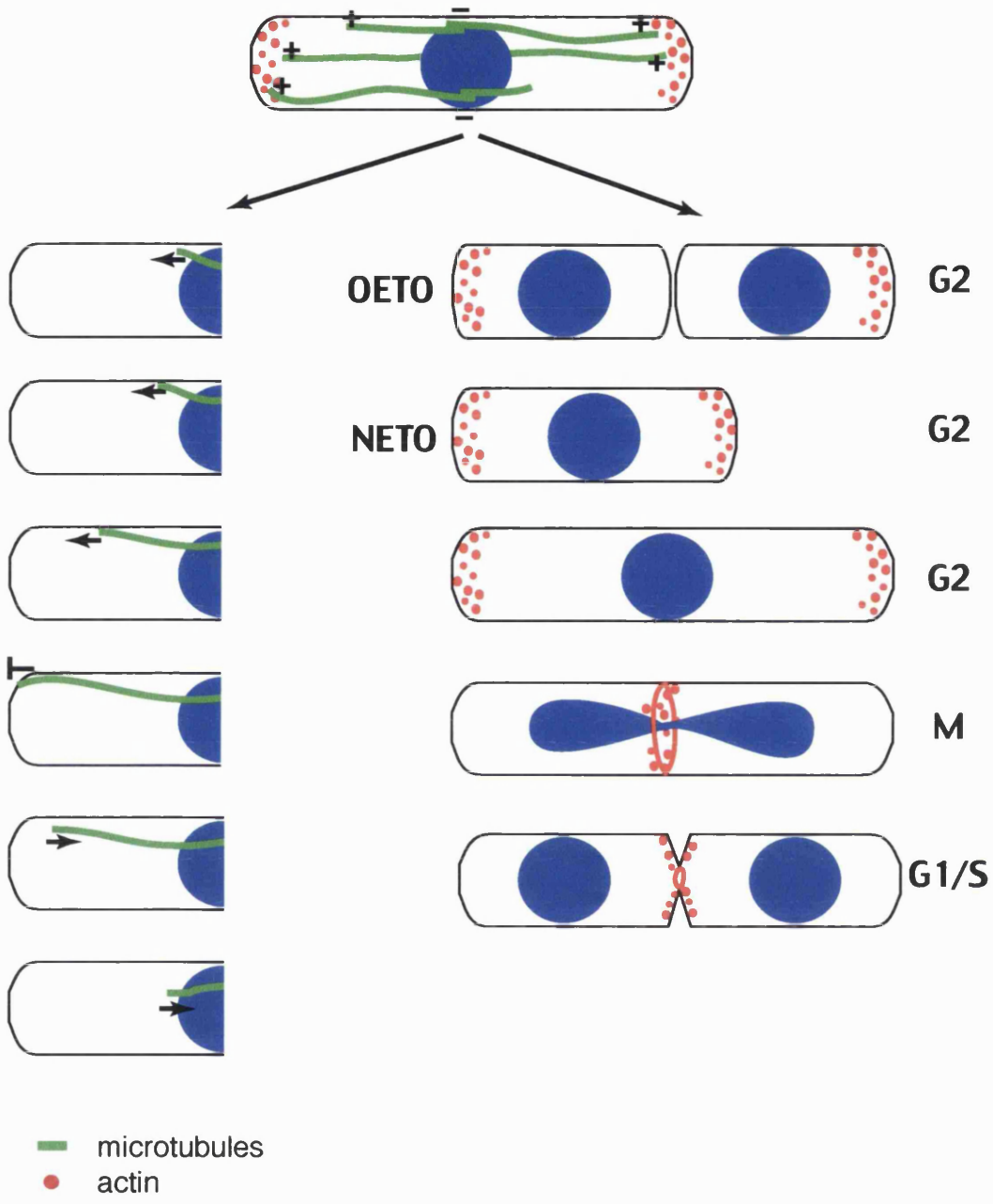

Figure 1.2 Microtubule and actin organisation.
Interphase microtubules are arranged as 3-5 antiparallel bundles with overlapping minus ends located at the cell centre, at sites adjacent to the nuclear membrane. Microtubules nucleate from the cell centre, growing along the length of the cell and stalling at the cell ends, and then undergo catastrophe back to the cell centre.
Patches are found at actively growing ends during interphase and relocate to the cell middle during cell division.

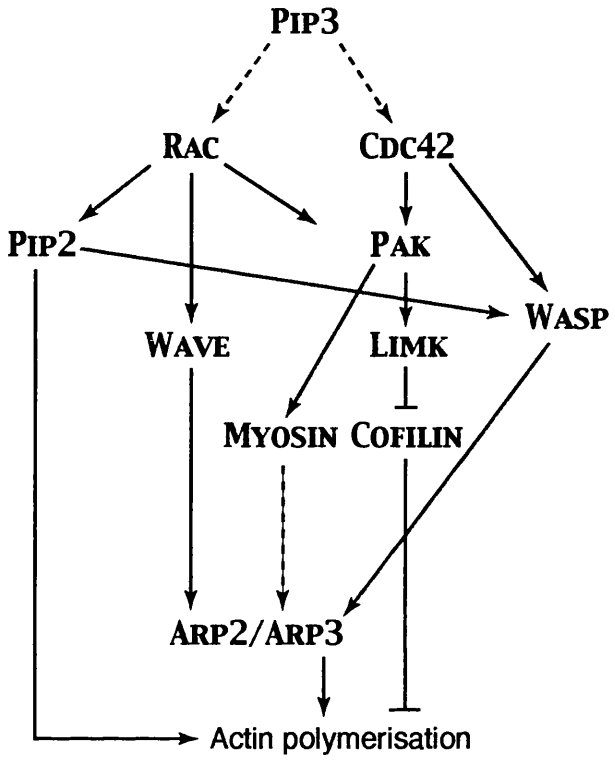

Figure 1.3 Model for actin polymerisation.
CDC42 via WASP, and RAC via WAVE, can stimulate the ARP2/ARP3 complex to activate actin polymerisation. RAC and CDC42 can also stimulate PAK, which inhibits cofilin via LIM kinase and activates myosin to induce ARP2/ARP3. RAC also stimulates PIP2 production. PIP2 then can activate WASP and can induce actin filament uncapping thus generating extra sites for actin polymerisation. PIP3 also stimulates actin polymerisation, possibly by activating RAC and CDC42 at the beginning of the cascade.

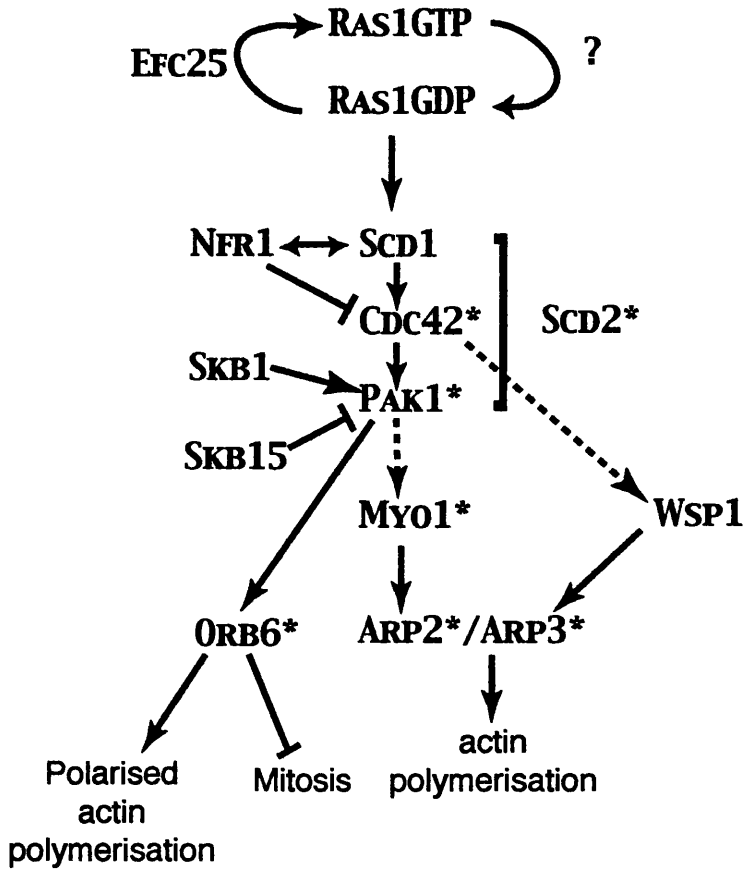

Figure 1.4 Vegetative actin polymerisation cascade.
During vegetative growth Efc25p acts as the Ras1p GEF, activating Ras1p. Ras1p then feeds into the Cdc42p/Pak1p pathway. Cdc42p is activated by the GEF Scd1p and Nfr1p, a transmembrane protein localising to vacuoles, is a negative regulator of Cdc42p. Active Cdc42p binds to Pak1p releasing its autoinhibition and activates actin polymerisation, possibly via Wsp1p. Active Pak1p stimulates Arp2/3 dependent actin polymerisation via Myo1p. Skb1p is another positive regulator and Skb15 is a negative regulator of Pak1p. Scd2, an SH3 containing protein, acts as a scaffold facilitating the interaction between Scd1p/Cdc42p/Pak1p. Pak1p also activates Orb6p, a Caseine Kinase II, involved in actin polymerisation and mitosis. All proteins marked "*" are known to localise to cell ends.

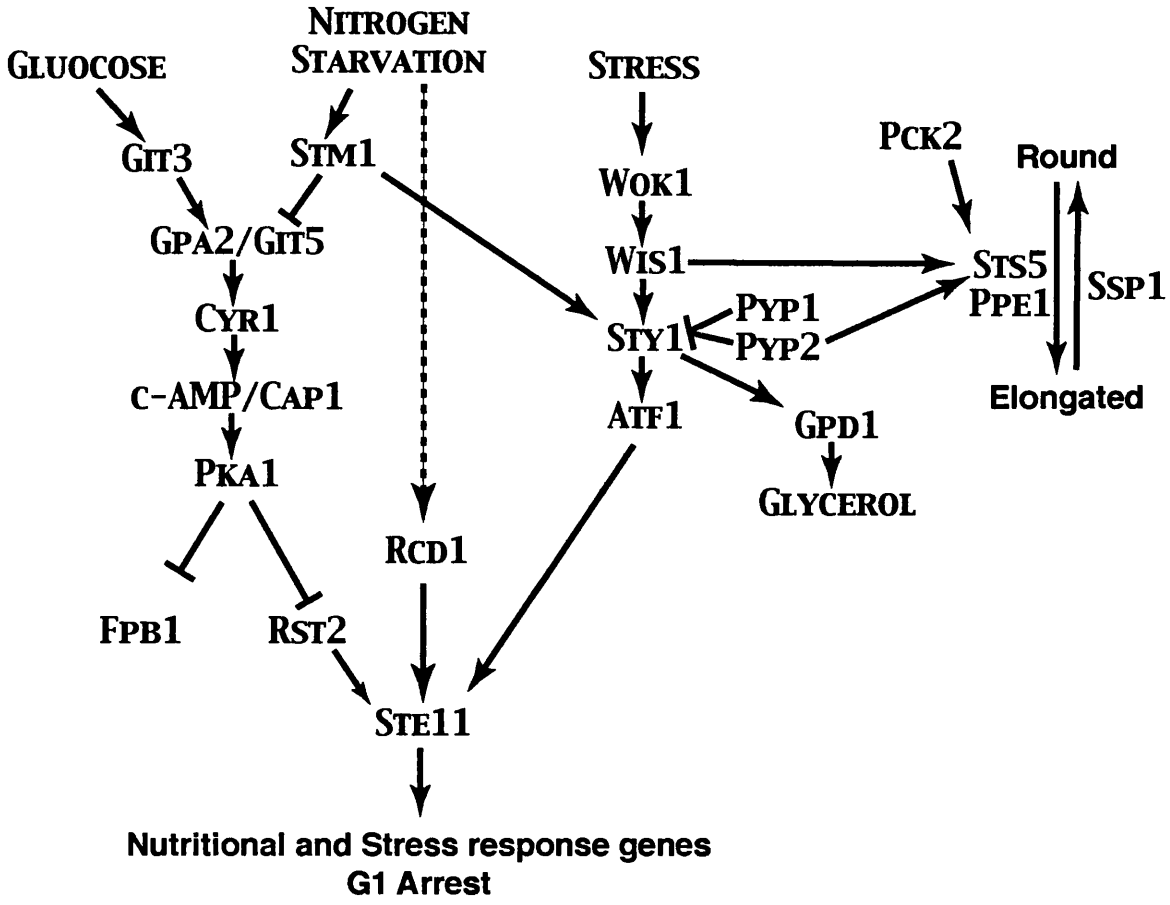

Figure 1.5. Nutrient and Osmotic Pathway.
In response to osmotic stress the MAPK cascade Wok1p/Wis1p/Sty1p is activated. This results in the activation of the transcription factor Atf1p, which induces Ste11p and production of glycerol via the glycerol-3-phosphate-dehydrogenase Gpd1p. Glycerol then provides osmotic protection to the cell. The MAPK Sty1p is inhibited by the phosphatases Pyp1p and Pyp2p. These proteins, with Pck2p and Wis1p, also regulate actin localisation via the phosphatases Sts5p and Ppe1p, and the kinase Ssp1p. Nitrogen starvation can also activate the MAPK Sty1p, via the seven transmembrane receptor Stm1p, and Ste11p via Rcd1p. Glucose availability is sensed via the Git3p transembrane receptor, which then activates a small trimeric G-protein complex comprising Gpa2p/Git5p. Gpa2p, the Galpha subunit, activates Cyr1p to induce cyclic AMP production. c-AMP associates with Cap1p (c-AMP associates protein) to activate Pka1p (Protein Kinase A). Pka1p then inhibits Fpb1p, which produces fructose and Rst2p, a transcription factor for Ste11p. Nitrogen starvaton inhibits Cyr1p, leading to the production of fructose and stimulation of Ste11p.

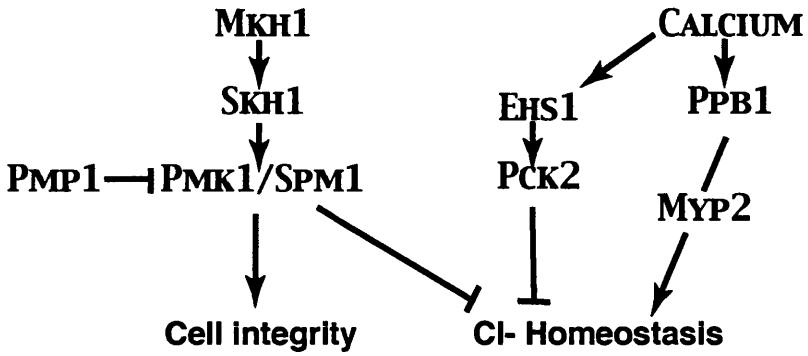

Figure 1.6 Cell integrity and Chloride homeostasis pathways.
Cell wall integrity is regulated by a MAPK cascade, comprising Mhk1pSkh1p/Pmk1p, which is inhibited by Pmp1p. This pathway also regulates Chloride ion homeostasis, together with the Calcium response pathway.
Increased Calcium levels activate Ehs1p, an integral membrane protein, which activates Pck2p to regulate cell wall composition and Chloride ion homeostasis. Increased Calcium also induces Ppb1p, which regulates Chloride ion homeostasis,

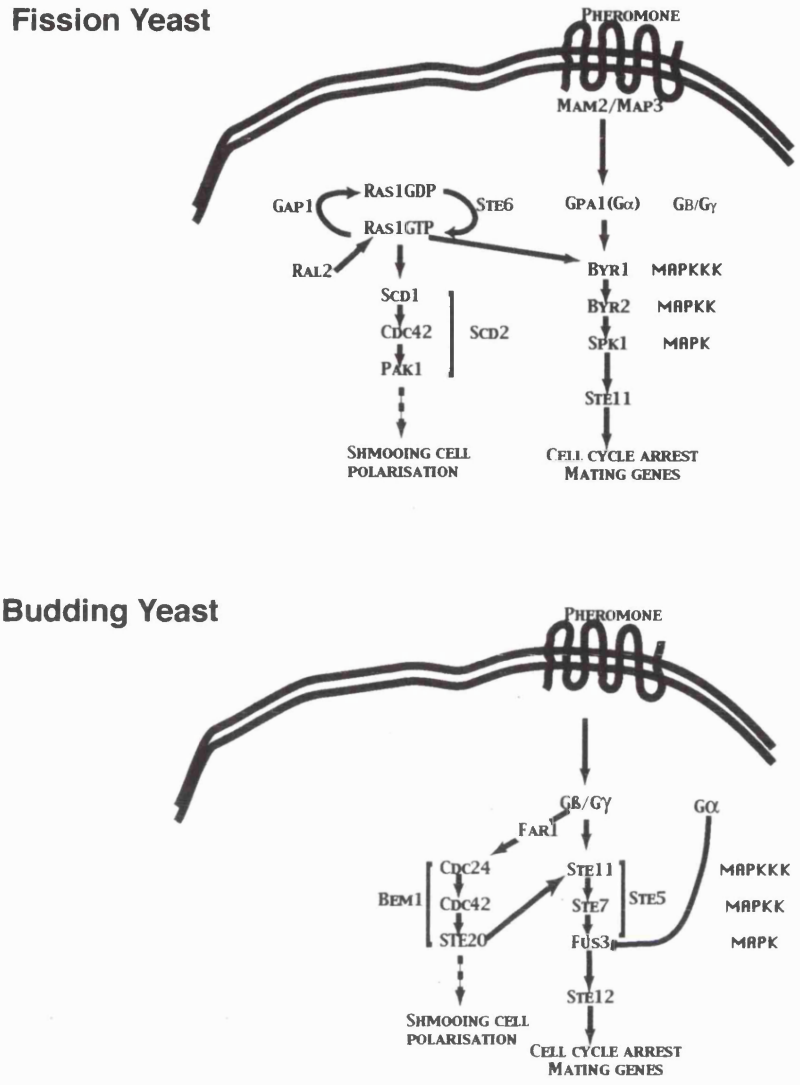

Fig 1.7 Pheromone response cascade.
In both cases a seven transmembrane-domains G-protein coupled receptor binds specifically to the opposite mating type pheromone and transmits the signal to the interior of the cell. G-alpha-beta-gamma dissociate to activate the downstream MAPK cascade, which leads to cell cycle arrest and to the expression of mating-specific genes. In fission yeast Ras1p then interacts with the polarisation machinery to generate a shmooing polarised projection. In budding yeast Far1 interacts with G-beta to bring Cdc24 to the shmooing site and activate the polarisation machinery.

Chapter 2

Role of Tea1p, Tea3p and Pom1p in the determination of cell ends during vegetative growth

2.1 Introduction

Fission yeast cells extend from their two ends to generate a rod-shaped cell with microtubules spanning the length of the cell and terminating at the cell end (See previous chapter for details). In order to maintain its cylindrical shape, cells have to elongate along a single axis and to achieve this growth zones have to be positioned at the two ends, exactly opposed to each other. Since microtubules play a role in positioning growth zones (Sawin and Nurse, 1998), it is important that they terminate at cell ends. The ends of the cell therefore act both as sites for growth and for microtubule termination. A critical issue for understanding the maintenance of fission yeast cell polarity is how the cell identifies its ends, such that growth is activated and microtubule stalling and depolymerisation are triggered at that location. Genetic analyses have identified several proteins involved in this process, including Tea1p, Pom1p and Tea3p. These proteins are located at cell ends (Fig 2.1), and appear to be involved in cell end identification and New End Take Off (NETO), when growth is activated at the second end. Tea1p and Pom1p are essential for maintenance of fission yeast's cylindrical cell shape: *tea1Δ* and *pom1Δ* cells are monopolar, bent and branched at low frequency, and in some cells microtubules curve round the cell ends (Bahler and Nurse, 2001; Bahler and Pringle, 1998; Mata and Nurse, 1997). *Tea3Δ* cells are also monopolar but do not bend or branch (Arellano et al., 2002). All three proteins localise to cell ends and so may be important for the cell to identify these locations for growth and for regulating microtubule termination.

In this chapter I describe the analysis of the roles of Tea1p, Tea3p and Pom1p in the determination of cell ends as sites for growth and for microtubular termination. I will

also briefly address the relationship between the actin and microtubule cytoskeletons. The second figure of this chapter describes work done by Manolo Arellano, a post-doctoral fellow in the lab, but all the rest of the work described in this chapter is my own.

2.2 Results

2.2.1 Cell growth patterns

Most wild type cells, start to grow from the end inherited from the mother cell after division (Old End) (Fig 2.2). To assess the contribution of Tea3p, Tea1p and Pom1p to the identification of cell ends for growth, Manolo Arellano investigated the ability of deletion mutants of each gene to re-identify their old ends after cell division and activate them as sites for growth. Manolo Arellano carried out time lapse photomicrography on wild type, *tea1Δ, tea3Δ* and *pom1Δ* mutant cells as well as the double deletions of these mutants. The triple deletion grew too poorly to work with. Single mutants and combination of double mutants were placed on agar pads and filmed, and the growth patterns were scored. As expected, nearly all the wild type cells were bipolar in their growth pattern and efficiently resumed growth from their old ends after cell division (Fig 2.2). In contrast *tea1Δ, tea3Δ* and *pom1Δ* cells were all mostly monopolar in their growth (Arellano et al., 2002; Bahler and Pringle, 1998; Mata and Nurse, 1997). The growth pattern of pairs of daughter cells after cytokinesis was monitored. Two types of behaviour were observed: pairs which re-initiated growth from a previously growing end (YES, Figure 2A) and pairs which failed to do so (NO, Fig 2.2A). *Tea3Δ* cells resumed growth from their old end after division, indicating that the cell inheriting a growing end had no

difficulty in re-identifying it as the appropriate site for growth after division (Figure 2A). In contrast, 14% of *tea1Δ* cells and 30% of *pom1Δ* cells failed to resume growth from a previously growing end (Fig 2.2A). The double mutants were significantly worse in re-directing cell growth to the old growing end after cell division. The *pom1Δ tea1Δ* and *pom1Δ tea3Δ* double mutants displayed the strongest phenotypes with around 60% of the cells being unable to select the old end as the site for growth (Fig 2.2A).

Further analysis revealed four possible growth patterns of the two daughter cells after cytokinesis, described in Figure 2B. Mutants unable to efficiently re-initiate growth at their previously growing end did not display a random growth pattern, but generally re-initiated growth from the new end generated at cytokinesis (see third column Fig 2.2B). This also applied to cells inheriting an end that had never grown, which initiated growth from the septation site (see second and third column Fig 2.2 B).

2.2.2 Tea1p, Tea3p and Pom1p play different roles as cell end identifiers for growth

The inability of *tea1Δ, pom1Δ* and the double mutants *tea1Δ pom1Δ* and *pom1Δ tea3Δ* to efficiently resume growth at the old end suggested that these mutants were either unable to re-localise the growth machinery away from the septation site to the old end or that they could not recognise the old end as a site for new growth because it was not properly marked. To distinguish between these two possibilities I investigated the ability of a wild type strain to relocalise actin after treatment with the drug LatrunculinA (LatA), an inhibitor of actin polymerisation. A LatA pulse raises the pool of free actin monomers, which triggers actin relocalisation to both ends in all cells, including those which have

not undergone NETO (Rupes et al., 1999). Cells blocked in the cell cycle before NETO with a monopolar growth pattern can switch to a bipolar growth pattern after a LatA pulse (Rupes et al., 1999). If an end is marked, actin should be able to relocalise back to that marked position. On the other hand, if a cell cannot identify its ends, actin will not be able to efficiently relocalise back to the ends and will become delocalised.

Figure 3 shows that *tea3Δ* cells are usually monopolar for actin during vegetative growth but, like wild type, frequently switched to being bipolar after a LatA pulse. This suggests that *tea3Δ* cells are able to identify their ends and that their monopolar growth pattern is probably due to a defect in triggering NETO. In contrast *tea1Δ* cells were less efficient at becoming bipolar and more cells exhibited delocalised actin. *Pom1Δ* cells did not become more bipolar for actin after LatA treatment but there was a 20% increase in cells exhibiting delocalised actin, suggesting that *pom1Δ* cells often failed to relocalise actin to any end. The double mutants became progressively worse in relocalising actin to their ends after a LatA pulse; *pom1Δ tea1Δ* exhibited the most extreme phenotypes with over 60% of cells displaying delocalised actin 1 hour after recovery (Fig 2.3). This suggests that more than 60% of these cells were unable to identify their ends. The result of the *tea1Δ* LatA pulse differs from that of Rupes et al., 1999. They found that *tea1Δ* cells could not switch at all to bipolar actin, whilst I found an increase from 27% to 48% in bipolar actin. The reason for this is unclear but may be due to differences in scoring or temperature between the experiments.

2.2.3 Tea1p plays a major role in the regulation of microtubular dynamics

I next examined the role that these cell end markers play in the specification of cell ends as sites for microtubule termination. To do so I examined the microtubular phenotype of *pom1Δ, tea1Δ, tea3Δ* and the double mutants at 25°C and 37°C. I concentrated on more extreme phenotypes and only scored microtubules that were clearly curling along the cell periphery back into the body of the cell. I did not score microtubules which just crossed the midline of the cell. Figure 4 shows that *tea1Δ* cells at high temperatures displayed microtubules bending round the cell ends, in accordance with previously published results (Mata and Nurse, 1997). In contrast *pom1Δ* and *tea3Δ* cells have almost wild type looking microtubules. *Tea3Δ pom1Δ* cells displayed only a minor microtubular defect, whilst cells with a *tea1Δ* in combination with either *tea3Δ* or *pom1Δ* had a clear defect in microtubules with, respectively, 24% and 37% of cells showing microtubules bending round the cell ends. To confirm that the high number of microtubules bending round the cell ends in *pom1Δ tea1Δ* cells was not solely due to the reduced cell length of the double mutant, I grew the cells in low HU concentration (2 mM), a drug which induces a cell cycle delay and therefore increases cell length, and then shifted the culture to 37°C. 35% of microtubules were curling round the ends in the HU treated cells compared to 34.5% of the untreated control. This indicates that the higher number of curling microtubules seen in *pom1Δ tea1Δ* cells is not because the cells are shorter than wild type.

To determine what causes the microtubules to bend round the cell end I monitored live microtubular dynamics in the *tea1Δ pom1Δ* strain, which exhibits the most extreme phenotype, and compared it to a wild type control (Fig 2.5). I visualised microtubules with a GFP tagged tubulin integrated into the genome (a gift from Dao-Chiao Ding (Ding et al., 1998), see Chapter 7, materials and methods for details). Cells were grown at 25°C, shifted up to 37°C from 45 minutes to 2 hours and then monitored using a confocal microscope. Microtubular dynamics did not appear to change significantly during this period. I characterised the microtubular dynamics and behaviour at the cell end for wild type and *pom1Δtea1Δ* strains. Figure 2.6 shows that there was no significant difference in the dwelling time, the number of microtubules crossing the mid-cell line at the cell end or the number of microtubules touching at the cell end. However there was a slight increase in the number of microtubules crossing over each other at the cell end in a *pom1Δ tea1Δ* strain (Fig 2.6B). Moreover, when microtubules crossed at the cell end in a *pom1Δtea1Δ* background they could bend over each other and bundle to generate an apparently continuous microtubule bundle which bent round the cell end (Fig 2.5 B). Although some microtubules did cross over at the cell end in the wild type strain this bundling was never observed (Fig 2.5 A). These microtubule bundles were very stable and in some cases could persist for the whole filming period.

The dwelling times in Figure 6A were scored only for individual microtubules that had clearly distinguishable ends. It is impossible to see individual microtubules in the bundles at the cell end and so they were not scored. Since these bundled microtubules,

which were very stable, were not scored, the dwelling times for the mutant could be longer than shown in Figure 2.6A.

2.2.4 Role of the microtubular cytoskeleton in actin relocalisation

The microtubular cytoskeleton has been implicated in determining the position of the growth zone but I did not find a strong direct correlation between microtubular and actin relocalisation defects. I therefore decided to determine the role of the microtubular cytoskeleton in actin relocalisation by investigating the ability of a wild type strain to relocalise actin after a Latrunculin A pulse in the presence of Carbendazim (MBC, a microtubule depolymerising drug, see Chapter 7, Materials and methods for details). Figure 7A shows that even in the absence of microtubules actin can relocalise to the cell ends within 50 minutes. I then monitored more carefully how this relocalisation occurred by taking time-points every 10 minutes after the LatA pulse. In both the treated and the control cells, immediately after the LatA wash-out, actin repolymerised at the cell ends, after that actin lost this cell end localisation, and then slowly relocalised to the cell ends over a 30 minute period. The pattern of relocalisation is different in the cells treated with MBC than in those treated with a DMSO control (Fig 2.7A). Overall, in the MBC treated sample, actin appeared to either delocalise rather slower or to a lesser extent but it generally could still relocalise to the cell ends.

Cells that are more defective in identifying their ends may be more reliant on the microtubule cytoskeleton to find their ends. To test this I monitored the ability of a *pom1Δ tea3Δ* strain to relocalise actin after a Latrunculin A pulse, in the presence of

MBC or DMSO, as a control. Actin appeared to relocalise less efficiently in the presence of MBC, although the ability of the control cells to relocalise actin depended on how long the cells had been on plates. The longer the cells had been stored on plates before starting the liquid culture, the higher the initial percentage of delocalised actin. In "older" cells actin relocalisation after a LatA pulse was also more defective and the difference between the MBC treated cells and the control became less dramatic (Fig 2.7B).

2.2.5 Contribution of the actin and the microtubule cytoskeletons to the determination of cell shape

Tea1Δ cells, which have a microtubule defect and *pom1Δ* cells, which have a growth and actin relocalisation defect, are known to branch upon shift to higher temperatures. I analysed whether the double mutants, which have more severe growth and actin relocalisation defects or microtubule defects, would result in greater numbers of T-shaped cells. Figure 2.8 show that *pom1Δ,* in combination with either *tea1Δ* or *tea3Δ* mutants, resulted in more T-shaped cells. *Pom1Δ tea1Δ*, which has the most severe cell end growth defect and microtubule defect, also has the highest number of T-shaped cells.

2.3 Discussion

Tea3p, which is required for NETO, is not a major cell end identifier for growth. In *tea3Δ* cells, after depolymerisation, actin switched from being monopolar to bipolar. However, the double mutant analysis suggests that Tea3p can play a minor role as an end identifier since *tea3Δ* cells in combination with either *tea1Δ* or *pom1Δ* produced more

cells which failed to become bipolar than any of the single deletions alone. Pom1p, on the other hand, is a major cell end identifier for cell growth. In its absence cells do not efficiently resume growth from their old end after septation, and actin fails to efficiently re-localise to cell ends after LatA treatment. The strongest phenotypes were produced by *pom1Δ* in combination with either of the other mutants, confirming Pom1p's role as a major cell end identifier. *Tea1Δ* cells had an intermediate phenotype between *tea3Δ* and *pom1Δ* with regard to the growth pattern and actin relocalisation. Neither Tea3p nor Pom1p are located at cell ends in *tea1Δ* cells (Arellano et al., 2002; Bahler and Pringle, 1998). This failure to localise correctly could result in those proteins not functioning efficiently, explaining the partial phenotype observed in *tea1Δ* cells. Alternatively, Tea1p could act both as a trigger of NETO and as a cell end identifier for growth.

Cells, which did not inherit a previously growing end, showed a marked preference for re-initiating growth at the new end, as did mutants exhibiting the most defective growth patterns. These observations suggest that cells which are unable to efficiently identify their old ends preferentially activate growth at the last place where actin was located; that is the site of septation which forms the new ends of the daughter cells after division. For all the mutants examined, the number of cells unable to resume growth from a previously growing end after cytokinesis was similar to the number of cells unable to relocate actin to the ends after a LatA pulse. This suggests that the mechanisms re-identifying ends after cytokinesis and maintaining cell end identity during interphase may be similar.

Cell ends are also sites for microtubular termination and Tea1p plays a role in regulating microtubules at the cell ends. In its absence, microtubules curve round the cell ends, confirming previous reports (Mata and Nurse, 1997). Cells of the double mutants *tea1Δ pom1Δ* and *tea1Δ tea3Δ* had more microtubules curving around the cell ends than *tea1Δ* cells, indicating that Tea3p and Pom1p also play some role in the regulation of microtubular organisation and that this only becomes apparent in the absence of Tea1p. Analysis of live microtubules showed that the microtubules curving back round the cell end in fixed cells are due at least in part to two microtubules growing from opposite sides of the cell which cross and bundle at the cell end. Although this does not occur at a high frequency, once formed these bundles are very stable. This stability could account for the higher number of microtubules seen to bend round the cell end in fixed cells.

Microtubules are not essential for the relocalisation of actin, which can occur in the absence of microtubules in wild type cells but appear to play some role in the relocalisation of actin when cell end identity for growth is defective, as in *pom1Δtea3Δ* cells. Although I could not find a strong influence of the actin cytoskeleton on the microtubules or vice-versa, the two cytoskeletons appear to collaborate to maintain the overall shape of the fission yeast cell. *Pom1Δ tea1Δ* cells, which have both a severe cell end memory and a microtubule defect, are also more frequently branched.

This chapter shows that in fission yeast Tea1p, Tea3p and Pom1p play a dual role: they identify cell ends as sites for growth thus localising actin, and they specify ends as sites for microtubular termination. Tea1p, Tea3p and Pom1p all contribute to both roles,

with Pom1p having the major role in identifying cell ends as sites for growth and Tea1p the major role in regulating microtubular dynamics.

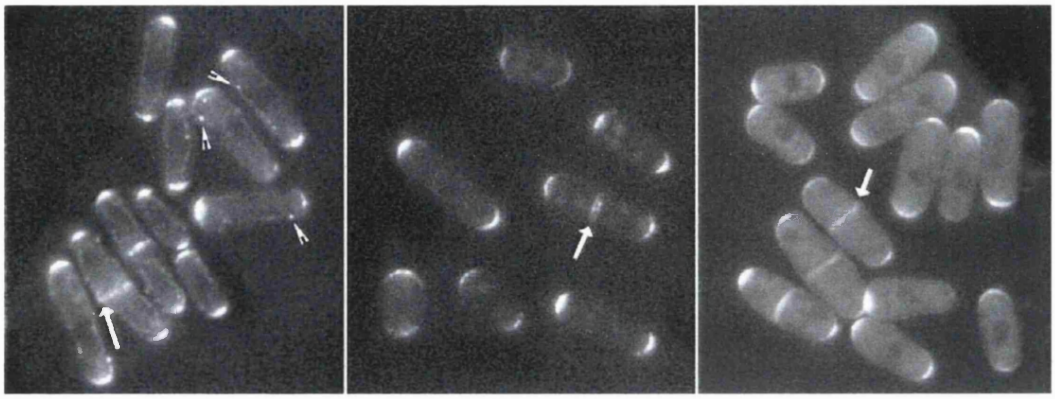

Tea1GFP Tea3GFP Pom1GFP

Figure 2.1. Tea1p, Tea3p and Pom1p localise to the cell ends.
Exponentially growing *tea1GFP*, *tea3GFP* and *pom1GFP* strains were photographed with a fluorescent microscope. All three proteins localise to the septum (arrows) as well as cell ends. Tea1GFP localises to the tips of microtubules (arrowhead).

A

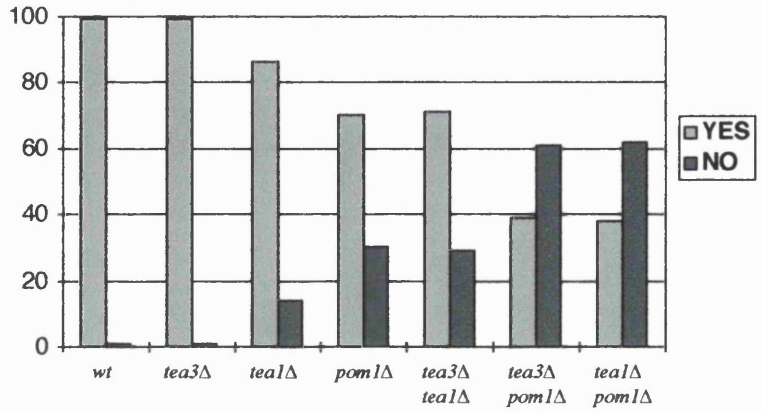

B

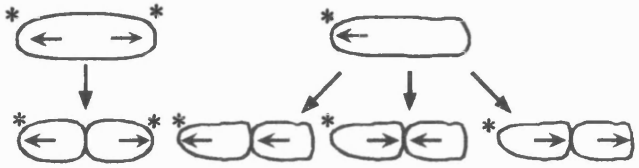

wt	96%	3%	1%	0%
tea3Δ	20%	79%	1%	0%
tea1Δ	8%	78%	14%	0%
pom1Δ	10%	60%	30%	0%
tea3Δtea1Δ	12%	59%	29%	0%
tea3Δpom1Δ	17%	22%	47%	14%
tea1Δpom1Δ	10%	28%	59%	3%
tea1Δtea3Δpom1Δ	6%	20%	66%	8%

Figure 2.2. Growth patterns.
(A) Cells were placed on an agar pad and filmed for 16 hours with a light microscope. The growth patterns of pairs of daughter cells after cell division were monitored and grouped into two categories: pairs of cells that could activate growth at a previously growing end (YES) and cells which could not (NO). Since most of the mutant cells were monopolar at cell division only one of the daughter cells inherited a growing end. We therefore scored as YES pairs in which the daughter inheriting the previously growing end chose it as a site for growth, the other cell could have resumed growth from either end. (B) Analysis of the 4 possible growth patterns observed in A. The cell end marked with an asterisk (*) had been growing in the previous cell cycle. In the case of the wild type control, both ends had been growing. The first two columns were grouped under YES in figure A and the last two columns were NO in figure B. All scores are expressed as percentages of total cells scored.

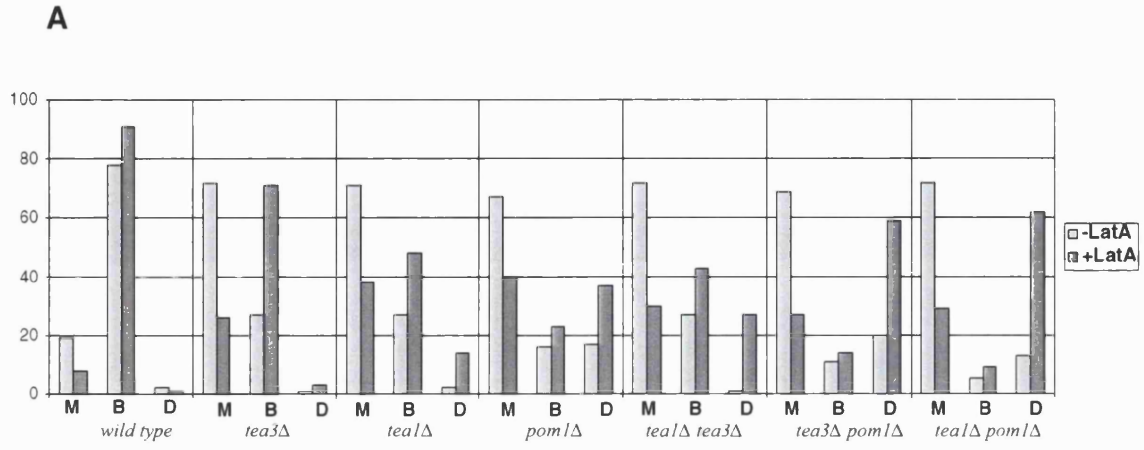

Figure 2.3. Actin scores.
Cells were grown in YE5S at 25˚C, 25 ml of culture were spun, resuspended in 1 ml YE5S, pulsed with LatA for 8 minutes, then washed once and allowed to recover for 1 hour in 25ml of pre-conditioned media. Cells were fixed in formaldehyde before and after the LatA pulse, stained with rhodamine phalloidin and scored for monopolar (M), bipolar (B) or delocalised (D) actin

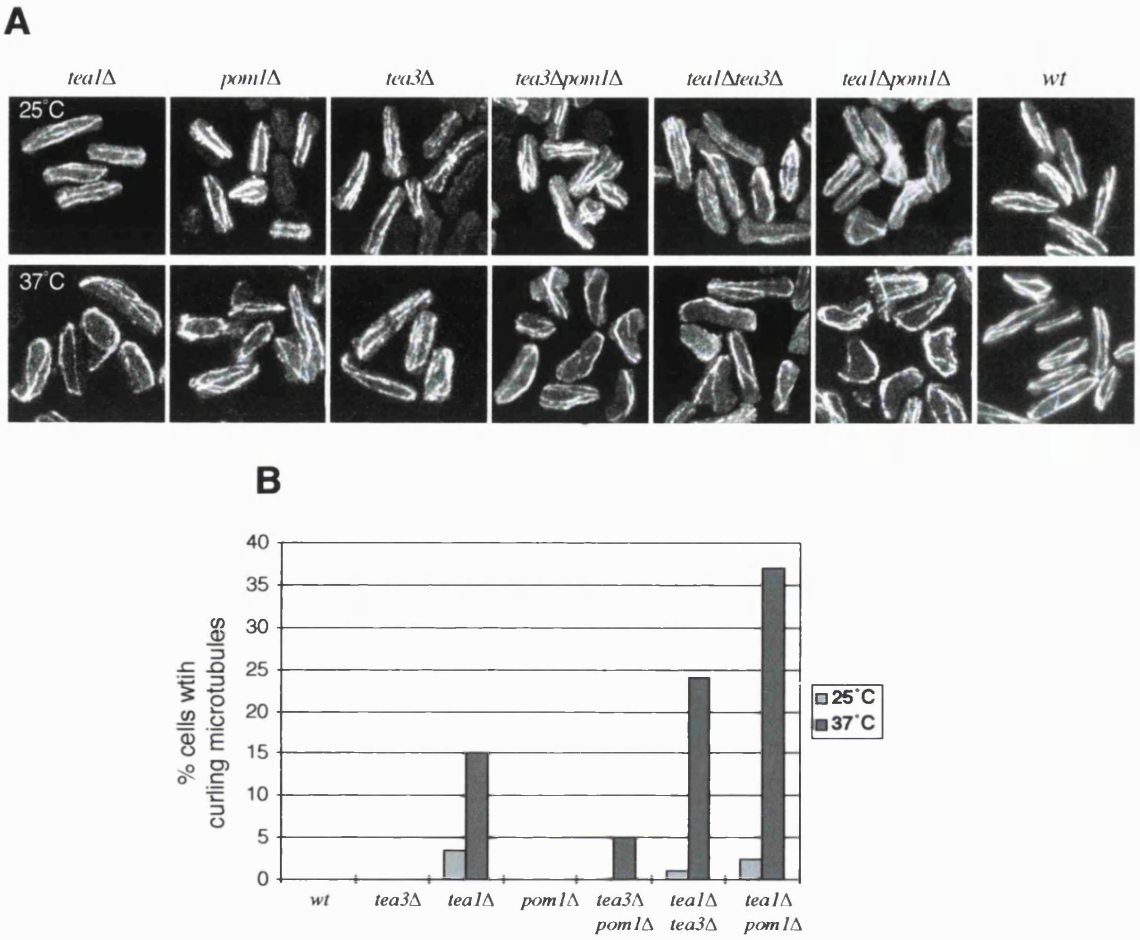

Figure 2.4. Microtubules bending round the ends.
Cells were grown at 25°C and shifted at 37°C for 2 hours. (A) Cells were then fixed and stained for microtubules and (B) the number of cells with microtubules bending round the ends was scored and expressed as a percentage of total cells scored. At least 100 cells were scored in three independent experiments. Bahler and Nurse, 2001, reported that *pom1Δ* cells display microtubules bending round the ends; the difference is probably due to our only scoring microtubules which curl back completely into the body of the cell.

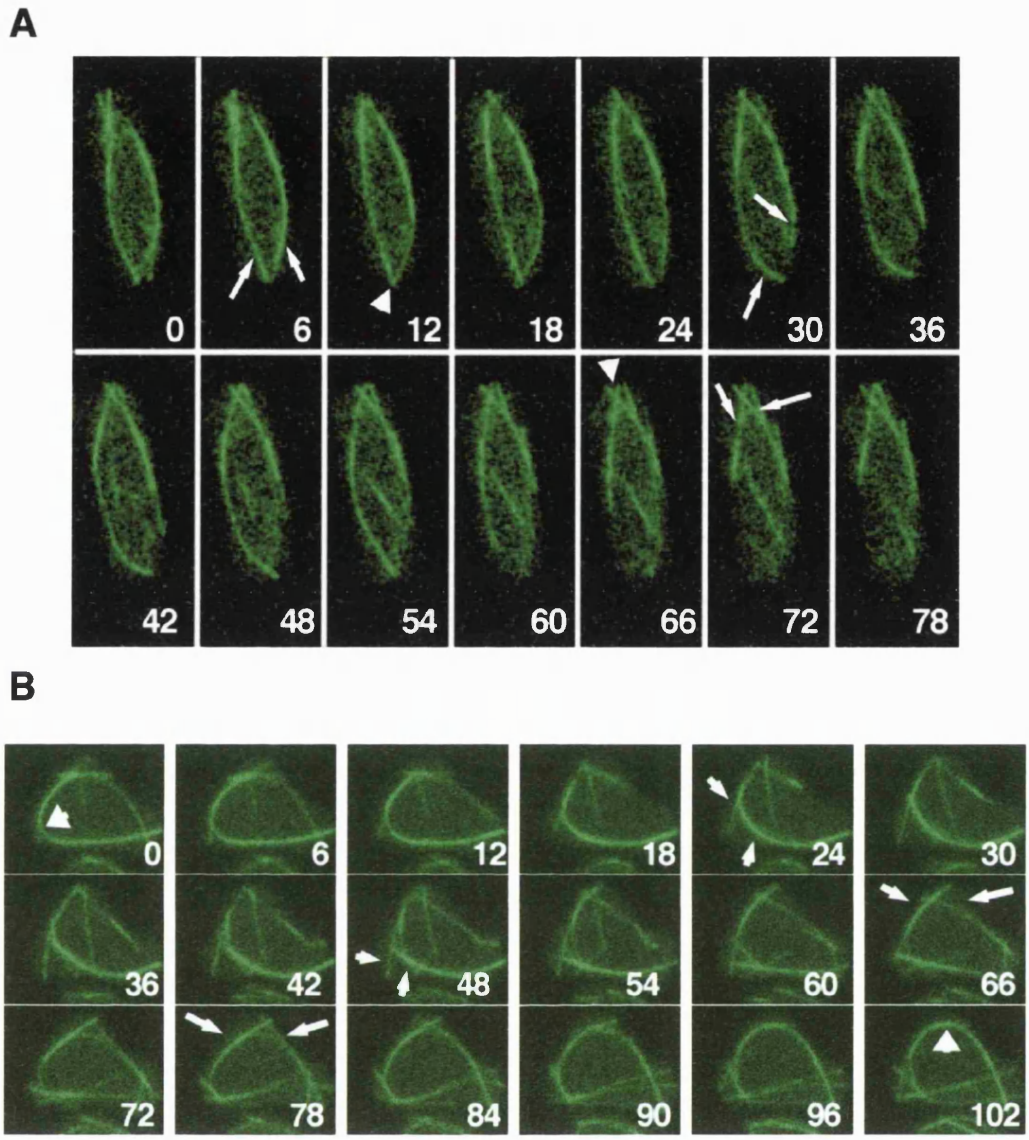

Figure 2.5. Live wild type and *pom1Δtea1Δ* microtubules at high temperatures.
(A)Wild type *nmt1atb2GFP* and (B) *Pom1Δtea1Δ nmt1atb2GFP* cells were grown in low thiamine at 25°C and then shifted to 37°C for 45 minutes. Live microtubules were filmed on a confocal microscope, taking frames every 6 seconds. The images shown are a projection of sections through the cell. Small arrows indicate individual microtubules and arrowheads show microtubules at the ends of the cell, crossing over in the wild type and bundling in the mutant.

A

	wild type	*pom1Δtea1Δ*	T-TEST
Dwelling time (sec)	150+/-90 (40)	118+/-83 (71)	0.06

B

MT crossing the midline MT meeting at cell ends MT crossing at cell ends

	wild type	*pom1Δtea1Δ*	chi-squared	P
MT crossing midline	42% (124)	39% (99)	0.37	0.47<P<0.61
MT meeting at cell ends	19% (119)	20% (101)	0.06	0.61<P<0.95
MT crossing at cell end	18% (119)	28% (101)	6.8	0.005<P<0.009

Figure 2.6. Characterisation of microtubular behaviour at the cell ends.

(A) Dwelling times at the cell ends were scored for live wild type and *pom1Δtea1Δ* microtubules shifted to 37˚C for up to 2 hours, numbers in bracket indicate the total number of microtubules scored. A T-TEST was performed between the two populations. (B) Microtubular behaviour at the cell ends was scored and a chi-squared test was performed, numbers in bracket indicate the total number of microtubules scored. The probability of the two populations being statistically the same is indicated under P.

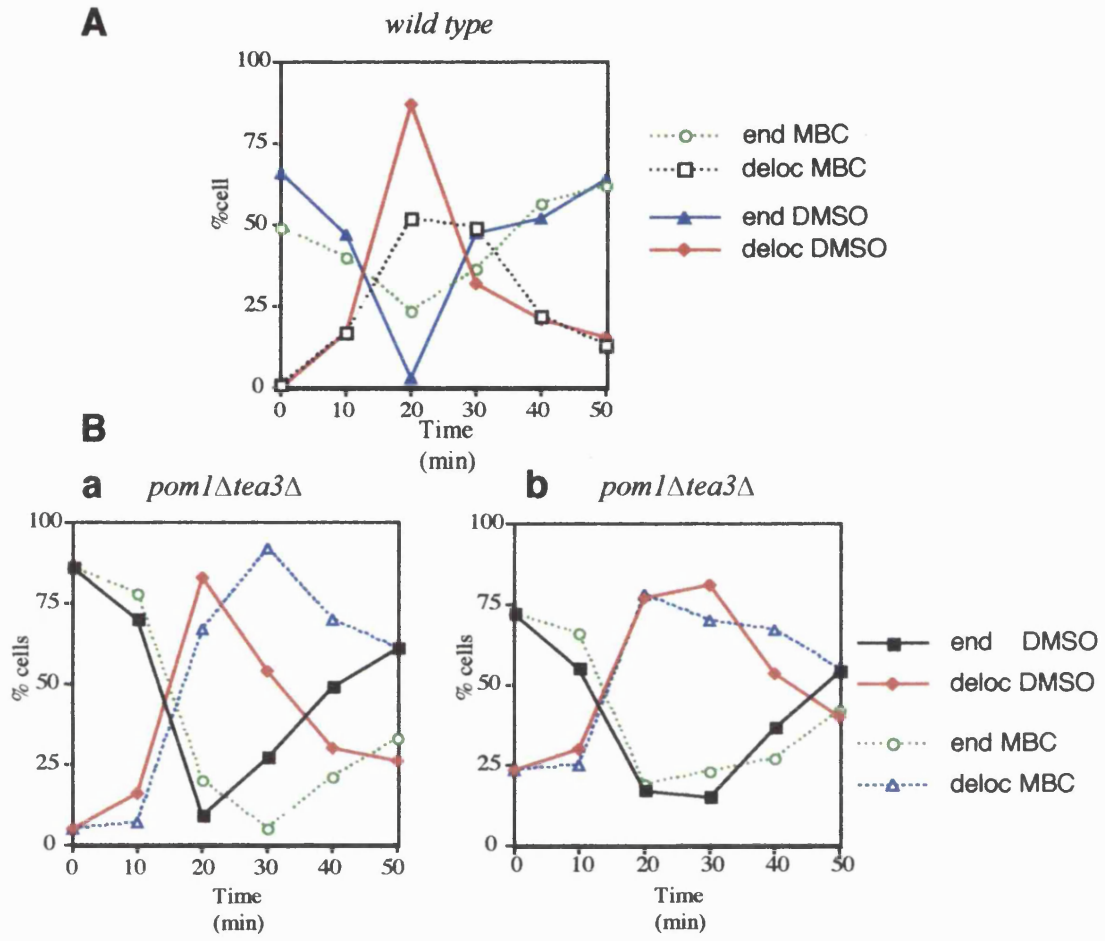

Figure 2.7. Actin relocalisation in the presence of MBC.
(A) Wild type cells were grown in YE5S at 25°C, treated with 25μg/ml MBC or DMSO as a control for 10 minutes and then pulsed with LatA (see materials and methods for details). Cells were allowed to recover for up to 50 minutes in YE5S with MBC or DMSO. Samples were taken every 10 minutes, fixed in formaldehyde, stained with rhodamine phalloidin and scored for cell end localised (end) or delocalised (deloc) actin. (B) *Tea3Δ pom1Δ* cells were treated as above. Two independent experiments are shown, in (a) the cells had been stored on plates for 2 days and in (b) for 3 days. The cell end localisation for wild type cells was mostly bipolar and for *pom1Δtea3Δ* was mostly monopolar. Scores are expressed as percentages of total cells scored.

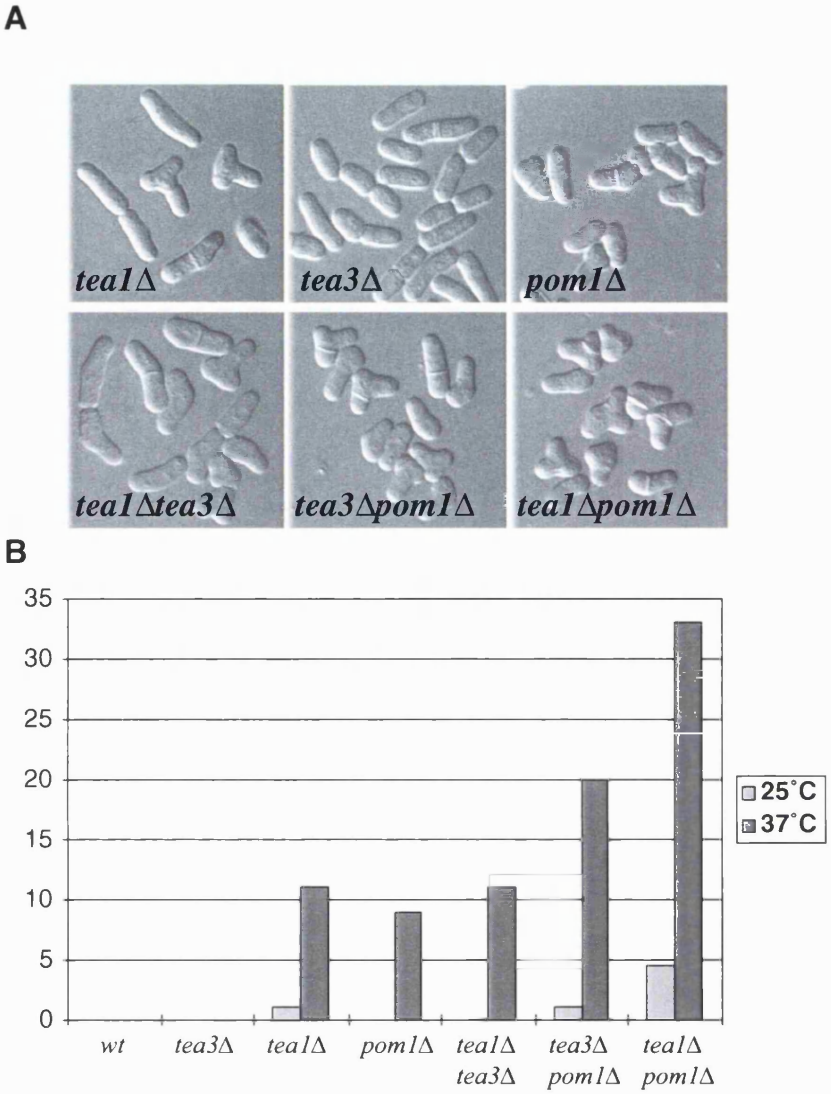

Figure 2.8. % T-shaped cells at different temperatures.
Cells were grown at 25˚C and shifted up to 37˚C for 2 hours. (A) Live cells were imaged with a light microscope and (B) scored for T-shaped cells. Scores are shown as percentages of total cells scored, at least 200 cells were scored in 2 independent experiments

Chapter 3

Analysis of the response to pheromone

3.1 Introduction

Fission yeast cells are characterised by two modes of growth: vegetative growth which is determined by a mechanism internal to the cell and shmooing growth, which occurs in repose to mating pheromones and is, therefore determined by an external signal.

Exponentially growing fission yeast cells switch to a shmooing mode of growth only if they are nitrogen starved in the presence of mating pheromones, thus responding to two independent signals: lack of nitrogen and presence of pheromone. In order to separate the two signals and to analyse the response to a single external signal, i.e. the mating pheromone, I used a h- *cyr1Δ sxa2Δ* strain, which responds to exogenously added pheromone in rich media (Imai and Yamamoto, 1994). *Cyr1+* encodes adenylyl cyclase, which produces cAMP and is switched off during nitrogen starvation (Kawamukai et al., 1991; Maeda et al., 1990). Deleting *cyr1+* abolishes the requirement for nitrogen starvation in mating, *cyr1Δ* cells can therefore mate in rich media (Kawamukai et al., 1991). *Sxa2+* encodes a secreted protease, specific to h- cells, which degrades the pheromone secreted by h+ cells (Imai and Yamamoto, 1992). When present, Sxa2p degrades any exogenous added pheromone before it had any effect, but *sxa2Δ* cells can respond to synthetic pheromone (Imai and Yamamoto, 1994). Using *cyr1Δ sxa2Δ* cells allows the analysis of only the response to the pheromone signal.

In this chapter I describe an initial characterisation of the switch between the vegetative and the shmooing mode of growth in the *cyr1Δ sxa2Δ* strain. I show that the switch is highly synchronous in this strain and that cells displays a wild type shmooing pattern, making the *cyr1Δ sxa2Δ* strain a good model system to investigate the switch to

shmooing growth. All experiments described are carried out with the h- *cyr1Δ sxa2Δ* strain in minimal medium with the addition of synthetic P-factor, the pheromone secreted by h+ cells.

3.2 Results

3.2.1 Cyr1Δsxa2Δ strain continues to shmoo over an 8 hour period

To determine if the *cyr1Δ sxa2Δ* strain was a good model system to investigate shmooing growth I analysed its response to the addition of pheromone. FACS analysis showed that cells, which during vegetative growth are mostly in the G2 phase of the cell cycle, arrested in the G1 phase of the cell cycle after the addition of pheromone (Fig 3.1C). Immediately after the addition of pheromone the septation index rose and cell length dropped (Fig 3.1A and B). This indicates that, in response to pheromone, cells are advanced into mitosis and therefore septate at a smaller cell size. After that the septation dropped index to 1.5% by 6 hours and remained low until 8 hours (Fig 3.1A), suggesting that cells arrest during this period and do not merely slow down in the G1 phase of the cell cycle. At the same time the cell length increased as the cells continued to extend during the cell cycle block (Fig 3.1B). I conclude that in response to pheromone the *cyr1Δ sxa2Δ* strain arrests in G1 within 6 hours and the cells are still actively growing 2 hours after the arrest.

3.2.2 Cells shmoo from the new end

Cells are know to extend in a monopolar manner in response to pheromone. To analyse if this was also the case for the *cyr1Δ sxa2Δ* strain, I gave exponentially growing cells a pulse of FITC labelled lectin, which stains the whole of the cell wall. I then washed the lectin out and allowed the cells to grow in the presence or absence of pheromone for 8 hours. I then counter-stained with calcofluor, which stains growing ends. Fig 3.2A shows that during vegetative growth calcofluor (green) stained both ends whereas in shmooing growth it mostly stained one end and lectin stained the other end. This establishes that in the presence of pheromone the cells grow only at one end.

After septation vegetative cells resume growth from the old end. To verify if this was also the case for cells that switched to a shmooing growth pattern, I mounted cells on agarose pads containing pheromone and filmed the cells for 12 hours. After septation cells started to extend off-axis from a single cell end (Fig 3.2B), generating very long and bent cells, characteristic of a shmooing growth pattern. I scored the growth pattern for each pair of daughter cells and found that the majority of daughter cells generated at cell division, initiated shmooing growth from the new end (Fig 3.2C).

3.2.3 The cytoskeleton is re-arranged in the switch to shmooing growth

Shmooing growth displays very different characteristics from vegetative growth: it is monopolar, cells are much longer and grow off-axis to generate a bent, shmooing

projection. I investigated if the cytoskeletal elements were rearranged to reflect this change in shape, by monitoring cells that switched to a shmooing growth mode.

Rhodamine phalloidin staining revealed that actin, which is mainly bipolar during vegetative growth, relocated to a single end and remained monopolar as the cells extended (Fig 3.3, middle panel). The switch in actin localisation can therefore be used to monitor the switch between bipolar vegetative growth and monopolar shmooing growth modes. As cells arrested, actin relocalised to one end with the switch from a bipolar vegetative pattern to a monopolar shmooing pattern being complete after 6 hours (Fig 3.4). The number of cells displaying delocalised actin was also scored but it did not change significantly in response to pheromone (Fig 3.4A).

To monitor microtubular behaviour I imaged live tubulin GFP after the addition of pheromone. During vegetative growth microtubules normally were seen as multiple parallel bundles spanning the length of the cell. After cells had septated in the presence of pheromone microtubules re-arranged to generate fewer, thicker bundles, originating from a single microtubule organising centre (MTOC) and mostly to one side of the cell (Fig 3.3, lower panel).

I conclude that both actin and microtubules are re-arranged during the switch to shmooing growth, in accordance with previously published results (Petersen et al., 1998; Petersen et al., 1998), and that the *cyr1Δ sxa2Δ* strain displays a wild type shmooing growth pattern.

The microtubules of shmooing cells appear very different to those in vegetative cells. I tested whether their polymerisation was also different by examining the

repolymerisation of microtubules after cold-shock. To exclude variations due to shmooing cells and their microtubules being longer, the vegetative control was treated with HU, a drug which blocks S-phase progression and therefore makes cells and microtubules longer.

After 40 min on ice both vegetative and shmooing microtubules were totally depolymerised (top panel Fig 3.5). Upon shift to 25°C the HU treated cells started to repolymerise their microtubules earlier than the pheromone treated cells, but after 11 minutes the pattern of microtubule growth was the same for the two samples. This suggests that although shmooing cells' microtubules initiate repolymerisation a little slower, after that they polymerise faster than vegetative microtubules.

3.2.4 Pheromone response in different conditions

To optimise the conditions for these experiments I analysed the response to different pheromone concentrations, to identify which concentration would give the most synchronous switch from vegetative to shmooing growth. I analysed the cell cycle arrest and the switch in actin localisation after the addition of different concentrations of pheromone, ranging from 0.15 μg/l to 6 μg/l. Cell cycle arrest occurred with roughly the same kinetics at all pheromone concentrations (Fig 3.6), but actin relocalisation became progressively slower at lower pheromone concentrations and no longer occurred at 0.15 μg/l of pheromone (Fig 3.7), even though the cells had arrested in G1. The morphological switch also appeared to reach a maximum rate at 3μg/l, after which higher pheromone concentrations did not increase the synchrony of the switch, possibly because the cell

cycle arrest, which always occurred at the same speed, became rate limiting. This suggests that there might be two different signalling cascades: one regulating the cell cycle arrest which is sensitive to very low amount of pheromone, and another with a higher threshold of sensitivity which controls the morphological switch.

It is known that mating efficiency drops at high temperatures. The analysis of the response to different pheromone concentrations revealed that there may be two pathways, one controlling cell cycle arrest and the other the morphological switch, either of which could be inhibited at high temperatures. Since the system I used allows cell cycle arrest and morphological responses to be monitored independently, I determined which of the two responses failed to occur at high temperatures. I added pheromone to cells at different temperatures and monitored cell cycle arrest by FACS analysis and the morphological switch by actin staining. Cell cycle arrest occurred with similar kinetics at all temperatures (Fig 3.8B) but actin did not become monopolar at 36°C, and even at 32°C the switch was not complete (Fig 3.8A). This suggests that at high temperatures cells can sense pheromone and arrest in the cell cycle but can not undergo the morphological switch from bipolar to monopolar actin. This could explain why cells can not mate at high temperatures.

Previous experiments suggested that at high pheromone concentrations the rate-limiting step might be the cell cycle arrest (see above). Since at high temperatures cell cycle arrest occurs but the morphological switch does not, I thought that arresting the cells in pheromone at 36°C and shifting them to 25°C might increase the synchrony of the morphological switch. This was indeed the case. The morphological switch at 25°C was

complete after 8 hours whereas after shift-down from 36°C to 25°C the switch occurred in just over one hour (Fig 3.9).

3.2.5 Roles of microtubules and actin during shmooing

Next I analysed the role of the cytoskeleton itself in the shmooing process. First I tested whether properly organised actin was required for shmooing. Since cells treated with pheromone at 36°C arrest in G1 with bipolar actin and do not activate monopolar shmooing growth (Fig 3.9), I arrested cells at 36°C in the presence of pheromone. I depolymerised actin using the drug LatA, and looked at the ability of the cells to shmoo. Not surprisingly, since polymerised actin is known to be essential for growth, cells were unable to shmoo in the presence of Latrunculin A (Fig 3.10).

Next I examined the requirement for an intact microtubular cytoskeleton, which is not essential for cell end extension during vegetative growth (Sawin and Nurse, 1998). I arrested cells at 36°C in the presence of pheromone, I then depolymerised microtubules with the drug MBC, and released the cells at 25°C to allow them to activate shmooing growth in the absence of microtubules (Fig 3.11C). I then monitored the rate of shmooing by looking at the relocalisation of actin from bipolar to monopolar. The switch from bipolar to monopolar actin localisation was unaffected by the absence of microtubules (Fig 3.11B). This demonstrates that microtubules play no role in the establishment of a single polarised growth zone during shmooing. However, some T-shaped cells were observed (Fig 3.11A and D), similar to the proportion seen in vegetative growth in the presence of MBC (Ken Sawin, personal communication), and calcofluor staining showed

that the growing area was very narrow and distorted (Fig 3.11A), suggesting that microtubules may play some role in the correct positioning and shaping of a growth zone within the cell.

3.3 Discussion

In this chapter I have shown that the *cyr1Δ sxa2Δ* strain is a good tool to analyse the switch between the vegetative and the shmooing growth pattern. After the addition of exogenous pheromone the strain arrests in the G1 phase of the cell cycle and switches to a shmooing growth mode, which displays the typical characteristics of the wild type shmooing pattern of conjugating cells. Microtubules re-arrange to generate thicker bundles, often connected to a single point, probably the Spindle Pole Body (SPB). Cells grow off-axis, only at one end and actin relocates to the single growing end. Since actin is mostly bipolar during vegetative growth I could monitor the relocalisation of actin from bipolar to monopolar and take that as an indicator of the morphological switch from vegetative to shmooing growth. Using this approach I found that microtubules themselves are not essential for the organisation of a single polarised projection. However, the generation of some T-shaped cells in the absence of microtubules, suggests that microtubules play some role in the correct positioning of the growth zone during shmooing. Microtubules could have a role in directing the polarised projection towards the pheromone source, but this possibility requires further investigation. Disrupting microtubules with TBZ concomitant with nitrogen starvation has been shown to totally inhibit projection tip formation (Petersen et al., 1998). This may be due to the fact that

actin as well as microtubules is disrupted in the presence of TBZ (Ken Sawin, personal communication) and lower amounts of TBZ were found to lead to the formation of H-shaped zygotes (Petersen et al., 1998). Using Latrunculin A I found that actin was essential for a polarised projection to be formed, consistently with previously published data showing that actin is essential for conjugation (Petersen et al., 1998).

Analysis of the growth pattern after the addition of pheromone revealed that cells initiated shmooing growth predominantly from the new end, in contrast to vegetativelly growing cells which re-initiate growth from the old end. During shmooing growth a new polarity is established, dictated by an external signal rather than by the internal landmarks. It is possible that the old cell end markers might no longer be recognised. The cell will therefore resume growth from the last place where the growth machinery was, the site of septation, as in the case of mutants lacking the internal cell end markers, described in the previous chapter.

I also analysed the response to pheromone under different conditions, independently monitoring the cell cycle arrest and the morphological switch. I found that the cell cycle arrest and the morphological switch display different characteristics. All pheromone concentrations and temperatures tested gave a good cell cycle block, suggesting that the cascade governing the cell cycle has a high sensitivity, responding to low pheromone concentrations, and that it is not influenced by temperature. The morphological switch, on the other hand is temperature sensitive, only occurring at low temperatures, and requires higher pheromone concentrations, with a graded response to lower pheromone concentrations. These results suggest that the reason that cells can not

mate efficiently above 30°C is because the morphological switch can not occur, so cells are not able to shmoo towards each other and conjugate. Most of the genes responsible for mating, including the pheromone and the pheromone receptor genes, are activated in response to pheromone. When a cell is in the vicinity of a mating partner, it will initially sense the very low amount of constitutively secreted pheromone and will respond by arresting in the G1 phase of the cell cycle and activating the pheromone response genes. This will lead to more pheromone being secreted and sensed, eventually resulting in the activation of shmooing growth which will allow the two cells to grow towards each other, meet and conjugate.

The most synchronous switch from vegetative to shmooing growth was observed at 25°C in response to 3μg/l of P-factor. At higher concentrations of pheromone the cell cycle arrest became rate limiting. This could be overcome by arresting the cells at 36°C in the presence of pheromone and then shifting the culture to 25°C to allow the morphological switch. Although this method increases the synchrony dramatically it also introduces a temperature shift, which in itself can effect the cells' physiology, and it could not be used in my subsequent analyses, using temperature sensitive mutants. I therefore decided to use 3μg/l of pheromone at 25°C for future experiments.

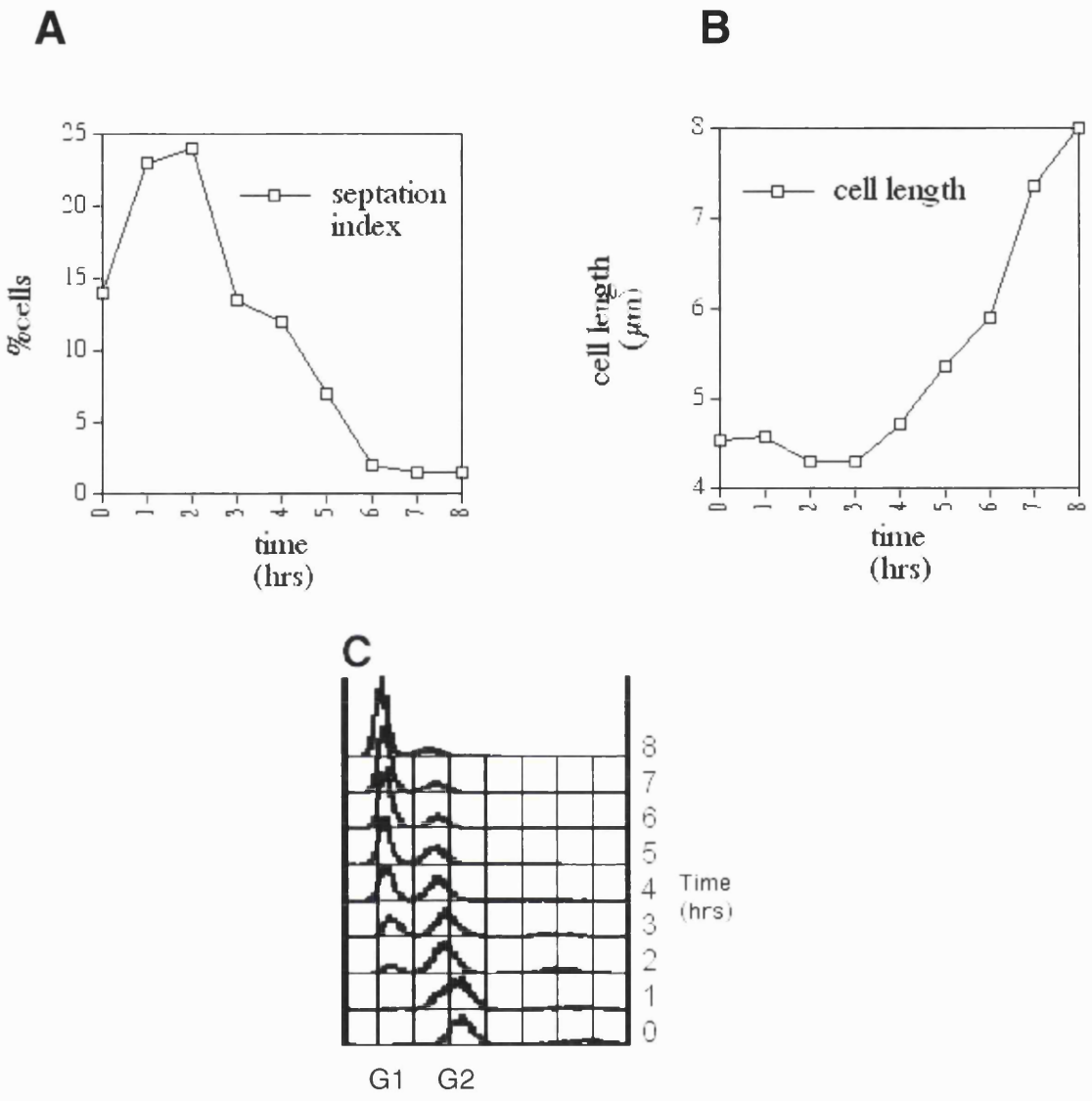

Figure 3.1. *Cyr1*Δ*sxa2*Δ strain in the presence of pheromone
3μg/ml of P factor was added at time 0. Samples were taken every hour. (A) Cells were stained with calcofuor and the sepation index was monitored. (B) Cells were imaged with a phase microscope mounted with a Hamamatsu camera and cell length was measured with NIH image. (C) Cells were fixed in ethanol and processed for FACS analysis

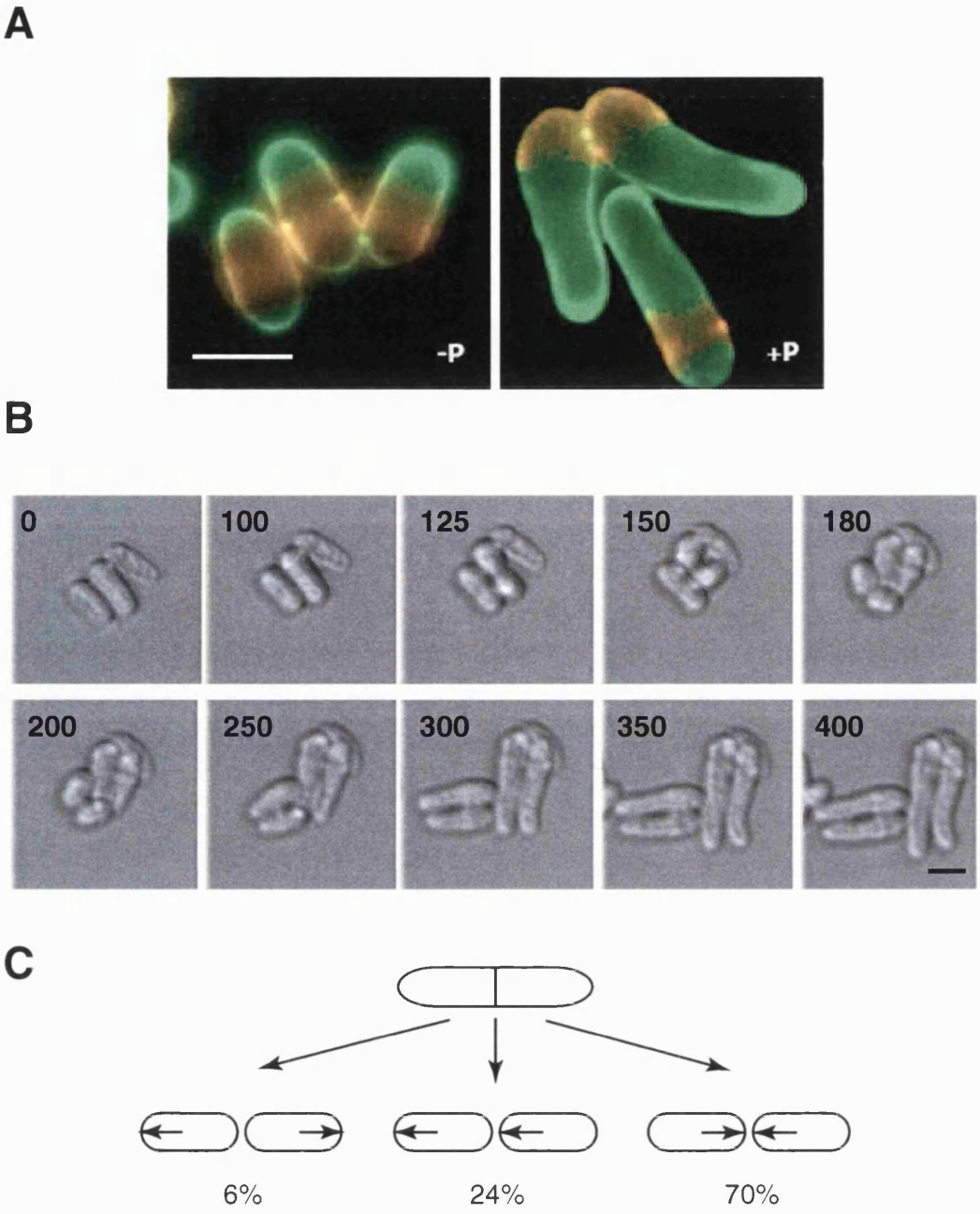

Figure 3.2. Pattern of growth in shmooing cells.
(A) The cell wall was stained with 1:1000 (from a 5mg/ml stock in water) FITC-lectin (red), for 10 minutes, the lectin was washed out and the cells were allowed to grow for 8 hours in the presence or absence of pheromone. Cells were then stained with calcofluor (green), which stains growing ends. The areas in red have not grown since the lectin pulse while the areas in green have. (B) 3µl of cell culture was places on a 1.5% agarose pad containing nutrients and pheromone, the cells were overlaid with a coverslip and sealed with wax.
Timelapse images were taken at 25˚C every 5 minutes for 12 hours. Selected frames are shown and the time is indicated in minutes. (C) Growth pattern of shmooing cells in (B) were scored. After septation cells exhibited 3 possible growth patterns. These are shown here, and scores are expressed as a percentage of total cells scored (n=66). Scale bar= 5µm.

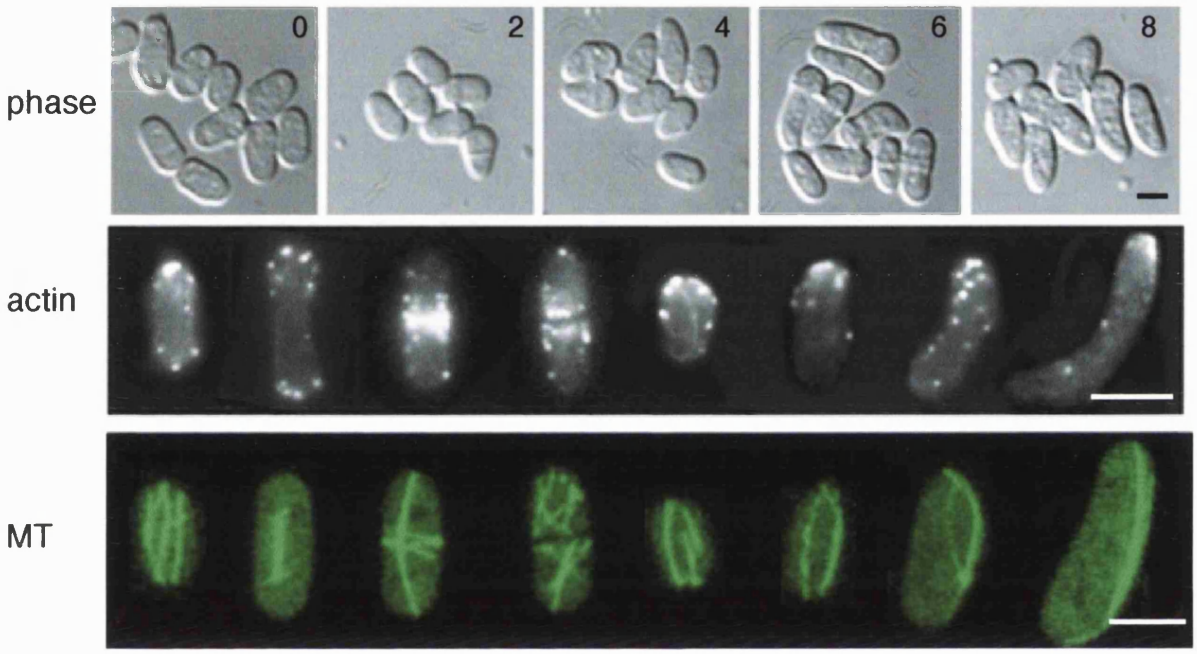

Figure 3.3. Arrangement of cytoskeletal elements.
(Upper panel) Pheromone was added to an exponentially growing *cyr1Δsxa2Δ* cell culture and phase images were taken every 2 hours. Numbers indicate time expressed in hours. (Middle panel) The cells from every timepoint were fixed in formaldehyde and stained for actin with rhodamine phalloidin. The various stages of the switch between vegetative and shmooing growth were imaged with a fluorescent microscope and selected cells are shown. (Lower panel) Pheromone was added to exponentially growing *atb2GFPcyr1Δsxa2Δ* cells and images were taken on a confocal microscope of cells at various stages. The images shown are a projection of sections through the whole cell. Scale bar= 3μm.

A

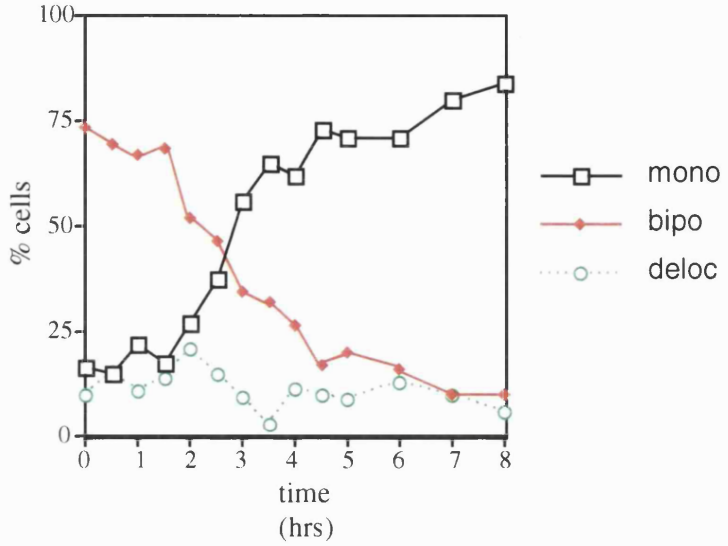

B

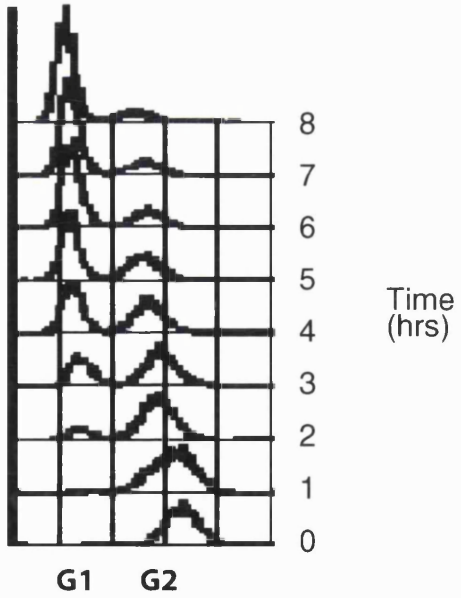

Figure 3.4. Actin relocalisation during shmooing.
(A)3µg/l of pheromone was added to *cyr1Δsxa2Δ* cells at time 0. Samples were taken every 30 minutes, fixed in formaldehyde and processed for actin staining. Actin localisation was then scored as monopolar, bipolar or delocalised. (B) Samples were taken every hour, fixed in 70% ethanol, and processed for FACS analysis.

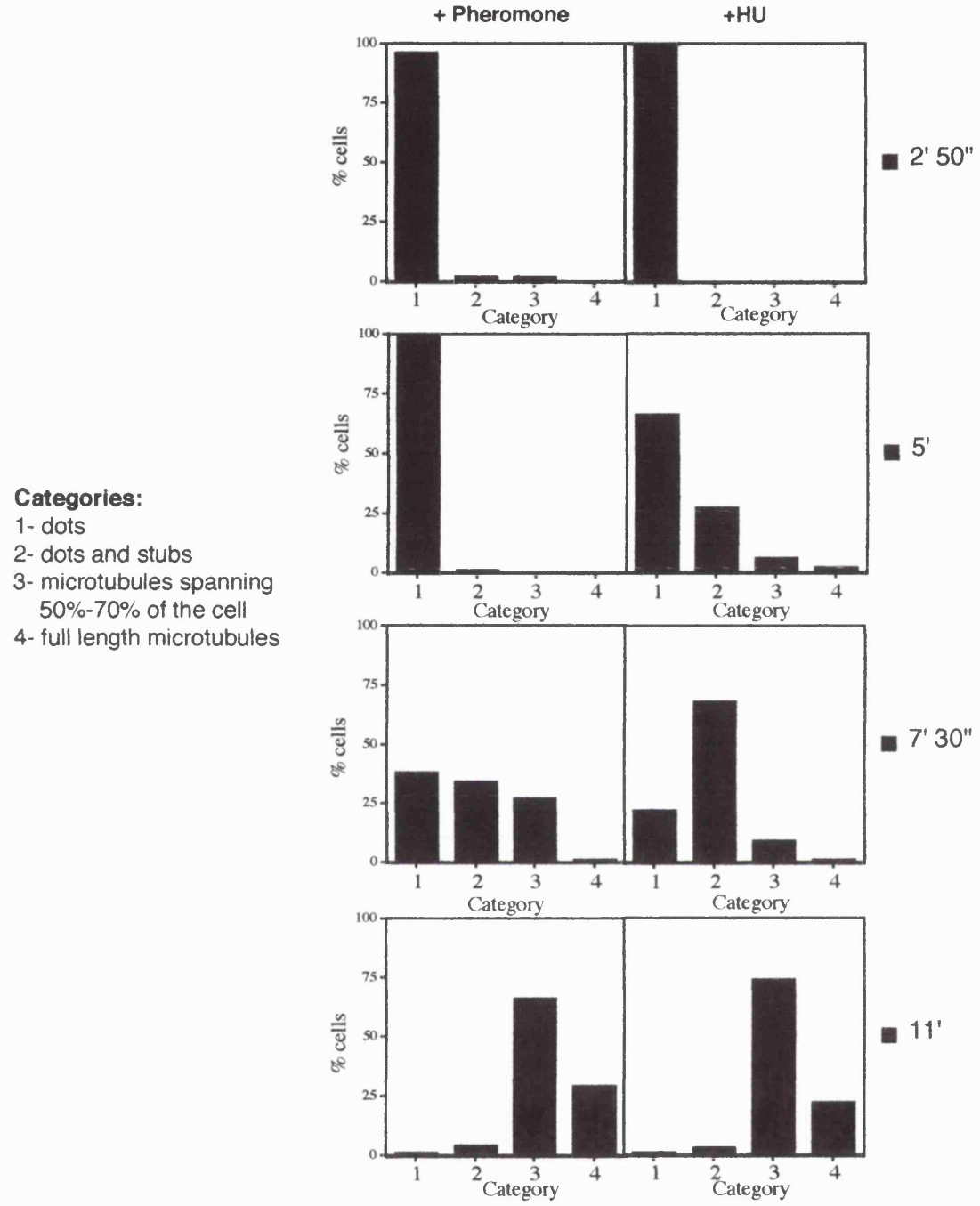

Figure 3.5. Cold shock recovery of microtubules.
1.5μg/l of pheromone or 11mM HU, as a control for long cells, were added to *cyr1Δsxa2Δ* exponentially growing cells, after 9 hours 25ml aliquots were placed on ice for 45 minutes. The aliquots were then placed in the 25˚C incubator and collected onto filters which were dropped in -80˚C methanol and placed at -20˚C. The time indicated are calculated from when the aliquots were taken from the ice to the time the cells were dropped into methanol and are not equally spaced because of different filtration times for different samples. Samples were then immunostained with anti-tubulin and scored. Scores are expressed as a % of total cells scored.

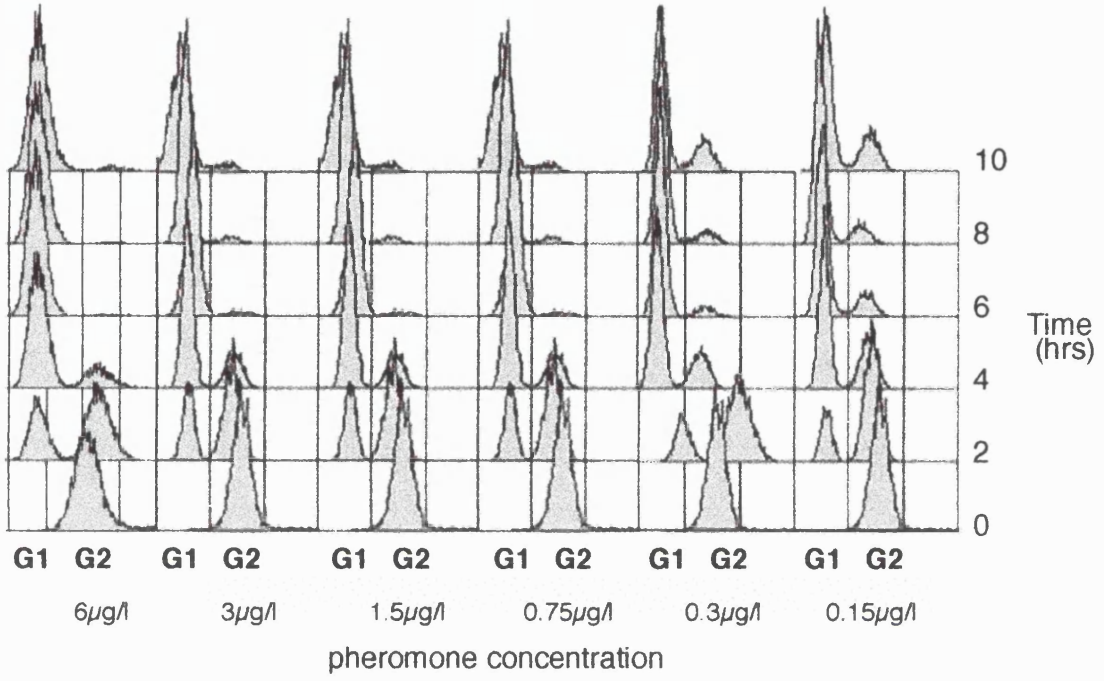

Figure 3.6. Cell cycle arrest at different pheromone concentrations.
Different amounts of pheromone were added to exponentially growing *cyr1Δ sxa2Δ* cells. Samples were takes every 2 hours, ethanol fixed and processed for FACS analysis.

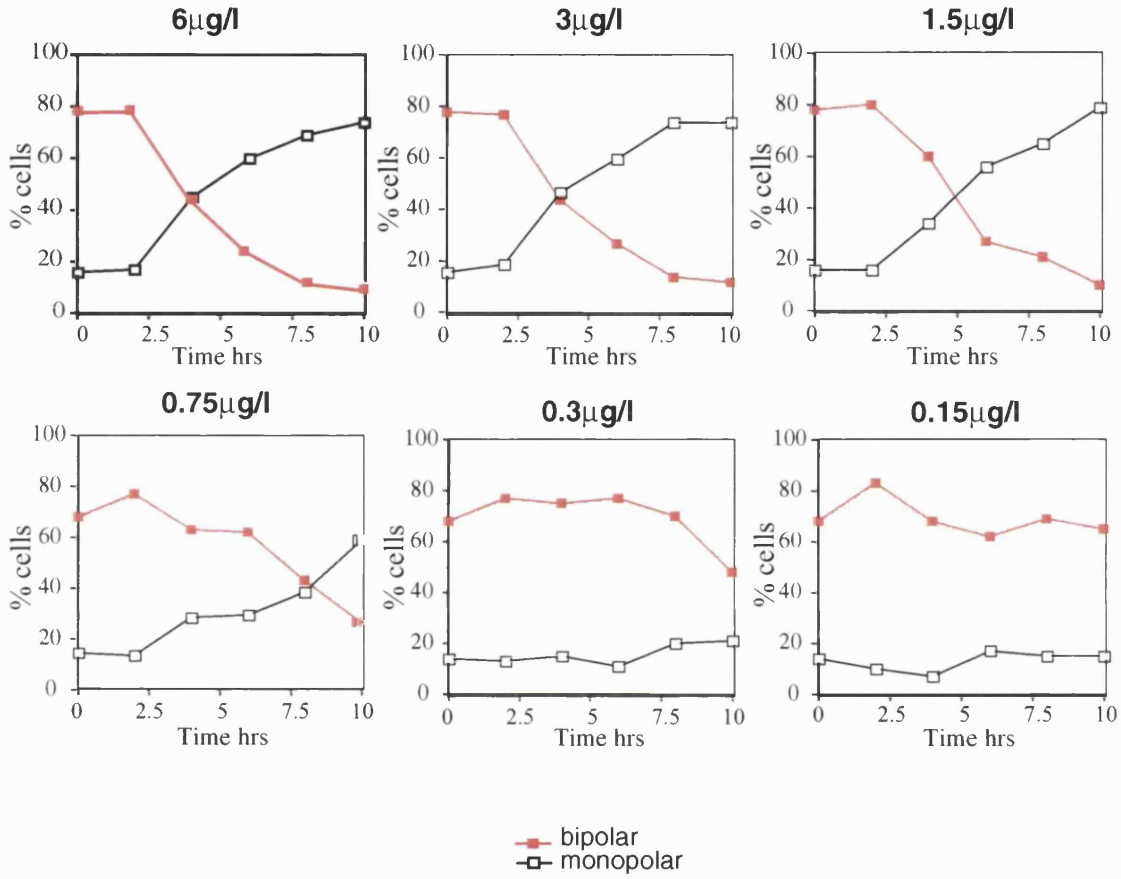

Figure 3.7. Actin relocalisation at different pheromone concetrations.
Exponentially growing *cyr1Δ sxa2Δ* cells were induced with different pheromone concentrations. Samples were takes every 2 hours, formaldehyde fixed and processed for actin staining. Actin localisation was then scored as monopolar or bipolar.

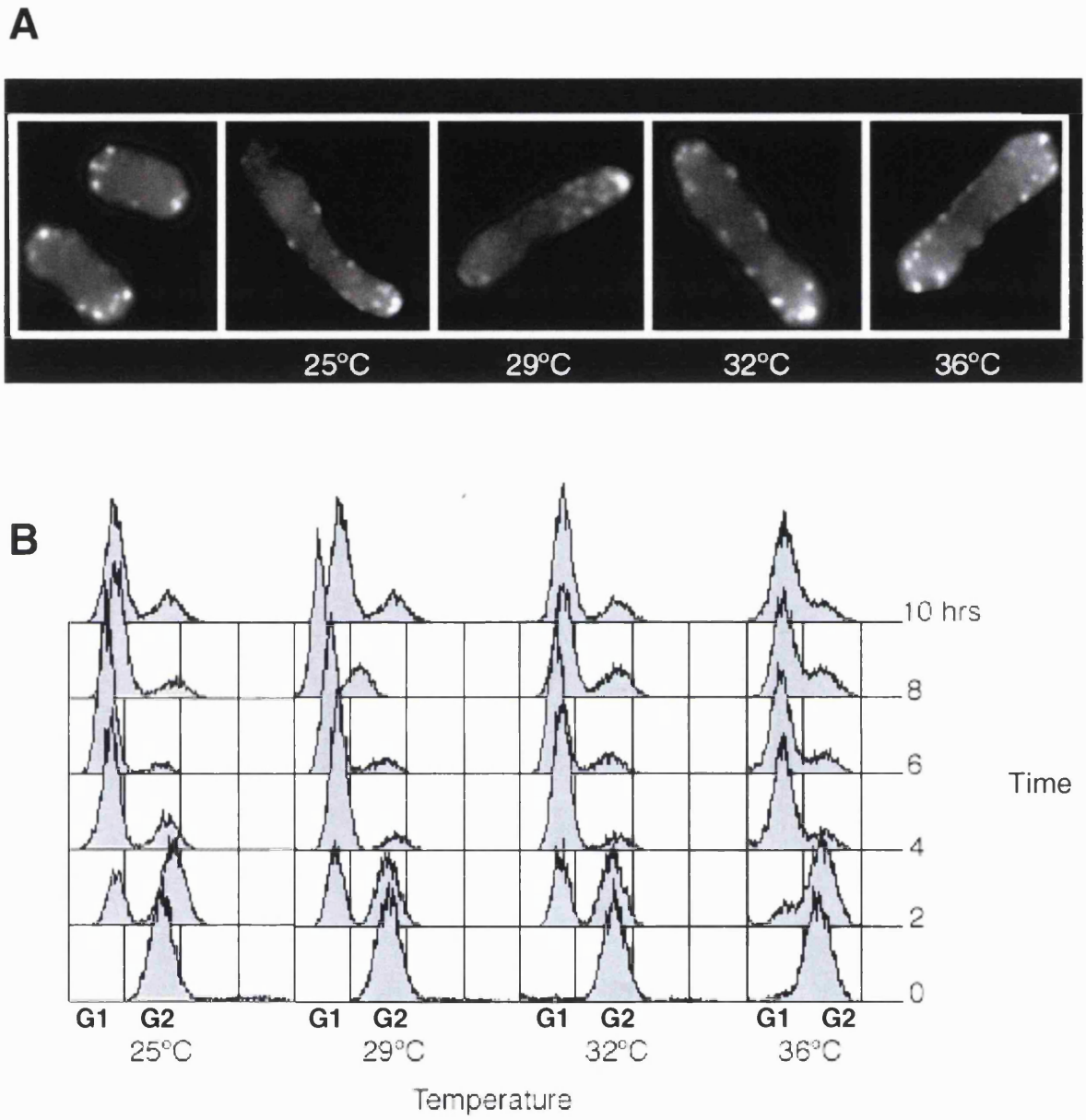

Figure 3.8. Pheromone response at different temperatures.
Pheromone was added at time 0 to cultures at different temperatures. (A) 8 hours after pheromone induction cells were fixed in formaldehyde and processed for actin staining. (B) Samples were taken every 2 hours, fixed in ethanol and processed for FACS analysis.

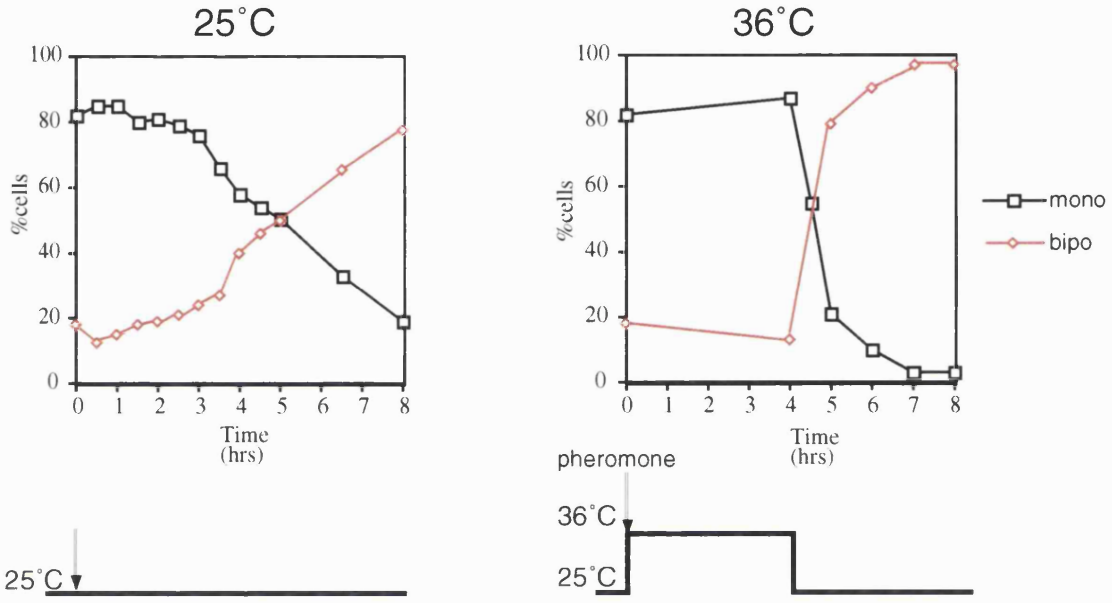

Figure 3.9. Temperature shift to induce shmooing.
Exponentially growing cells were treated with pheromone and left at 25˚C or shifted to 36˚C for 4 hours and then shifted down to 25˚C. Samples were taken at the indicated timepoints, fixed in formaldehyde, stained for actin and scored for monopolar or bipolar actin.

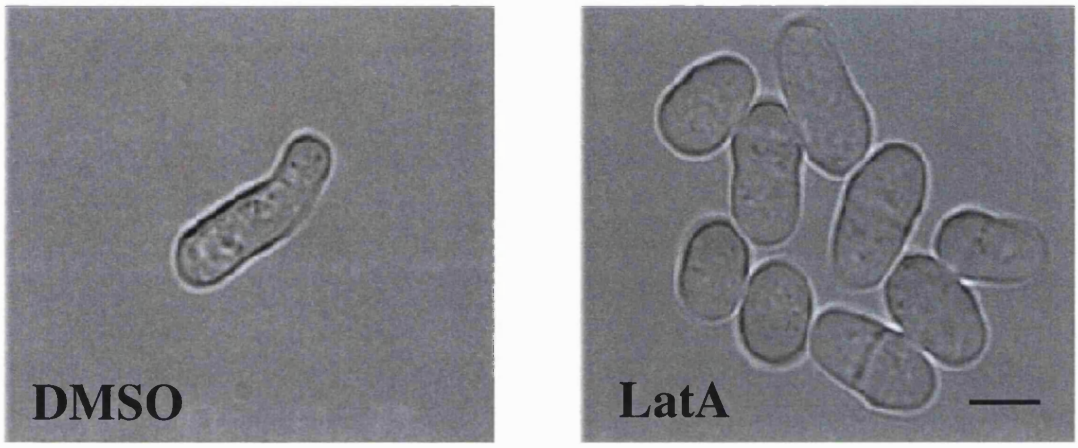

Figure 3.10. Effect of Latrunculin on shmooing.
Cells were treated with 3µg/ml of P factor for 4 hours at 36˚C, cells were then shifted to 25˚C for 3 hours in the presence of 200µg/ml of LatA or DMSO, as a control, and visualised under the light microscope. Scale bar=5µm.

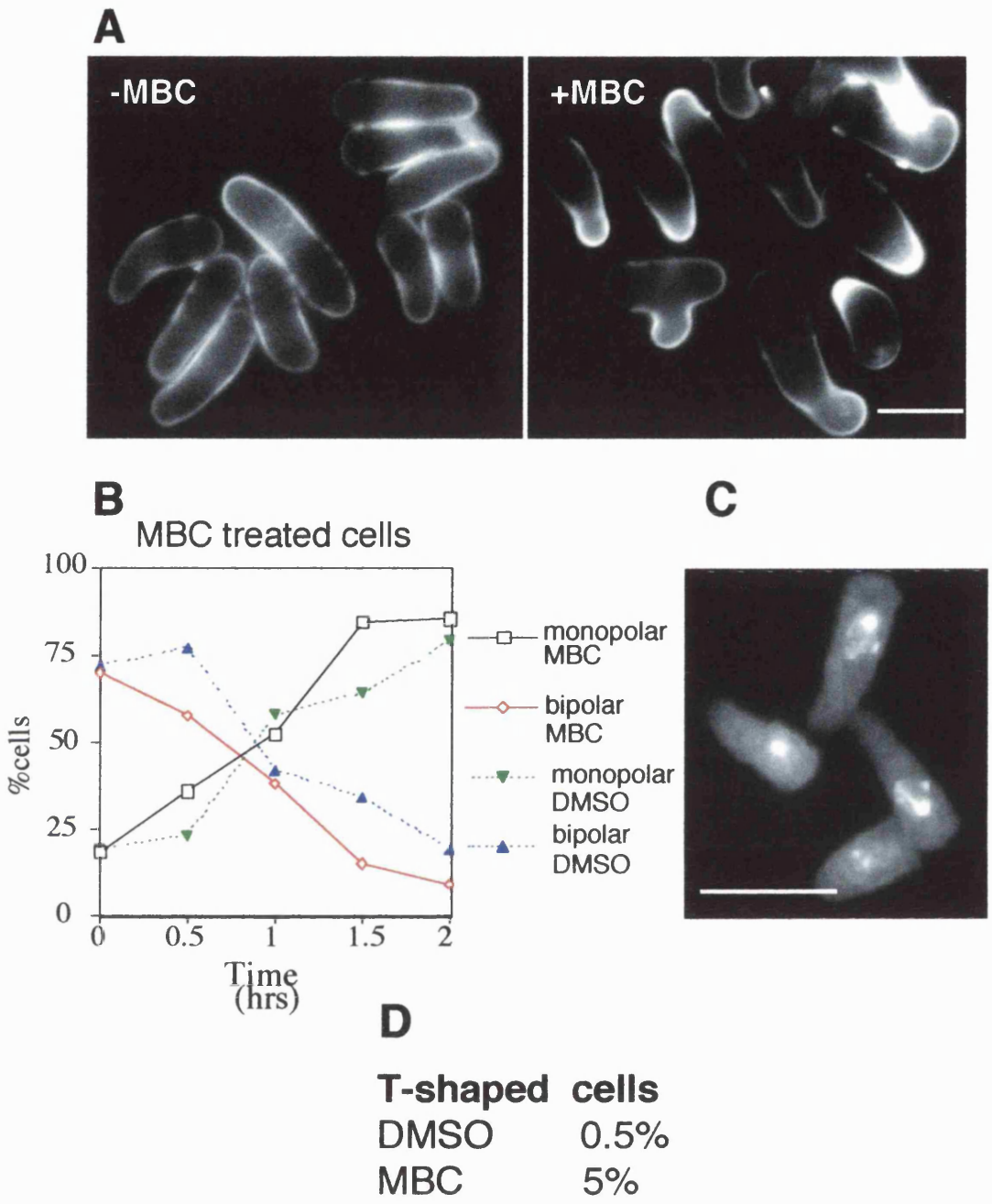

Figure 3.11. Effect of MBC on shmooing
Cells were arrested at 36°C in the presence of 3μg/l P factor for 4 hours, 25μg/ml of MBC or DMSO, as a control, were added and the cells were shifted to 25°C to induce shmooing. (A) 4 hours after shift-down cells were stained with calcofluor and visualised with a fluorescent microscope. (B) Samples were taken every 30 minutes, fixed in formaldehyde, stained with rhodamine phalloidin to visualise actin and scored for actin localisation. Times shown are calculated from the shift to 25°C (C) Cells treated with MBC were fixed in methanol at the end of the time course and processed for tubulin immunofluorescence to verify that no microtubules were present. (D) After 4 hours shift-down the number of T-shaped cells was scored. Scale bar, 5μm.

Chapter 4

Regulatlon of extrinsic cell growth

4.1 Introduction

In the previous chapter I have shown that the vegetative and the shmooing mode of growth of fission yeast display very different characteristics. This suggests that the two growth modes are regulated differently. In this chapter I investigate how the externally directed shmooing cell growth is regulated, analysing factors which direct intrinsic cell growth and possible regulators of extrinsic growth, such as the pheromone receptor, in the switch from vegetative to shmooing growth. All experiments have been carried out in a *cyr1Δ sxa2Δ* strain (Imai and Yamamoto, 1994)

Cell end markers like Tea1p, Tea3p and Pom1p play an essential role in maintaining cell shape during vegetative growth. In Chapter 2 I showed that all three contribute, to differing extents, to the determination of cell end identity and regulation of microtubular dynamics during vegetative growth. Pom1p plays a major role in the identification of cell ends as sites for growth and Tea1p in the regulation of microtubular dynamics. In the presence of pheromone, Tea1p has been found to delocalise from the cell ends, consistent with it being part of a vegetative specific machinery that becomes shut down in shmooing cells, to allow growth to occur away from the long axis of the cell (Mata and Nurse, 1997). Two further factors, Tea2p and Tip1p, which act upstream in the Tea1 pathway, also play a role in microtubular dynamics and cell polarity (Browning et al., 2000; Brunner and Nurse, 2000). In the absence of either of these factors microtubules are short and cells are bent and branched at a low frequency. The CLIP 170-like protein Tip1p forms a complex with Tea2p (D. Brunner and P. Nurse, unpublished

data), a kinesin-like protein, and both are found at the tips of microtubules and at the ends of cells (Browning et al., 2000; Brunner and Nurse, 2000). Tea2p and Tip1p may collaborate with Tea1p in the regulation of microtubular dynamics during vegetative growth (Browning et al., 2000; Brunner and Nurse, 2000; Mata and Nurse, 1997). Apart from factors determining the position of the growth zones, there are core-components which are thought to directly contribute to actin polymerisation. One of these is Scd2-Ral3p, a scaffold protein which is thought to facilitate the interaction between Cdc42p and Shk1-Pak1-Orb2p (Chang et al., 1999; Chang et al., 1994), and control actin polymerisation. This protein is known to play a role both during vegetative growth and during mating, suggesting that the core-machinery is the same. Ral3p should therefore be a useful positive control for a factor involved in shmooing growth.

Shmooing growth is thought to be regulated by pheromone secreted by cells of the opposite mating type. The positional information from the pheromone gradient therefore has to be detected and relayed to the inside of the cell to direct formation of a mating projection. The obvious candidate for this job is the pheromone receptor. In this chapter I also analyse the behaviour of the Mam2p P-factor receptor in response to pheromone, to determine its role in directing cell growth during shmooing. All experiments presented in this chapter were carried out in the *cyr1Δ sxa2Δ* background, unless otherwise stated.

4.2 Results

4.2.1 Pom1 is not a cell end marker for shmooing growth

I investigated the differences between the vegetative and shmooing growth modes by looking at the behaviour of various morphological factors. I first examined the role of Pom1p in the pheromone response. Pom1p plays a major role in the establishment of cell polarity as a marker of cell ends for growth (Bahler and Pringle, 1998) (see Chapter 2). I examined the levels of Pom1HA by Western blotting at different time points after pheromone addition and found that they remain essentially constant during the pheromone time course (Fig 4.1A). If Pom1p exerts a similar role in cell morphogenesis during shmooing growth as it does in vegetative growth, it might be expected to localise to the same place within the cell. To investigate this I analysed the Pom1GFP in live cells in the presence or absence of pheromone. Pom1GFP, which is located at the cell ends during vegetative growth, became distributed more generally throughout the cell after addition of pheromone (Fig 4.1B).

The delocalisation of the protein suggests that it might no longer play a role in directing polarised cell growth during shmooing. To investigate this I analysed the role of Pom1p by looking at the ability of *pom1Δ* cells to shmoo. FACS analysis showed that the cells responded to pheromone, arresting with similar kinetics to wild type (Fig 4.2A). Actin was mostly monopolar during vegetative growth, but as soon as pheromone was added, the proportion of cells with monopolar actin dropped and that of cells with delocalised actin increased (Fig 4.2B). Close comparison of actin localisation for the first two hours in *pom1Δ* and a wild type strains (Fig 4.2C) showed a marked difference

between the two. In wild type cells actin remained bipolar for the first 1.5 hours, whereas in *pom1Δ* cells delocalised actin increased within 0.5 hours.

In wild type monopolar cells actin becomes bipolar upon commitment to mating, and then relocalises to the shmooing end (Petersen et al., 1998). Pom1p therefore may be required to maintain the cell end localisation of actin during the early stages of the switch to shmooing growth. The subsequent establishment of a monopolar localisation for actin was also slower and less efficient in *pom1Δ* cells. Even after 6.5 hours, only 65% of the cells were monopolar for actin and 27% of cells still had delocalised actin (Fig 4.2B), whereas by this time point over 90% of wild type cells were monopolar for actin (see Fig 4.17). From these results Pom1p appears to play some role in the establishment of cell polarity during shmooing. To confirm if this was the case I analysed the recovery of actin localisation at the cell ends after a LatA pulse (see materials and methods for details). The *cyr1Δ sxa2Δ* background does not seem to have a dramatic effect on the relocalisation of actin (Fig 4.3). The wild type and *pom1Δ* strains, in the *cyr1Δ sxa2Δ* background, after a LatA pulse during vegetative growth gave a similar result to the exponentially growing cells in Chapter 2 (Fig 4.3). On the contrary shmooing wild type cells after a LatA pulse could not relocalise actin to one end after 1 hour recovery, displaying 65% delocalised actin and even after 2 hours recovery actin had not totally relocalised to one end (Fig 4.3). This also indicated that the shmooing end is not as strongly marked as a vegetatively growing end. There was also no increase in cells with bipolar actin, suggesting that the second end can not be recognised as a site for growth. The shmooing *pom1Δ* strain showed 75% delocalised actin at 1 hour, that dropped to

35% after 2 hours recovery. This was slightly higher than wild type, but the deletion of Pom1p already displayed 20% delocalised actin at time 0, suggesting that lack of Pom1p does not have a major effect on actin relocalisation after a LatA pulse during shmooing. I conclude, that Pom1p is not a cell end marker for growth during shmooing and does not play a role in the establishment of cell polarity determined by an extrinsic signal. To confirm this I monitored the ability to mate of a *h90 pom1Δ* strain in a wild type background. Figure 4.4 shows no difference between wild type and *pom1Δ* cells' mating ability. Pom1p is therefore not required for mating.

If Pom1p is a vegetative specific cell end marker, maybe it needs to be switched off for the new shmooing cell polarity to be established. The over-expression of Pom1p might therefore block the switch from vegetative to shmooing growth. To test this I expressed *pom1+* from the full strength inducible *nmt1* promoter on a plasmid, and monitored the cells' ability to arrest and shmoo in the presence of elevated amounts of Pom1p. The *nmt1* promoter drives moderate levels of expression even when fully repressed in the presence of thiamine. Moderate levels of Pom1p overexpression (+thiamine Fig 4.5) delayed both the cell cycle arrest and the actin relocalisation and full induction (-thiamine Fig 4.5) delayed the two responses even further. Full induction led to a very high level of delocalised actin, and eventually resulted in cell death; the switch to shmooing growth might therefore be slow because the cells are sick. But the results from the moderate over-expression suggest that the presence of elevated amounts of Pom1p delays the cell cycle arrest, and the morphological switch.

4.2.2 Tea3p is not required for shmooing growth

I next examined the role of another cell end marker, Tea3p which is required to induce the switch to bipolar cell growth during vegetative growth and has an overlapping role as a cell end marker (See chapter 2) with Tea1p and Pom1p. Vegetative cells undergo a transient bipolar phase before switching to monopolar shmooing growth (Petersen et al., 1998). I analysed if Tea3p was required for this switch to the bipolar intermediate stage and whether it was a cell end marker for shmooing growth. The protein level did not change after the addition of P-factor (Fig 4.6A) but Tea3GFP relocalised to the cell periphery and was no longer concentrated at the cell ends as during vegetative growth (Fig 4.6B).

I then analysed the ability of a *tea3+* deletion mutant to shmoo. The cells arrested with similar kinetics to the wild type (Fig 4.7A) and the relocalisation to a monopolar shmooing stage appeared faster than the wild type situation. The initial proportion of monopolar cells was already high so it was difficult to distinguish which cells were vegetatively growing and which were shmooing. No switch to the intermediate bipolar stage was observed suggesting that Tea3p is required for cells to switch to the bipolar intermediate stage. I conclude that Tea3p is not required for shmooing growth itself but it is required for the transient bipolar stage.

4.2.3 Behaviour of Tea1p, Tea2p and Tip1p in the switch to shmooing growth

Microtubular dynamics appear very different in shmooing cells. I therefore analysed the role of Tea1p, Tea2p and Tip1p, which are key regulators of microtubular

dynamics in vegetative growth, during the switch to shmooing growth. The levels of Tea1p, Tea2p and Tip1p protein remained essentially constant after pheromone addition (Fig 4.8A). The only change I detected was a different pattern of bands for Tip1p and Tea1p after 2.5 hours in pheromone (marked by arrows in Fig 4.8A, B). Phosphatase treatment suggests that the new faster migrating form for Tea1p may be due to dephosphorylation (Fig 4.8C). I conclude that all three proteins are present in the cell during shmooing growth, although they might be differentially phosphorylated compared with vegetatively growing cells. The result for Tea1p differs from previously published data (Mata and Nurse, 1997) and is due to a more complete extraction procedure during the sample preparation in the present study. Mata collected the cells, boiled them and broke the cells using glass beads, he then spun the samples and only took the supernatant for further analysis; we never spun the samples and loaded the whole extract onto the gel.

I then analysed the localisation of GFP tagged versions of the three proteins in live cells in the presence or absence of pheromone. Tea1GFP (Behrens and Nurse, 2002), which replaces the endogenous Tea1p, fully rescues the mutant phenotype of *tea1Δ* cells. Cells with Tea2GFP or Tip1YFP appear to be wild type during vegetative (Browning et al., 2000) and shmooing growth. During vegetative growth Tea1GFP, Tip1YFP and Tea2GFP localise to cell ends and to a few dots on microtubules (Behrens and Nurse, ; Browning et al., 2000) (A. Decottignie, unpublished results) (Fig 4.9). After pheromone addition, Tea1GFP became mostly lost from the growing end and was redistributed along the cell periphery at the non growing larger end (Fig 4.9). After pheromone addition Tea2GFP and Tip1YFP were also reduced at the growing end, accumulating at the non-

growing end and in the cytoplasm, often as dots in a row (Fig 4.9). The same relocalisation was observed for Tea2GFP during an h90 mating (Fig 4.10). In conjugating cells Tea2GFP was found to localise to the non growing ends with some dots in the cytoplasm (Fig 4.10). This demonstrates that the delocalisation of these factors is also observed in cells undergoing normal conjugation. I conclude that Tea1p, Tea2p and Tip1p are no longer specifically located at the growing ends of shmooing cells, and therefore may not be required for polarising cellular growth in these cells as they are in vegetatively growing cells.

Tea2p and Tip1p are known to be associated during the vegetative cell cycle (Damian Brunner, personal communication) and Tea2p may be the motor protein that transports Tea1p to the ends of the cell (Browning et al., 2000). These factors might therefore co-localise during vegetative growth and if they no longer have a role in shmooing growth their association might fall apart. Visualisation of Tea2GFP in combination with Tip1YFP revealed that Tea2p always co-localises with Tip1p in the presence and absence of pheromone (Fig 4.11B). In contrast, analysis of Tea1GFP in combination with Tip1YFP revealed that there is a 10 fold increase in the number of Tea1GFP dots that do not co-localise with Tip1YFP in the presence of pheromone (Fig 4.11A and C). Most of the free Tea1p dots localise to the peripheral region near the non-growing end (Fig 4.11A). The Tea1p in the cytoplasm may still be on microtubules where it is co-localised with Tip1p, but once it reaches the cell end it diffuses along the periphery of the cell, whilst Tip1p remains more concentrated at the cell tip. Therefore during shmooing growth the colocalisation of Tip1p and Tea2p is maintained, but the

colocalisation of Tea1p and Tip1p, and by inference Tea1p and Tea2p, is reduced. Although the co-localisation of Tea1p with Tea2p is reduced, the Tea1p complex size remains the same in the presence and absence of pheromone (Fig 4.12). The smaller molecular weight Tea1p fraction seen in +pheromone is not reproducible. This suggests that the majority of the Tea1p complex is still intact.

4.2.4 Tea1p and Tip1p association with microtubules

It is thought that cells predominantly respond to pheromone in the G1 phase of the cell cycle (Stern and Nurse, 1998). Therefore, when cells enter G1 in the presence of pheromone, the properties of microtubules or Tea1p may be altered, reducing the association between them. To test this possibility, I compared the efficiency of Tea1p binding to re-polymerising microtubules in G2 arrested cells which do not respond to pheromone, and in G1 cells which do respond to pheromone. Live Tea1GFP images (Fig 4.13 a and b) during a G2 block in the absence and in the presence of pheromone, show short linear arrays of dots, similar to the re-polymerising microtubule arrays seen by tubulin immunostaining (Fig 4.13 a and b) of the same population. This suggests that Tea1GFP may co-localise with re-polymerising microtubules. On the contrary, when cells enter G1 and become responsive to pheromone, Tea1GFP is no longer found on re-polymerising microtubules (Fig 4.13c).

I confirmed that the Tea1GFP dots corresponded with microtubules in G2 arrested cells by repeating the experiment using an untagged *tea1+* strain, fixing the cells in methanol and co-staining for tubulin and Tea1p in the same cells. Cells arrested in G2 without pheromone (Fig 4.14A) and G2 cells with pheromone (Fig 4.14B) show Tea1 on

microtubules. As before, after entry into G1 in the presence of pheromone (Fig 4.14C), Tea1p is not found on microtubules.

The lack of association of Tea1p with microtubules in cells responsive to pheromone could mean Tea1p is no longer efficiently transported along microtubules and so does not accumulate at the growing end of the cell. In contrast, Tip1p, which is still found at the end of microtubules during shmooing (Fig 4.15A), can still associate with growing microtubule in G1 cells treated with pheromone (Fig 4.15B). A lack of microtubular association is therefore unlikely to be the reason for Tip1p not accumulating at growing cell ends (Fig 4.9).

4.2.5 Phenotype of cells lacking Tea1p, Tea2p and Tip1p

Tea1p, Tea2p and Tip1p are delocalised in response to pheromone, suggesting they might not be required during shmooing. To investigate this I examined the microtubular phenotype in *tea1Δ, tea2.1* and *tip1Δ* cells treated with pheromone. Microtubules of vegetatively growing *tea1Δ* cells are slightly longer than wild type and some can curl around the cell ends (Mata and Nurse, 1997), whereas in *tea2.1* (a null mutant) and *tip1Δ* cells' microtubules are shorter and rarely reach the cell ends (Browning et al., 2000; Brunner and Nurse, 2000; Verde et al., 1995). If these factors no longer have a role during shmooing growth, then microtubules should look like wild type after pheromone treatment. This was indeed the case. All three mutants were able to detect and respond to pheromone by arresting in G1, as shown by FACS analysis (Fig 4.17B), and displayed wild type microtubules (Fig16 A, B and C). Control vegetative

cells arrested in HU still showed the mutant phenotype demonstrating that the effect was not related to cell elongation (Fig 4.16 B and C).

During vegetative growth Tea1p, Tip1p and Tea2p also affect the ability of a cell to position a growth zone correctly (Browning et al., 2000; Brunner and Nurse, 2000; Mata and Nurse, 1997). Therefore I investigated the ability of the three null mutants to correctly reorganise a single growth zone during the switch from vegetative to shmooing growth. Actin relocalisation was used to monitor the switch from bipolar vegetative growth to monopolar shmooing growth. Cells were only scored as being monopolar if they showed no actin or only one actin dot at the other end. Many monopolar mutants, including *tea1Δ*, are monopolar for growth and show actin localised mainly at the growing end but often have a few dots of actin at the non-growing end and therefore would have been scored as bipolar. The assay gives an accurate indication of the switch to a shmooing growth pattern during vegetative growth, which shows no actin at all at the non-growing end.

In vegetative wild type cells actin was initially bipolar, and after 2.5 hours in pheromone it became monopolar in 50% of the cells (Fig 4.17A), indicating that half of the cells have activated shmooing growth by 2.5 hours. In contrast all three mutants responded more rapidly, relocalising actin in 50% of the cells within 1.5 hours (Fig 4.17A). These results show that Tea1p, Tea2p and Tip1p are not required to reorganise a shmooing tip, and in fact, their presence can cause some delay in the switch to the new growth mode. To analyse the effect of faster shmooing rates on mating I scored the number of fused cells in a time course for mating in h90 wild type and mutant strains.

Tea2.1 and *tip1Δ* strains mated faster than wild type suggesting that the faster shmooing rates may lead to faster conjugation (Fig 4.18), in contrast *tea1Δ* cells mated at the same rate as wild type. It is possible that Tea1p could be required for a subsequent step in the mating pathway or for efficient arrest during nitrogen starvation. After 6 hours without nitrogen, I observed more septating cells in *tea1Δ* than in wild type (data not shown), suggesting that *tea1Δ* cells might have difficulties arresting in the nitrogen block, and this would slow down the mating.

Since the presence of Tea1p and Tea2p were inhibitory for the switch to shmooing growth their overexpression might inhibit the switch. To verify this possibility I expressed Tea1p and Tea2p from a *nmt1* promoter on a plasmid. Long periods of overexpression were lethal to the cell, however 14 to 23 hours of overexpression provided higher levels of protein than normal (Fig 4.19B) without being lethal. Cells overexpressing Tea1p or Tea2p were still able to shmoo (Fig 4.19A). I conclude that elevated levels of Tea1p and Tea2p do not have a major effect on the ability of a cell to switch to a shmooing mode of growth.

4.2.6 Ral3p and Mam2p do play a role in shmooing growth

Key regulators of polarity in vegetative cells do not appear to play a role in shmooing growth and are delocalised in the presence of pheromone. I analysed if this was also the case for Ral3p, a morphological factor that is known to play a role in mating and that is a key regulator of the core actin polymerisation machinery.

I monitored the localisation of a slightly over-expressed Ral3GFP protein. Ral3GFP was localised to both ends during vegetative growth and to the shmooing

projection during shmooing growth (Fig 4.20), in accordance with previous reports that it plays a role in polarity during shmooing. This also suggests that the core actin polymerisation machinery might be the same even if the mechanism positioning it is different during vegetative and shmooing growth.

A candidate for localising the actin polymerisation machinery to the shmooing projection is the pheromone receptor, Mam2p. If this were the case it should localise to the shmooing projection. I tagged Mam2p with GFP and MYC and monitored the protein's levels after the addition of pheromone. In the presence of pheromone the protein was greatly induced (Fig 4.21A), in accordance with previous reports (Kitamura and Shimoda, 1991). The smear observed in the gel is probably because of secondary modifications of the protein, like glycosylation, and because it is a membrane protein, which might be retarded from entering the gel. I then monitored Mam2GFP localisation by mating a Mam2GFP h- strain to a wild type h+ strain. After nitrogen starvation the protein was localised throughout the membrane (Fig 4.21 Ba) but when the cell starts to shmoo Mam2GFP localised only to the shmooing projection (Fig 4.21 Bc). After fusion Mam2GFP could diffuse to its mating partner's membrane (Fig 4.21 Bd) and in the final stages of the mating process Mam2GFP was found in very bright vesicles and was excluded from the spores (Fig 4.21Be and Bf). To be able to direct actin localisation Mam2p has to localise to the shmooing end before actin. I monitored Mam2mycp and actin localisation in cells fixed at various stages after the addition of pheromone (Fig 4.22). Mam2p is expressed to very high levels and readily internalised for recycling, the signal from Mam2GFPp inside live cells was so bright that it masked the membrane

signal, making it impossible to monitor membrane Mam2GFPp localisation in live cells. On the other hand, in fixed cells only the membrane fraction was immunostained. Mam2mycp became monopolar faster than actin (Fig 4.22 B), consistent with the idea that it might direct actin localisation.

4.2.7 Screen to identify novel mutants

In order to identify novel factors required to establish shmooing cell polarity I screened a bank of mutants for abnormal shmooing morphology. The mutants were generated via a his-tagged mutagenesis (See materials and methods for details). Briefly, a linear fragment containing the *his+* gene was transformed in a *his-* strain using a protocol which would maximise non-homologous recombination and should have allowed the fragment to insert randomly into the genome. The *his+* cells were then selected for prototrophs, which had taken up the fragment. The cells were then replica plated onto pheromone containing plates and visually screened for mutants displaying abnormal shmooing morphology. 10000-15000 mutants were screened and 55 mutants were picked. Upon re-checking some were diploids, unstable or did not show a mutant phenotype and therefore were discarded. 16 did arrest, were haploids and displayed abnormal morphology. I prepared genomic DNA from these strains and sequenced the junction to identify the insertion site. I successfully identified 14 insertion sites and found that the fragment had either inserted into mitochondrial DNA or in intragenic regions. I conclude that the *his+* fragment does not integrate randomly within the genome but preferentially into intragenic or mitochondrial DNA and therefore it is not a suitable method to generate random mutants in coding genomic sequences.

4.3 Discussion

In this chapter I have shown that the five morphological factors Pom1, Tea3p, Tea1p, Tea2p and Tip1p, required for cell polarisation in vegetative growth, do not play a role in polarising cell growth in pheromone. In the presence of pheromone these factors are all present in the cell but are no longer localised to the growing end. Tea1p and Tip1p display a different banding pattern, which might be due to differences in phosphorylation (Damian Brunner, personal communication, this study) and these modifications might contribute to their delocalisation.

After addition of pheromone to cells, actin first becomes bipolar and then relocalises to the shmooing end (Petersen et al., 1998). This may be an initial re-setting step, which allows the cell to pick either end for shmooing growth, depending on which one is experiencing the higher pheromone concentration. Pom1p may be important for marking the cell ends for this initial relocalisation step since actin becomes delocalised in *pom1Δ* cells after pheromone addition. Tea3p is also required for this step; *tea3Δ* cells do not become bipolar after pheromone addition but remain monopolar suggesting that Tea3p is required to trigger relocalisation of actin to both ends in this intermediate step. But neither Pom1p or Tea3p are required for the establishment of cell polarity during shmooing growth; *tea3Δ* cells shmooed very efficiently and shmooing *pom1Δ* cells recovered from a LatA pulse as well as wild type cells. The LatA pulse also revealed that cell ends during shmooing growth are not as strongly marked as vegetatively growing ends.

In vegetative growth Tea1p is thought to be transported along microtubules in association with Tea2p and Tip1p. Live imaging data suggest that Tea1p and Tip1p mostly co-localise during vegetative growth, but in the presence of pheromone there is an increase in free Tea1p. Most free Tea1p is localised to sites near the cell cortex close to the non-growing end, suggesting that the complex is less strongly held together and falls apart when it reaches the cell ends. On the other hand, Tip1p and Tea2p, which also co-localise during vegetative growth (D. Brunner, personal communication, this study), still co-localise in the presence of pheromone, suggesting that their association remains intact. These results support the idea that the co-localisation of Tea1p with Tip1p-Tea2p is not as strong during shmooing growth as it is during vegetative growth.

In response to pheromone, Tea1p also no longer appears to associate efficiently with microtubules and this could explain why Tea1p does not accumulate at the cell ends. Since Tea1p may act as an anchoring factor for Tea2p and Tip1p at the cells ends (Browning et al., 2000; Brunner and Nurse, 2000) the loss of Tea1p from the growing end may also stop the cell end accumulation of Tea2p and Tip1p. Microtubular dynamics might also be different during shmooing, since their appearance is different, and this could contribute to the loss of morphological factors from one end. The loss of association between Tea1p and microtubules was only observed in G1 and not G2 cells with pheromone. This suggests that the decision to set up a new, shmooing polarised projection or to maintain the old vegetative growth pattern is made during G1 and cannot be made in G2 cells until they have completed division and entered G1 of the next cell cycle.

In the presence of pheromone, *tea1Δ, tip1Δ and tea2.1* exhibit wild type microtubules, suggesting that Tea1p, Tea2p and Tip1p do not play a major role in regulating microtubular dynamics during shmooing. In fact, the presence of these factors seems to be inhibitory for shmooing growth, because in response to pheromone all the mutants set up the new shmooing pattern of growth faster than the wild type cells. FACS analysis showed that the mutants arrested with similar kinetics to wild type cells indicating that the response to pheromone occurs normally, and that it is only the switch to shmooing growth that is accelerated in these mutants. In the absence of any of these factors the vegetative system is probably partially defective and can be dismantled more easily, allowing the new mode of growth to be activated faster.

The machinery involved in positioning growth zones during vegetative growth is no longer required for shmooing cell growth. On the other hand, Ral3p, which is directly involved in actin polymerisation, is still localised to the growing end and *ral3* mutants are known to be defective in shmooing (Fukui and Yamamoto, 1988). This suggests that there might be a core polymerisation machinery which is always the same but its localisation is dictated by different mechanisms in response to intrinsic or extrinsic signals. The pheromone receptor is a good candidate for directing the polymerisation machinery during shmooing growth. Mam2p is highly expressed in response to pheromone and it localises to the shmooing end before actin, consistent with it having a role in directing the localisation of the growth zone in shmooing.

I have shown that the morphological factors Tea1p, Tea2p, Tip1p, Tea3p and Pom1p, involved in setting up and maintaining an internally established axis for

vegetative cell growth, are not required for shmooing growth. Ral3p, which is involved in actin polymerisation more directly, still plays a role in both modes of growth. On the other hand, the pheromone receptor, Mam2p, which is only expressed in response to pheromone, appears to be involved in establishing cell polarity specifically in response to pheromone.

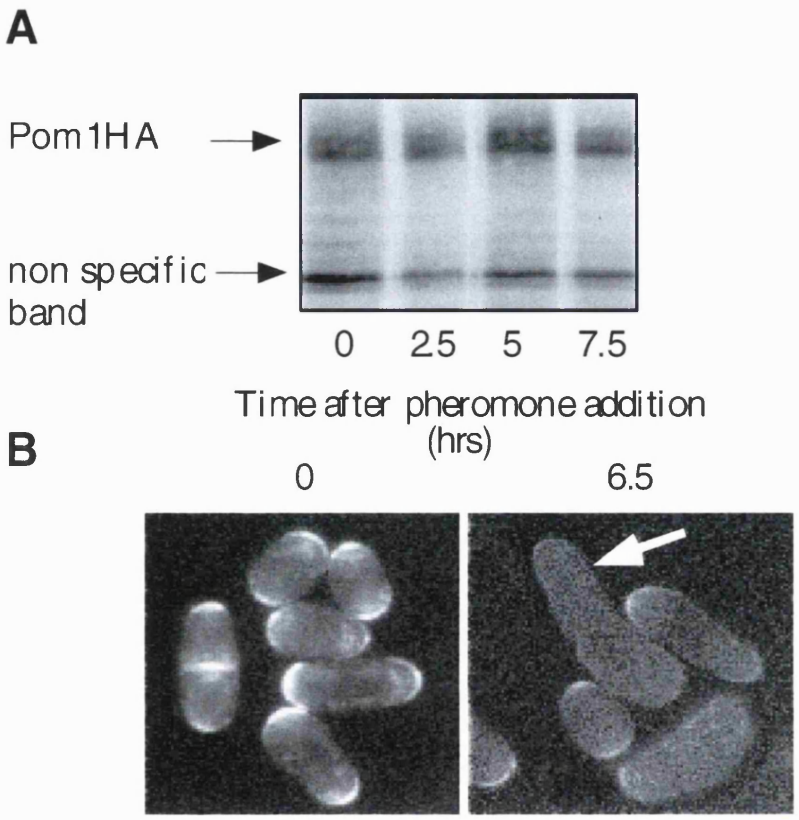

Figure 4.1. Pom1p behaviour in the presence of pheromone.
3μg/ml of P factor was added at time 0 to a *cyr1Δsxa2Δpom1HA* strain (A) or a *cyr1Δsxa2Δpom1GFP* strain (B). (A) Western blot of total cell extracts, probed with anti-HA antibody to visualise Pom1p. (B) Pom1GFP in live cells at time zero and after 6.5 hours in pheromone. The arrow indicates the longest shmoo which shows Pom1GFP diffused throughout the cell.

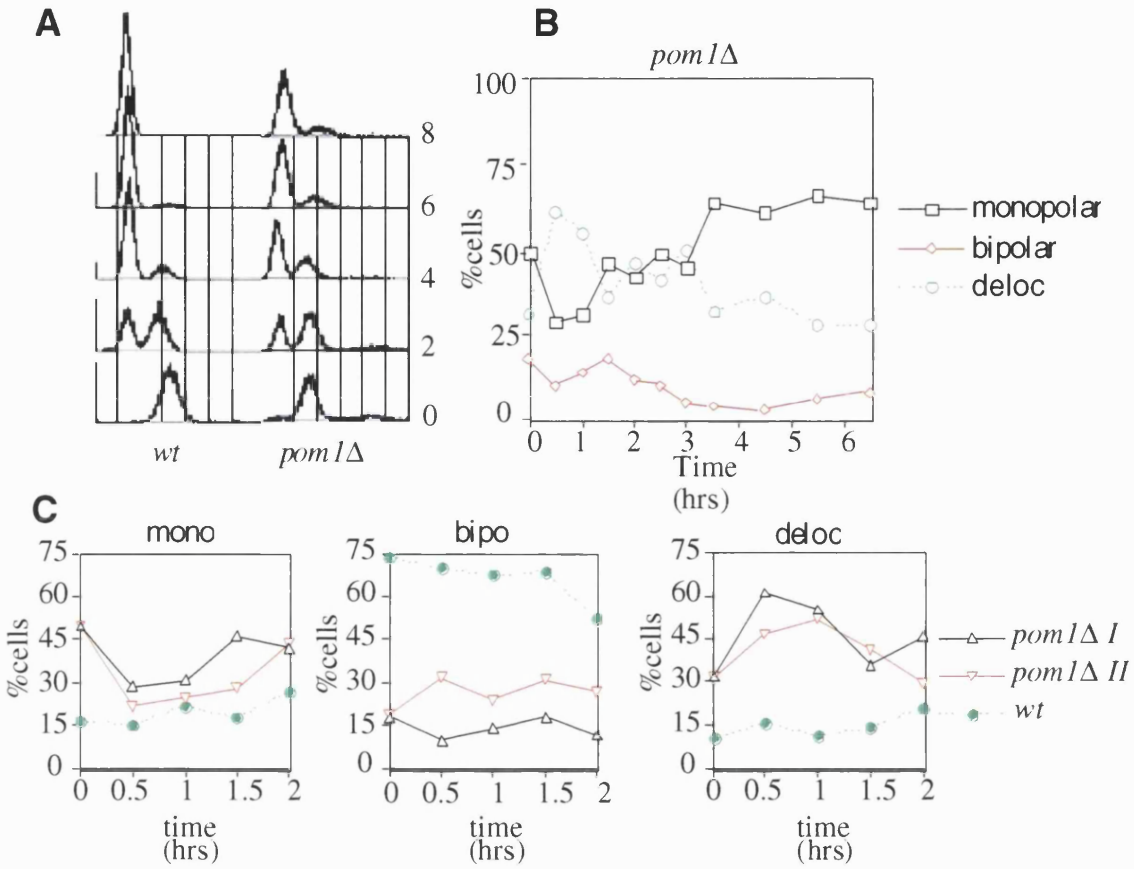

Figure 4.2. Effect of *pom1*Δ on shmooing
3μg/ml of P factor was added at time 0 to a *pom1*Δ*cyr1*Δ*sxa2*Δ, (A) Samples were taken every 2 hours, fixed in ethanol and processed for FACS analysis. (B)Samples were taken every 30 minutes, fixed in formaldehyde, stained with rhodamine phalloidin to visualise actin and scored for actin localisation. (C) The first 2 hours of the time course for two independent experiments (I and II) are plotted together with a wild type control to show the rise in delocalised actin and the reduction in monopolar actin for *pom1*Δ cells.

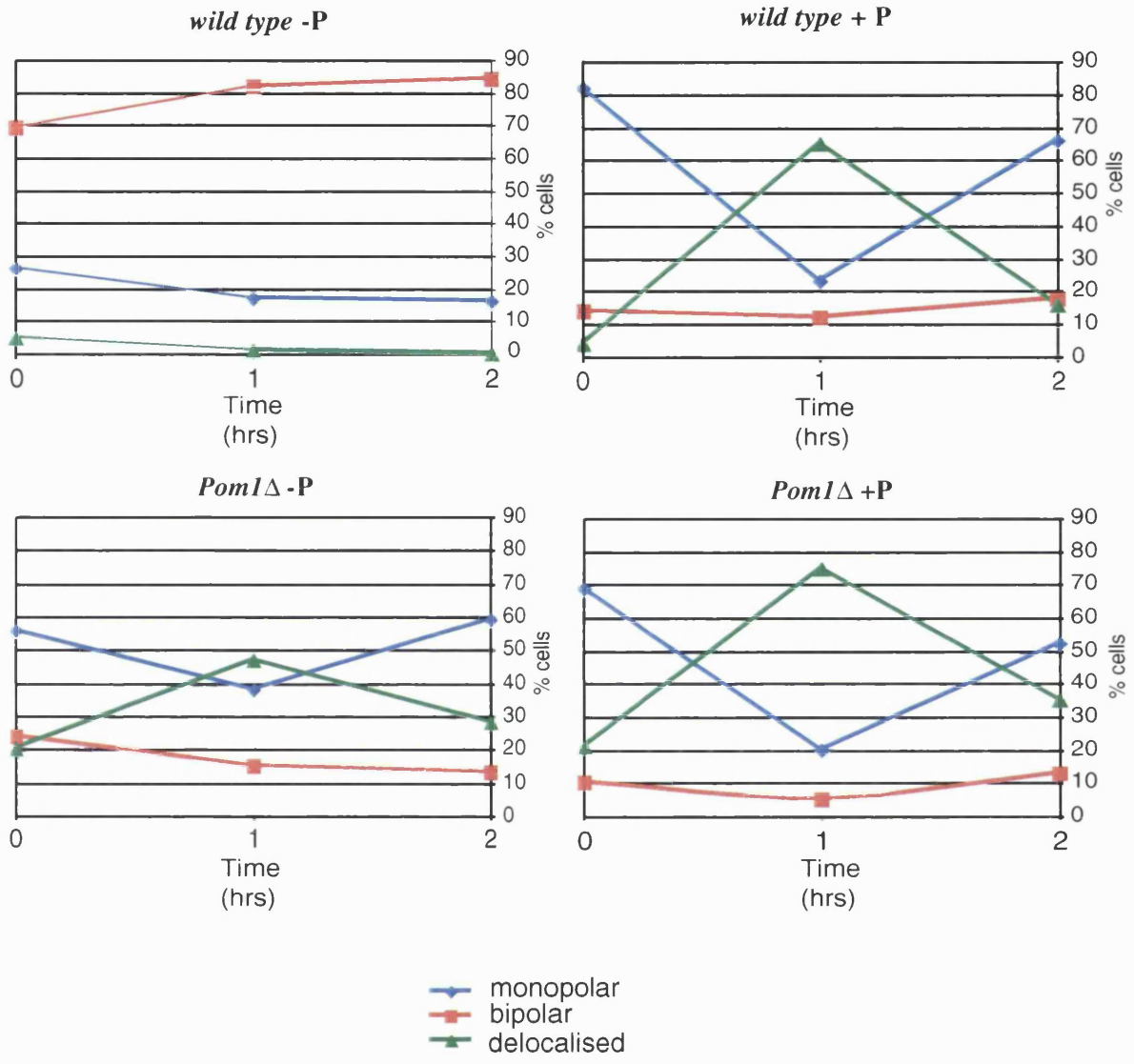

Figure 4.3. Actin relocalisation after a LatA pulse.
Exponentially growing *cyr1Δsxa2Δ* and *cyr1Δsxa2Δpom1Δ* cells were treated with 3µg/l of pheromone (+P) or not (-P), and allowed to grow for a further 5 hours. Cells were then pulsed with 5µM LatA (from a 200µM stock in DMSO) for 8 minutes and allowed to recover for up to 2 hours in pre-conditioned medium (see materials and methods for details). Cells were fixed in formaldehyde before the LatA pulse, after 1 hour and after 2 hours recovery. Cells were then processed for actin staining and actin localisation was scored.

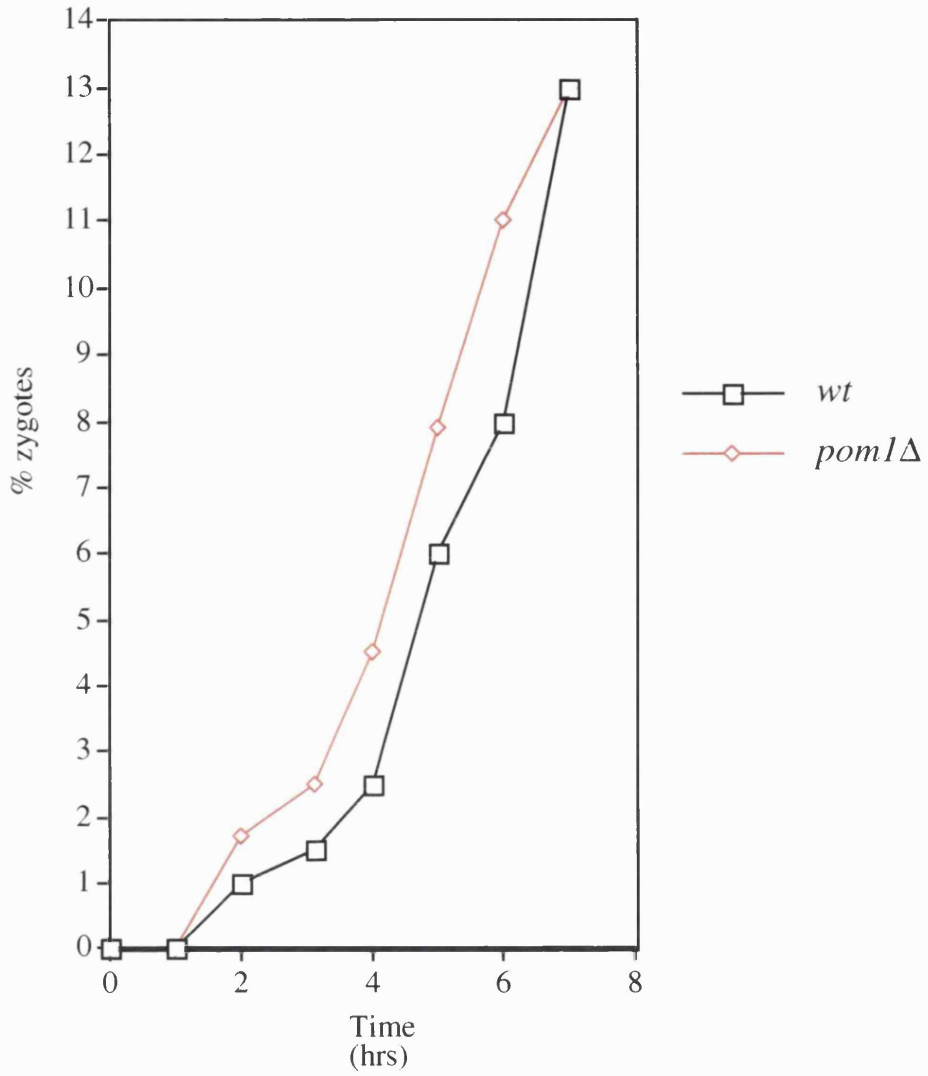

Figure 4.4. *pom1*Δ h90 matings.
h90 wild type and *pom1*Δ strains were grown overnight in full nitrogen and low glucose medium (10g/l) to 2*10E7 cells/ml, cells were then spun and re-suspended in low glucose, nitrogen free medium at 1*10E6 cells/ml to induce mating and fused cells were scored every hour, at least 200 cells were scored for each time point.

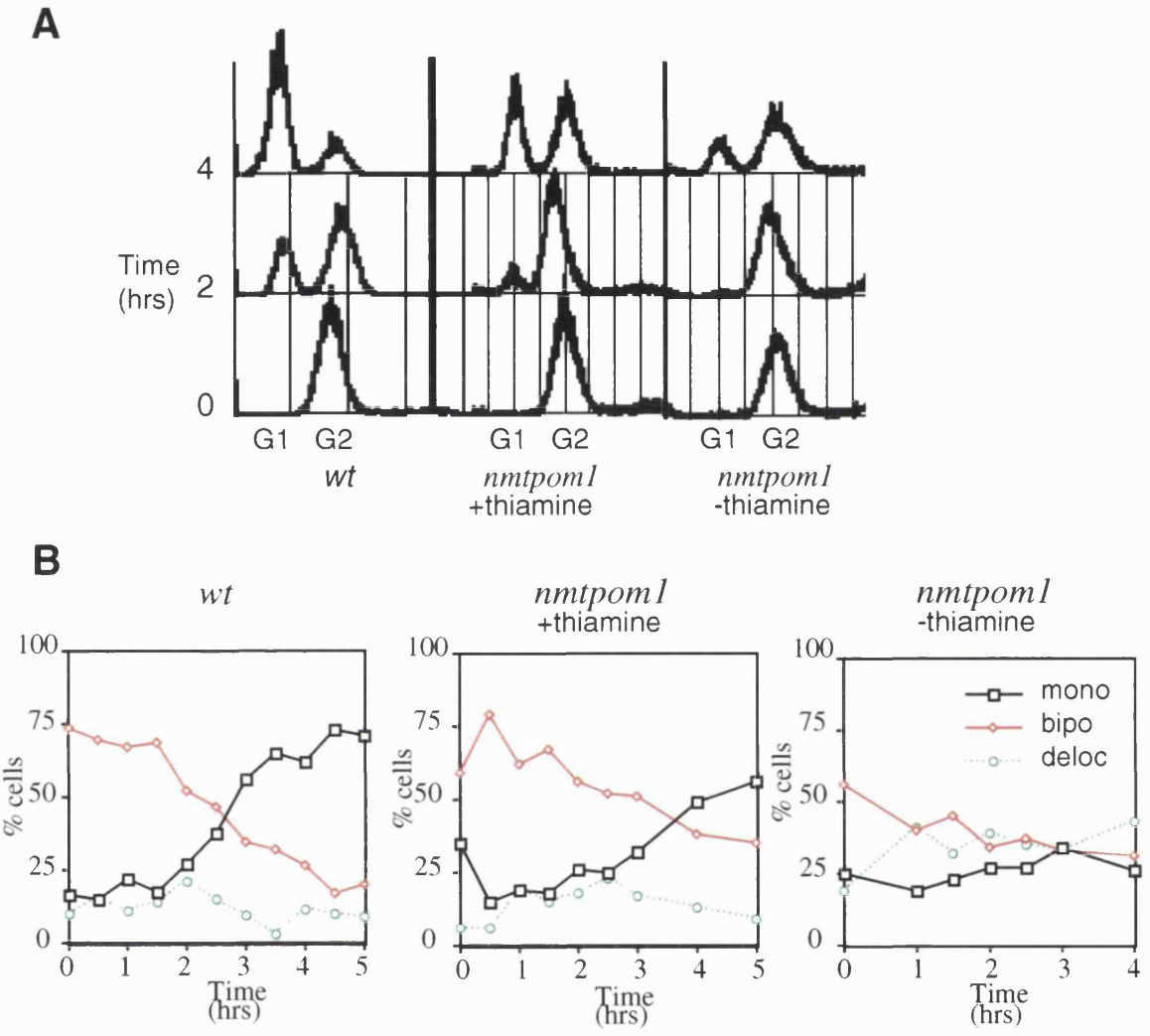

Figure 4.5. Pom1p overexpression.
Cyr1Δsxa2Δ expressing *nmt1-pom1* from a plasmid were grown with or without thiamine for 24 hours, 3µg/l of pheromone was added and (A) samples were taken every 2 horus, fixed in ethanol and processed for FACS analysis. (B) Samples were taken every 30 minutes, fixed in formaldehyde, processed for actin staining and scored for actin localisation. A typical wild type FACS and actin profile is shown for comparison.

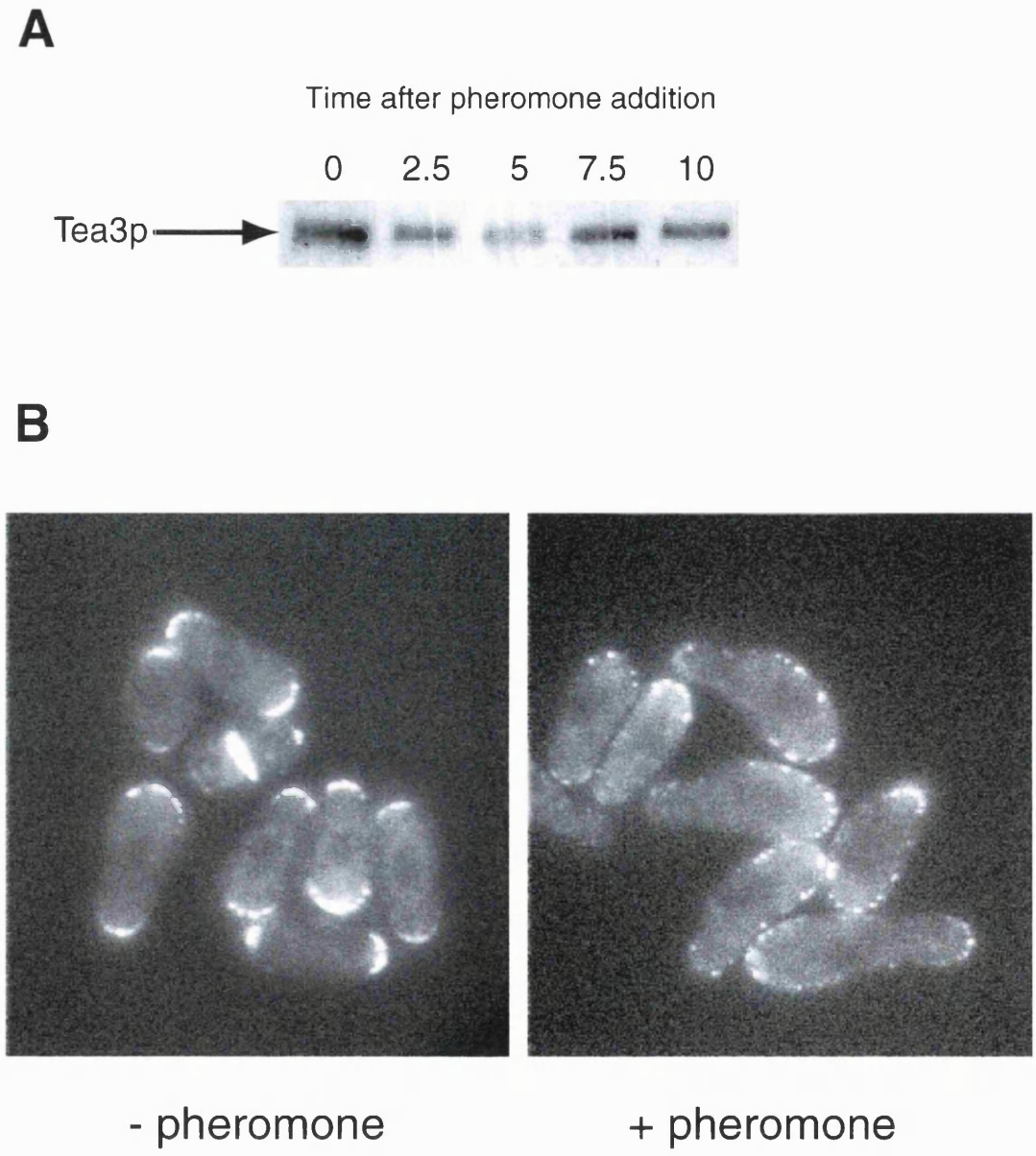

Figure 4.6. Tea3p behaviour in the presence of pheromone.
(A) Pheromone was added to a *cyr1Δsxa2Δ* and western blots of total cell extracts from different timepoints were probed with anti-Tea3 antibody. (B) Tea3GFP was imaged before pheromone addition and 6 hours after the addition of pheromone.

A

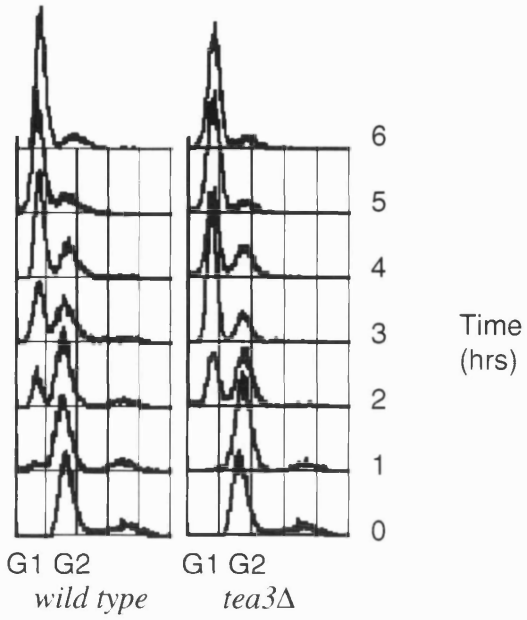

B

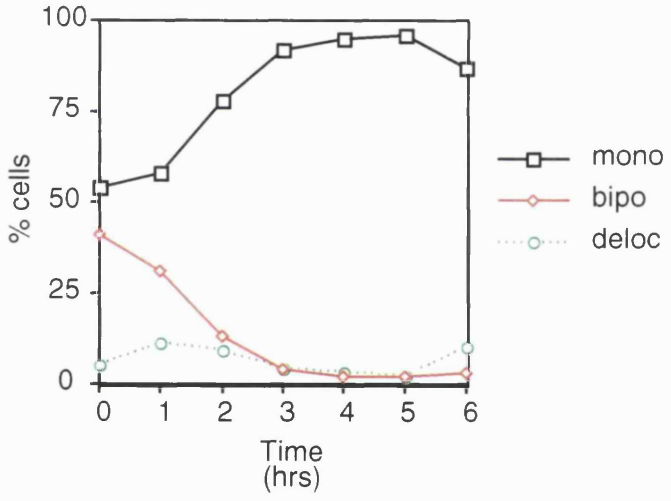

Figure 4.7. Response of *tea3*Δ cells to pheromone.
Pheromone was added to exponentially growing *tea3*Δ*cyr1*Δ*sxa2*Δ cells and (A) samples were taken every hour, fixed in ethanol and processed for FACS analysis. (B) Samples were taken every hour, fixed in formaldehyde, processed for actin staining and scored for actin localisation.

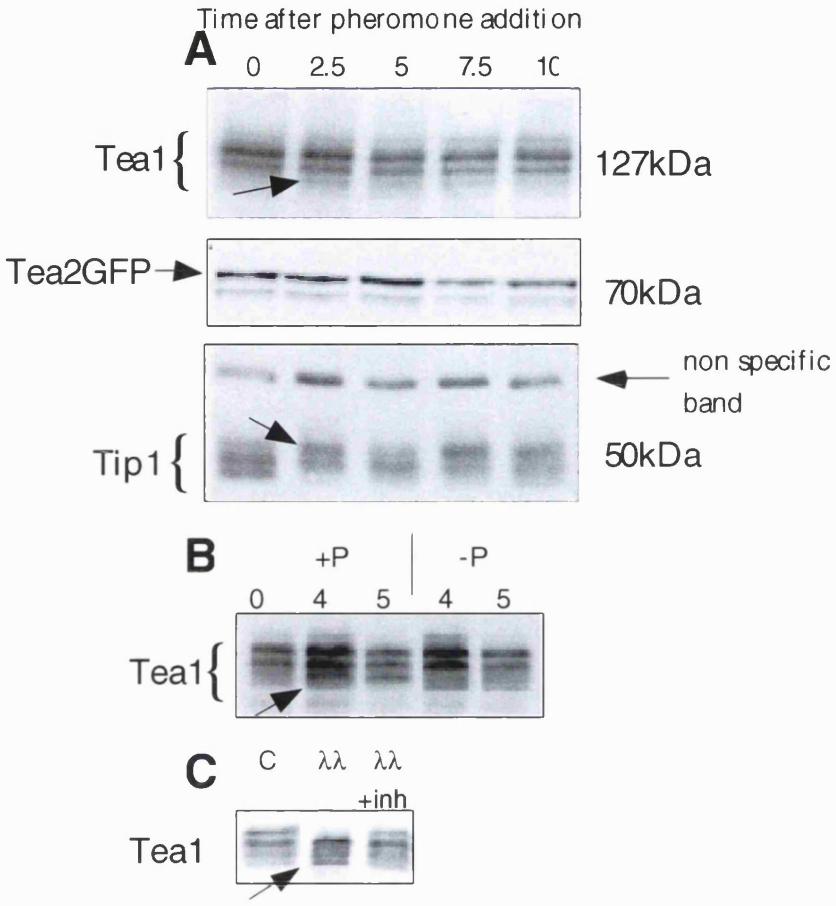

Figure 4.8. Protein levels during a pheromone time course.
(A) Western blot of total cell extracts from a pheromone time course probed with anti-Tea1, anti-GFP for Tea2GFP and anti-Tip1 antibodies. New forms of proteins appearing after pheromone addition are marked by arrows. (B) Cells were shifted to 36˚C in the presence or in the absence of pheromone for 4 hours. Cells at 36˚C in the presence of pheromone arrest in G1 but do not activate the shmooing growth mode. Cells were then released at 25˚C to allow synchronous progression into shmooing growth. Samples were taken at time 0, after 4 hours at 36˚C and after 1 hour release and western blots were carried out on total cell extracts for Tea1p. (C) Native cell extracts were made from vegetativelly growing cells and treated with Lambda phosphatase in the absence -λλ- or in the presence -λλ+inh- of phosphatase inhibitors, an untreated sample is run as a control -C-. Western blots were probed for Tea1p

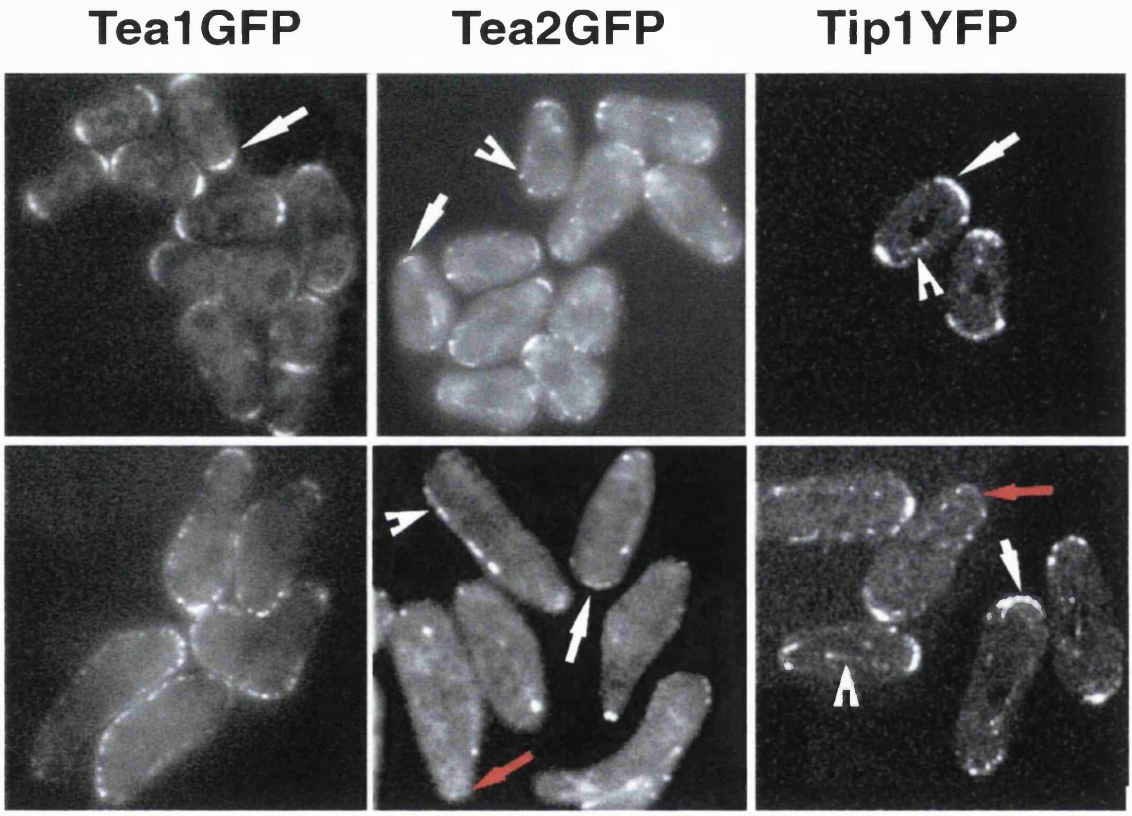

Figure 4.9. Tea1p, Tea2p and Tip1p delocalise in the presence of pheromone. Exponentially growing *cyr1Δsxa2Δtea1GFP, cyr1Δsxa2Δtea2GFP, cyr1Δsxa2Δtip1GFP* (upper panels) were induced with 3μg/l pheromone for 6 hours (lower panels) and then photographs were taken. The cell end localisation is marked by white arrows and to the lack of cell ends localisation is marked by red arrows. White arrowheads indicate microtubular localisation.

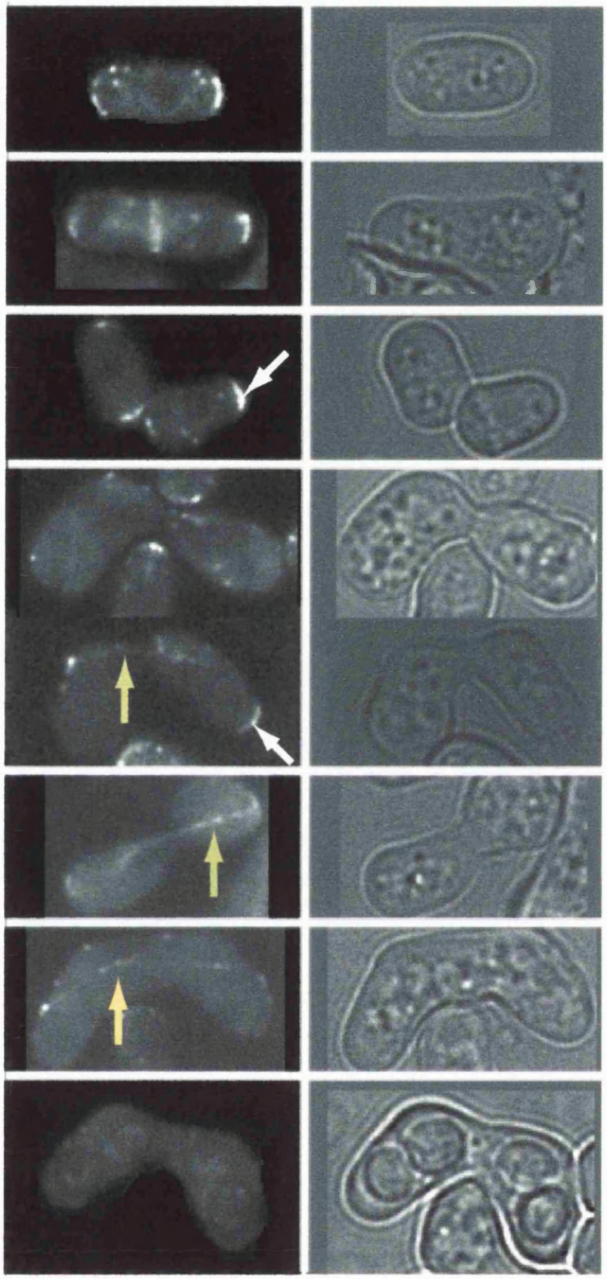

Figure 4.10. Tea2GFP localisation during a wild type mating.
Tea2GFP h90 cells were mated overnight on glutamate plates and photographs were taken of various stages of mating. White arrown indicate the cell end localisation and the yellow arrows the microtubular localisation.

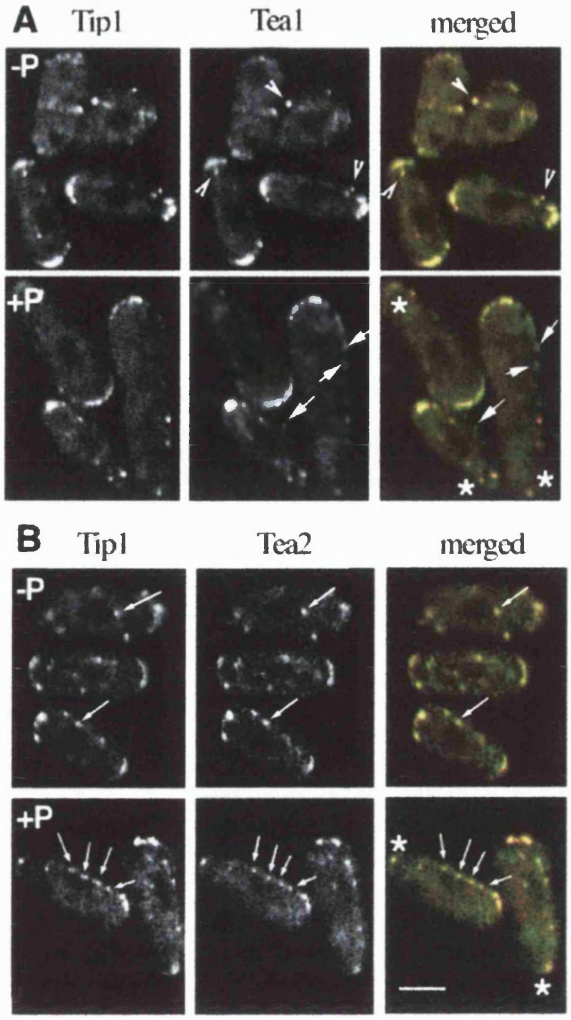

C

Quantitation of the colocalisation of Tea1GFP with Tip1YFP

	-pheromone	+pheromone
Free Tea1p	1.5% (n=193)	17% (n=95)
Free Tip1p	16% (n=227)	23% (n=102)

Figure 4.11. Tea1p, Tip1p and Tea2p partially delocalise in the presence of pheromone.

(A) *tip1YFPtea1GFPcyr1Δsxa2Δ* (B) and *tip1YFPtea2GFPcyr1Δsxa2Δ* strains were used to determine colocalisation in vivo. Cells were grown in minimal medium without or with pheromone for 5 (A) or 7 (B) hours. Pictures were taken with a confocal microscope using YFP and CFP filters which allow excitation and detection each fluorophore separately. The more narrow ends, here marked by *, are known to be growing from previous calcofluor and actin stainings. The arrows in A indicate the Tea1GFP dots co-localising with Tip1YFP in the absence of pheromone but not in the presence of pheromone. In B the arrows indicate the Tea1GFP dots co-localising with Tip1YFP both in the presence and absence of pheromone. Scale bar, 3μm. (C) The colocalisation of Tip1YFP and Tea1GFP was quantitated for *tea1GFP tip1YFP cyr1Δsxa2Δ* strain in the absence and in the presence of pheromone. The number of Tip1YFP dots without any Tea1GFP and the number of Tea1GFP dots without any Tip1YFP was scored and expressed as percentages of the total number of dots scored (n). Scale bar=3μm.

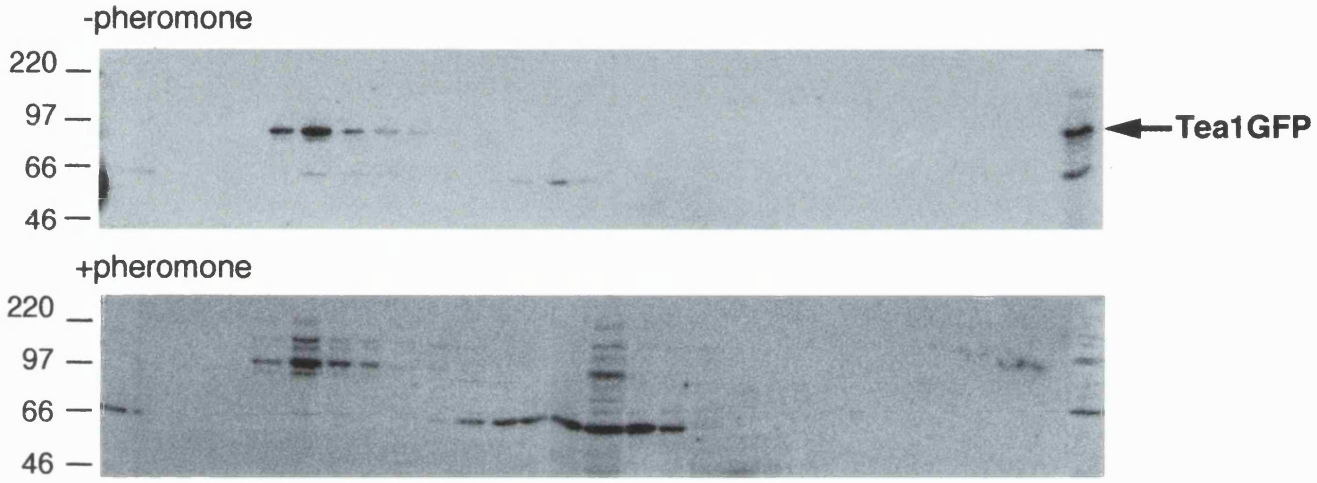

Figure 4.12. Tea1p gel filtration.
Tea1GFP cyr1Δsxa2Δ cell extracts without or with pheromone for 8 hours were mixed with *cyr1Δsxa2Δ* cell extracts with or without pheromone, respectively, so that all samples would have equal levels of proteases, which are induced upon mating.
Gel filtration was carried out as described in the materials and methods and the fractions were run on a SDS-acrylamide gel and western blotted with GFP antibodies.

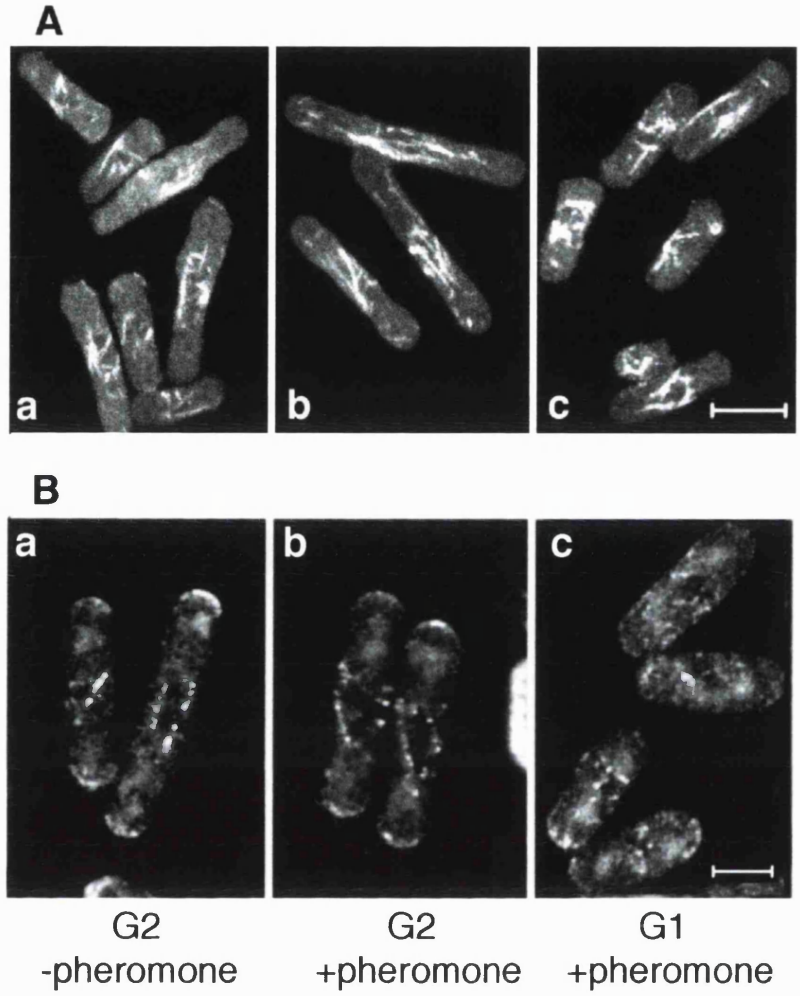

Fig 4.13. Tea1 localisation in the presence of pheromone in G2 and G1.
A *cdc25-22cyr1Δsxa2Δtea1GFP* strain was arrested in G2 at 36˚C for 90 minutes, pheromone was then added, cells were incubated for a further 2 hours and then released into cell cycle progression at 25˚C in the continued presence of pheromone. Samples were taken at three different time points: (a) when cells were arrested in G2 at 36˚C in the absence of pheromone, (b) after having been incubated with pheromone for 2 hours at 36˚C, (c) and after cells had been allowed to enter G1 at 25˚C in the continued presence of pheromone. Cells from each time point were treated with MBC, a microtubule depolymerising drug, to totally depolymerise microtubule, the drug was then washed out and microtubules were allowed to repolymerise for 50 seconds. (A) Cells were fixed in methanol and processed for tubulin immunofluorescence while (B) Tea1GFP was imaged live on a confocal microscope (see Materials and Methods for details). Scale bar, 5μm.

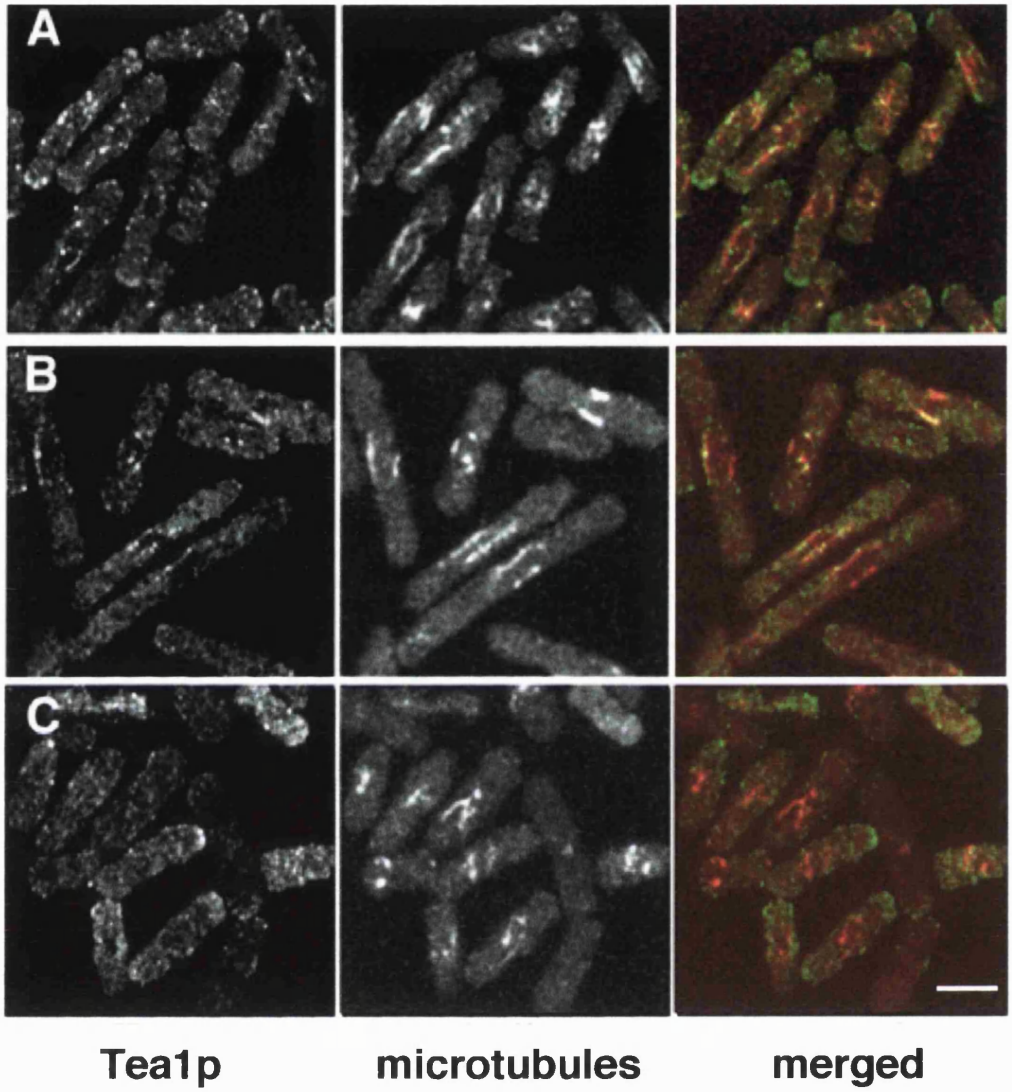

Figure 4.14. Tea1 localisation in the presence of pheromone in G2 and G1.
A *cdc25-22cyr1Δsxa2Δ* strain was arrested in G2 at 36˚C for 90 minutes, pheromone was added, cells were incubated for a further 2 hours and then released into cell cycle progression at 25˚C in the continued presence of pheromone. Samples were taken at three different time points: (A) after cells had been arrested in G2 at 36˚C in the absence of pheromone, (B) after having been incubated with pheromone for 2 hours at 36˚C, (C) after cells had been allowed to enter G1 at 25˚C in the continued presence of pheromone. Cells from each time point were treated with MBC, a microtubule depolymerising drug, to totally depolymerise microtubules, the drug was then washed out and microtubules were allowed to repolymerise for 50 seconds. Cells were fixed in methanol and processed for tubulin and Tea1p immunofluorescence. Scale bar=3μm.

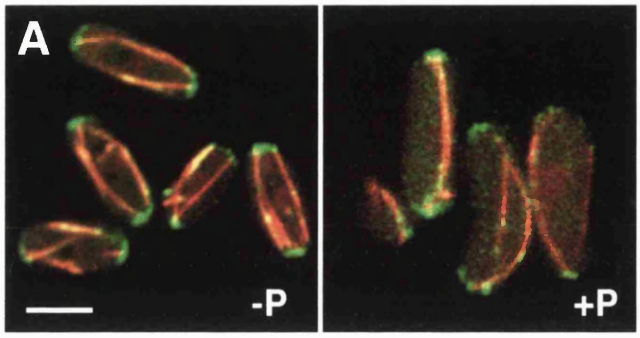

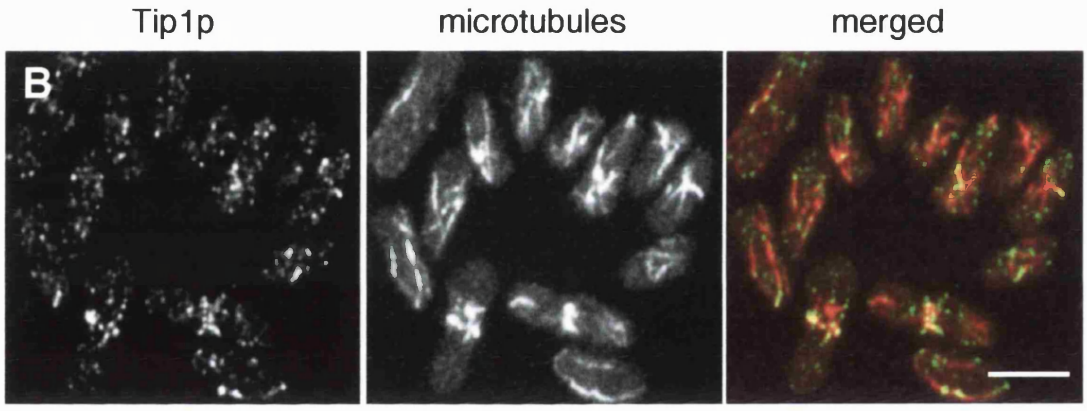

Figure 4.15. Tip1 and microtubules during shmooing.
(A) *Tip1YFP atb2CFP cyr1*Δ*sxa2*Δ cells were grown for 6 hours in the absence of thiamine without pheromone (-P) or with 3μg/ml of pheromone (+P), and photographs were taken with a confocal microscope. Images shown are single planes through the cell middle. (B)A *cdc25-22cyr1*Δ*sxa2*Δ strain was arrested in G2 at 36˚C for 90 minutes, pheromone was added, cells were incubated for a further 2 hours and then released into cell cycle progression at 25˚C in the continued presence of pheromone. Cells were treated with MBC, a microtubule depolymerising drug, to totally depolymerise microtubule, the drug was then washed out and microtubules were allowed to repolymerise for 50 seconds. Cells from the last timepoint were fixed in methanol and processed for tubulin and Tip1p immunofluorescence. Scale bar= 3μm.

A

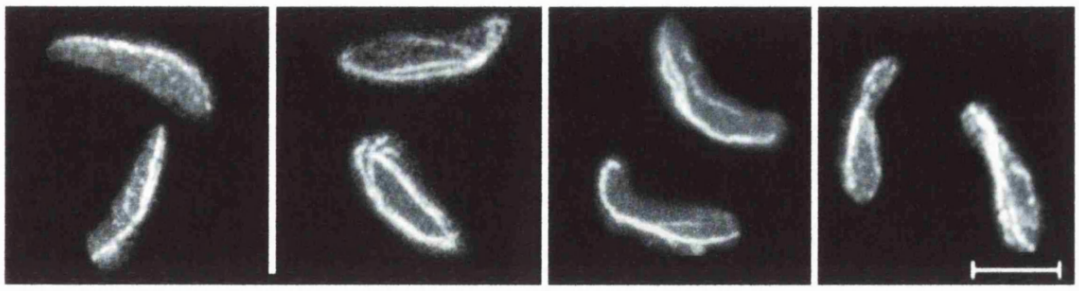

B

Microtubule length in the presence and absence of pheromone

mutant	mean cell length	mean MT length	TTEST
wt +HU	7.35±1.60	7.06±1.61	0.13
wt +P	7.00±2.26	6.80±2.17	0.59
Tea2.1+HU	6.02±1.82	4.34±1.26	1.09E-5
Tea2.1+P	6.44±1.40	6.44±1.40	0.933
Tip1Δ+HU	6.86±1.68	4.90±1.82	1.83E-12
Tip1Δ+P	6.86±1.96	6.58±2.10	0.20

C

Mutant	+HU	+P
wt	3%	20%
tea1Δ	17%	23%
tip1Δ	0%	25%
tea2.1	0%	25%

Figure 4.16. *Tea1Δ*, *tip1Δ* and *tea2.1* microtubules in the presence of pheromone
(A) Cells were treated with 3μg/ml P factor for 9 hrs, then fixed in methanol and cells were stained with anti-tubulin antibody. (B) The length of microtubules and the length of the cells was measured with NIH image in μm for three independent experiments (n=100x3). The length of the microtubules was then compared with the length of the cells with a T-TEST which gave an indication of how similar the microtubules length was to the cell length, a T-TEST value of 1 means that the length of microtubules is the same as the length of the cell. (C) The percentage of cells with microtubules curving round their ends was scored for wild type and mutants cells treated with P factor or HU, as a control, for 8 hours. At least 100 cells were scored in three independent experiments. Scale bar, 3μm.

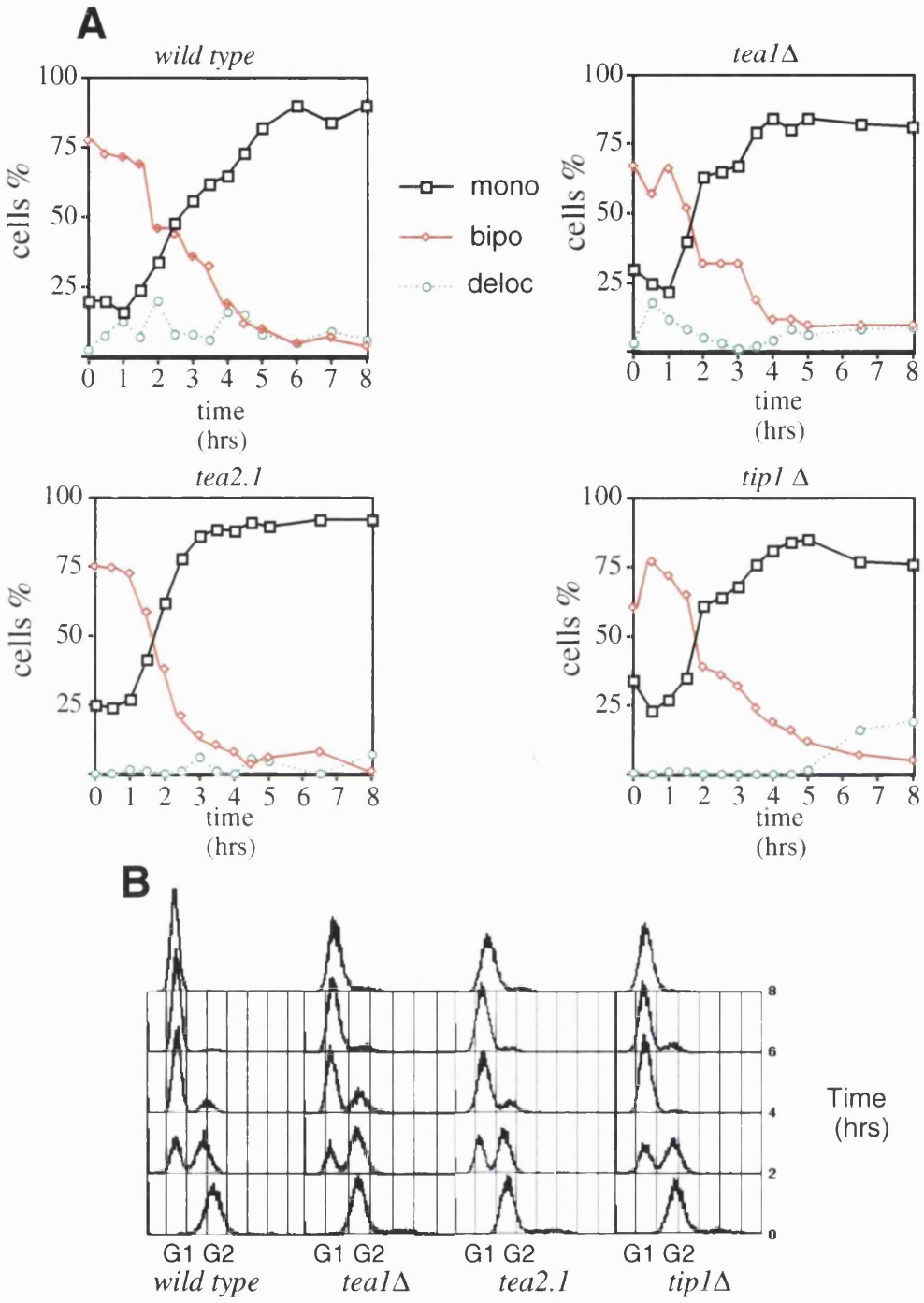

Figure 4.17. Actin relocalisation in the mutants strains.
3µg/ml of P factor was added at time 0. (A) Samples were taken every 30 minutes, fixed in formaldehyde for 40 minutes and stained for actin with rhodamine phalloidin. Actin localisation was scored for each time point. (B) Samples were taken every 2 hours, fixed in ethanol and processed for FACS analysis.

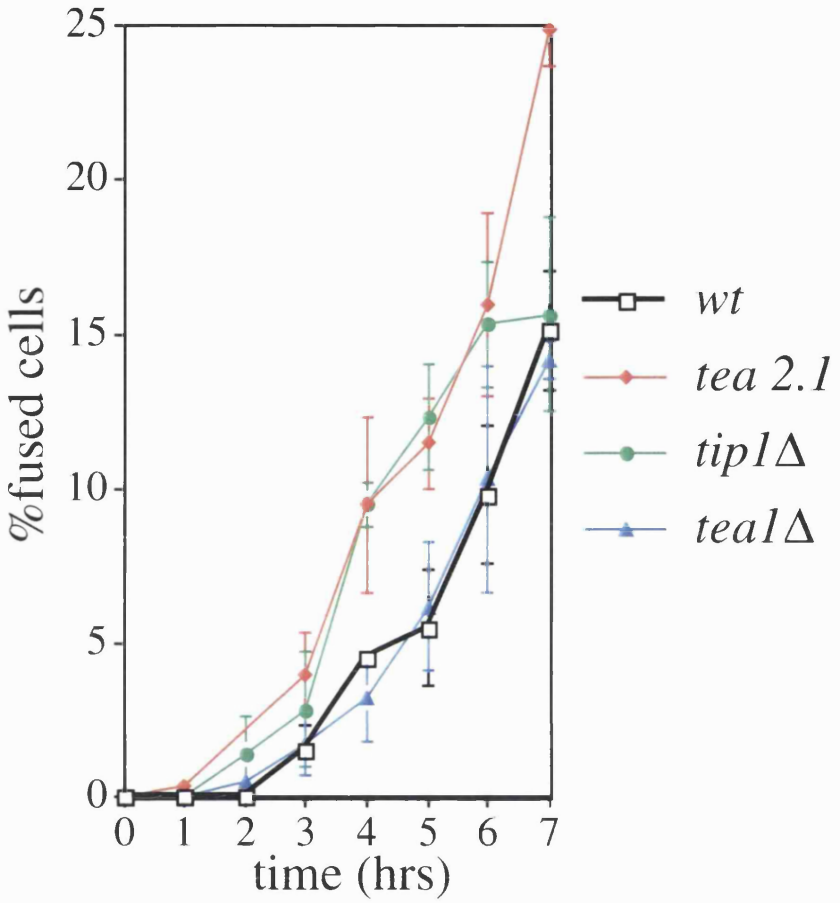

Figure 4.18. h90 mutants' matings.
h90 wild type and mutant strains were grown overnight in full nitrogen and low glucose medium (10g/l) to 2*10E7 cells/ml, cells were then spun and re-suspended in low glucose, nitrogen free medium at 1*10E6 cells/ml to induce mating and fused cells were scored every hour. Experiments were repeated at least three times and at least 200 cells were scored for each time point, standard deviation was calculated and error bars are shown.

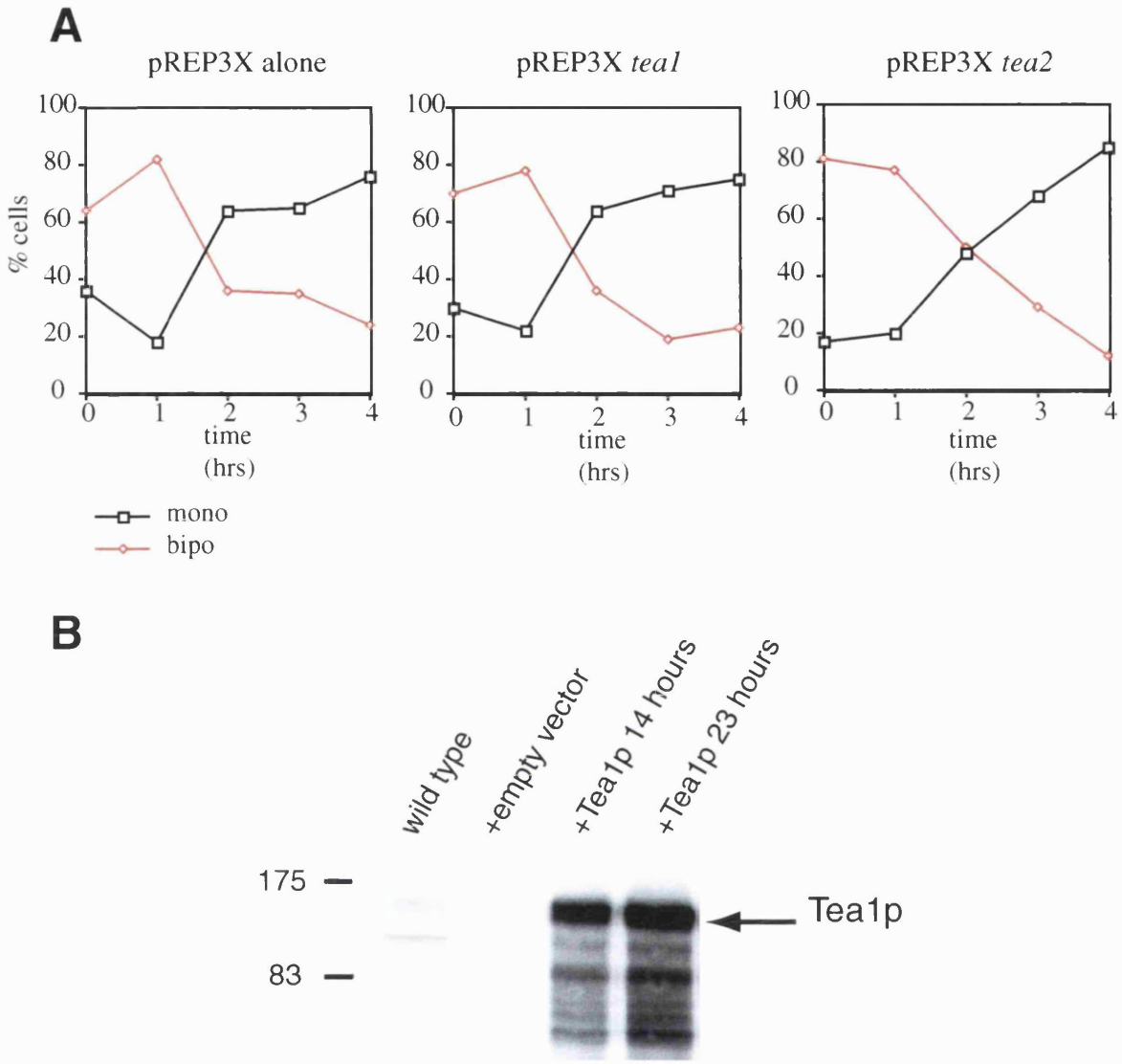

Figure 4.18. Effect of Tea1p and Tea2p overexpression.
A *cyr1Δsxa2Δ* strains expressing either Tea1p or Tea2p from a plasmid, under the control of the *nmt1* promoter, were grown for 14 hours in -thiamine medium, a control culture carrying an empty plasmid was used as a control. 3µg/l of pheromone was added to each culture and samples were taken every hour, fixed in formaldehyde and processed for actin staining and scored for actin localisation. (B) Samples were taken from a wild type culture, one carrying the empty pREP3X and one carrying the pREP3X-*tea1+*, induced for 14 hours and 23 hours. Western blots of total cell extracts were carried out and probed with anti-Tea1 antibody.

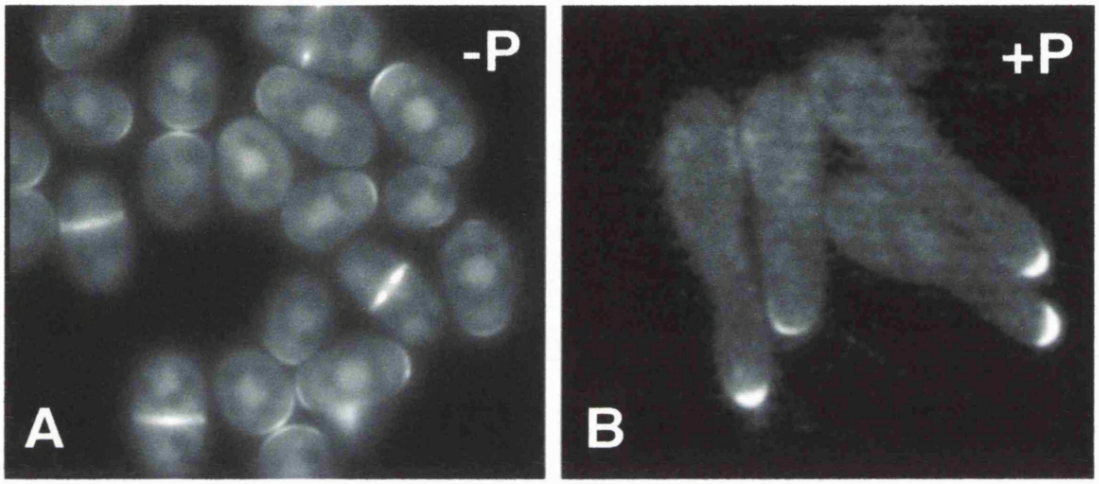

Figure 4.20. Ral3p localisation during shmooing.
(A) *cyr1Δsxa2Δ nmt1ral3GFP* were grown over-night in the absence of thiamine,(B) pheromone was then added for 9 hours to induce shmooing, at the same time thiamine was added to stop Ral3p levels from becoming too high and affecting shmooing morphology,

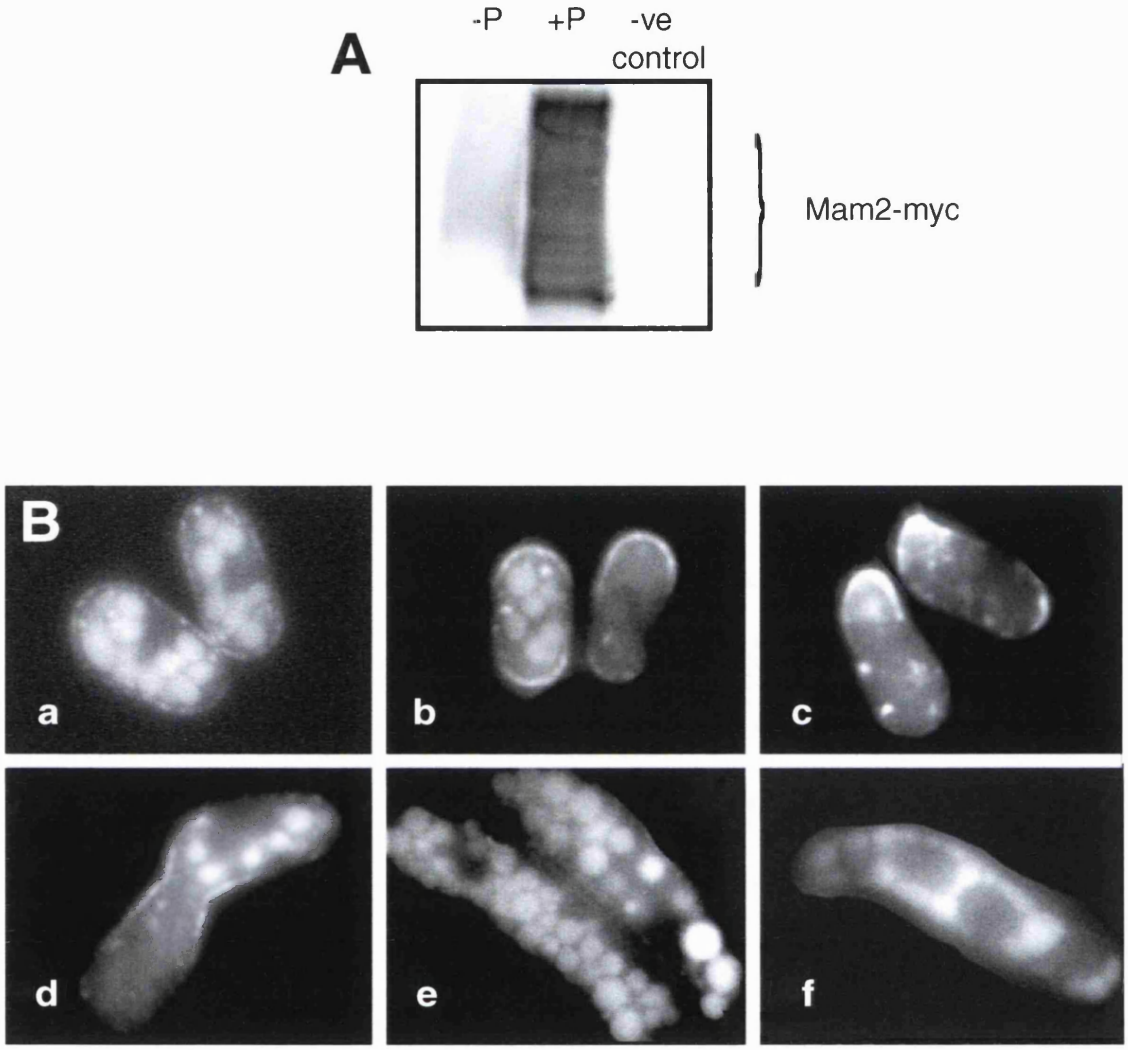

Figure 4.21. Mam2 is induced during shmooing and localises to the mating projection.

(A) *Mam2 myc cyr1Δsxa2Δ* cells were induced with pheromone for 5 hours,extracts were made at time 0 and after 5 hours and probed with anti-myc. (B) *Mam2GFP h-* was crossed to *wild type h+* on plates and photographs were taken of the various stages of mating.

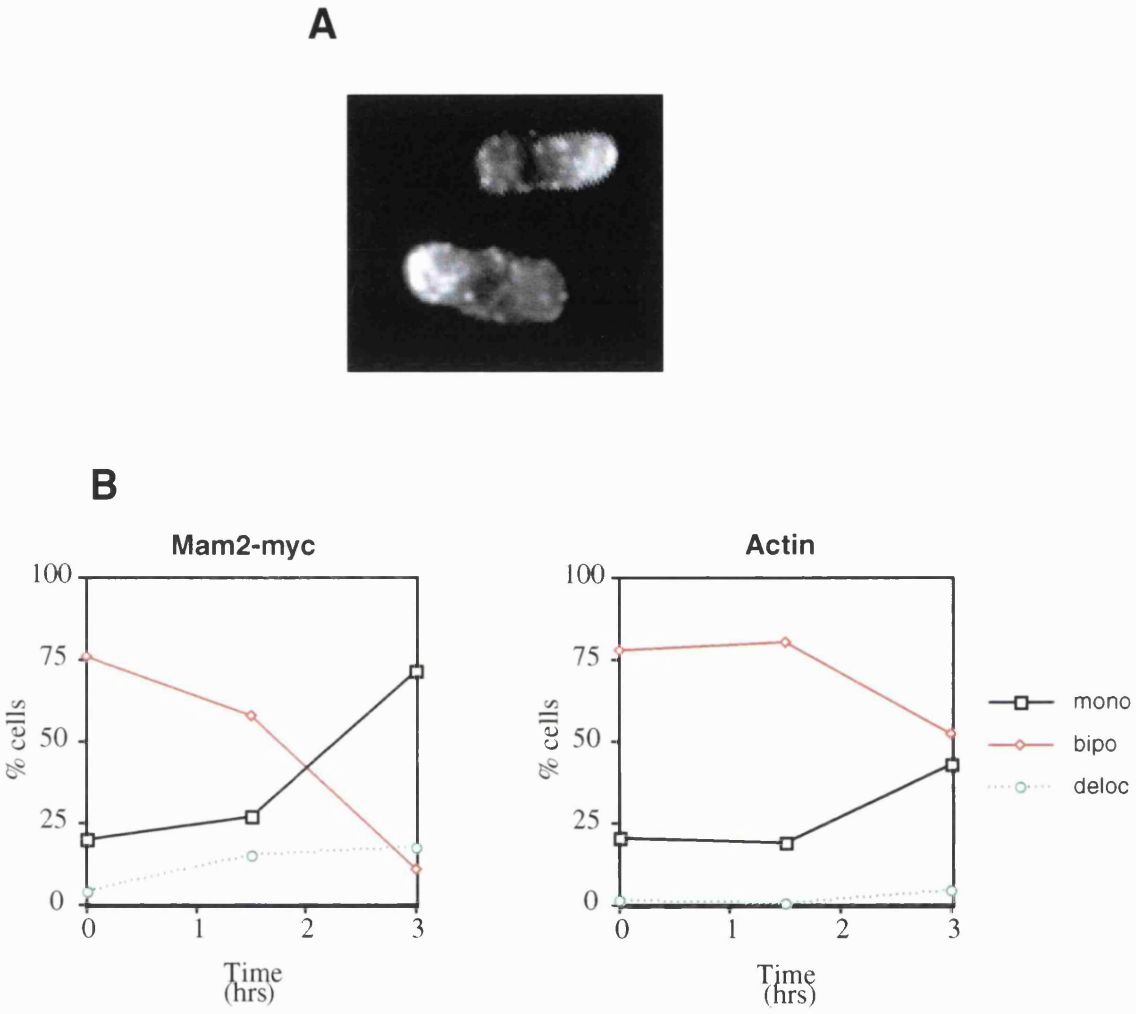

Figure 4.22. Mam2 localisation during shmooing.
(A) *Mam2myc cyr1Δsxa2Δ* cells were treated with 1.5μg/l of pheromone for 5 hours, cells were fixed in formaldehyde and stained with anti-myc antibody. (B) *Mam2myc cyr1Δsxa2Δ* cells were treated with 1.5μg/l of pheromone, samples were taken every 1.5 hours, fixed in formaldehyde and immunostained with anti-myc to visualise Mam2-myc and with rhodamine phalloidin to visualise actin. Monopolar or bipolar localisation of the two proteins was then scored.

Chapter 5

Regulation of microtubular dynamics during shmooing

5.1 Introduction

In the previous chapter I described how morphological factors, involved in regulating microtubular dynamics during vegetative growth, are not involved in the regulation of microtubular dynamics during shmooing. The mutant screen designed to provide me with morphological factors specific for shmooing cell growth failed to identify any mutants. I therefore took a candidate gene approach and looked for possible homologues of the vegetative specific factors, that could take on their roles during shmooing growth. I have shown that Tip1p, which is involved in stabilising microtubules during vegetative growth plays no role in shmooing growth. Tip1p has a homologue in fission yeast: Ssm4p, a glued-type protein (Fig 5.1) (Brunner and Nurse, 2000[Yamashita, 1997 #716). Ssm4 is transcribed during mating and an over-expressed GFP-tagged version localises to microtubules (Yamashita et al., 1997), and therefore it could be involved in microtubule regulation during shmooing.

The *ssm4+* gene encodes a protein with the same domain structure as Tip1p, with a coiled coil region and a CAP-Gly microtubule binding domain (Yamashita et al., 1997), but does not have the serine rich region or the carboxy-terminal metal binding motif of Tip1p (Fig 5.2). Ssm4p has the same domain structure as Glued (Fig 5.2). Glued is part of the dynactin complex, which interacts with cytoplasmic dynein and microtubules and is required for most of dynein-mediated cellular activities (Gill et al., 1991; Holzbaur et al., 1991; Quintyne et al., 1999; Schafer et al., 1994; Waterman-Storer and Holzbaur, 1996). Cytoplasmic dynein is a minus-end-directed motor protein, which performs essential functions in vesicular transport, spindle organisation, and nuclear migration (Karki and

Holzbaur, 1999)((King, 2000). Dhc1p, dynein heavy chain and Dlc1p, dynein light chain are involved in the regulation of microtubular dynamics during mating in fission yeast (Miki et al., 2002; Yamamoto et al., 1999).

In this chapter I analyse the role of Ssm4p in the regulation of microtubular dynamics during mating and show that it collaborates with the CLIP-170 homologue Tip1 to generate a shmooing microtubular array. As in the previous chapter, all experiments were carried out in the *cyr1Δsxa2Δ* background unless otherwise stated.

5.2 Results

5.2.1 *Ssm4Δ* cells do not display any horsetail nuclear movement

Ssm4p, a homologue of Tip1p, is transcribed during mating and it localises to microtubules (Yamashita et al., 1997). It therefore is a good candidate for regulator of microtubules in shmooing cells. To verify this I analysed the effect of a deletion of *ssm4* on microtubule dynamics. Shmooing cells, like zygotes, are known to display a characteristic "horsetail" nuclear movement, in which the nucleus oscillates back and forward in the cell (Ding et al., 1998). This movement is driven by microtubules, which also display a typical oscillatory dynamics during shmooing and are linked to the nucleus probably via the Spindle Pole Body (SPB) (Ding et al., 1998; Svoboda et al., 1995) (Fig 5. 3). Mutant strains which display abnormal microtubular dynamics, like *dhc1* and *dlc1* mutants, also show defective nuclear movement (Miki et al., 2002; Yamamoto et al., 2001; Yamamoto et al., 1999). Monitoring the nuclear oscillations is therefore a good and

easy way to check if microtubular dynamics are defective. I expressed a GFP-tagged nuclear marker in *ssm4Δ* and wild type cells and analysed the nuclear movement in response to pheromone. Whereas wild type cells displayed a clear movement of the nucleus spanning the whole of the cell length, *ssm4Δ* hardly showed any nuclear movement, with the nucleus being mostly stationary in the middle of the cell (Fig 5.4 A and B). This suggests there might be a defect in the dynamics of microtubules in *ssm4Δ* shmooing cells, which results in the lack of any oscillatory nuclear movement. An alternative explanation is that in *ssm4Δ* cells the nucleus is not linked to the SPB or the microtubules, and therefore can not be pulled as the microtubules oscillated. To rule this out I analysed the localisation of the nucleus relative to the SPB and the microtubules in *ssm4Δ* cells. I fixed vegetative and shmooing *ssm4Δ* cells and immunostained them for tubulin and Sad1p, a SPB marker (Hagan and Yanagida, 1995), and visualised the nucleus with DAPI (4',6-diamidino-2-phenylindole, dihydrochloride.), a fluorescent DNA dye. The nucleus was always touching the SPB and the microtubules (Fig 5.5), suggesting that they were still associated. A lack of association with the SPB is therefore unlikely to be the reason for the absence of nuclear movement in *ssm4Δ* cells.

5.2.2 *Ssm4Δ* cells display defective microtubular dynamics

I next analysed the microtubular dynamics in wild type and *ssm4Δ* cells. To generate this oscillatory movement, microtubular dynamics at opposite ends of the cell might be co-ordinated, with microtubules polymerising at one end whilst depolymerising at the opposite end. I will refer to this as "co-ordinated" behaviour. To verify if wild type microtubules exhibited co-ordinated behaviour I monitored live microtubular dynamics

during shmooing, measuring microtubule length at each timepoint (Fig 5.6B) and calculating whether they were polymerising or depolymerising. Each cell end had 1-5 microtubules at a given time. I compared the dynamics of microtubules at the same end for each time-point and in 80% of cases the majority of microtubules displayed similar dynamics. I took this as a "consensus dynamics" for an end. I then compared the consensus dynamics at both cell ends for each time-point and analysed if they exhibited co-ordinated behaviour, discounting stalling microtubules. In 80% of cases microtubules at opposite cell ends displayed opposite dynamics (Fig 5.6 A and B, see materials and methods for details).

One way the oscillatory movement could be generated is by the SPB moving on the plus ends of polymerising microtubules. This assumes that the polarity of the microtubules is switched compared to vegetative growth, with minus ends being at the cell ends and the plus ends at the SPB. Another way is for the microtubule plus ends to remain at the cortex and pull or push on the SPB as they grow and shrink. To investigate the polarity of microtubules I bleached a portion of a microtubule and monitored the recovery of the fluorescence. If the plus ends were at the SPB then the distance between the SPB and the bleached area should change as the SPB moves on polymerising microtubules. If, on the other hand, the plus ends are at the cell end and the minus ends at the SPB, the distance between the SPB and the bleached area should not change and it should always recover from the side closer to the SPB, as a new microtubule polymerises. This was indeed the case, the distance between the bleached area and the SPB did not change. The bleached area moved in the same direction as the SPB (Fig 5.7A and B) and

it always recovered from the SPB (Fig 5.7A). Fig 5.7A also shows that a new microtubule could polymerise along a pre-existing bundle. Occasional sliding of microtubules was observed (Fig 5.7B), but this was never dramatic and probably was not a major contributor to nuclear movement. I conclude that microtubules are polymerised from the SPB and that the plus ends of microtubules are distal to the SPB and the minus ends at the SPB.

The horsetailing nucleus could therefore either be pulled by the microtubules ahead of the nucleus or pushed by those behind. It has been proposed that this movement is driven by a pulling force generated on microtubules at the cell ends (Yamamoto et al., 2001). Since microtubules do not curl around the body of the cell, they must depolymerise as they are pulled. To confirm that a pulling force was acting on depolymerising microtubules I bleached a small area on a microtubule, added MBC and monitored microtubules' dynamics as they depolymerised. After MBC addition the bleached area moved towards one end of the cell. Because microtubules were all depolymerising after the addition of the drug, movement must be due to a pulling force exerted on the shrinking microtubules as they depolymerised (Fig 5.8A).

Microtubules of *ssm4Δ* shmooing cells did not appear to oscillate. Microtubule bundles appeared thicker than wild type bundles, suggesting that there are more microtubules per bundle. Their length also did not change significantly over the filming period (Fig 5.9A and B). Fluorescence intensity along the bundle, did change, suggesting that individual microtubules might be growing and shrinking but that there was no co-ordination of the bundle as a whole (Fig 5.10). There was also no co-ordination of the

dynamics at the opposite ends of the cell; only in 35% of cases did microtubules display opposite dynamics at opposite ends (Fig 5.9B). Monitoring recovery of a bleached microtubule showed that *ssm4Δ* microtubules always recovered from the SPB, suggesting they had the same polarity as wild type, with the minus ends in the middle of the cell and the plus ends at the cell ends (Fig 5.11). To verify if a pulling force was generated on shrinking microtubules, I bleached a small area on a microtubule and then depolymerised microtubules with MBC monitoring the behaviour of the bleached area. The bleached area did not move as microtubules depolymerised, and the microtubules shrank back to a stud in the middle of the cell (Fig 5.8B). This suggests that a pulling force in not generated on shrinking microtubules and, unlike wild type cells, that microtubules are not anchored at the cortex and therefore depolymerise back to the SPB in the cell centre.

In *ssm4Δ* cells, apart from the lack of pulling force, the microtubular array seemed different to that found in wild type cells, appearing more bundled. I investigated this further by analysing the appearance of microtubular bundles in fixed wild type and *ssm4Δ* cells. I found that there were fewer Microtubule Organising Centres (MTOC) in *ssm4Δ* cells, but the same number of bundles per MTOC (Fig 5.12), suggesting that the increased bundling might be due to a difference in the nucleation of microtubules rather than in cross-linking along the microtubules. To monitor differences in how microtubules were polymerised I analysed the repolymerisation of microtubules after MBC washout. After microtubule depolymerisation there were slightly more stubs in wild type than in *ssm4Δ* cells (2.8 vs. 2). Upon MBC washout, most of the wild type cells repolymerised from 2 seeds whereas the majority of *ssm4Δ* cells repolymerised from one seed only (Fig

5.13 and 5.14). This suggests that there is a difference in microtubule nucleation between wild type and *ssm4Δ* cells. I conclude that in the absence of Ssm4p, microtubular bundles are thicker, that the co-ordination within the bundle and between opposite cell ends is lost, and that microtubules are no longer anchored or able to generate a pulling force at the cell cortex.

5.2.3 Ssm4p is localised along microtubules and at the SPB

It has been published that *ssm4+* is only transcribed during mating and that an overexpressed Ssm4GFP localises to microtubules (Yamashita et al., 1997). If Ssm4p has an analogous role to Tip1p during shmooing it should be expressed in response to pheromone and be localised to microtubules when expressed at endogenous levels. To investigate this I tagged the endogenous Ssm4 with HA and GFP, and then analysed the protein levels during vegetative and shmooing growth in a *cyr1Δ sxa2Δ* mutant strain. The tags did not effect the function of the protein since the nucleus was still able to oscillate in the tagged strains. Ssm4HA was not detectable during vegetative growth but its level increased after 6 hours in the presence of pheromone (Fig 5.15), indicating that the protein is induced during shmooing growth. Ssm4GFP fluorescence, which was not detectable during vegetative growth (data not shown) became visible in response to pheromone and was arranged in linear arrays that co-localised with microtubules. This fluorescence became dispersed when the cells were treated with MBC (Fig 5.15B and C). This suggests that the protein is localised along microtubules. Ssm4GFP also appeared as a bright dot in the cell body, coincident with the SPB marker Sad1p (Hagan and Yanagida, 1995), and at a point where microtubules touched the cortex (Fig 5.15B,

arrows). This pattern of localisation resembles that of Dhc1p (Yamamoto et al., 2001). Ssm4GFP was filmed in shmooing cells and fluorescence was found along microtubules in dots that appeared mostly stationary with respect to the microtubule (Fig 5.16). The bright dot at the SPB oscillated back and forth in the cell (Fig 5.16), yellow arrow. The fluorescence at the microtubules' tips seemed to increase when microtubules stalled or depolymerised (Fig 5.16, white arrow), but it did not appear to accumulate when microtubules were extending. Since microtubules pulling on the SPB were also depolymerising, the fluorescence at the tip ahead of the moving SPB became very bright, similar to what has been found for Dhc1p (Yamamoto et al., 2001). This indicates that Ssm4p can bind to depolymerising or stalling ends of microtubules

I have shown that Tip1p, which carries a CAP-Gly microtubule binding motif can efficiently bind to repolymerising microtubules (Fig 4.15B in Chapter 4), and so I checked if the same was true for Ssm4p. I depolymerised microtubules with MBC, mounted the cells on a slide and then washed the MBC out with fresh media and filmed Ssm4GFP as microtubules repolymerised. Soon after the MBC had been washed out linear arrays of fluorescence appeared and extended, resembling the pattern of repolymerising microtubules (Fig 5.17). This suggests that Ssm4p, like Tip1p, can very efficiently bind to microtubules.

5.2.4 Ssm4p interacts with Dhc1p

Glued type proteins are known to be part of the dynactin complex, which also includes dynein heavy chain. Dhc1p in *S. pombe* is required for the horse-tail nuclear movement occurring during meiotic prophase and for the regulation of microtubular

dynamics during mating (Yamamoto et al., 2001). Dhc1p is required to generate a pulling force on microtubules at the site where microtubules contact the cortex and accumulates at that site. This localisation pattern is similar to that seen for Ssm4p during shmooing. In the absence of Ssm4p the pulling force is no longer generated, I analysed whether the absence of Ssm4 p had any effect on Dhc1p localisation.

In *ssm4Δ* cells Dhc1p was still found at the SPB (Fig 5.18, yellow arrows) but its fluorescence along microtubules was reduced and it no longer accumulated at sites where the microtubules contacted the cortex (Fig 5.18). This could explain why no pulling force is generated in the absence of Ssm4p. I conclude that Ssm4p is required for efficient binding of Dhc1p to microtubules and for its accumulation at microtubular tips, but not for its association to the SPB.

Various reports have shown that glued type proteins co-immunoprecipitate with dynein (Karki and Holzbaur, 1995; Vaughan and Vallee, 1995; Waterman-Storer and Holzbaur, 1996). I investigated if this was also the case in fission yeast by constructing a strain in which Ssm4p and Dhc1p were tagged with different peptides in a *cyr1Δ sxa2Δ* strain. Co-immunoprecipitations were carried out after pheromone induction. Immunoprecipitation of Ssm4HA in shmooing cells brought down Dhc1MYC and vice-versa (Fig 5.19), indicating that Ssm4p and Dhc1p are part of the same complex.

5.2.5 Tip1p and Ssm4p collaborate to allow the switch to shmooing microtubular dynamics

Tip1p is required to stabilise microtubules in vegetative cells, whereas Ssm4p appears to be required to co-ordinate the dynamics but not to directly stabilise

microtubules in shmooing cells. Tip1p is still present during shmooing growth, and possibly is able to partially substitute for the absence of Ssm4p. To address this I monitored microtubular dynamics in a *tip1Δ* and a double deleted strain, *ssm4Δ tip1Δ*. Microtubular dynamics in a *tip1Δ* varied from cell to cell. In certain cases microtubules appeared to have lost the co-ordination between opposite ends (Fig 5.20A and B) even if microtubules were still able to generate a pulling force on the SPB (yellow arrows Fig 5.20A), and in others microtubules appeared almost wild type (Fig 5.20C). Overall the co-ordination between opposite ends was found to be 73%, which is not statistically significantly different from wild type. This confirms that Tip1p does not play a major role in the regulation of microtubular dynamics during shmooing.

On the contrary, the double mutant *ssm4Δ tip1Δ* displayed a dramatically different microtubular pattern from wild type shmooing cells, which appeared similar to vegetative cells. There were more microtubule bundles arranged parallel to each other, spanning the whole cell length and terminating at the cell end. They were less bright, and no longer displayed opposite dynamics at opposite cell ends (Fig 5.21A and B). This suggests that there are less microtubules per bundle and that their dynamics have lost co-ordination. I conclude that both Ssm4p and Tip1p play a role in the switch of microtubular behaviour from a vegetative to a shmooing array.

CLIP-170 like proteins have also been found to interact with the dynactin complex (Coquelle et al., 2002), and I have shown that Tip1p collaborates with Ssm4p in the regulation of shmooing cells' microtubular dynamics. Therefore I investigated if Tip1p also played a role in localising Dhc1p and Ssm4p. Dhc1GFP and Ssm4GFP

localisation was wild type in the absence of Tip1p (Fig 5.22A and C) and Tip1YFP localisation was wild type in *ssm4Δ* cells (Fig 5.22B), but in the double mutant *ssm4 Δtip1Δ,* Dhc1GFP had totally lost its microtubular localisation, although it retained its SPB localisation (Fig 5.22C). Dhc1GFP also co-localised with Tip1-YFP at the tips of microtubules in response to pheromone (Fig 5.23B), suggesting they might interact.

On the other hand Ssm4GFP and Tip1YFP only partially overlapped at the tips of microtubules (Fig 5.23A), suggesting that they might not directly interact. I conclude that Tip1p might interact with Dhc1p and that it collaborates with Ssm4p to localise Dhc1p appropriately.

5.2.6 *Ssm4Δ tip1Δ* cells can shmoo

Ssm4 Δtip1Δ cells display vegetative-like microtubules even in the presence of pheromone, I analysed if this had any effect on the ability of these cells to shmoo. I monitored the ability of mutant cells to arrest and to relocalise actin in response to pheromone. *Ssm4Δ* and *ssm4Δ tip1Δ* cells were able to arrest in response to pheromone with the same kinetics as wild type cells (Data not shown). Both *ssm4Δ* and *ssm4Δ tip1Δ* cells could relocalise actin to one end, even faster than wild type (Fig 5.24), although the high number of vegetative monopolar cells in the double mutant makes it harder to distinguish between shmooing and monopolar vegetative cells. This high proportion of monopolar cells during vegetative growth suggests that Ssm4p might play some role during vegetative growth too, even if its expression levels are very low. I conclude that Ssm4p is not required for setting up a single shmooing projection and that defective

shmooing microtubular dynamics has no effect on the ability of the cell to relocalise actin to a single end.

During vegetative growth, defective microtubular dynamics does not necessarily effect the number of sites of growth but it does effect the overall cell shape, resulting in bent or branched cells (Browning et al., 2000; Brunner and Nurse, 2000; Mata and Nurse, 1997; Sawin and Nurse, 1998). I therefore analysed the cells shape of *ssm4Δ* or *ssm4Δ tip1Δ* cells by counting the number of T-shaped shmoos and measuring the angle of the bent shmooing projection, taking as 0˚ a straight cell. *Tip1Δ* cells displayed a slightly increased shmooing angle (Fig 5.25B), which is probably due to their defective vegetative morphology (Brunner and Nurse, 2000). The double mutant displayed a very low number of T-shaped cells and had a slightly larger shmooing angle, but it already displayed some T-shaped cells during vegetative growth (Fig 5.25 B). It is therefore hard to determine if this is a result of an initial defective vegetative shape or if it is a result of the defective microtubular dynamics.

I conclude that Ssm4p does not play a role in setting up shmooing cell polarity, and that defective microtubular dynamics in shmooing cells does not have a dramatic effect on cell shape. In particular, the apparent vegetative-like microtubular array does not induce the cells to grow straighter.

5.3 Discussion

In this chapter I have shown that Ssm4p, a Glued-type homologue, is required for the regulation of microtubular dynamics during shmooing, and that it collaborates with

Tip1p to generate a shmooing array of microtubules. The localisation of Ssm4p and its deletion phenotype resemble that of Dhc1p, and the two proteins are found in the same complex. This indicates that Ssm4p is a functional homologue of Glued.

In *ssm4Δ* cells the nucleus can not undergo "horsetail" movement, on the contrary it remains stationary in the centre of the cell. To generate the oscillatory horsetail nuclear movement microtubular dynamics at opposite ends of the cell have to be co-ordinated so that as microtubules polymerise at one end they depolymerise at the other. This co-ordination is lost in *ssm4Δ* cells. Bundles appear a lot thicker and more stable, but close examination of the bundles revealed that individual microtubules were growing and shrinking within the bundle but there was no co-ordination of the bundle as a whole. In the absence of Ssm4p microtubules were no longer pulled at the cortex, which explains why the nucleus is not able to oscillate in *ssm4Δ* cells. Ssm4GFP localises to microtubules and the SPB, and it accumulates to the tips of depolymerising microtubules, this pattern is similar to that of Dhc1p localisation (Yamamoto et al., 2001). Ssm4p is found in the same complex as Dhc1p, suggesting that they might interact at those locations. In *ssm4Δ* cells Dhc1GFP fluorescence along microtubules is reduced and it no longer accumulates at the site where microtubules contact the cortex. Ssm4p is therefore required for efficient binding of Dhc1p to microtubules and to stabilise Dhc1p at microtubule tips as microtubules depolymerise. Dhc1p is thought to generate this pulling force at the site where microtubules contact the cell cortex (Yamamoto et al., 2001), and because it is unable to accumulate there in the absence of Ssm4p, it will not be able to pull on microtubules in *ssm4Δ* cells.

Analysis of microtubules repolymerising after MBC wash-out showed that in *ssm4Δ* cells only 1 seed could nucleate a microtubular array, whereas in wild type cells microtubules repolymerise mostly from 2 seeds. This suggests that Ssm4p might also play a role in microtubular nucleation that does not act via dynein, since Dhc1p is still localised at the SPB.

The homologue of Ssm4p, Tip1p, is a CLIP-170 like protein. CLIP-170 like proteins have also been implicated in dynein function. However Tip1p appears to have no role in localising Dhc1p or Ssm4p in fission yeast and has only a minor role in the regulation of microtubular dynamics during shmooing. Surprisingly, the double mutant *ssm4Δ tip1Δ* could not localise Dhc1GFP along microtubules and was completely unable to generate a shmooing microtubular array. This suggests that Ssm4p and Tip1p collaborate in the co-ordination of microtubular dynamics during shmooing to generate the characteristic oscillatory movement. The microtubular array in *ssm4Δ tip1Δ* cells looked more like a vegetative array but this did not appear to have any major effect on the ability of the cells to set up a proper shmooing polarised projection.

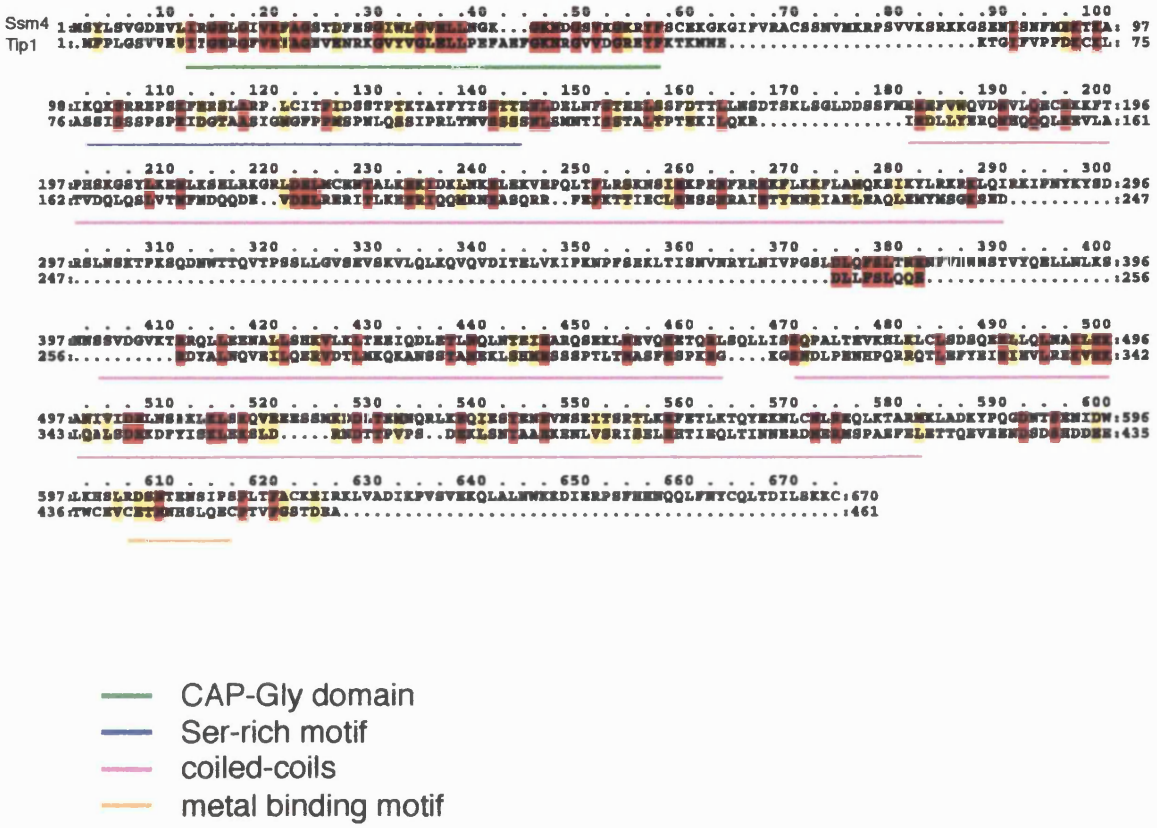

Fig. 5.1 Alignment of Ssm4p with Tip1p.
The two proteins were aligned with ClustalX and visualised with Macboxshade, residues in red are identical and residues in yellow are similar. The identity between the two proteins is 40% in the CAP-Gly domain and 20% in the colied-coil regions. Tip1p has a serine rich and a metal binding motif that Ssm4p does not have.

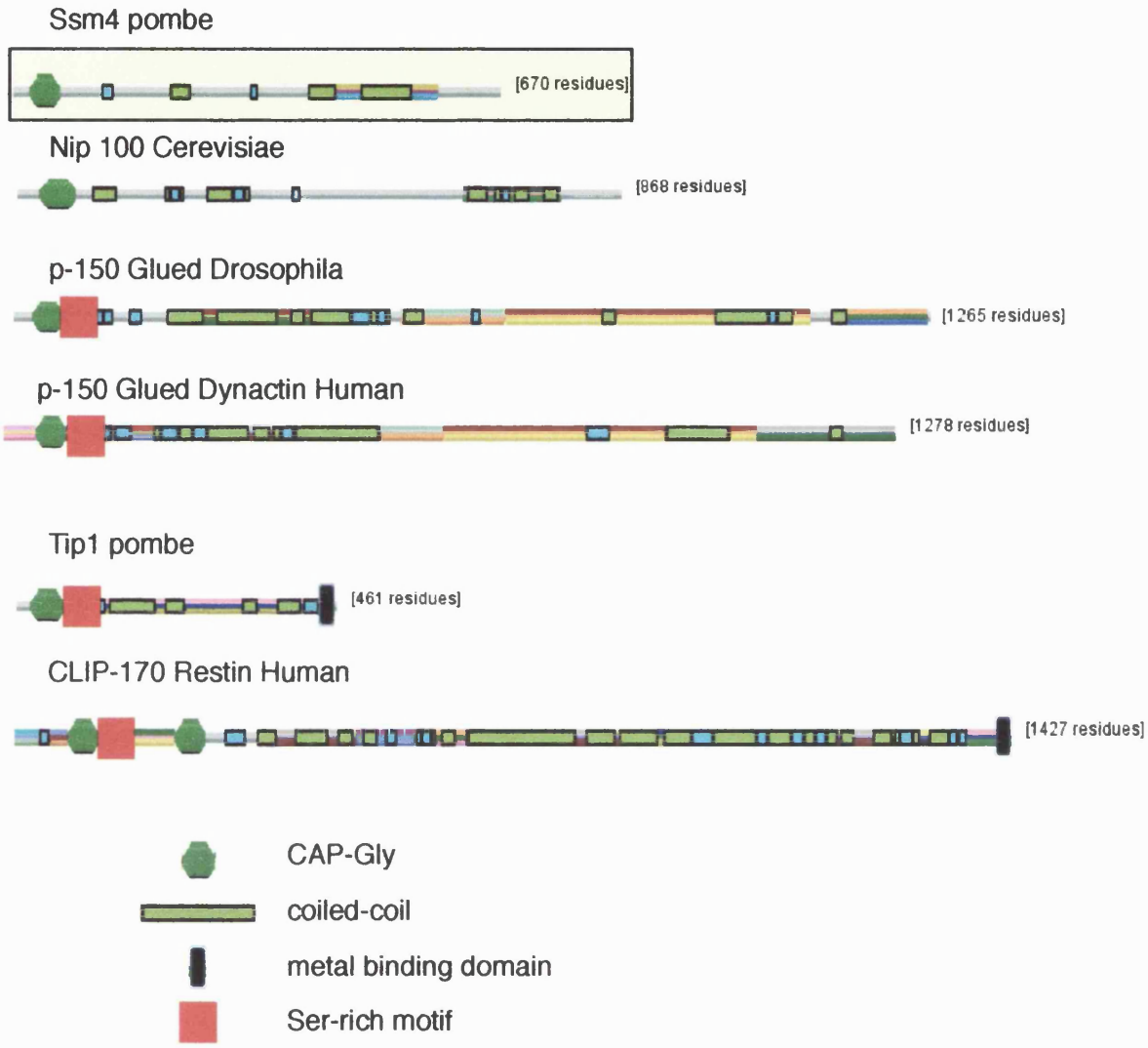

Fig 5.2 Domain arrangement of Ssm4p and its homologues.
Ssm4p is characterised by a microtubule binding CAP-Gly domain at the N-terminus, followed by a series of coiled-coil domains towards it C-terminus. This arrangement is similar to that of all the p-150 Glued-dynactin family. CLIP-170 like proteins, like Tip1p, have a similar domain arrangement plus a metal binding domain at the C-terminus.

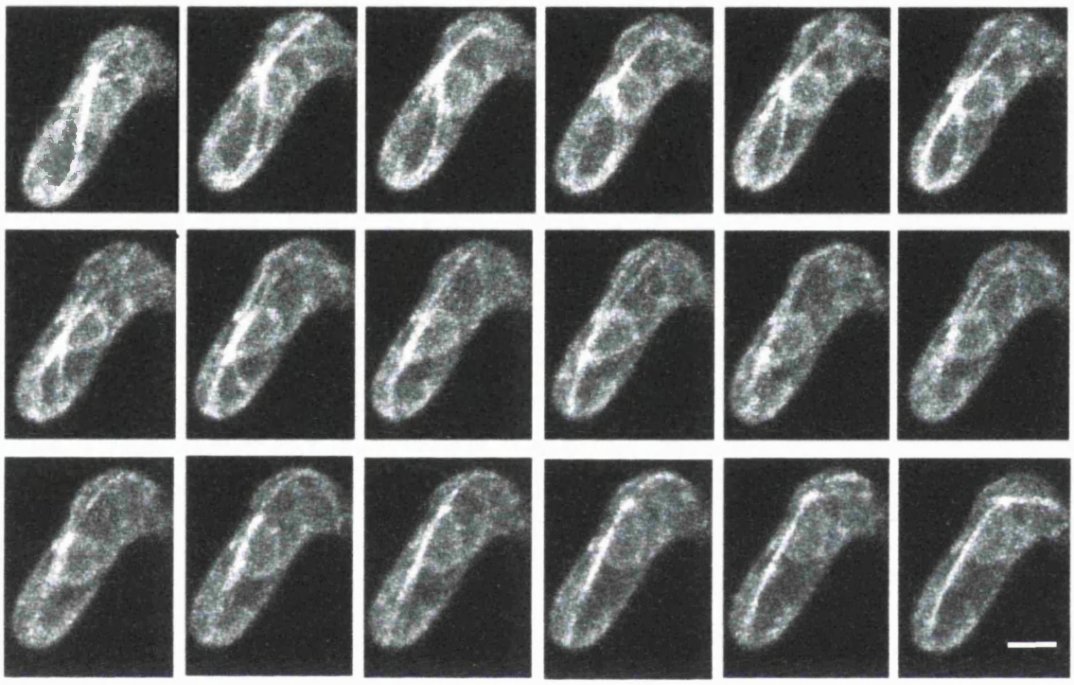

Fig 5.3 The nuclear movement is driven by microtubular dynamics.
Cyr1Δsxa2Δnmt1atb2GFP cells carrying a plasmid expressing *cut11GFP*, which localises to the nuclear envelope, were treated with pheromone for 6 hours. The cells were then imaged every 12 seconds with a confocal microscope. Images shown are projections of sections through the whole cell. Scale bar, 3μm.

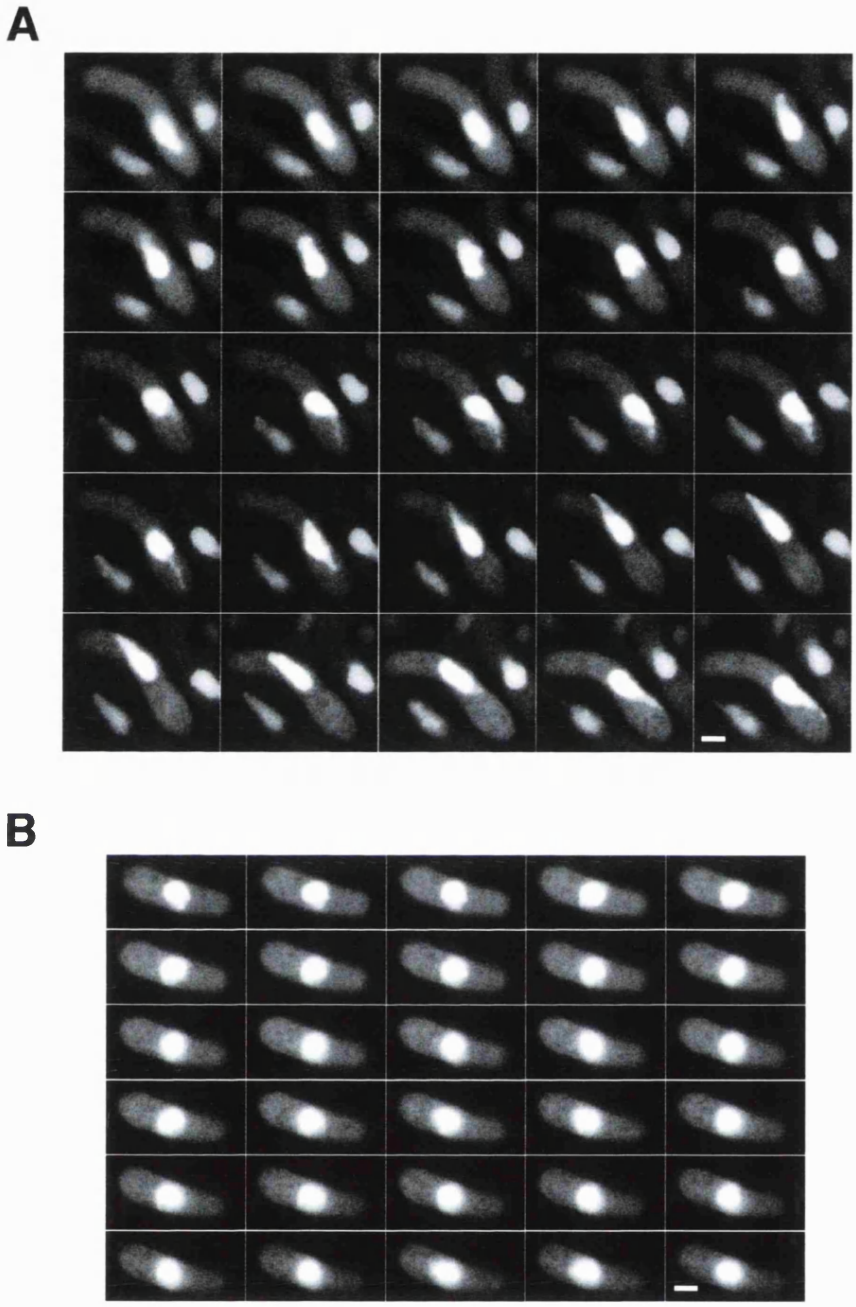

Fig 5.4 Nuclear movement in wild type and *ssm4*Δ cells.
(A) Wild type and (B) *ssm4*Δ cells were transformed with a plasmid carrying a nuclear GFP marker, the cells were then treated with pheromone for 6 hours, placed on a slide and filmed with a fluorescent microscope. Images were taken every 30 seconds.Scale bar, 3μm.

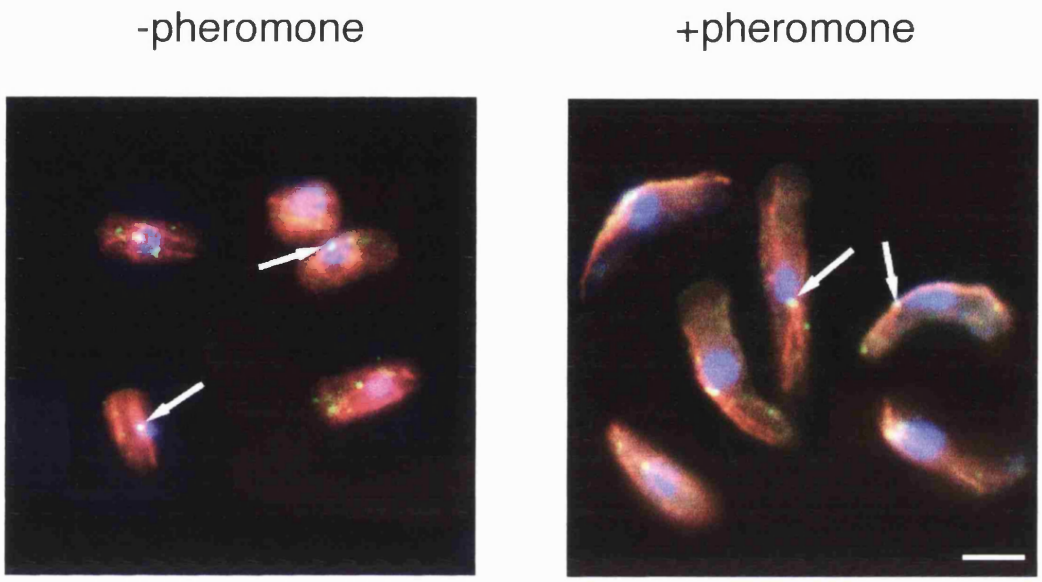

Fig 5.5 SPB association with the nucleus.
Cyr1Δsxa2Δssm4Δ cells were grown in the absence or the presence of 3μg/l of pheromone for 6 hours. Cells were fixed and immunostained with anti-tubulin (red) and anti-Sad1 (green) , which marks the SPB. The cells were mounted in media containing DAPI, which stains the nucleus (blue) and imaged with a fluorescent microscope. Scale bar, 3μm.

A

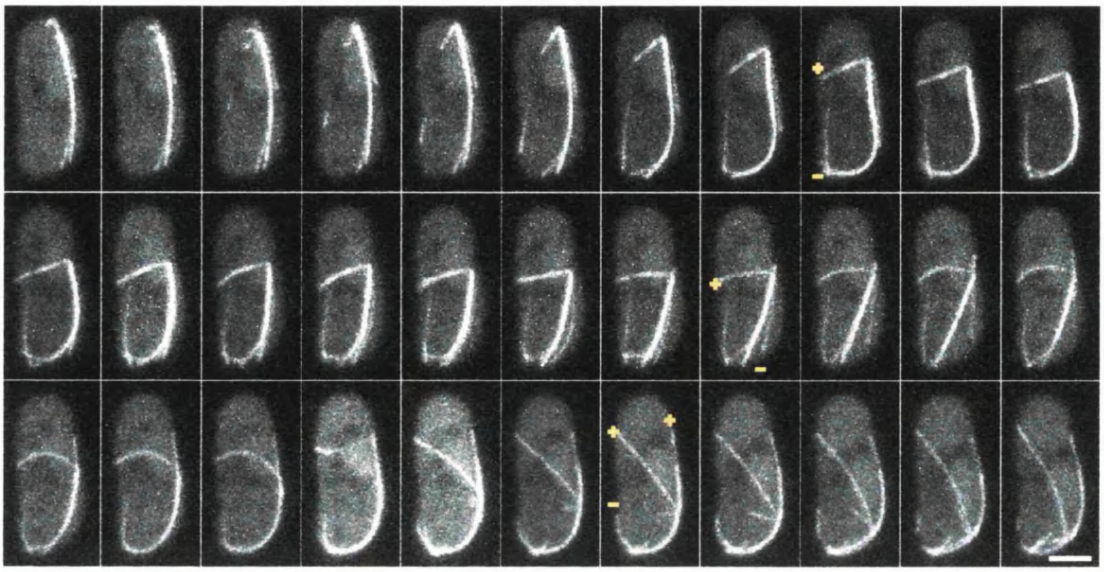

B

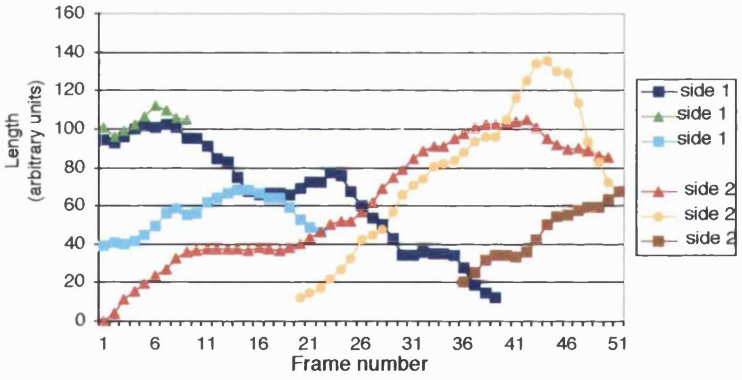

co-ordination at opposite cell ends **80%**

Fig 5.6 Microtubular dynamics in wild type cells.

Cyr1Δsxa2Δnmt1atb2GFP cells were treated with pheromone for 5-6 hours. (A) Cells were then imaged every 6 seconds on a confocal microscope. Images shown are projections of sections through the whole cell. (B) Microtubules' lengths for single cells were measured distinguishing which side of the cell they lie in. The diagram describes the dynamics of the microtubules of a typical cell. The concordance of dynamics at each cell end and discordance between opposite cell ends was then calculated as a percentage of total time points, 8 cells were scored for a total of 45 minutes imaging time. Scale bar, 3μm.

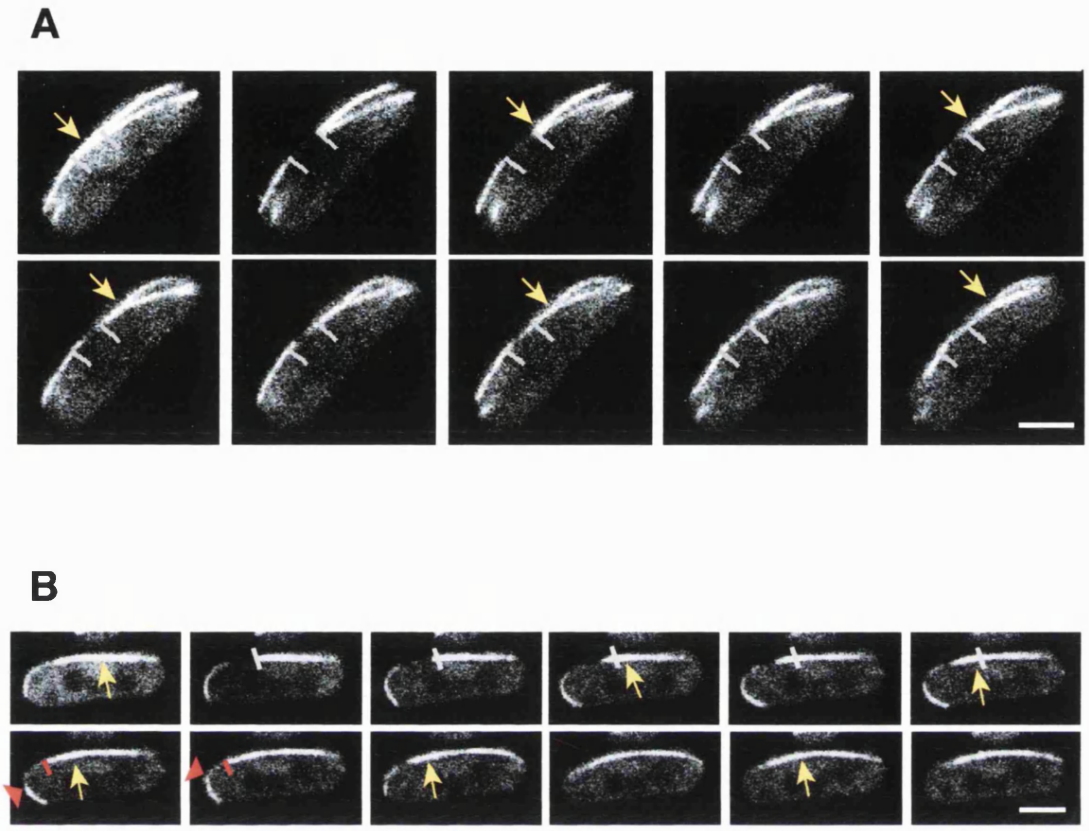

Fig 5.7 Microtubule bleaching and recovery in the wild type cells.
Cyr1Δsxa2Δnmt1atb2GFP were induced with pheromone for 5-6 hours, placed on a lectin-coated glass bottom dish, bleached with a localised laser beam and then filmed every 6 seconds to monitor the pattern of recovery. Images show a single plane through the middle of the cell. The yellow arrows indicates the position of the SPB. The grey lines mark the bleached area. (A) The bleached area moves in the same direction as the SPB, and the distance between the SPB and the further boundary of the bleached area remains the same, the fluorescence recovers from the boundary closer to the SPB. (B) The red mark indicated the boundary of the bleached area closer to the SPB and the arrow the boundary further from the SPB. The bleached area shrinks and the distance between the further boundary and the SPB reduces even though the distance between the SPB and the closer boundary remains the same. This suggets that the microtubule is sliding back towards the SPB. Scale bar, 3μm.

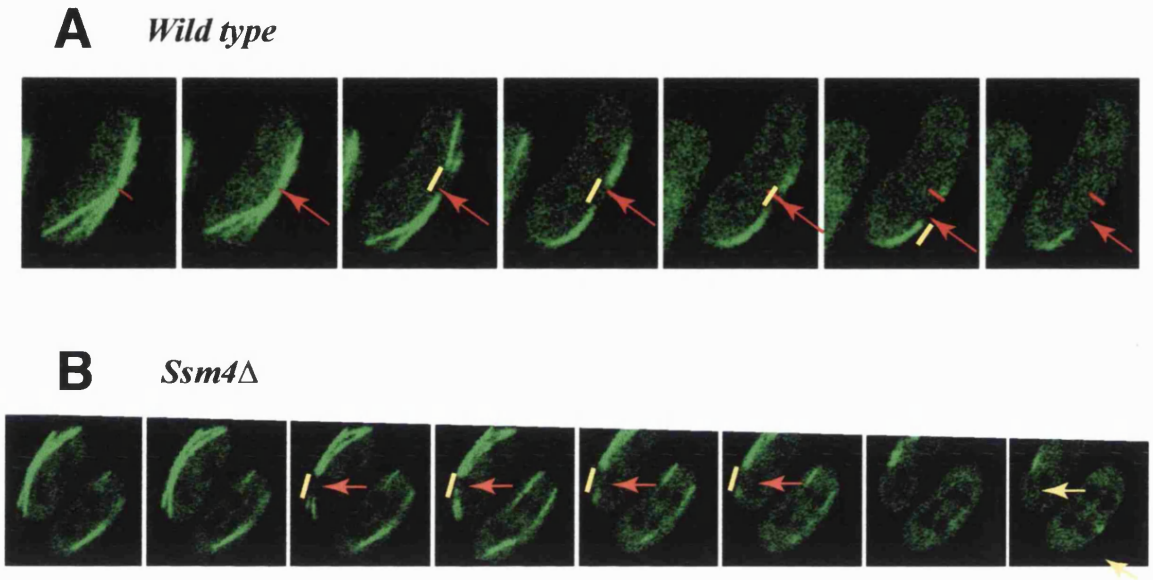

Fig 5.8 *Ssm4*Δ cells do not generate a pulling force on microtubules.
(A) *Cyr1Δsxa2Δnmt1atb2GFP* and (B) *Cyr1Δsxa2Δssm4Δnmt1atb2GFP* cells were induced with pheromone for 6 hours. Cells were then mounted on a lectin-coated glass bottom dish. Microtubules were bleached with a pulse of laser light, MBC was then added to depolymerise the microtubules and the cells were filmed with a confocal microscope (see materials and methods for details). Images shown are single planes through a cell. The red arrows marks a fixed spot and the yellow lines mark the bleached area. The yellow arrows mark the stubs remaining after microtubules had depolymerised.

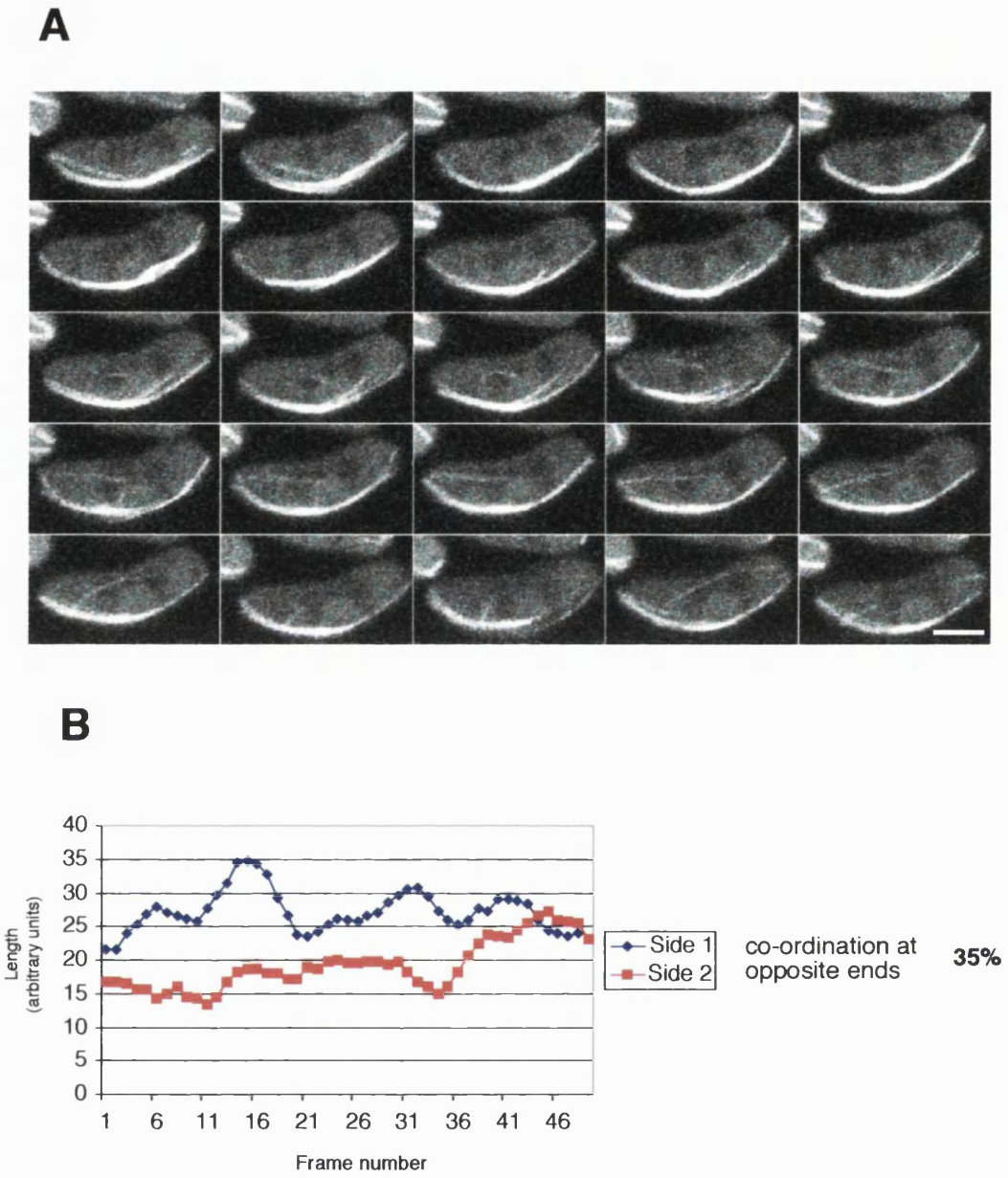

Fig 5.9 Microtubule bundles in *ssm4Δ* cells are less dynamic and do not oscillate.

Cyr1Δsxa2Δssm4Δ nmt1atb2GFP cells were treated with pheromone for 5-6 hours. (A) Cells were then imaged every 12 seconds on a confocal microscope. Images shown are projections of sections through the whole cell. (B) The length of microtubules in single cells were measured distinguishing which side of the cell they lie in. The diagram describes the dynamics of the microtubules of the cell in (A). The concordance of dynamics at each cell end and between opposite cell ends was then calculated as a percentage of total time points, 4 cells were scored for a total imaging time of 20 minutes. At least 10 cells for a total of 50 minutes imaging time were observed and they all exhibited a similar behaviour. Scale bar, 3μm.

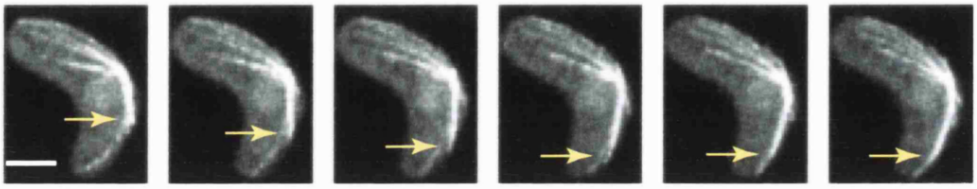

Fig 5.10 Microtubules grow and shrink in *ssm4*Δ cells.
*Cyr1*Δ*sxa2*Δ*nmt1GFPatb2ssm4*Δ cells were induced with pheromone for 6 hours. Cells were imaged every 7 seconds on a confocal microscope. Images shown are projections of planes through the cell. The yellow arrow indicates where there is a change of fluorescence along a bundle, suggesting a microtubule is growing along another. Scale bar, 3μm.

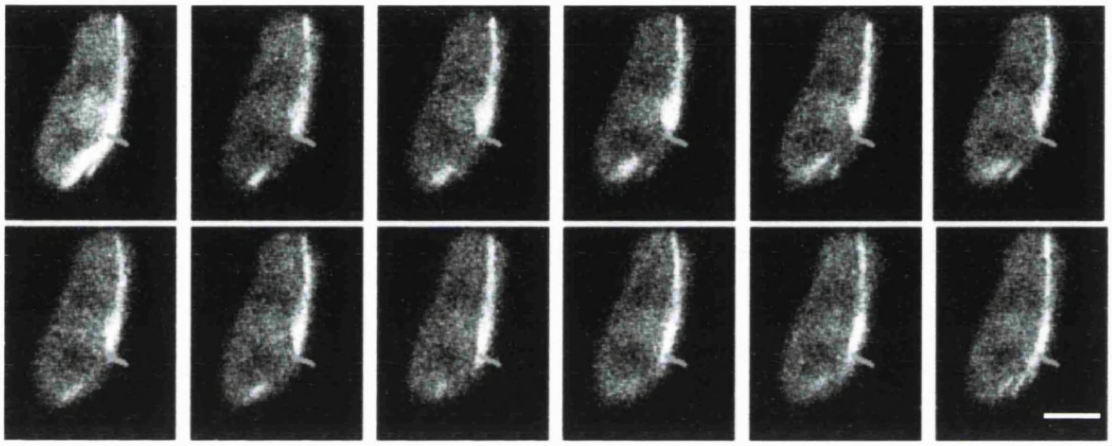

Fig 5.11 Bleaching and recovery of *ssm4*Δ cells' microtubules.
*Cyr1*Δ*sxa2*Δ*ssm4*Δ*nmt1atb2GFP* cells were induced with pheromone for 5-6 hours, placed on a lectin-coated glass bottom dish, bleached with a localised lasar beam and then filmed every 6 seconds to monitor the pattern of recovery. Images show a single plane through the middle of the cell. Scale bar, 3μm.

A

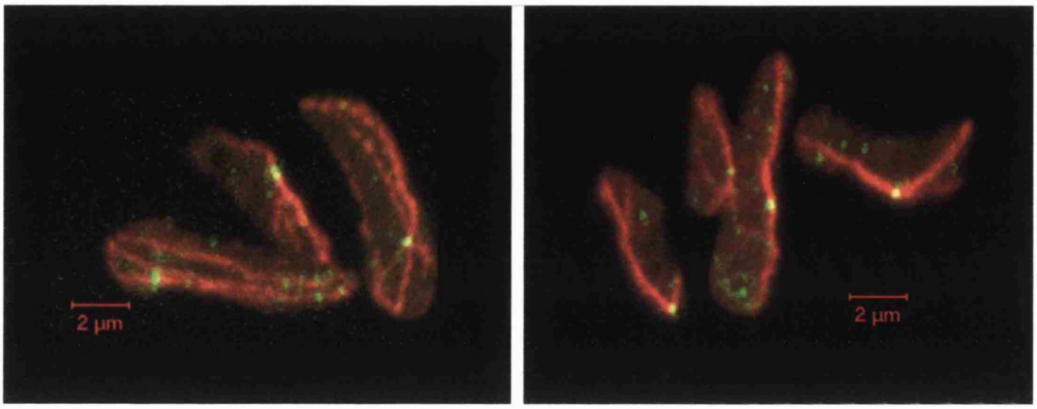

wild type *ssm4Δ*

B

Microtubules per SPB

Strain	1	2	3	4	
wt	54	39	5	1	(n=44)
ssm4Δ	47	40	12	1	(n=68)

C

Number of Microtubule organising centres

Strain	1	>1	
wt	48	52	(n=300)
ssm4Δ	63	37	(n=300)

Fig 5.12 Microtubule bundles in *ssm4Δ* cells.
(A) *Cyr1Δsxa2Δ* and *cyr1Δsxa2Δssm4Δ* cells were induced with 3µg/l pheromone for 6 hours, cells were then fixed in methanol and immunostained for tubulin (red) and Sad1(green), which stains the SPB. (B) The number of microtubules going though each SPB was scored. (C) The number of microtubule organising centres was scored. If all microtubules were seen to go through one point it was scored as one, otherwise it was scored as more than one. All numbers are percentages of total number of cells scored.

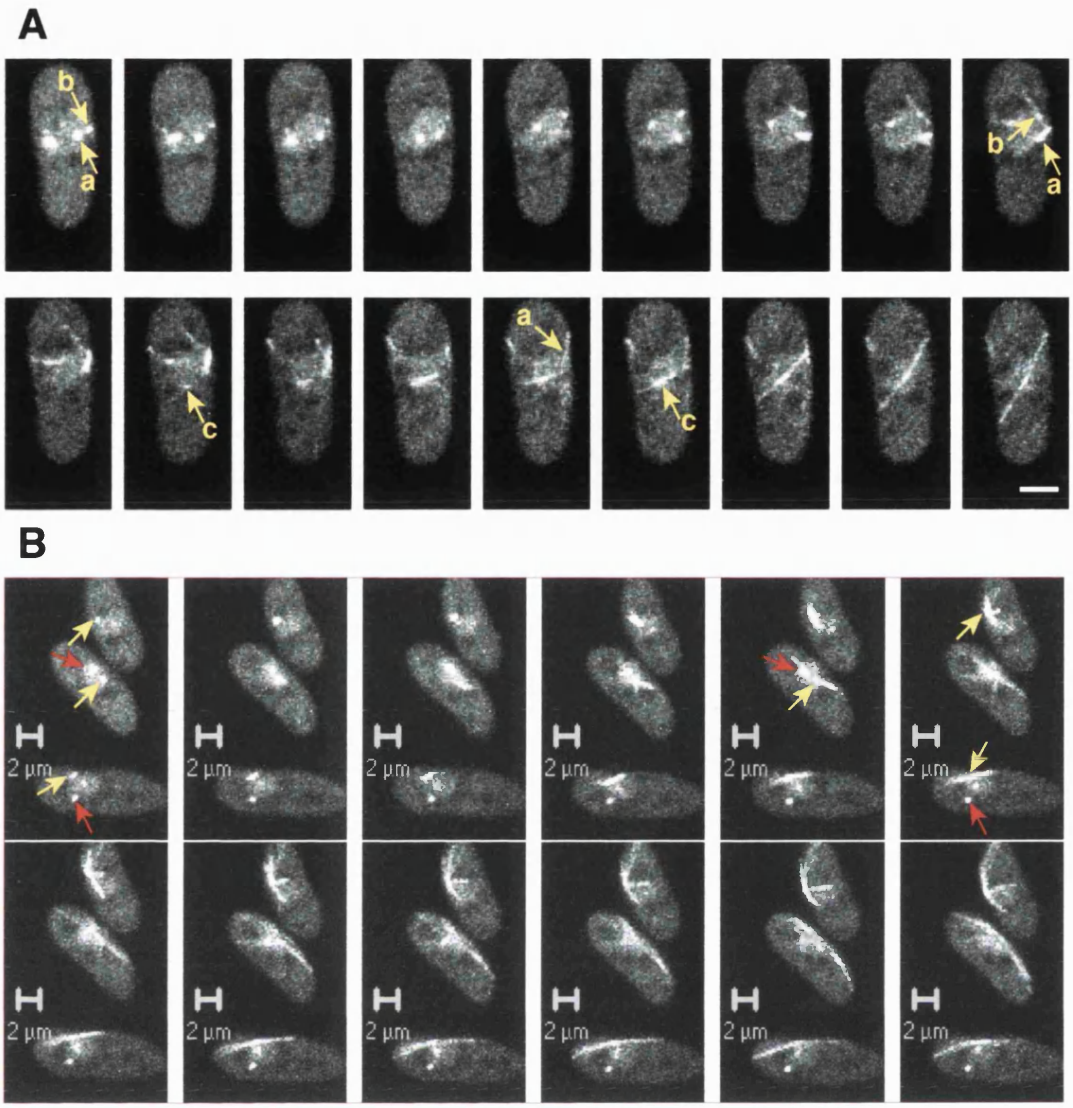

C

	MT repolymerised from one seed	MT repolymerised from >1 seed		
		then bundled	then 1 disappeared	generated 2 arrays
wild type n=17	25%	45%	20%	10%
*ssm4*Δ n=18	61%	28%	0%	11%

Fig 5.13 Repolymerisation of wild type and *ssm4*Δ microtubules.
(A) *Cyr1Δsxa2Δnmt1atb2GFP* and (B) c*yr1Δsxa2Δssm4Δnmt1atb2GFP* cells were treated with pheromone for 6 hours and MBC was added to the media to depolymerise microtubules. Cells were then placed on a lectin coated dish, MBC was diluted out with pre-conditioned media and the cells were filmed with a confocal microscope by taking images every 6 seconds. (See materials and methods for details). The yellow arrows show seeds which start to repolymerise whereas red arrows those that will not. (C) Different patterns of repolymerisation were observed and scored: microtubules could repolymerise from one or from multiple seeds. If more than one seed nucleated microtubules, the newly formed microtubules could either bundle together (a and c), or one seed could start to repolymerise a microtubule but then disassemble and disappear (b), or multiple seeds could give rise to multiple stable array of microtubules. Scale bar, 2µm.

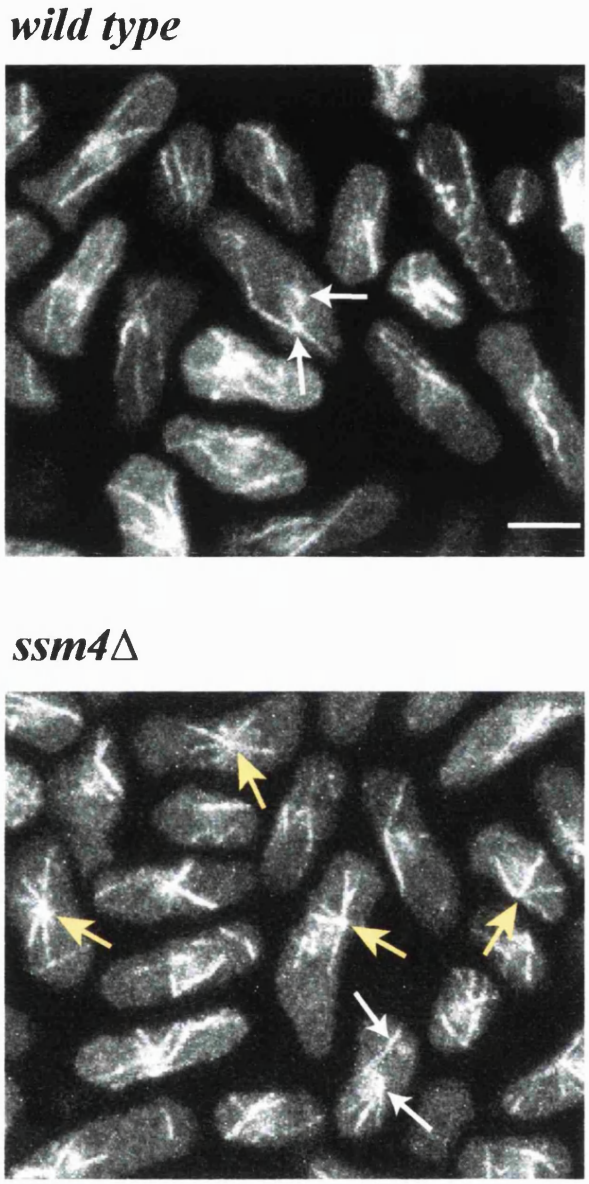

Fig 5.14 *Ssm4Δ* microtubules mostly repolymerise from one seed.
Cyr1Δsxa2Δnmt1atb2GFP and *cyr1Δsxa2Δnmt1atb2GFPssm4Δ* cells expressing tubulin GFP were grown in the presence of pheromone for 6 hours. MBC was added to depolymerise microtubules and 10mls of cells were collected onto a millipore filter. The cells were washed for 1 minute with fresh media to allow microtubules to partially repolymerise, and then fixed in methanol. Fixed tubulin GFP was visualised with a confocal microscope. Images shown are projections of sections through the cell. Yellow arrows indicate microtubules repolymerising from one MTOC. White arrows indicate microtubules repolymerising from more than one MTOC. Scale bar, 3μm.

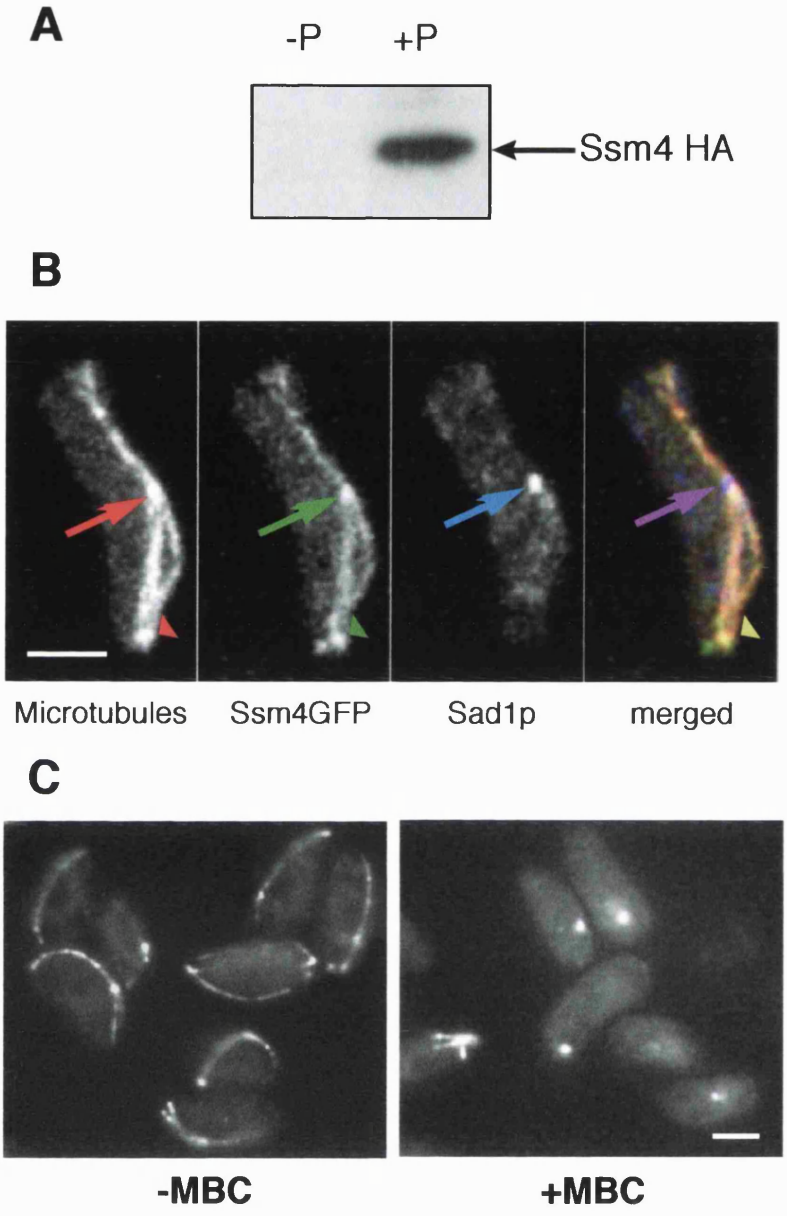

Fig 5.15 Ssm4p expression and localisation.
(A) *Cyr1Δsxa2Δssm4HA* cells were grown in the absence (-P) and in the presence (+P) of pheromone for 6 hours. Boiled cell extracts were carried out as described in the materials and methods, and western blots were probed with anti-HA antibody. (B) *Cyr1Δsxa2Δssm4GFP* were induced for 6 hours with pheromone, cells were then fixed in methanol and immunostained with anti-tubulin and anti-Sad1 antibodies. Arrows indicate the SPB (Spindle Pole Body) and arrowheads the point where microtubules contact the cell surface. (C) *Cyr1Δsxa2Δssm4GFP* were induced for 6 hours with pheromone, treated with MBC (a microtubule depolymerising drug) and imaged on a fluorescent microscope before and after the treatment. Scale bar, 3μm.

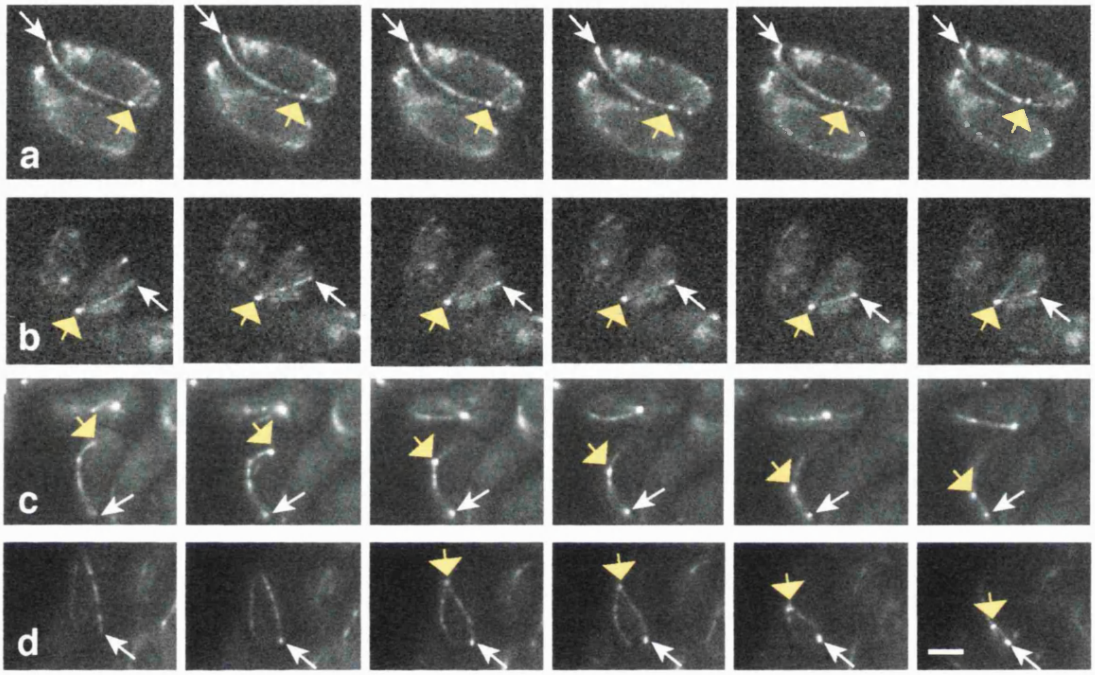

Fig 5.16 Ssm4p accumulates at the tips of depolymerising microtubules.
Cyr1Δsxa2Δssm4GFP cells were induced with pheromone for 6 hours, placed on a slide and filmed with a fluorescence microscope. Frames are 8-10 seconds apart. White arrows point to the microtubule tips and yellow arrows to the fluorescent dot at the SPB. The microtubular tip is anchored in a fixed position at the tip in a,c and d and the SPB is moving towards it as the microtubule depolymerises. In b, the SPB is not moving and the microtubule is depolymerising back towards it. Scale bar, 3μm.

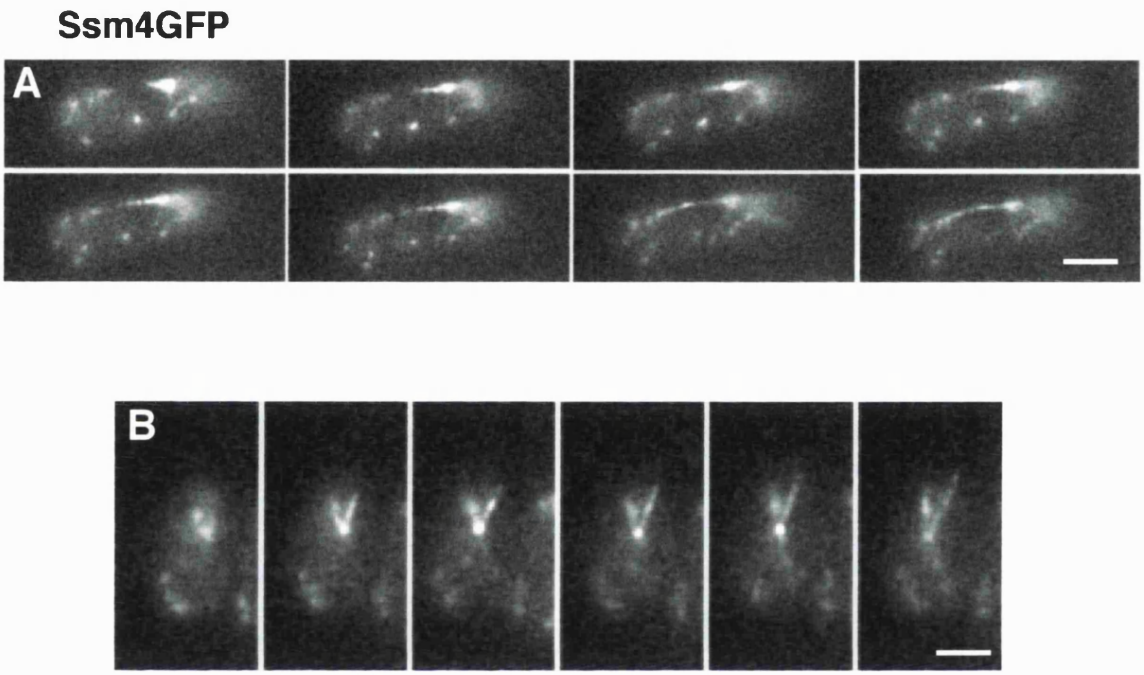

Fig 5.17 Ssm4GFP localisation as microtubules repolymerise.
Cyr1Δsxa2Δssm4GFP cells were grown in pheromone for 6 hours, MBC was then added for 5-15 minutes to depolymerise microtubules. Cells were placed on a lectin-coated coverslip and inverted onto a slide to create a small flow-through chamber. The MBC was washed out with fresh media to repolymerise microtubules and cells were filmed every 12 seconds with a fluorescent microscope.A and B are two different cells from different experiments. Scale bar, 3μm.

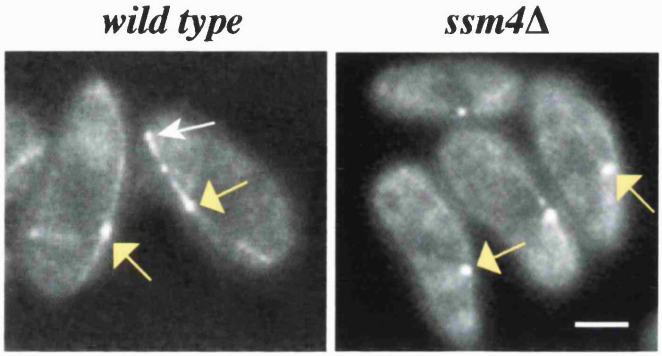

Fig 5.18 Dhc1p does not accumulate at microtubule tips in *ssm4*Δ cells.
*Cyr1*Δ*sxa2*Δ*dhc1GFP* and *cyr1*Δ*sxa2*Δ*ssm4*Δ*dhc1GFP* cells were treated with pheromone for 6 hours. Cells were placed on a slide and visualised with a fluorescent microscope. Yellow arrows indicate the fluorescence at the SPB and white arrows the fluorescente at the microtubule tips. Scale bar, 3μm.

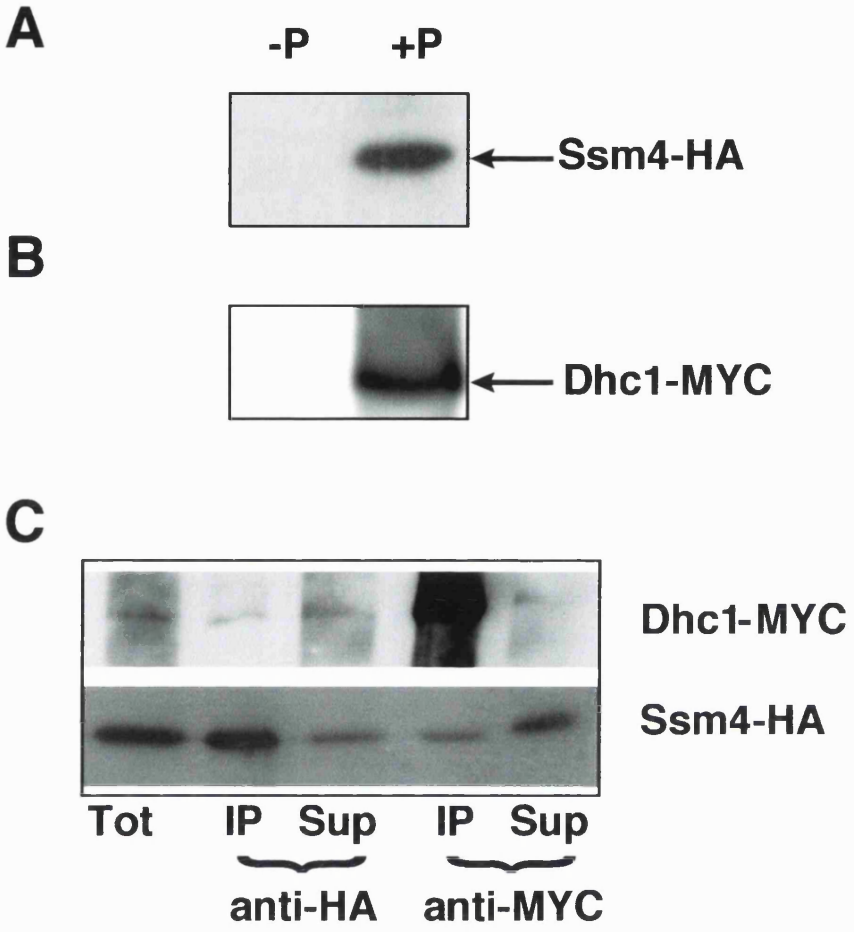

Fig 5.19 Ssm4p and Dhc1p are found in the same complex.
(A) *Cyr1Δsxa2Δssm4HA* and (B) *cyr1Δsxa2Δdhc1myc* cells were treated with pheromone for 6 hours. Western blots of total cell extracts were carried out at time 0 and after the pheromone treatment. Blots were probed with anti-HA and anti-MYC antibodies. (C) *Cyr1Δ sxa2Δ dhc1MYC ssm4HA* cells were induced with pheromone for 6 hours. Native cell extracts were immunoprecipitated with anti-HA and anti-MYC antibodies. Western blots of IPs, supernatants and total cell extracts were carried out as described in the materials and methods, and probed with HA and MYC antibodies.

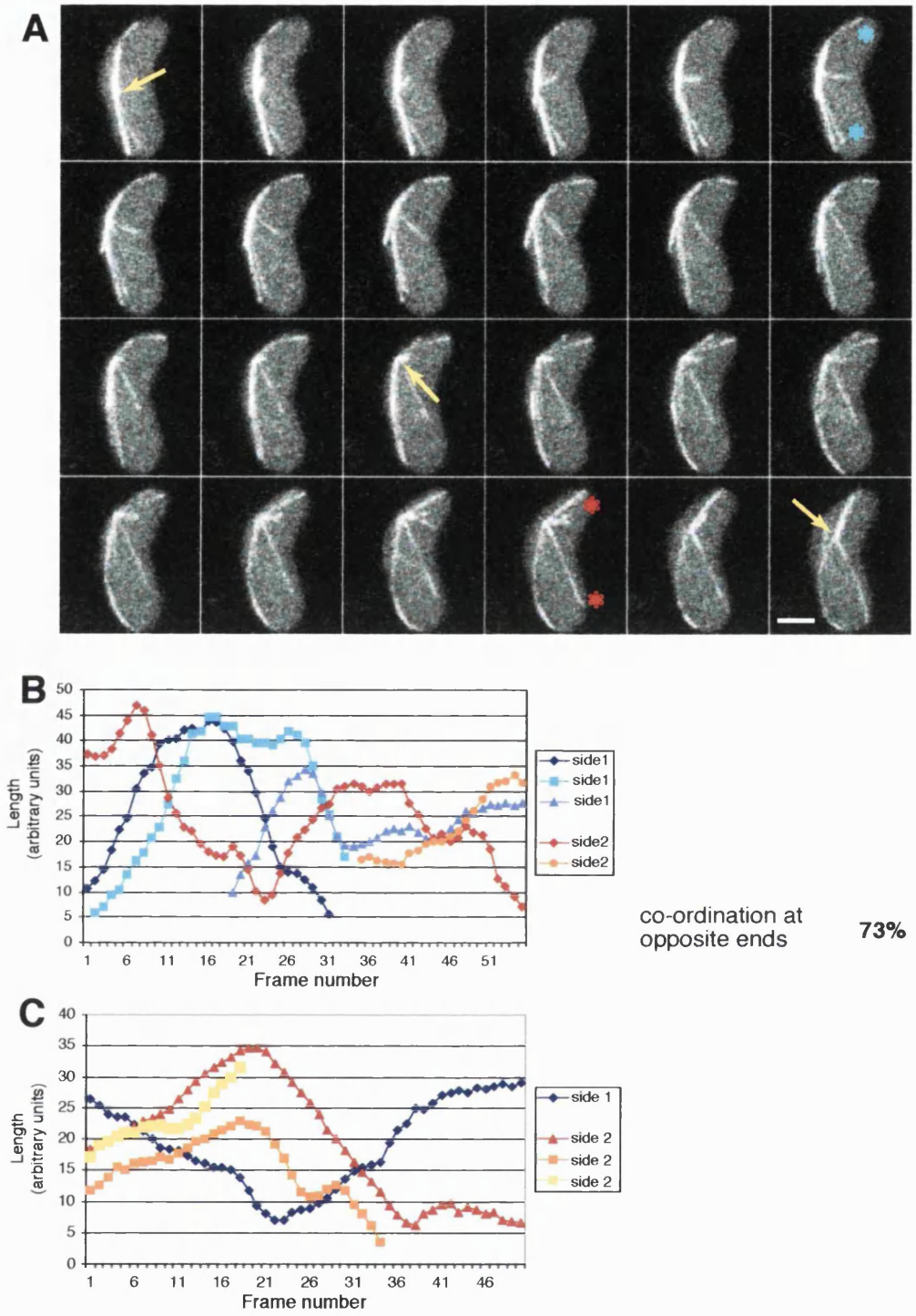

Fig 5.20 Microtubular dynamics in *tip1*Δ cells.

*Cyr1*Δ*sxa2*Δ*tip1*Δ*nmt1atb2GFP* cells were treated with pheromone for 5-6 hours. (A) Cells were then imaged every 6 seconds on a confocal microscope. Images shown are projections of sections through the whole cell. Yellow arrows show the position of the SPB, which is oscillating. Light blue asterisks mark two shrinking microtubules at opposite sides of the cell and red asterisks mark two growing microtubules at opposite ends of the cell. (B) Microtubules' lengths for single cells were measured distinguishing which side of the cell they lie in. The diagram describes the dynamics of the microtubules of the cell in (A). (C) Diagram of another cell showing more wild type dynamics. The concordance of dynamics at each cell end and between opposite cell ends was then calculated as a percentage of total time points, 8 cells were scored for a total of 45 minutes imaging time. Scale bar, 3μm.

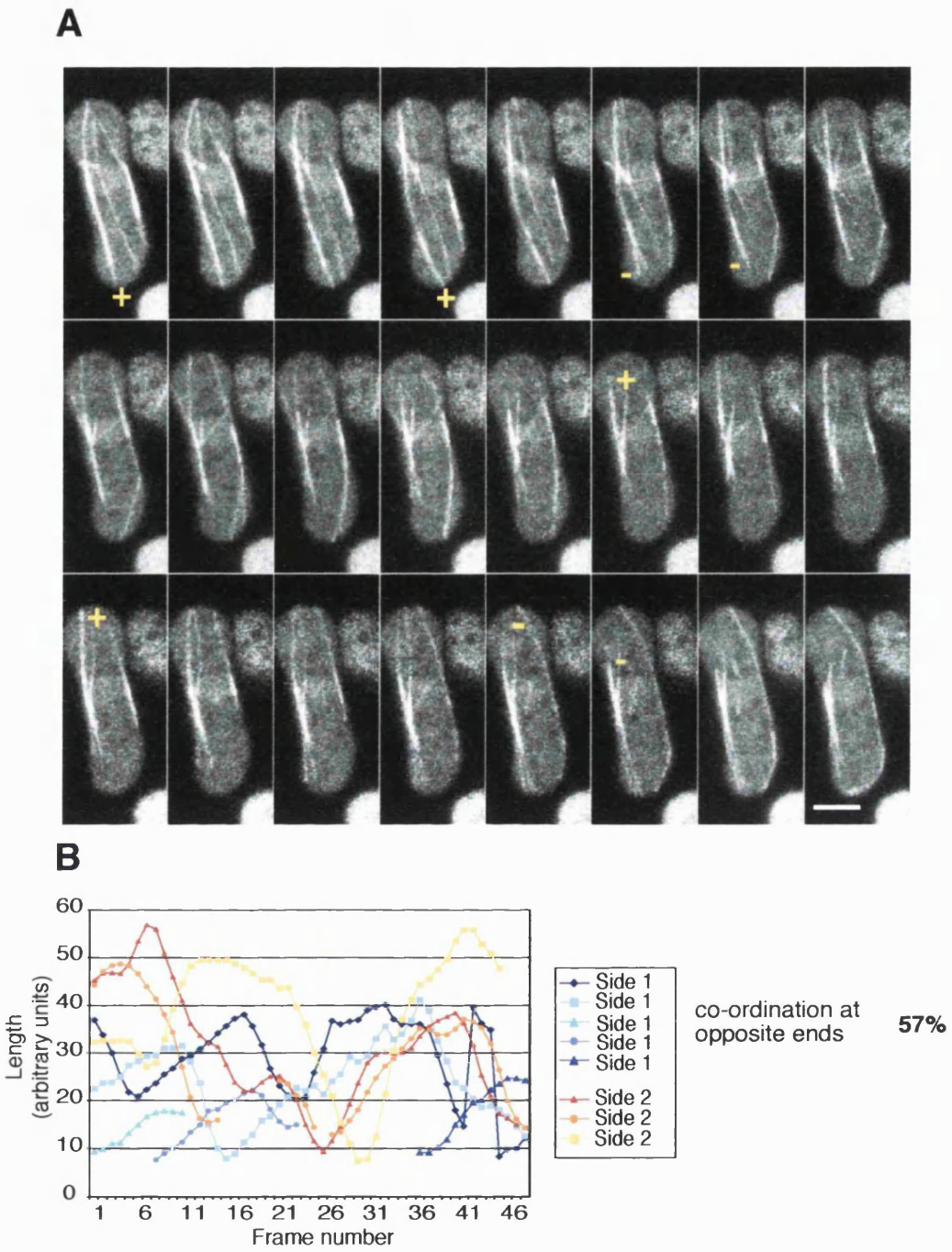

Fig 5.21 Microtubular dynamics in *ssm4Δtip1Δ* cells

Cyr1Δsxa2Δtip1Δssm4Δnmt1atb2GFP cells were treated with pheromone for 5-6 hours. (A) Cells were then imaged every 6 seconds on a confocal microscope. Images shown are projections of sections through the whole cell, "+" indicate growing microtubules and "-" indicate shrinking microtubules. (B) Microtubules' lengths for single cells were measured distinguishing which side of the cell they lie in. The diagram describes the dynamics of the microtubules of the cell in (A). The concordance of dynamics at each cell end and between opposite cell ends was then calculated as a percentage of total time points, 4 cells were scored but at least 10 were observed for a total imaging time of at least 50 minutes. Scale bar, 3μm.

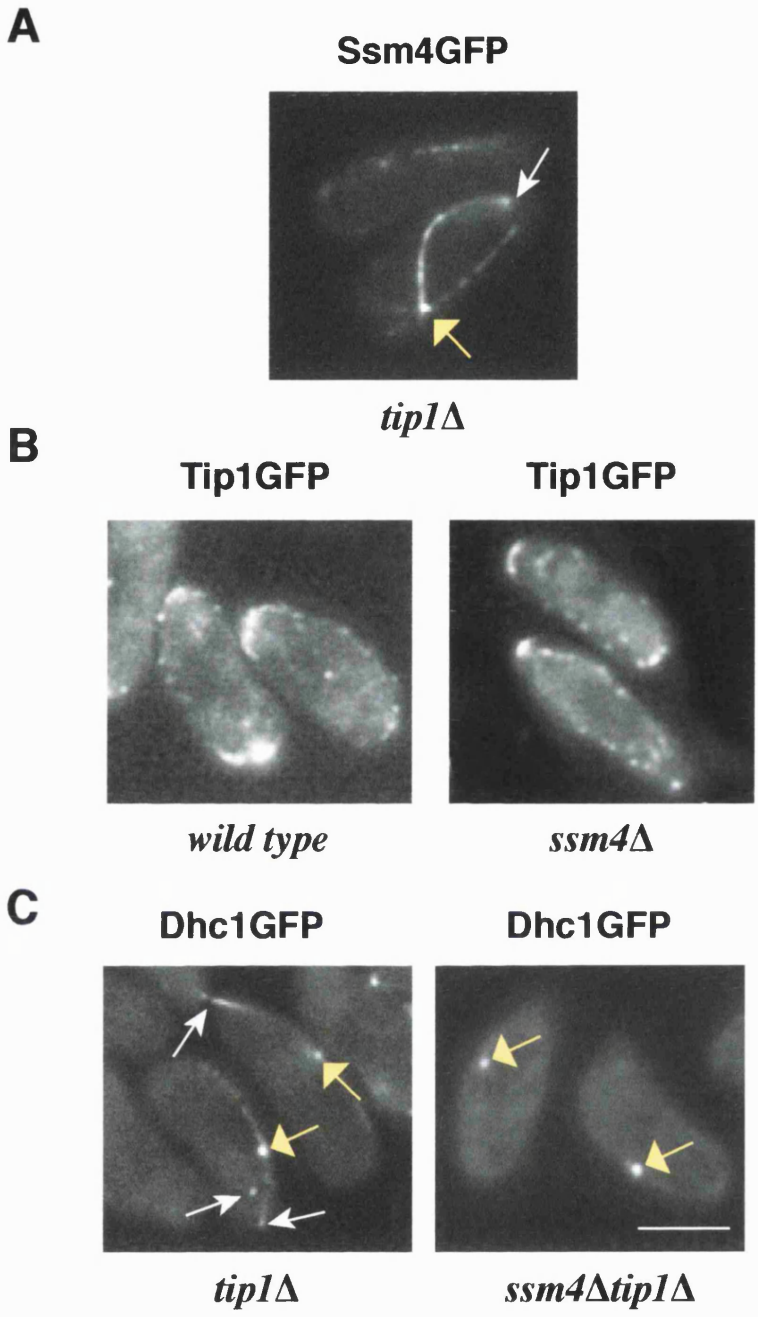

Fig 5.22 Ssm4GFP, Tip1GFP and DhcGFP localisation.
(A)*Cyr1Δsxa2Δtip1Δssm4GFP*, (B) *cyr1Δsxa2Δtip1GFP*, *cyr1Δsxa2Δtip1GFPssm4Δ*, (C) *cyr1Δsxa2Δtip1Δdhc1GFP* and *cyr1Δsxa2Δtip1Δssm4Δdhc1GFP* cells were grown in pheromone for 6 hours and then imaged with a fluorescent microscope. The white arrows indicate the microtubule tips and the yellow ones the SPB. Scale bar, 4μm.

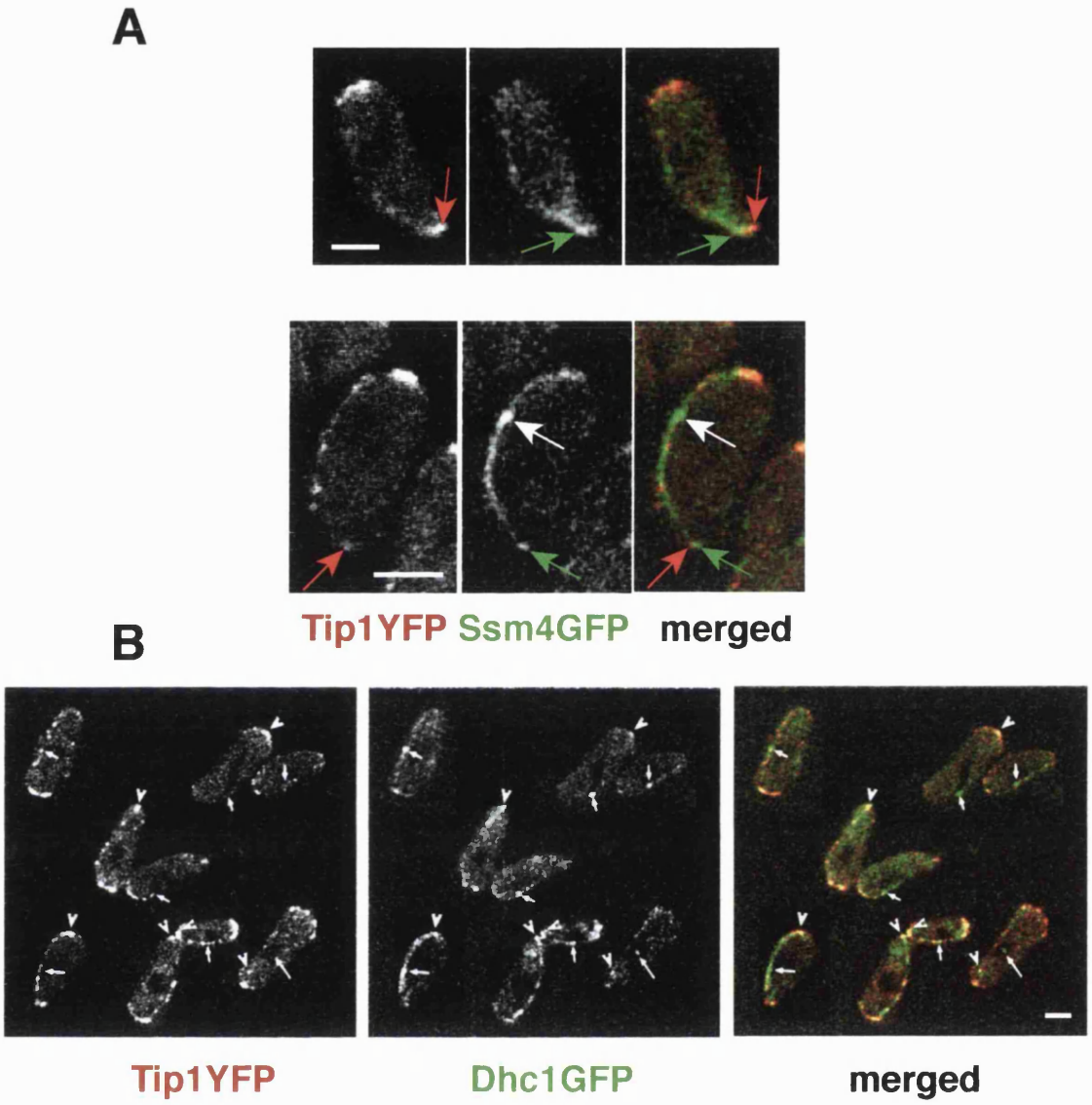

Fig 5.23 Ssm4-Tip1 and Tip1-Dhc1 co-localisation.
(A) *Cyr1Δsxa2Δssm4GFPtip1YFP* and (B) *cyr1Δsxa2Δdhc1GFPtip1YFP* cells were grown in the presence of pheromone for 6 hours. The cells were then imaged with a confocal microscope with YFP-CFP specific filters which can separate the YFP from the GFP signal. White arrows indicate the SPB and coloured arrows the signal at the microtubule tips. Scale bar, 3μm.

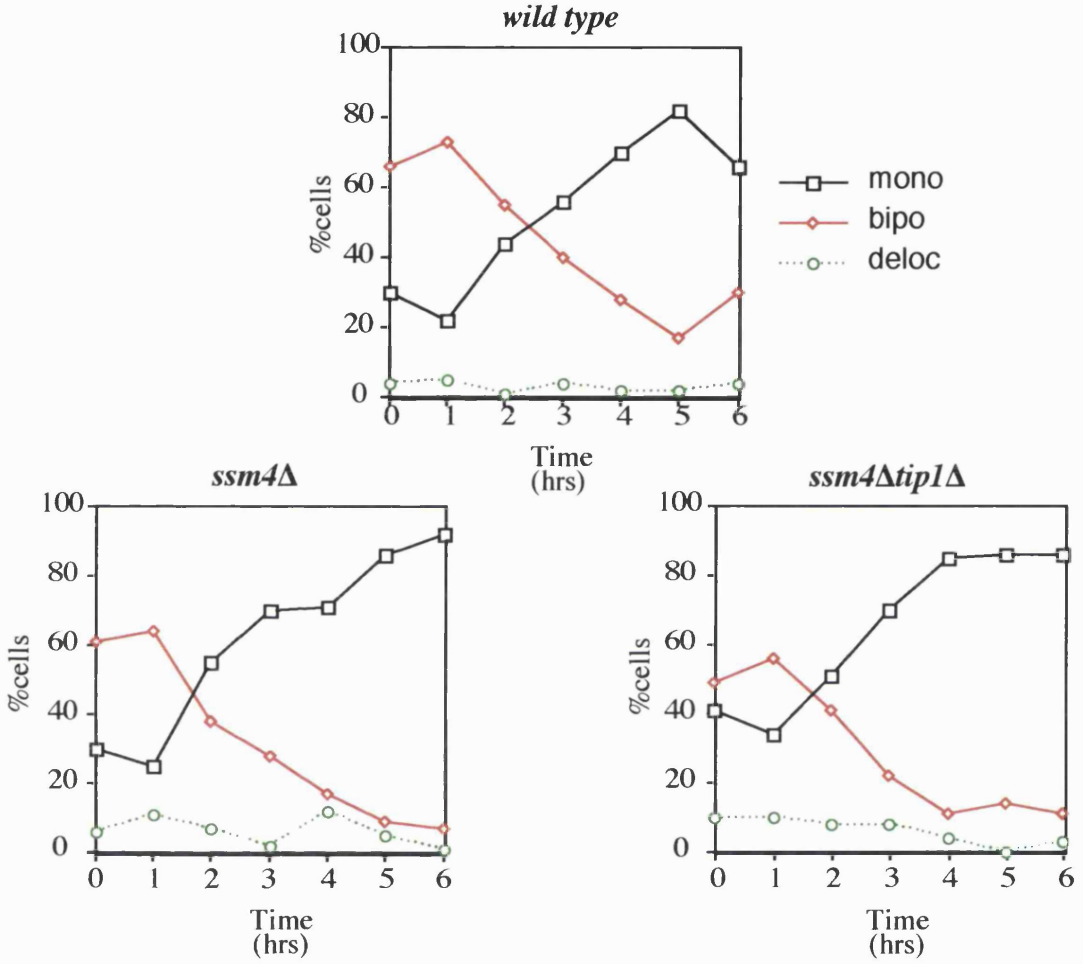

Fig 5.24 Actin relocalisation in *ssm4Δtip1Δ* cells.
Cyr1Δsxa2Δ, *cyr1Δsxa2Δssm4Δ* and *cyr1Δsxa2Δssm4Δtip1Δ* cells were grown in minimal, 3μg/l of pheromone was added to each culture at time 0, samples were taken every hour, fixed in formaldehyde and stained for actin. Cells were then score for monopolar, bipolar and delocalised actin.

A

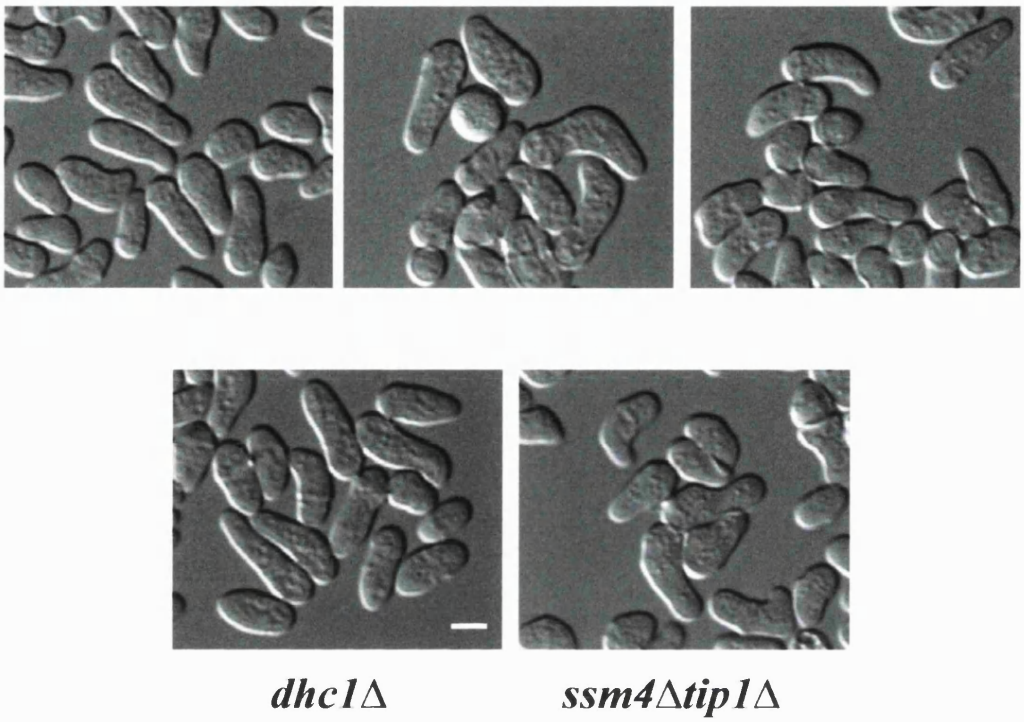

B

strain	n° of T-shaped cells		angle of shmoo	T-TEST
	-P	+P		
wild type	0	0	22.7°(n=71)	NA
tip1Δ	0	0	28.9°(n=72)	0.15
ssm4Δ	0	0	21.1°(n=60)	0.68
dhc1Δ	0	0	24°(n=70)	0.73
ssm4Δtip1Δ	0.5	2	34 °(n=112)	0.004

Fig 5.25 Appearance of mutant shmoos.

(A) Wild type and mutants cells were grown in the presence of pheromone for 6 hours. Cells were then placed on a slide and photographed using DIC optics. (B) Cells were scored for T-shaped cells before and after 6 hours in pheromone, at least 200 cells were scored. The angle of the shmooing projection was measuered using NIH image. A T-TEST between each mutant and the wild type was calculated to investigate if the angle of the shmoo was statistically significantly different. Scale bar, 3μm.

Chapter 6

General Discussion

6.1 Discussion

6.1.1 Determination of intrinsic cell polarity

During vegetative growth fission yeast cells are rod shaped, they extend along a single axis from their two ends, with microtubules spanning the length of the cell and actin localising to the growing cell ends (Hagan and Hyams, 1988; Marks et al., 1986). At every major growth transition, such as NETO and after cytokinesis, fission yeast cells re-position growth to the ends, in order to keep their linear shape. No external signals direct this process and the cell relies on an internal mechanism to locate its ends and position the growth machinery there.

Cell ends could be either re-identified at each growth transition or they could be marked by a particular factor laid down at the previous cell cycle. Microtubules are thought to be crucial for the cell to identify its ends: in the presence of TBZ, when microtubules are short, cells can not localise growth to the ends and become T-shaped (Sawin and Nurse, 1998). This suggests that cells find their ends *de-novo* at each cell cycle, and that this requires microtubules. However, mutants with clear microtubular defects, like *tea1Δ, tea2Δ* or *tip1Δ,* display only a small proportion of T-shaped cells, although cells do appear bent, suggesting that growth is not precisely located. This indicates that most of the time cells can form a growth zone at cell ends even in the absence of a fully functional microtubular array. It is possible that microtubules are mostly required to ensure that cells extend along a single axis.

In *S. cerevisiae* microtubules are not required for directing cell polarity. Landmarks laid down at the previous cell cycle direct bud formation. These landmarks

bind Cdc24 in the subsequent cell cycle to localise actin polymerisation and growth (Casamayor and Snyder, 2002). In *Drosophila melanogaster* neuroblasts a similar system applies. Bazooka, which is apically localised in the progenitor cells, directs the localisation of Inscuteable and Partner of Inscuteable (PINS) in the neuroblasts, leading to asymmetric cell division (Schaefer et al., 2001).

Many factors have been identified in *S. pombe* which locate to the cell ends and are required for cell polarity. These are good candidates for cell end markers, which could direct cell polarity in two ways:

1. They could trigger microtubule depolymerisation at the cell ends, allowing the microtubular array to terminate at the cell ends and therefore deliver growth components there.
2. They could mark cell ends as sites for growth, localising actin and growth components directly.

In the second chapter I analysed the role of three cell end markers, Tea1p, Tea3p and Pom1p in identifying cell ends as sites for growth and for microtubule termination. I could separate the two functions because I analysed their role in localising growth at low temperatures, when microtubules were essentially wild type.

I found that these three factors play three distinct but partially overlapping functions. Tea3p plays a major role as a trigger for NETO; Tea1p is a regulator of microtubule dynamics; and Pom1p is a cell end identifier for growth. Double mutants display synthetic interactions, which suggests that all three markers collaborate, at least partly, in every function. After displacement of actin from the cell ends, *tea1Δ pom1Δ*

and *tea3Δ pom1Δ* cells are unable to re-identify cell ends and localise actin, even at a temperature where the microtubular array is essentially wild type. This suggests that these factors play a direct role in localising the actin polymerisation machinery to cell ends during cell growth and that they do not act via the microtubule cytoskeleton. The number of cells unable to identify cell ends after actin delocalisation during the cell cycle matches the number of cells unable to re-initiate growth from the old end after cell division. This suggests that the same factors maintaining cell end identity during the cell cycle, are marking cell ends for growth after cytokinesis. Pom1p, Tea1p and Tea3p are located at the cell ends throughout the cell cycle. Fission yeast, like budding yeast, therefore relies on the positioning of landmarks laid down at the previous cell cycle to direct cell growth at the subsequent cell cycle. These landmarks act as a cell end memory system, which allows the cell to re-identify its ends after actin has been displaced, both during cell growth and after cytokinesis. Other cell end markers, like Bud6p or For3p (Feierbach and Chang, 2001; Glynn et al., 2001) might also be part of the landmark system, identifying cell ends as sites for growth.

Microtubules do not play an essential role in localising growth zones during exponential growth, since actin can relocalise to cell ends just as well in the presence or absence of microtubules. However, in the experimental conditions used, any cell end markers present would have been already at the cell ends. But microtubules may be required to initially get markers to the ends and thus contribute to cell polarisation. Tea1p is delivered to the cell ends by microtubules, and other cell end markers, like Pom1p and Tea3p, require Tea1p to accumulate at the cell ends. In the absence of a wild type

microtubular array these factors can still localise but not as efficiently, and cells often grow bent (Beinhauer et al., 1997; Browning et al., ; Brunner and Nurse, 2000). Microtubules therefore, might facilitate the localisation of cell end landmarks, or they might be required to deliver cell end markers and growth components at precisely opposing locations, thus guaranteeing linear growth.

During exponential growth, even when cell end markers and microtubules are missing, actin eventually relocalises to the ends of the cell after being displaced. This suggests that in the absence of cell end markers, actin and growth have an affinity for cell ends. Perhaps, the cell membrane or the cell wall also plays a role in localising growth zones. Inositol derivatives have been involved in actin polymerisation (Takenawa and Itoh, 2001), and the cell wall is known to be important for cell polarity (Ribas et al., 1991). Cell ends are normally sites of recent growth and might have a different membrane or cell wall composition from the cell middle, which could facilitate actin polymerisation and therefore growth. This would also explain why cells lacking cell end markers resume growth from the new end, the site with the newest cell wall and membrane composition. Maybe landmarks are required to relocalise growth from the site of septation to the old end, ensuring the cell first grows away from its sister to explore new space, in search for more nutrients.

Landmarks are also involved in triggering NETO. This is again an active transition, which could not be driven by static membrane composition. Cell end markers could collaborate with membrane and cell wall components in a local feedback mechanism to concentrate growth to a particular site. Tea1p and Tea3p have limited

homology to the ERM family of proteins. ERMs cross-link actin filaments with the plasma membrane (Louvet-Vallee, 2000) and are involved in a positive feedback process at the leading edge of the plasma membrane involving Rho and Phosphatidylinositol (4,5) bisphosphate (PIP2), an activator of ERM whose production is induced by Rho. Active Rho recruits ERM proteins to the plasma membrane and activates them via PIP2 and an unknown kinase. Active ERM can block Rho-GDI, a Rho inhibitor, thus activating Rho further, in a positive feedback pathway localised at the plasma membrane (Reviewed by (Tsukita and Yonemura, 1999)). Rho and Inositol derivatives are involved in regulating cell wall and membrane composition in *S. pombe*. A similar positive feedback could therefore operate in *S. pombe* to localise growth to the cell ends but no evidence for this has so far emerged. Pom1p is a member of the Dyrk family of dual specificity protein kinases (Becker and Joost, 1999) that have been implicated in actin polymerisation (van Es et al., 2001). It is possible that Tea1p, Tea3p and Pom1p may have functions related to their homologues in multicellular eukaryotes in regulating actin behaviour to ensure proper cellular organisation. How Tea3p, Tea1p and Pom1p link to the actin cytoskeleton is still not known. Tea3p's homology to ERM proteins is especially high in the actin binding region, Tea1p contains a Kelch motif, which can associate with actin (Reviewed in (Adams et al., 2000)), and recent evidence suggests that there might be an interaction between Tea1p and Pak1p (Qyang et al., 2002). Thus there might be a direct connection between these proteins and the actin polymerisation machinery.

Actin and cell end markers are delocalised during nitrogen starvation (Rupes et al., 1997), suggesting these cells might have lost all "memory" of cell polarity. Yet cells

resume growth in a straight line when they are returned to rich medium. Actin is also transiently delocalised upon shift to high temperatures (K.Leonhard, unpublished observation), which might also displace cell end markers. Interestingly, mutants defective in microtubular dynamics or cell end "memory" exhibit a dramatic increase in the number of branches formed upon exit from nitrogen starvation (M. Arellano, unpublished observation) or shift to high temperatures. This suggests that microtubules and cell end markers play a more important role under these conditions than they do in steady state exponential growth. Mutants with defective microtubules but no severe cell end memory defect (like *tea1Δ*), or mutants that can not identify their cell ends efficiently but have no severe microtubule defect (like *tea3Δ pom1Δ*), show an increase in T-shaped cells upon shift to high temperature. Mutants with both a microtubule and a cell end memory defect exhibit an even stronger increase in T-shaped cells. The microtubule array is highly dynamic and it might be involved in re-identifying the ends of a rod-shaped cell after markers have been lost. Microtubules could then deliver cell end markers, which will direct growth. This process might allow the cell to reposition the growth zones in response to changing environmental conditions and re-establish cell polarity.

During vegetative exponential cell growth microtubules, cell end identifiers, and cell membrane and wall composition could feedback into each other to maintain linear cell growth. After cell division, cell end markers might direct the localisation of the growth machinery and collaborate with membrane and wall components to limit the localisation of the growth zones to the cell ends. The microtubules then might orient along the long axis of the cell thereby delivering more cell end markers, which will then

identify the ends of the two daughter cells generated at septation (Fig 6.1). This system would be designed to maintain cells growing in a straight line during exponential growth.

6.1.2 Determination of extrinsic cell polarity

6.1.2.1 Role of vegetative morphological factors

Pheromones secreted by a partner of opposite mating type induce a new mode of cell growth, which is extrinsically determined. Pheromone signalling triggers two responses: cell cycle arrest in the G1 phase and a morphological switch. The cell cycle arrest is sensitive to low pheromone concentrations and is also temperature independent, whereas the morphological switch is only brought about in response to high pheromone concentrations and is temperature sensitive. Although only one MAPK cascade has been identified as being responsible for both pheromone responses it is possible that it activates two different targets at different concentrations, one responsible for the cell cycle arrest and the other for the morphological switch. The same has also been observed in *S. cerevisiae;* lower pheromone concentrations are required to induce cell cycle arrest than to induce projection formation (Moore, 1983). Patterning during development is also brought about by the sequential activation of distinct developmental processes in response to different threshold values of the same morphogenic gradient (Irvine and Rauskolb, 2001). This suggests that modulating one signal to trigger different responses is a conserved mechanism.

During shmooing none of the vegetative cell end markers, Tea1p, Pom1p and Tea3p appear to play a role in directing cell polarity. These factors are not required for a cell to set up a shmooing polarised projection and they are no longer concentrated at the

growing areas. But before cells switch to a monopolar shmooing growth pattern, they undergo an intermediate bipolar stage in the G1 phase of the cell cycle (Petersen et al., 1998). This may be an initial re-setting step, which allows the cell to pick either end for shmooing growth, depending on which one is experiencing the higher pheromone concentration. Tea3p and Pom1p play a role in this intermediate bipolar stage. Tea3p is required to trigger the relocalisation to both ends, because in its absence the cell can not undergo the bipolar intermediate stage. Pom1p is involved in recognising the two ends, since in *pom1Δ* cells actin is removed from one end but is not relocated efficiently to the two ends, leading to an increase in delocalised actin. This suggests that the relocalisation to both ends is not achieved by activating actin polymerisation at the second end but via a transient actin delocalisation, similar to the process suggested for NETO (Rupes et al., 1999). These experiments also indicate that at this stage the cell still recognises its vegetative ends, and only after an end has been chosen is the vegetative polarisation machinery shut down. Although cells do undergo this bipolar transition as they switch from vegetative to shmooing growth, most cells appear to initiate shmooing growth from the new end generated at cytokinesis. In these experiments cells were exposed to a uniform pheromone concentration and not to a pheromone gradient. *S. cerevisiae* cells exposed to very high or uniform pheromone concentrations initiate a default shmooing pathway. This default pathway initiates growth near the incipient bud site and is regulated by different factors to normal shmooing growth (Dorer et al., 1995). *S. pombe* cells exposed to a uniform pheromone concentration could also be executing a default pathway. This "default" shmooing growth pattern is strikingly similar to that of

vegetative cells lacking cell end markers. In both cases there are no landmarks to direct growth, either because they have been deleted, or because they are no longer recognised and there is no exogenous gradient to direct extrinsic cell growth. Perhaps, in the absence of any localisation signal growth will always resume from the new end. Alternatively, there might be no gradients in the wild and shmooing growth might be always initiated from the new end in fission yeast. Matings in the wild normally occur between h90 cells after nitrogen starvation. Starved cells are very close to each other and so a gradient might not be able to form. Most h90 cells also switch mating type after cytokinesis and therefore the closest mating partner is the sister cell, which is closest to the new end. Cells initiating shmooing from the new end have a higher chance of meeting a mating partner and therefore fission yeast cells might always shmoo from the new end.

Tea1p, Tea2p and Tip1p, which during vegetative growth regulate microtubular dynamics, are not implicated in microtubular dynamics during shmooing, indicating that both the actin and the microtubule cytoskeleton are regulated in a different manner during extrinsic growth. Tea1p, Tea2p and Tip1p appear to inhibit the switch to the shmooing growth mode, suggesting the vegetative microtubular array has to be actively dismantled in response to pheromone before the new extrinsic mode of growth can be established.

Factors which are part of the intrinsic polarisation machinery, could be inactivated either by degradation, protein modification or delocalisation as the role of these proteins in directing cell polarity relies on their localisation at cell ends (Bahler and Nurse, 2001; Behrens and Nurse, 2002). All factors are still present during shmooing but some, like Tea1p and Tip1p, are differentially phosphorylated and this might play a role in their

inactivation. The binding of CLIP-170 to microtubules is known to be regulated by phosphorylation (Rickard and Kreis, 1991), but Tip1p's binding to microtubules is just as efficient in the presence of pheromone. Moreover Tea1p, Tea2p, Tea3p, Tip1p and Pom1p are delocalised in response to pheromone. As Tea3p, Pom1p, Tea2p and Tip1p are dependant on Tea1p to localise to the cell ends, the triggering of Tea1p's delocalisation will ensure that these other morphological factors will not be able to localise either. In shmooing cells Tea1p can no longer concentrate at the cell ends but it is still localised to the cell periphery. Tea1p is transported along microtubules to the cell ends and as Tea1p's binding to microtubules is reduced during shmooing, its diffusion away from the ends could be quicker than its delivery. Alternatively, the concentration of Tea1p at the cell ends during vegetative growth could be due to a positive feedback process between Tea1p and other cell end factors, if this feedback were switched off during shmooing then Tea1p would no longer be able to concentrate at the cell end.

None of the known vegetative morphological markers therefore play a role in directing cell growth but does the actin polymerisation machinery still play a role? In *S.cerevisiae* (Nern and Arkowitz, 2000; O'Shea and Herskowitz, 2000; Shimada et al., 2000), the core polarisation machinery is directed to the internal landmarks during vegetative growth and to the externally marked site during shmooing growth. This might be the case also in *S. pombe.* Ral3p, a direct regulator of the core polymerisation machinery, is still required for shmooing, as are other regulators of actin polymerisation, like Scd1p, Ras1p and Ral2p (Chang et al., 1994; Fukui et al., 1989; Fukui and Yamamoto, 1988). Ral3p is localised to the growing end, indicating that it might play a

direct role in organising actin polymerisation and growth at that site. This suggests that the core polymerisation machinery, like in *S. cerevisiae*, is the same during intrinsic and extrinsic growth and that shmooing specific morphological factors are involved in positioning the core actin polymerisation at the shmooing tip. As Mam2p (Kitamura and Shimoda, 1991), the pheromone receptor, clusters to the shmooing end before actin, it is likely to mark the end where growth should occur in response to pheromone. Adapter molecules might then act as a bridge between the actin cytoskeleton and the pheromone receptor. This role in *S. cerevisiae* is carried out by Far1 (Nern and Arkowitz, 2000; Shimada et al., 2000) but as no Far1 homologue is present in *S. pombe*, it is possible that no such adapter exists in *S. pombe.* In *S. cerevisiae* the actin polymerisation machinery has to be actively diverted from the bud landmarks to the pheromone receptor. In *S. pombe* the vegetative cell end identifiers appear to be switched off in pheromone and the growth machinery might therefore automatically re-direct to the pheromone receptor.

When actin is displaced from the end during shmooing growth it relocalises much more slowly than in vegetative growth, suggesting that growing ends are less strongly marked during shmooing growth. As there are now no internal landmarks identifying cell ends, the cell might have to rely on a continuos external signal to direct polarised cell growth, this is provided by the pheromone receptor. Receptor clustering in *S. cerevisiae* requires actin (Ayscough and Drubin, 1998), and so when actin is displaced in *S. pombe* the receptor might also disperse. The receptor then has to re-cluster before it can mark the cell end and direct actin localisation, and this whole process might take longer. Cell end marking might also be a lot more dynamic than during vegetative growth, and feedback

to the actin cytoskeleton for its maintenance. This could allow the cell to rapidly adjust to changes in the direction of the external signal. During shmooing, the landmark for growth is positioned by an external signal and the cell must recognise that signal and position its growth site accordingly, thus altering its current cell shape. The externally determined cell polarity is designed to alter cell shape to follow the external signal. In vegetative growth the landmarks for cell polarisation are set up internally and once the cell shape has been established the cell must be able to read that shape and maintain it, despite changing external conditions, and this polarity machinery might therefore be more robust.

6.1.2.2 Role of mating specific microtubule regulators

The vegetative regulators of microtubular dynamics no longer play a role during shmooing growth. On the other hand a new set of regulators is induced, including the dynein complex (Yamamoto et al., 1999). During vegetative growth, this highly conserved minus end directed motor does not play a role in the regulation of microtubular dynamics or nuclear positioning, perhaps because the nucleus does not need to travel long distances. In contrast, during shmooing growth, the nucleus oscillates back and forth along the whole length of the cell and dynein appears to play a central role (Yamamoto et al., 2001; Yamamoto et al., 1999).

Ssm4p is involved in the same cellular activities as dynein and it interacts with the dynein complex in fission yeast, strongly suggesting that Ssm4p is a functional as well as a sequence homologue of p150-Glued, a component of the dynein-activating dynactin complex.

The oscillatory horsetail nuclear movement is powered by microtubules (Ding et al., 1998). A pulling force is exerted at the cortex on depolymerising microtubules, which drives the nucleus and SPB to one end of the cell. Once the nucleus reaches the cell end, the pulling force at that end stops and the microtubules at the opposite end start to depolymerise pulling the nucleus in the opposite direction (Yamamoto et al., 2001). For this mechanism to work four conditions have to be met: 1. The whole microtubule bundle has to depolymerise at the same time, 2. A pulling fore has to be generated on the microtubules, 3. The microtubules have to be anchored, probably to the cortex, as they depolymerise, 4. Microtubular dynamics at opposite ends of the cell have to be co-ordinated, with microtubules polymerising at one end as they depolymerise at the other, thereby ensuring that movement occurs continuously and smoothly. When the pulling force at one end stops, the opposite microtubule tip is already in the vicinity of the opposite cell end, ready to establish a productive interaction with the cortex and pull the nucleus in the opposite direction. All these conditions are lost in *ssm4Δ* cells. Microtubules grow and shrink independently within a bundle, a pulling force is not generated on depolymerising microtubules, microtubules are not anchored at the cell end, and opposite ends do not display opposite dynamics. Whereas p150-Glued proteins have been shown to stabilise microtubules (Vaughan et al., 1999), Ssm4p appears to be required to co-ordinate microtubules dynamics. Also, in *ssm4Δ* cells Dhc1p can no longer accumulate at the site where microtubules contact the cell cortex. Dhc1p is thought to generate the pulling force that drives the nuclear oscillations at that site (Yamamoto et al., 2001), and therefore might not be able to pull on microtubules in *ssm4Δ* cells, explaining

the lack of pulling forces in this mutant. Dhc1p fluorescence on microtubules is also reduced in *ssm4Δ* cells. In vitro studies have also shown that p150-Glued enhances dynein's binding to microtubules (King and Schroer, 2000) and in *Neurospora crassa* dynactin is required for efficient binding of dynein to microtubules (Kumar et al., 2000). Although previous experiments have suggested that the dynein-dynactin complex could bind polymerising or anchored microtubules (Minke et al., 2000), this study shows that Ssm4p accumulates on the tips of stalling or depolymerising microtubules, even when they are not anchored. How this is achieved in not clear. One possibility is that Ssm4p might be slowly moving towards microtubule plus ends, when microtubules stall or depolymerise, Ssm4p reaches the microtubule end, accumulating there. Here, Ssm4p could be directly required to stabilise Dhc1p and activate its pulling force. Alternatively, the altered microtubular dynamics in *ssm4Δ* cells with microtubules growing and shrinking independently within a bundle, could limit the accumulation of Dhc1p at the tip of the bundle.

The dynactin complex is also known to regulate dynein motor activity by directly influencing its ATPase activity (Kumar et al., 2000), and increasing its processivity (King and Schroer, 2000). Ssm4p might therefore regulate dynein both by activating its motor activity and by localising it to the microtubule tips where it can exert its pulling force.

CLIP-170 like proteins have also been implicated in dynein function; CLIP-170 co-localises with dynein and dynactin (Dujardin et al., 1998), co-immunoprecipitates with dynein intermediate chain (Coquelle et al., 2002) and is involved in localising dynactin (Valetti et al., 1999). However, this interaction is mediated by LIS-1 (Coquelle

et al., 2002), and I could not find a significant homologue in the pombe genome database. Tip1p, a CLIP-170 like protein, is not required for Dhc1p or Ssm4p localisation in fission yeast and only partially co-localises with Ssm4p, suggesting it might not be directly regulating the dynein-dynactin complex in fission yeast. Deletion of *tip1* leads to less bright microtubules, suggesting they might be less bundled. On the contrary, deletion of *ssm4* leads to brighter and probably more bundled microtubules. The double mutant *tip1Δ ssm4Δ* displays a more severe phenotype than the sum of the two individual phenotypes, leading to an almost vegetative microtubule array. Ssm4p and Tip1p could act independently of each other, regulating two different aspects of shmooing microtubular dynamics, both of which have to be absent for the microtubule array to completely disassemble. For example Tip1p might affect bundling of microtubules, as in its absence bundles appear less bright, whereas Ssm4p might co-ordinate microtubular dynamics within a bundle and between opposite ends of the cell. In the absence of both, microtubules are neither bundled nor co-ordinated, and as a consequence take on the appearance of a vegetative microtubular array. Alternatively, Tip1p might partially substitute for Ssm4p function in *ssm4Δ* cells and only when both proteins are missing is the real function of Ssm4p unveiled. Ssm4p, a p150 Glued homologue, therefore ensures nuclear movement in two ways: it is required to co-ordinate microtubular dynamics within a bundle and between opposite cell ends, and to regulate anchoring and pulling on depolymerising microtubules at the cell cortex, generating the characteristic oscillatory shmooing microtubular array. The vegetative microtubular pattern might be a basic state of microtubular organisation to which the cell can revert.

Microtubule capture at the cell cortex has been observed in a variety of organisms, and is typically followed either by stabilisation, shrinkage or sliding of the microtubule array. Often these events lead to nuclear movement or re-orientation, and they appear to be regulated by a conserved set of factors (for a review (Gundersen, 2002)). Two major pathways responsible for these events have been identified. The first is involved in microtubule capture and shrinkage in *S. cerevisiae* and microtubule stabilisation in fibroblasts, and does not involve dynein. It relies on activation by Rho of formin, which then interacts with an EB1 homologue, via an unknown factor, to capture microtubules (Gundersen, 2002). The second pathway requires dynein-dynactin, and is involved in MTOC reorientation in a variety of organisms and in microtubule capture and sliding in *S. cerevisiae*, where the nucleus is pulled in the mother-daughter neck. The same components are also involved in the spindle rotation leading to the asymmetric cell division of the one cell stage *C. elegans* embryo. In mammalian cells dynein-dynactin is regulated by PAR6-PKCζ , which is activated by CDC42 (Etienne-Manneville and Hall, 2001). In *S. pombe* dynein activity has to be switched on and off at each oscillation, the homologues of CDC42 and PKC, Cdc42p or Rho1p and Pck1p, could be located at the cell ends and provide the regulatory on/off switch required for the horsetail movement. For pulling to occur, the dynein motor has to be anchored to microtubules on one side and to the cell cortex on the other. How this is achieved is not well understood. Some possible candidates for a cortical dynein anchor have been described. LIS1 localises to microtubules and to the cell cortex (Faulkner et al., 2000) and *LIS1* mutations in *Drosophila* displace dynein from the cortex (Swan et al., 1999). In mammalian cells

spectrin associates with ARP1, a component of dynactin, to link dynein to vescicular organelles (Holleran et al., 1996) but no spectrin involvement in linking dynein to the cortex has been described. Dynein also binds ß-catenin to tether microtubules to adherens junctions (Ligon et al., 2001). Adenomatous Polyposis Coli, APC, is another possible candidate, since in mammalian cells APC localises to the plasma membrane and to microtubules via EB1 (Askham et al., 2000; Nathke et al., 1996). EB1 also binds to dynein and therefore could provide a link to APC as a cortical anchor (Berrueta et al., 1999). No homologues to any of these putative anchors exist in *S. pombe*, except for the EB1 homologue Mal3p, which might interact with dynein and could provide a link to a cortical anchor. In *S. cerevisiae* Num1 localises to the bud tip and it interacts with microtubules in a dynein-mediated fashion, suggesting it could be the link between dynein and the cortex in this system (Farkasovsky and Kuntzel, 2001). *S. pombe* does have a weak Num1 homologue (SPBC216.02), which could be involved in anchoring dynein to the cortex. Further studies in S.pombe will be required to identify the cortical dynein anchor.

A possible model for horsetail nuclear movements could involve 3 steps (Fig 6.2):

1. The microtubules ahead of the nucleus depolymerise as they are pulled by Dhc1p. Ssm4p activates Dhc1p motor activity and ensures that the microtubules can interact with the cortical anchor and that the whole bundle depolymerises as one. The microtubules behind the nucleus polymerise more slowly than the ones ahead are being depolymerised and so they are pulled away from the cell end and can not interact with the cortical anchor.

2. When the overlap region reaches the end of the cell, microtubules can no longer depolymerise and they dissociate from their cortical anchor. The dynein-dynactin complex, which is moving in the minus direction, is no longer anchored at the cortex and so it moves towards the SPB. A Rho-like switch, located at the overlap region, could inactivate the dynein-dynactin complex when it reaches this region, causing it to dissociate from the cortical anchor.

3. When microtubules lose their cortical anchor they are no longer pulled, and the microtubules behind are able to grow until they reach the cortical anchor at the opposite end. The anchor, or another factor at the cell ends, might induce microtubules to pause. Ssm4p then accumulates at the microtubule tips, generating a stable interaction with the cortex and triggering microtubule depolymerisation. Dhc1p accumulates at the tips of microtubules, stabilised by Ssm4p, which also activates Dhc1p motor's activity to pull the nucleus in the opposite direction. Alternatively once the SPB has reached the cell end it could send a signal to the opposite microtubule tip, activating it for an interaction with the cortical anchor.

Although the horsetail oscillatory nuclear movement is specific to fission yeast mating, the molecular basis of it appears to be conserved with nuclear movement in other organisms. It might follow the same basic principles: it is dynein-dynactin based, dynein must be anchored to the cell end to generate a pulling force on the nucleus, and dynein's motor activity has to be highly regulated, with possibly a Rho protein acting as the on/off switch.

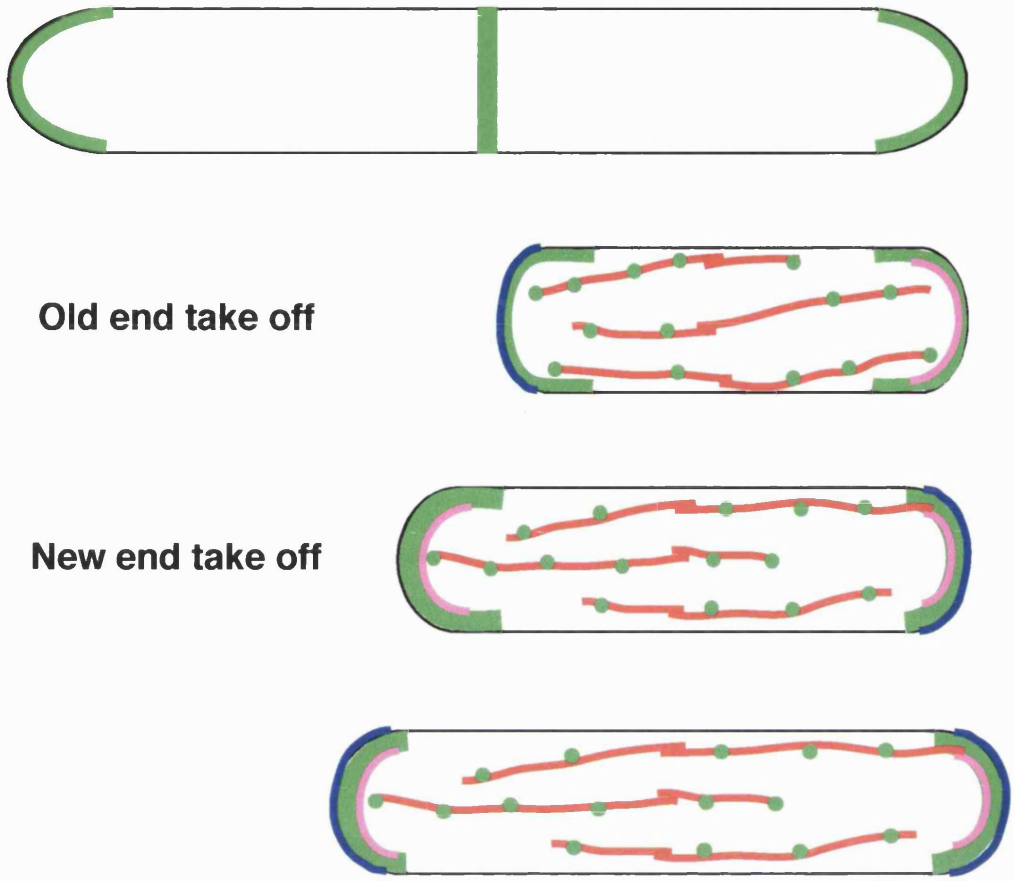

Figure 6.1 Model for vegetative growth.
(A) At cytokinesis cell end markers are found at the cell ends and at the site of septation.
(B)The new born cell has new membrane and cell wall cell at the New End, but it also inherits cell end markers which direct growth to the old end, initiating Old End Take Off.
(C) New membrane is formed at the site of growth which feeds-back into the cell end marker system tightening the growth zone. Microtubules deliver cell end markers to the two cell ends, maintaining the two ends exacly opposed to each other.
(D) Cell end markers trigger New End Take Off,initiating bipolar cell growth.

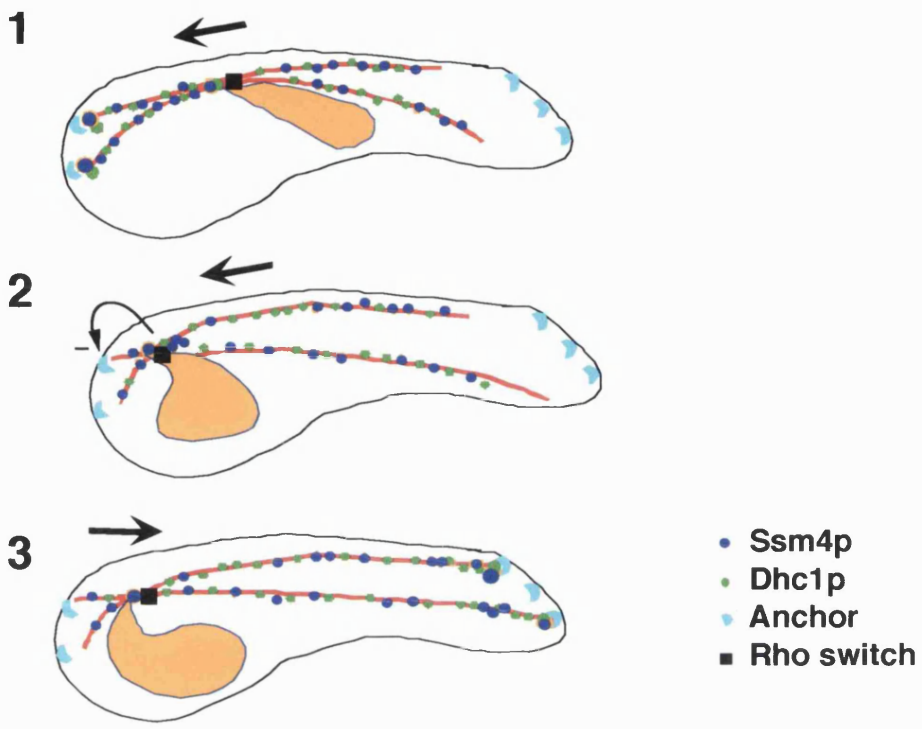

Fig 6.2 Model for microtubular oscillations.
See text for details

Chapter 7

Materials and methods

7.1 Materials and methods

7.1.1 Fission yeast physiology and maintenance

7.1.1.1 Gene and protein nomenclature

The gene and protein nomenclature followed in this thesis is based on (Kohli, 1987). Fission yeast gene names are three letter words followed by a number, expressed in lower case italicised letters (e.g. *cdc10*). The wild type gene is marked with a "+" after the gene name (e.g. *cdc10+*) and a mutant allele is indicated by the gene name followed by the allele number (e.g. *cdc10-129*), all in lower case italics. A deletion is marked with a "Δ" after the gene name (e.g. *cdc10Δ*). To indicate that a particular gene has been substituted with another, the deleted gene is followed by "::" and the name of the replacing gene (e.g. *ssm4Δ::kanR*). The protein encoded by a particular gene has the same name, but with the first letter in upper case and the rest in lower case, not italicised, followed by a "p" (e.g. Cdc10p). If a gene has been fused to another DNA sequence, the name of the individual DNA sequences is expressed in the order they would be found in the genome with no spaces if the two sequences would generate a single fused protein product. *ssm4GFP kanR* means that the *ssm4* gene has been fused to *GFP* and that the kanR gene follows the fusion. When genes are expressed from plasmids the gene name is preceded by the name of the plasmid and a "p" (e.g. pREP3X*tea1+*). *S. cerevisiae* gene names are three capital letter words, followed by a number, all italicised (e.g. *BNI1*), and the corresponding protein has the first letter in upper case, followed by lower case (eg.

7.1.1.2 Strain growth and maintenance

The strains of *S. pombe* used in this study are listed in Table 1. All strains were derived from wild type h-972 and h+975 (Leupold, 1950). Media were prepared as described previously. Complete medium YE5S, minimal medium EMM and mating glutamate medium were used, supplemented with amino-acids when required (MacNeill and Fantes, 1993; Moreno et al., 1991). Standard methods were used for growth, storage, and maintenance of strains (Moreno and Nurse, 1994). Strains were kept as frozen stocks and thawed on agar plates when required. Liquid cultures were inoculated from a patch into the desired medium and grown overnight. When large cultures were required a pre-culture in YE5S was grown for 24 hours, and that was used to inoculate the larger liquid culture. All cells were grown at 25°C unless otherwise stated.

Table 7.1 Fission yeast strains

Strain	Genotype	Reference
PN 4385	*tea1GFP kanR leu1-32 ura4-D18 h+*	Cell Cycle laboratory
PN 3227	*tea3GFP kanR h-*	Cell Cycle laboratory
PN 3141	*pom1GFP kanR h-*	Cell Cycle laboratory
PN 2853	*ura4-D18 leu1-32 h+*	Cell Cycle laboratory
PN 1686	*tea1Δ::ura4 ura4-D18 leu1-32 h-*	Cell Cycle laboratory
PN 3256	*tea3Δ::kanR ura1-D18 leu1-32h+*	Cell Cycle laboratory
MA 82	*pom1Δ::ura4 ura4-D18 leu1-32*	Cell Cycle laboratory
PN 2	*wt h90*	Cell Cycle laboratory
PN 3810	*tea1Δ::ura4 ura4D18 h90*	Cell Cycle laboratory
PN 3808	*tea2.1 h90*	This study
PN 3809	*tip1Δ::kanR h90*	This study
PN 2467	*tea2GFP(kanR) ura4D18 h90*	This study
PN 3834	*pom1Δ::ura4 h90*	This study
PN 3043	*tea1Δ::ura4 pom1Δ::ura4 ura4-D18 leu1-32 h+*	This study

TN 130	*tea1Δ::ura4 tea3Δ::his3 his3-D1 ura4-D18 leu1-32*	This study
PN 3258	*pom1Δ::ura4 tea3Δ::kanR ura4-D18 leu1-32 h+*	This study
PN 3741	*cyr1Δ::LEU2 sxa2Δ::ura4 leu1-32 ura4D18 h-*	(Imai and Yamamoto, 1994)
PN 1379	*cyr1Δ::LEU2 sxa2Δ::ura4 leu1-32 ura4D18 h+*	Cell Cycle laboratory
PN 1689	*cyr1Δ::LEU2 sxa2Δ::ura4 tea1Δ::ura4 leu1-32 ura4D18 h-*	(Mata and Nurse, 1997)
PN 3162	*cyr1Δ::LEU2 sxa2Δ::ura4 pom13HA ura4 ura4-D18 leu1-32 h-*	(Bahler and Pringle, 1998)
PN 3177	*cyr1Δ::LEU2 sxa2Δ::ura4 pom1Δ::his3 leu1-32 ura4D18 h-*	This study
PN 3301	*cyr1Δ::LEU2 sxa2Δ::ura4 tip1Δ::kanR leu1-32 ura4-D18 h-*	This study
PN 3303	*cyr1Δ::LEU2 sxa2Δ::ura4 tea2-1 leu1-32 ura4-D18 h-*	This study
PN 3749	*cyr1Δ::LEU2 sxa2Δ::ura4 pom1GFP kanR leu1-32 ura4-D18 h-*	This study
TN 135	*cyr1Δ::LEU2 sxa2Δ::ura4 tip1YFP kanR tea1GFP(kanR) leu1-32 ura4D18 h-*	This study
TN 136	*cyr1Δ::LEU2 sxa2Δ::ura4 tip1YFP kanR tea2GFP(kanR) leu1-32 ura4D18 h-*	This study
TN 127	*cyr1Δ::LEU2 sxa2Δ::ura4 tea1GFP kanR leu1-32 ura4D18 h-*	This study
TN 22	*cyr1Δ::LEU2 sxa2Δ::ura4 tea2GFP kanR leu1-32 ura4D18 h-*	This study
TN 133	*cyr1Δ::LEU2 sxa2Δ::ura4 tip1YFP kanR leu1-32 ura4D18 h -*	This study
PN 3827	*cyr1Δ::LEU2 sxa2Δ::ura4 cdc25-22 tea1GFP kanR ura4-D18 leu1-32 h-*	(Stern and Nurse, 1997)
TN 23	*cyr1Δ::LEU2 sxa2Δ::ura4 int nmt1GFPral3 leu1-32 ura4D18 ade6-704 h-*	This study
PN 2668	*cyr1Δ::LEU2 sxa2Δ::ura4 mam2GFP kanR leu1-32 ura4D18 h-*	This study
PN 2667	*cyr1Δ::LEU2 sxa2Δ::ura4 mam2MYC kanR leu1-32 ura4D18 h-*	This study
PN 4483	*cyr1Δ::LEU2 sxa2Δ::ura4 tea3Δ::kanR leu1-32 ura4D18 h-*	This study
PN 4482	*cyr1Δ::LEU2 sxa2Δ::ura4 tea3GFP kanR leu1-32 ura4D18 h-*	This study
PN 1701	*cyr1Δ::ura4 sxa2Δ::ura4 leu1-32 ura4D18 ade6-704 h-*	This study
TN 158	*cyr1Δ::ura4 sxa2Δ::ura4 nmt1-GFP-atb2 leu1-32 ura4D18 h-*	This study
TN 96	*cyr1Δ::ura4 sxa2Δ::ura4 ssm4Δ::kanR leu1-32 ura4D18 h-*	This study
TN 165	*cyr1Δ::ura4 sxa2Δ::ura4 nmt1-GFP-atb2 ssm4Δ::kanR leu1-32 ura4D18 h-*	This study
TN 236	*cyr1Δ::ura4 sxa2Δ::ura4 tip1Δ::kanR leu1-32 ura4D18 h-*	This study
PN 3855	*cyr1Δ::ura4 sxa2Δ::ura4 tip1Δ::kanR ssm4Δ::kanR leu1-32 ura4D18 h-*	This study
PN 3785	*cyr1Δ::ura4 sxa2Δ::ura4 ssm4GFP kanR leu1-32 ura4D18 h-*	This study
PN 3783	*cyr1Δ::ura4 sxa2Δ::ura4 ssm4HA kanR leu1-32 ura4D18 h-*	This study
TN 380	*cyr1Δ::ura4 sxa2Δ::ura4 ssm4Δ::kanR dhc1GFP kanR leu1-32 ura4D18 h-*	This study
PN 3454	*cyr1Δ::ura4 sxa2Δ::ura4 dhc1GFP kanR leu1-32 ura4D18 h-*	This study
TN 364	*cyr1Δ::ura4 sxa2Δ::ura4 tip1Δ::kanR dhc1GFP kanR leu1-32 ura4D18 h-*	This study
TN 360	*cyr1Δ::ura4 sxa2Δ::ura4 tip1Δ::kanR ssm4GFP kanR leu1-32 ura4D18 h-*	This study
PN 4314	*cyr1Δ::ura4 sxa2Δ::ura4 dhc1MYC kanR leu1-32 ura4D18 h-*	This study
TN 342	*cyr1Δ::ura4 sxa2Δ::ura4 ssm4HA kanR dhc1MYC kanR leu1-32 ura4D18 h-*	This study
TN 362	*cyr1Δ::ura4 sxa2Δ::ura4 ssm4Δ::kanR tip1Δ::ura4 dhc1GFPkanR leu1-32 ura4D18 h-*	This study

TN 336	*cyr1Δ::ura4 sxa2Δ::ura4 tip1YFP kanR ssm4Δ::kanR leu1-32 ura4D18 h-*	This study
PN 4361	*cyr1Δ::ura4 sxa2Δ::ura4 tip1YFP kanR ssm4GFP kanR leu1-32 ura4D18 h-*	This study
TN 290	*cyr1Δ::ura4 sxa2Δ::ura4 tip1YFP kanR dhc1GFP kanR leu1-32 ura4D18 h-*	This study

Table 7.2 Fission yeast plasmids

Description	Reference
pREP3X *tea1*	Cell Cycle Laboratory
pREP3X *tea2*	Cell Cycle Laboratory
pREP3X *pom1*	(Bahler and Pringle, 1998)
pREP3X *cut11GFP*	(West et al., 1998)
pREP3X *nuclearGFP*	(Sawin and Nurse, 1996)
pREP3X GFPatb2	(Ding et al., 1998)
pAF1	(Ohi et al., 1996)
pRL72	(Glynn et al., 2001)

7.1.1.3 Strain construction

All double mutant strains not in the *cyr1Δsxa2Δ* background were generated by crossing single mutants followed by tetrad dissection and selection of colonies from a tetrad that gave a 2:2 segregation wild type: mutant phenotype. All multiple mutant strains in the *cyr1Δsxa2Δ* background were constructed by sequentially crossing in the desired allele and analysing random spores to select for mutations, appropriate markers and mating type. The *cyr1Δsxa2Δh-* background was usually selected by pheromone sensitivity. When multiple constructs bore the same marker, the colonies were visually screened for the appropriate tag or deletion. *Dhc1* and *ssm4* tags and deletions, which could not be visually selected in a vegetative population, were identified by colony PCR using primers CO9+DPL85 for *ssm4* constructs and TN55+CO18 for *dhc1* constructs.

Strains carrying tagged *dhc1+* and *ssm4+* were generated by a PCR-based gene targeting method (Bahler et al., 1998), using primers DPL100+TN38 for *ssm4+* and TN56+TN57 for *dhc1+*. Briefly, the desired tag and a kanamycin resistance gene (*KanR),* conferring resistance to the drug G418, were amplified from a plasmid using long primers with 60-80 base-pairs sequence homology to the genomic region flaking the desired insertion site. The resulting PCR product was transformed in a *cyr1Δsxa2Δ* strain and the presence of the construct was selected for by plating cells on YE5S with the drug G418 (Sigma). The insertion at the correct site was then confirmed by colony PCR, using a primer binding to the genomic sequence and a primer binding to the inserted fragment.

Table 7.3 Oligoes

DPL 100 Forward primer for *ssm4* tagging

ATATCGAGCGACCCAGTTTTCATCACAATCAACAGCTATTTAATTATTGTCAGTTAACAGACA
TTCTTTCCAAAAAATGCCGGATCCCCGGGTTAATTAA

TN 38 Reverse primer for *ssm4* tagging

CATTAATGATAAATTCGTTAAAATATGGCAGTTAAGATTAGAAGCTAATTTTCGGCGGCTATT
AATAAATTGAATTATATATCTCGAATTCGAGCTCGTT

TN 56 Reverse primer for *dhc1* tagging

GAAAAAATTATACTAGGAGTTTTAATGGGAGGACAATAAAAGTTACGACAAAGTCTTTAGTA
AACAACAAATAGGAATTCGAGCTCGTTTAAAC

TN57 Forward primer for *dhc1* tagging

CCACCGGGCTGGTTGGACATACCGGAAAACAGTAAGCGAAAGAGAACTGATATTTATTTTAG
TATGTGCATTCGGATCCCCGGGTTAATTAA

DPL 85 Reverse primer for checking *ssm4* tags and deletion

GAAGCTAATTTTCGGCGGTAAAC

CO9 Common forward primer for checking tags and deletion

CAGGTGCGACAATCTATC

TN55 Forward primer for checking *dhc1* tags and deletion

GTTTATGGACCGAAGG

CO18 Common reverse primer for checking tags and deletion

GTCACATCATGCCCCTGAGC

T3 Primer binding pAF promoter, that sequences across the restriction site cut in the genomic region flanking the insertion

ATTAACCCCTCACTAAAGGGA

BS250 Primer binding pAF, that sequences the insertion junction

TTTTTGGGGTCGAGGTGC

7.1.1.4 Induction of gene expression from the nmt1 promoter

The nmt1 promoter is derived from that of the *nmt1* gene which is required for thiamine biosynthesis, it is repressed by the presence of 5μg/ml of thiamine, although some low level expression occurs even in the presence of thiamine (Maundrell, 1990). All strains carrying genes expressed from the nmt1 promoter, integrated or on a plasmid, were always grown on plates containing full thiamine. All plasmids used in this study were derived from pREP3, which carries the nmt1 promoter to drive gene expression. To induce over-expression cells were directly inoculated from plates into thiamine-free liquid medium. *Atb2GFP* and *nuclearGFP* fully induced were lethal to the cells, therefore to visualise tubulin and nuclei cells were grown in low thiamine (0.07 μg/ml), which induces *atb2GFP* and *nuclearGFP* expression to a level which allows the GFP signal to be visualised but that is not deleterious to the cell. *Nmt1atb2CFP* gives a very weak signal and so had to be fully. A stationary phase culture was inoculated into medium lacking thiamine and allowed to grow for 6 hours before imaging.

7.1.1.5 Microtubule depolymerisation

All microtubule depolymerisation experiments were carried out by adding 25μg/ml Carbendazim (MBC) from a 200X stock freshly in DMSO, directly to the culture for at least 10 minutes. This ensured microtubules were totally depolymerised.

7.1.1.6 Latrunculin pulses

Cells were grown at 25°C in YE5S, 20 mls of a mid-log culture were then spun at 2500 rpm for 3 minutes and resuspended in 1ml of YE5S with 10μM of latrunculin A (LatA) (from a 50X stock in DMSO)(Spector et al., 1983) for 8 minutes to allow total depolymerisation of the actin cytoskeleton. Cells were then spun again and resuspended in 20 mls of YE5S media and allowed to recover for 1 hour, after which cells were fixed and stained for actin. The control population was not spun or treated with DMSO because we found that actin was transiently delocalised even by a short spin or by DMSO.

For actin repolymerisation in the absence of microtubules MBC was added to the culture for 10 minutes, then samples were treated with LatA as above. After samples were resuspended in YE5S samples were taken every 10 minutes and fixed in formaldehyde and then processed for actin staining.

7.1.1.7 Pheromone induction experiments

Cyr1Δsxa2Δ cells were grown in EMM liquid medium with leucine, adenine and uracil. 3μg/ml of P-factor (from a 5mg/ml stock in DMSO) was added to induce the cells into shmooing, unless otherwise stated.

7.1.1.8 Arrest in Hydroxyurea

Hydroxyurea (HU) is a drug which inhibits the enzyme ribonucleotide reductase and results in the depletion of nucleotides. Addition of 11mM of HU to an exponentially growing culture arrests the population in early S-phase but allows the cells to continue to grow, generating elongated cells. This was used as a control in the pheromone experiments to distinguish between the effect of having longer cells and the effect of pheromone.

7.1.1.9 Flow cytometric analysis

$2X10^6$ and $2X10^7$ cells were fixed in –20°C 70% ethanol and stored at 4°C. To process samples for FACS, 300μl of cells were rehydrated in 3 ml of 50mM Na_3Citrate and spun at 2000RPM at 4°C for 5 minutes. Cells were then resuspended in 1ml 50mM Na_3Citrate containing 0.1mg RNaseA and 1μg/ml propidium iodide and incubated at 37°C for 2-4 hours. Samples were then sonicated for 10-20 seconds on setting 6 in a Soniprep 150 sonicator (MSE), FACS analysis was carried out on a Becton Dickinson scan as previously described (Sazer and Sherwood, 1990).

7.1.1.10 Mating assay

Modified from (Bahler et al., 1993). Cells were grown at 25°C in EMM with 10g/l glucose and full nitrogen to a titre of $1\text{-}2x10^7$ cells/ml. Cells were harvested and diluted to $2\text{-}3x10^6$ cells/ml in EMM with10g/l glucose and no nitrogen. Cells were shaken gently to allow mating partners to come together, samples were taken every hour and the number of zygotes scored.

7.1.2 Molecular biology techniques

7.1.2.1 Transformation of plasmids and PCR products

Cells were transformed according to the modified lithium acetate (LiOAc) method described by (Bahler et al., 1998). For each transformation $2X10^8$ cells of an exponentially growing culture in YE5S were collected by centrifugation, rinsed in H_2O and Lithium Acetate/ TE (0.1M Lithium Acetate, 10mM Tris-HCl, 1mM EDTA, PH7.5). Cells were incubated at 29°C in PEG/Lithium Acetate/ TE (30% PEG 4000, 0.1M Lithium Acetate, 10mM Tris-HCl, 1mM EDTA, PH7.5) with 10μg carrier sperm DNA, and 1μg of plasmid DNA or 10μg of PCR product for homologous integrations. After 40 minutes 43μl of DMSO were added to the samples and they were heat-shocked for 5 minutes at 42°C. For plasmids, cells were plated on two EMM plates lacking leucine. All plasmids used were pREP3X, which carry *LEU2* as a selectable marker and the full strength *nmt1* promoter (Maundrell, 1990) driving expression. For homologous integration cells were plated on YE5S plates and then replica-plated twice onto G418-containing YE5S plates.

7.1.2.2 Western Blotting

Cells were washed once in Stop buffer (150 mM NaCl, 50 mM NaF, 1 mM NaN3, 10 mM EDTA pH 8.0) and boiled for 6 minutes in HB buffer (25mM MOPS pH 7.2, 15mM $MgCl_2$, 15mM EGTA, 1% Triton X100). When native extracts were required cells were not boiled. Protein extracts were made by breaking cells with glass beads in HB buffer with protease inhibitors (1mM PMSF, 20μg/ml leupeptin, 20μg/ml aprotinin) and phosphatase inhibitors (60mM β–glycerophosphate, 12mM p-nitrophenylphosphate,

0.1mM sodium vanadate) (Moreno et al., 1991). Extracts were then recovered by making a whole in the bottom of the eppendorf tube and spinning the extracts at 7000RPM into a new tube. Cell extracts were boiled in 2x sample buffer (160mM Tris-HCl, pH 6.8, 20% glycerol, 4% SDS, 200mM DTT and 0.02% Bromophenol Blue) and 50 μg of each sample were run on an 8% SDS-polyacrylamide gel (Laemmli, 1970). SDS-polyacrylamide gels for Tea1p and Tip1p were prepared using a 203.25/1, mono/bisacrylamide mix and samples were run on long gels. Dhc1p was run on a 7% 30/0.3 acryl/bisacryl SDS-polyacrylamide gel. The proteins were blotted to Immobilon TM-P membrane (Millipore) and blocked overnight in PBS with 10% milk and 0.1% Tween 20. Membranes were then incubated with the primary antibody for at least 4 hours, rinsed with PBS+Tween three time, incubated with the secondary antibody, rinsed again and then detected using ECL (Amersham). The primary antibodies used were polyclonal anti-Tea1 at 1:1000 (Mata and Nurse, 1997), anti-Tip1 at 1:2000 (Brunner and Nurse, 2000), anti-Tea3 at 1:2000 (Arellano et al., 2002) and polyclonal anti-GFP at 1:1000 (a gift from Ken Sawin, Wellcome Trust Centre for Cell Biology, Institute of Cell and Molecular Biology, University of Edinburgh, UK), and monoclonals 16B12 anti HA at 1:2000 (BABCO) and 9E10 anti MYC at 1:2000. Secondary antibodies used were horseradish peroxidase conjugated anti-rabbit or anti-mouse (Amersham) at 1:2000.

7.1.2.3 Colony PCR

A colony was picked and resuspended in 30 μl PCR mix (42 μl water, 5 μl 10x Taq reaction buffer, 0.5 μl 10 mM each dNTP, 1 μl 50 μM of each primer) and boiled for

5 min. The remaining PCR mix with 0.5 μl Taq polymerase (2.5 U) was then added and a PCR was performed according to standard protocols (Sambrook et al., 1989).

7.1.2.4 Phosphatase assay

Native cell extracts were made as described in HB buffer (25mM MOPS pH 7.2, 15mM $MgCl_2$, 15mM EGTA, 1% Triton X100) with the Protease Inhibitor Set (Roche). Cell extracts were then incubated with Lambda Phosphatase (New England Biolabs) in its buffer supplemented with 2mM MnCl for 25 minutes at 30°C in the presence or absence of phosphatase inhibitors (60mM β–glycerophosphate, 12mM p-nitrophenylphosphate, 0.1mM sodium vanadate). The reactions were stopped by the addition of 2X sample buffer and boiling for 3 minutes.

7.1.2.5 Immunoprecipitations

Native cell extracts were made as described in HB buffer with the Protease Inhibitor Set (Roche) and phosphatase inhibitors, allowing 10% cell breakage.

Anti-HA (1:200) antibody or anti-MYC antibodies (1:200) were pre-bound to protein G beads for 1 hour. Extracts were incubated with the beads for 2 hours at 4°C. The beads were washed 3 times in buffer with inhibitors and then boiled in the presence of sample buffer to release the bound complex. Boiled samples were then loaded on a 7% 30/0.3 acryl/bisacryl SDS-polyacrylamide gel and detected as described above.

7.1.2.6 Gel filtration

$5x10^8$ cells were collected from a *tea1GFPcyr1Δsxa2Δ* culture, either vegetativelly growing or treated with pheromone for 6 hours and mixed with $5x10^8$ cells from a *cyr1Δsxa2Δ* culture treated in an opposite manner. The extracts were mixed to

make sure that the results were not due to different enzymatic activities of the extracts. Cell extracts were made as described, using Buffer A (20mMTris/HCl pH7.5, 20% glycerol, 0.1mM EDTA, 1mM 2-mercaptoethanol, 5mM ATP) with protease inhibitors (Boheringer complete) and allowing 50% cell breakage.

Extracts were then spun for 5 minutes at 3K on a bench-top centrifuge, the supernatant was spun again at 100,000g for 25 minutes and then loaded on a Superose-6 column equilibrated with BufferA containing 100mM NaCl without protease inhibitors. Thirty-two 75μl fractions were collected and 30μl of each fraction was then loaded on a 10% gel and processed as usual for western blotting. Tea1GFP was detected using GFP antibody.

7.1.2.7 His-tagged mutagenesis

The protocol used was modified from (Hoffman and Welton, 2000). Cells were grown to a density of $4x10^7$ cells/ml, 10^8 cells were collected and incubated over-night in 0.5mls PEG/Lithium Acetate/ TE (30% PEG 4000, 0.1M Lithium Acetate, 10mM Tris-HCl, 1mM EDTA, PH7.5) with 1-3μg of linearised pAF, carrying the *his3+* gene, and 10μg of carrier herring sperm DNA (Sigma). This protocol facilitates non-homologous integration. Cells were then plated onto EMM with all supplements apart from histidine (EMM-his) to select for integrants. Cells were replica plated again to EMM–his, when colonies became visible they were replica-plated onto pheromone containing plates and screened after 12-16 hours. Colonies displaying a mutant phenotype were picked and patched to a YE5S plate and then back to selective medium to check for stability of the

integration. Colonies that were stable and still showed a mutant phenotype upon re-screening were sequenced.

To determine the insertion site, the region around the inserted fragment was cloned and sequenced. Genomic DNA was prepared according to (Hoffman and Winston, 1987). Briefly, 10 mls of saturated culture were harvest by centrifugation, and washed in H_2O. Cells were suspended in 0.2 ml of 2% triton X-100, 1% SDS, 100mM NaCl, 10mM Tris-HCl (pH 8.0), 1mM EDTA and 0.2 ml of phenol: chloroform: isoamyl alcohol (25:24:1). Cells were then broken with glass beads and spun, the upper aqueous layer was transferred to fresh tube and ethanol precipitated with 1/10 volumes 3M NaOAc, pH 5.2 plus 2.5 volumes 100% ethanol and washed with 70% ethanol. The dry pellet was resuspend in 100μl TE+RnaseA, incubated at 37°C for 1 hour, ethanol precipitated again and resuspended in 50μl TE. The genomic DNA was digested with an enzyme cutting in pAF, and re-ligated according to standard procedures (Sambrook et al., 1989). Ligations were phenol/chloroform extracted, ethanol precipitated and transformed into bacteria for amplification (Sambrook et al., 1989). Plasmid minipreps were prepared with QUIAGEN kits, according to manufacturer's instructions and sequenced with primers T3 and BS250 according to standard protocols (ABI Prism BigDye terminator cycle sequencing ready reaction kit, Applied Biosystems). The sequence would give the genomic region around the integration site.

7.1.3 Microscopy

7.1.3.1 Image acquisition

Confocal images were acquired with a laser scanning confocal LSM150 microscope (Zeiss), fluorescent microscopy was carried out with a Zeiss Axioplan microscope mounted with a chilled CCD camera (Hamamatsu, C4742-95) and controlled by Kinetic Imaging AQM software (Kinetic Imaging). Phase and DIC images were taken with a Zeiss Axioplan microscope mounted with a chilled CCD camera (Hamamatsu, C5985).

Acquired images were processed with Adobe Photoshop 5.5.

7.1.3.2 Calcofluor staining

3μl of live cells were placed on a slide with 1μl of Calcofluor (from a 10mg/ml solution in H_2O), cells were then imaged on the fluorescent microscope with a 360 nm excitation /480 nm emission filter.

7.1.3.3 DAPI staining

3μl of fixed cells were placed on a slide and allowed to dry, they were overlaid with 3μl DAPI (1μg/ml DAPI, 1mg/ml p-phenylenediamine which acts as antifade, 50% glycerol) to stain the nuclei and a coverslip. Cells were then imaged on the fluorescent microscope with a 360 nm excitation /480 nm emission filter.

7.1.3.4 Phase and DIC imaging

3 μl of cells were placed on a glass slide and overlaid with a glass coverslip. Cells were viewed by DIC or phase microscopy with a Zeiss Axioplan microscope and pictures were taken.

7.1.3.5 Time lapse imaging of cells

Cells were routinely harvested by centrifugation at 2000 rpm/min, placed onto a layer of EMM+5S agar medium 0.5 mm thick, sealed with a mixture of lanolin:parafine (1:1), and images were recorded with a phase-contrast microscope at 1 minute intervals for 12 hours using a thermostatic chamber adjusted to 32°C for growth pattern analysis and to 25°C for shmooing cells.

7.1.3.6 Actin staining

Cultures were added directly to one-fifth volume pre-warmed 16% EM-grade formaldehyde (TAAB), and fixed for 30-40minutes at 25°C or 20 minutes at 37°C. Cells were then washed 3 times in 1 ml of (PEM), extracted for 30 seconds with PEM/1% Triton X-100, and washed 3 additional times in PEM. For staining, 3.5 μl of the rhodamine phalloidin were added to 0.5μl of cell pellet. Cells were then left overnight at 4°C. To visualise actin, 0.5 μl of stained cells were spotted onto a glass slide, followed by 2.5 μl of a mounting medium (50% Glycerol, 100mM Tris pH8, 1 mg/ml phenylene diamine as antifade) and cells were then imaged with a fluorescent microscope.

7.1.3.7 Immunofluorescence

Cells were fixed in –80°C methanol for 10-60 minutes to visualise tubulin, Tea1p, Tip1p and Sad1p. Cells were then washed 3 times in 1 ml of PEM, digested at 37°C in PEMS (PEM+ 1.2 M sorbitol) with 0.05mg/ml zymolyase and 0.1 mg/ml novozyme, until ~60% of the cells were digested. Cells were then extracted for 30 seconds with PEMS/1% Triton X-100, and washed 3 additional times in PEMS. Primary antibodies used were TAT1 monoclonal antibody (a gift from Prof. K. Gull, University of

Manchester, UK; (Woods et al., 1989)) at 1:50, anti-Tea1 at 1:1000 (Mata and Nurse, 1997), anti-Tip1 at 1:200 (Brunner and Nurse, 2000), anti-Sad1 at 1:5000 (Hagan and Yanagida, 1995). The secondary antibodies were goat anti-mouse Alexa 546 (Molecular Probes), anti-rabbit Alexa 488 and anti-rabbit Cy5 at 1:1000. To visualise cells, 1.5 μl of stained cells were spread onto a glass slide, allowed to dry, and then overlaid with 2.5 μl of mounting medium (50% Glycerol, 100mM Tris pH8, 1 mg/ml phenylene diamine as antifade) and a coverslip. Cells were then imaged with a fluorescent microscope. When cells were prepared for imaging with a confocal microscope, cells were spun onto a 1mg/ml ConcanavalinA coated coverslip, the coverslip was then rinsed with water and overturned onto 1.5μl of mounting medium on a slide. Images were taken with a Zeiss LSM 510 laser scanning confocal microscope.

7.1.3.8 Live imaging of GFP

For individual timepoints on the confocal and all imaging on the fluorescent microscope, cells were mounted on a glass slide in a volume of growth medium sufficient to trap but not to squeeze the cells. For time-lapse imaging on the confocal microscope 30μl of cells were placed on 35mm glass bottom dishes (MatTek Corporation) coated with 20μg/ml Soybean Lectin (Biochem). A GFP specific filter was used to visualise GFP alone, both on the confocal and the fluorescent microscope. To visualise GFP during shmooing, cells were imaged 5 to 6 hours after pheromone induction. During this period cells seemed to present constant behaviour. For confocal time-lapse imaging at 37°C, the dishes were pre-heated to 37°C before adding the cells, all media and dishes were kept at

37°C in a heating block and the microscope and stage used were inside a chamber heated to 37°C.

The nucleus was visualised with a nuclear GFP marker identified by (Sawin and Nurse, 1998), expressed from a plasmid, and imaged with a fluorescent microscope. Live microtubules were visualised with *nmt1-GFP-atb2* integrated into the genome (Ding et al., 1998) in the case of wild type and *ssm4Δ* cells and expressed from a plasmid in all other cases. Microtubules were generally visualised with the confocal microscope. *Tip1Δ* microtubules were not always bright enough to be monitored with a confocal microscope and therefore were sometimes monitored with a fluorescent microscope. For imaging of Tip1p and tubulin, a *tip1YFP* strain carrying the plasmid pRL72, which expresses *atb2CFP* from the nmt1 promoter was used (Glynn et al., 2001).

YFP-GFP and YFP-CFP colocalisation was monitored on the confocal microscope. A single section through the middle of the cell was taken using a YFP optimised filter set to visualise Tip1YFP and a CFP optimised filter set for GFP or CFP tagged proteins. YFP was excited at 514 nm and detected with a LP530 filter, GFP and CFP were excited at 458 nm and detected with a LP475 filter. The images were collected by line scanning and the two channels were excited sequentially at very high speed. Because of laser variability the amplitude gain and the offset were adjusted every time to ensure that there was no significant crossover between channels and all imaging was then carried out with the same settings.

7.1.3.9 Assay of Tea1p and Tip1p binding to microtubules

A *cdc25-22 cyr1Δsxa2Δ* culture, with or without *tea1GFP*, was grown overnight at 25°C to 4*10E6 cells/ml, shifted to 36°C for 90 minutes to arrest cells in G2 and then 3μg/ml of P factor was added. After a further 2 hours, the cells were shifted to 25°C for 2 hours and 20 minutes to allow progression into G1. Samples were taken for microtubular repolymerisation at 90 minutes, just before the shift-down and at the end of the time course.

25μg/ml of MBC (Carbendazim) were added to a cell culture for 10 minutes at 36°C or 15 minutes at 25°C to totally depolymerise microtubules. To visualise tubulin, cells were collected onto Millipore filters (0.45μm pore size) and washed for 50 seconds with minimal medium without MBC to allow partial repolymerisation of the microtubules. The filters were then dropped into 20ml of –70°C methanol to fix the cells, which were then processed as described for immunofluorescence. For visualisation of Tea1GFP in live cells, 50 μl of cells with MBC were placed on 35mm glass bottom dishes (MatTek Corporation) coated with 20μg/ml Soybean Lectin (Biochem), which allows the cells to stick without moving while the media is changed. The dish with the cells was placed on an inverted LSM 510 confocal microscope and 1ml of preconditioned media without MBC was added to the dish. This diluted the MBC to a concentration that allowed microtubules to repolymerise, and the cells were imaged 50 seconds later. For experiments carried out at 36°C, the dishes were pre-heated to 36°C before adding the cells, all media and dishes were kept at 36°C in a heating block and the microscope and stage used were inside a chamber heated to 36°C.

7.1.3.10 Bleaching of microtubules

Cells were prepared as above and filmed on an inverted confocal microscope. A small area along a microtubule was selected each time and bleached with 600nm laser on 75% power and using as many iterations as needed, these had to be determined every time because of laser variability. After the bleaching, microtubules were depolymerised with 1 ml of pre-conditioned media with MBC, rapid adjustments to the focus were sometimes needed. Cells were continuously filmed throughout the experiment.

7.1.3.11 Repolymerisation of microtubules

Microtubules were depolymerised with MBC. For confocal imaging, cells were placed dish as described above, 1ml of fresh medium was then added to the dish to dilute out the MBC and cells were filmed as microtubules repolymerised. Typically images were taken every 6 seconds.

For imaging with a fluorescent microscope, 30μl of cells were placed on a 20μg/ml Soybean Lectin (Biochem)-coated cover-slip for 2-3 minutes. The cover-slip was then inverted onto 2 strips of double-stick tape placed at the edges of a slide, creating a small chamber where medium could be flown through. While the cells were being filmed, 300μl of fresh medium were added on one side of the chamber, while a tissue on the other side absorbed the excess liquid, ensuring a good flow-through. Typically images were taken every 6 seconds.

7.1.4 Data analysis

7.1.4.1 Graphs

All bar charts were drawn in Microsoft Excel (Microsoft Office 1998) and all line charts in Cricket Graph III 1.5.2.

7.1.4.2 Quantification of fixed microtubules

The length of microtubules in fixed cells was measured with NIH image 1.61 PPC. At least 100 microtubules were scored for each sample. All the statistical analysis: calculation of mean values, standard deviation and T-test was carried out in Microsoft Excel (Microsoft Office 1998).

7.1.4.3 Quantification of microtubular dynamics

For vegetative microtubules, microtubules were filmed with a confocal microscope and dwelling times were calculated from the time the microtubule contacted the end of the cell to the time it underwent catastrophe and lost contact with the cell end.

The lengths of live shmooing microtubules were measured in LSM 5 Image Browser and plotted in Microsoft Excel. The length of a microtubule at each timepoint was compared to the previous timepoint, if the microtubule length was increasing microtubule dynamics was marked as polymerising (+), if microtubule length was decreasing the microtubule was marked as depolymerising (-) and if the microtubule length was the same the microtubule was marked as stalling (0). The dynamics of microtubules was calculated for each timepoint and then the dynamics of all microtubules at the same end was compared. At any given timepoint 1-5 microtubules were found at one end and in 75% of cases the majority of microtubules at a single end displayed the

same dynamics, they were polymerising, depolymerising or stalling. We called this consensus dynamics. We then compared the consensus dynamics of both ends for each timepoint to verify whether they were the same or different. In the comparison between opposite ends, timepoints which presented stalling "consensus dynamics", which occurred 9% of the time, were discounted.

All numerical analysis of both vegetative and shmooing microtubular dynamics was carried out in Excel spreadsheets (Microsoft Excel, Microsoft Office 1998), with the aid of appropriate formulas.

7.1.4.4 Protein analysis tools

Sequences, which needed to be aligned, were saved in a single BBEdit Lite 4.6 file, aligned with ClustalX (1.81) and imported into MacBoxshade 2.15 to create the graphic output. Proteins with similar domain structure were identified and the domain structure imported from Pfam database.

Bibliography

Adames, N. R. and Cooper, J. A. (2000). Microtubule interactions with the cell cortex causing nuclear movements in Saccharomyces cerevisiae. *J Cell Biol* **149**, 863-74.

Adams, J., Kelso, R. and Cooley, L. (2000). The kelch repeat superfamily of proteins: propellers of cell function. *Trends Cell Biol* **10**, 17-24.

Allan, V. (2000). Dynactin. *Curr Biol* **10**, R432.

Arai, R. and Mabuchi, I. (2002). F-actin ring formation and the role of F-actin cables in the fission yeast Schizosaccharomyces pombe. *J Cell Sci* **115**, 887-98.

Arellano, M., Coll, P. M. and Perez, P. (1999). RHO GTPases in the control of cell morphology, cell polarity, and actin localization in fission yeast. *Microsc Res Tech* **47**, 51-60.

Arellano, M., Durán, A. and Pérez, P. (1996). Rho1 GTPase activates the (1,3)beta-D-glucan synthase and is involved in *Schizosaccharomyces pombe* morphogenesis. *The EMBO Journal* **15**, 4584-4591.

Arellano, M., Niccoli, T. and Nurse, P. (2002). Tea3p Is a Cell End Marker Activating Polarized Growth in Schizosaccharomyces pombe. *Curr Biol* **12**, 751-6.

Askham, J. M., Moncur, P., Markham, A. F. and Morrison, E. E. (2000). Regulation and function of the interaction between the APC tumour suppressor protein and EB1. *Oncogene* **19**, 1950-8.

Ayscough, K. R. and Drubin, D. G. (1998). A role for the yeast actin cytoskeleton in pheromone receptor clustering and signalling. *Curr Biol* **8**, 927-30.

Bahler, J. and Nurse, P. (2001). Fission yeast Pom1p kinase activity is cell cycle regulated and essential for cellular symmetry during growth and division. *Embo J* **20**, 1064-73.

Bahler, J. and Pringle, J. R. (1998). Pom1p, a fission yeast protein kinase that provides positional information for both polarized growth and cytokinesis. *Genes Dev* **12**, 1356-70.

Bahler, J., Wu, J.-Q., Longtine, M. S., Shah, N. G., McKenzie III, A., Steever, A. B., Wach, A., Philippsen, P. and Pringle, J. R. (1998). Heterologous modules for efficient

and versatile PCR-based gene targeting in *Schizosaccharomyces pombe*. *Yeast* **14**, 943-951.

Bahler, J., Wyler, T., Loidl, J. and Kohli, J. (1993). Unusual nuclear structures in meiotic prophase of fission yeast: a cytological analysis. *J Cell Biol* **121**, 241-56.

Balasubramanian, M. K., Helfman, D. M. and Hemmingsen, S. M. (1992). A new tropomyosin essential for cytokinesis in the fission yeast *S. pombe*. *Nature* **360**, 84-87.

Balasubramanian, M. K., Hirani, B. R., Burke, J. D. and Gould, K. L. (1994). The *Schizosaccharomyces pombe cdc3*$^{+}$ gene encodes a profilin essential for cytokinesis. *The Journal of Cell Biology* **125**, 1289-1301.

Banuett, F. (1998). Signalling in the yeasts: an informational cascade with links to the filamentous fungi. *Microbiology and Molecular Biology Reviews* **62**, 249-274.

Becker, W. and Joost, H. G. (1999). Structural and functional characteristics of Dyrk, a novel subfamily of protein kinases with dual specificity. *Prog Nucleic Acid Res Mol Biol* **62**, 1-17.

Behrens, R. and Nurse, P. (2002). Roles of fission yeast tea1p in the localization of polarity factors and in organizing the microtubular cytoskeleton. *J Cell Biol* **157**, 783-93.

Beinhauer, J. D., Hagan, I. M., Hegemann, J. H. and Fleig, U. (1997). Mal3, the fission yeast homologue of the human APC-interacting protein EB-1 is required for microtubule integrity and the maintenance of cell form. *J Cell Biol* **139**, 717-28.

Berrueta, L., Tirnauer, J. S., Schuyler, S. C., Pellman, D. and Bierer, B. E. (1999). The APC-associated protein EB1 associates with components of the dynactin complex and cytoplasmic dynein intermediate chain. *Curr Biol* **9**, 425-8.

Bezanilla, M., Forsburg, S. L. and Pollard, T. D. (1997). Identification of a second myosin-II in Schizosaccharomyces pombe: Myp2p is conditionally required for cytokinesis. *Mol Biol Cell* **8**, 2693-705.

Blanchoin, L., Pollard, T. D. and Mullins, R. D. (2000). Interactions of ADF/cofilin, Arp2/3 complex, capping protein and profilin in remodeling of branched actin filament networks. *Curr Biol* **10**, 1273-82.

Bone, N., Millar, J. B., Toda, T. and Armstrong, J. (1998). Regulated vacuole fusion and fission in Schizosaccharomyces pombe: an osmotic response dependent on MAP kinases. *Curr Biol* **8**, 135-44.

Browning, H., Hayles, J., Mata, J., Aveline, L., Nurse, P. and McIntosh, J. R. (2000). Tea2p is a kinesin-like protein required to generate polarized growth in fission yeast [In Process Citation]. *J Cell Biol* **151**, 15-28.

Brunner, D. and Nurse, P. (2000). CLIP170-like tip1p spatially organizes microtubular dynamics in fission yeast. *Cell* **102**, 695-704.

Bu, W. and Su, L. K. (2001). Regulation of microtubule assembly by human EB1 family proteins. *Oncogene* **20**, 3185-92.

Busson, S., Dujardin, D., Moreau, A., Dompierre, J. and De Mey, J. R. (1998). Dynein and dynactin are localized to astral microtubules and at cortical sites in mitotic epithelial cells. *Curr Biol* **8**, 541-4.

Butty, A. C., Pryciak, P. M., Huang, L. S., Herskowitz, I. and Peter, M. (1998). The role of Far1p in linking the heterotrimeric G protein to polarity establishment proteins during yeast mating. *Science* **282**, 1511-6.

Calonge, T. M., Nakano, K., Arellano, M., Arai, R., Katayama, S., Toda, T., Mabuchi, I. and Perez, P. (2000). Schizosaccharomyces pombe rho2p GTPase regulates cell wall alpha-glucan biosynthesis through the protein kinase pck2p. *Mol Biol Cell* **11**, 4393-401.

Carnero, E., Ribas, J. C., Garcia, B., Duran, A. and Sanchez, Y. (2000). Schizosaccharomyces pombe ehs1p is involved in maintaining cell wall integrity and in calcium uptake. *Mol Gen Genet* **264**, 173-83.

Casamayor, A. and Snyder, M. (2002). Bud-site selection and cell polarity in budding yeast. *Curr Opin Microbiol* **5**, 179-86.

Chang, E., Bartholomeusz, G., Pimental, R., Chen, J., Lai, H., Wang, L., Yang, P. and Marcus, S. (1999). Direct binding and In vivo regulation of the fission yeast p21-activated kinase shk1 by the SH3 domain protein scd2. *Mol Cell Biol* **19**, 8066-74.

Chang, E. C., Barr, M., Wang, Y., Jung, V., Xu, H.-P. and Wigler, M. H. (1994). Cooperative interaction of *S. pombe* proteins required for mating and morphogenesis. *Cell* **79**, 131-141.

Chang, F. and Nurse, P. (1996). How fission yeast fission in the middle. *Cell* **84**, 191-194.

Chausovsky, A., Bershadsky, A. D. and Borisy, G. G. (2000). Cadherin-mediated regulation of microtubule dynamics. *Nat Cell Biol* **2**, 797-804.

Chen, C. R., Li, Y. C., Chen, J., Hou, M. C., Papadaki, P. and Chang, E. C. (1999). Moe1, a conserved protein in Schizosaccharomyces pombe, interacts with a Ras effector, Scd1, to affect proper spindle formation. *Proc Natl Acad Sci U S A* **96**, 517-22.

Chenevert, J. (1994). Cell polarization directed by extracellular cues in yeast. *Mol Biol Cell* **5**, 1169-75.

Chikashige, Y., Ding, D. Q., Funabiki, H., Haraguchi, T., Mashiko, S., Yanagida, M. and Hiraoka, Y. (1994). Telomere-led premeiotic chromosome movement in fission yeast. *Science* **264**, 270-3.

Collins, C. A. and Vallee, R. B. (1989). Preparation of microtubules from rat liver and testis: cytoplasmic dynein is a major microtubule associated protein. *Cell Motil Cytoskeleton* **14**, 491-500.

Colussi, P. A. and Orlean, P. (1997). The essential Schizosaccharomyces pombe gpil+ gene complements a bakers' yeast GPI anchoring mutant and is required for efficient cell separation. *Yeast* **13**, 139-50.

Coquelle, F. M., Caspi, M., Cordelieres, F. P., Dompierre, J. P., Dujardin, D. L., Koifman, C., Martin, P., Hoogenraad, C. C., Akhmanova, A., Galjart, N. et al. (2002). LIS1, CLIP-170's key to the dynein/dynactin pathway. *Mol Cell Biol* **22**, 3089-102.

Daniels, R. H. and Bokoch, G. M. (1999). p21-activated protein kinase: a crucial component of morphological signaling? *Trends Biochem Sci* **24**, 350-5.

Degols, G., Shiozaki, K. and Russell, P. (1996). Activation and regulation of the Spc1 stress-activated protein kinase in Schizosaccharomyces pombe. *Mol Cell Biol* **16**, 2870-7.

Desautels, M., Den Haese, J. P., Slupsky, C. M., McIntosh, L. P. and Hemmingsen, S. M. (2001). Cdc4p, a contractile ring protein essential for cytokinesis in Schizosaccharomyces pombe, interacts with a phosphatidylinositol 4-kinase. *J Biol Chem* **276**, 5932-42.

DeZwaan, T. M., Ellingson, E., Pellman, D. and Roof, D. M. (1997). Kinesin-related KIP3 of Saccharomyces cerevisiae is required for a distinct step in nuclear migration. *J Cell Biol* **138**, 1023-40.

Ding, D.-Q., Chikashige, Y., Haraguchi, T. and Hiraoka, Y. (1998). Oscillatory nuclear movement in fission yeast meiotic prophase is driven by astral microtubules as revealed by continuous observation of chromosomes and microtubules in living cells. *Journal of Cell Science* **111**, 701-712.

Dorer, R., Pryciak, P. M. and Hartwell, L. H. (1995). Saccharomyces cerevisiae cells execute a default pathway to select a mate in the absence of pheromone gradients. *J Cell Biol* **131**, 845-61.

Drubin, D. G. and Nelson, W. J. (1996). Origins of cell polarity. *Cell* **84**, 335-44.

Drummond, D. R. and Cross, R. A. (2000). Dynamics of interphase microtubules in Schizosaccharomyces pombe. *Curr Biol* **10**, 766-75.

Dujardin, D., Wacker, U. I., Moreau, A., Schroer, T. A., Rickard, J. E. and De Mey, J. R. (1998). Evidence for a role of CLIP-170 in the establishment of metaphase chromosome alignment. *J Cell Biol* **141**, 849-62.

Dujardin, D. L. and Vallee, R. B. (2002). Dynein at the cortex. *Curr Opin Cell Biol* **14**, 44-9.

Echeverri, C. J., Paschal, B. M., Vaughan, K. T. and Vallee, R. B. (1996). Molecular characterization of the 50-kD subunit of dynactin reveals function for the complex in chromosome alignment and spindle organization during mitosis. *J Cell Biol* **132**, 617-33.

Egel, R. (1971). Physiological aspects of conjugation in fission yeast. *Planta* **98**, 89-96.

Egel, R. (1989). Mating-Type Genes, Meiosis and Sporulation: Academic Press Inc.

Elion, E. A. (2000). Pheromone response, mating and cell biology. *Curr Opin Microbiol* **3**, 573-81.

Eng, K., Naqvi, N. I., Wong, K. C. and Balasubramanian, M. K. (1998). Rng2p, a protein required for cytokinesis in fission yeast, is a component of the actomyosin ring and the spindle pole body. *Curr Biol* **8**, 611-21.

Etienne-Manneville, S. and Hall, A. (2001). Integrin-mediated activation of Cdc42 controls cell polarity in migrating astrocytes through PKCzeta. *Cell* **106**, 489-98.

Evangelista, M., Pruyne, D., Amberg, D. C., Boone, C. and Bretscher, A. (2002). Formins direct Arp2/3-independent actin filament assembly to polarize cell growth in yeast. *Nat Cell Biol* **4**, 32-41.

Facanha, A. L., Appelgren, H., Tabish, M., Okorokov, L. and Ekwall, K. (2002). The endoplasmic reticulum cation P-type ATPase Cta4p is required for control of cell shape and microtubule dynamics. *J Cell Biol* **157**, 1029-39.

Farkasovsky, M. and Kuntzel, H. (2001). Cortical Num1p interacts with the dynein intermediate chain Pac11p and cytoplasmic microtubules in budding yeast. *J Cell Biol* **152**, 251-62.

Farshori, P. and Holzbaur, E. L. (1997). Dynactin phosphorylation is modulated in response to cellular effectors. *Biochem Biophys Res Commun* **232**, 810-6.

Faulkner, N. E., Dujardin, D. L., Tai, C. Y., Vaughan, K. T., O'Connell, C. B., Wang, Y. and Vallee, R. B. (2000). A role for the lissencephaly gene LIS1 in mitosis and cytoplasmic dynein function. *Nat Cell Biol* **2**, 784-91.

Feierbach, B. and Chang, F. (2001a). Cytokinesis and the contractile ring in fission yeast. *Curr Opin Microbiol* **4**, 713-9.

Feierbach, B. and Chang, F. (2001b). Roles of the fission yeast formin for3p in cell polarity, actin cable formation and symmetric cell division. *Curr Biol* **11**, 1656-65.

Fujita, A., Vardy, L., Garcia, M. A. and Toda, T. (2002). A Fourth Component of the Fission Yeast gamma-Tubulin Complex, Alp16, Is Required for Cytoplasmic Microtubule Integrity and Becomes Indispensable When gamma-Tubulin Function Is Compromised. *Mol Biol Cell* **13**, 2360-73.

Fukata, M., Watanabe, T., Noritake, J., Nakagawa, M., Yamaga, M., Kuroda, S., Matsuura, Y., Iwamatsu, A., Perez, F. and Kaibuchi, K. (2002). Rac1 and Cdc42 capture microtubules through IQGAP1 and CLIP-170. *Cell* **109**, 873-85.

Fukui, Y., Kaziro, Y. and Yamamoto, M. (1986). Mating pheromone like diffusible factor released by *Schizosaccharomyces pombe*. *EMBO J.* **5**, 1991-1993.

Fukui, Y., Miyake, S., Satoh, M. and Yamamoto, M. (1989). Characterization of the *Schizosaccharomyces pombe ral2* gene implicated in activation of the *ras1* gene product. *Molecular and General Genetics* **9**, 5617-5622.

Fukui, Y. and Yamamoto, M. (1988). Isolation and characterization of Schizosaccharomyces pombe mutants phenotypically similar to ras1. *Mol Gen Genet* **215**, 26-31.

Gachet, Y., Tournier, S., Millar, J. B. and Hyams, J. S. (2001). A MAP kinase-dependent actin checkpoint ensures proper spindle orientation in fission yeast. *Nature* **412**, 352-5.

Gaglio, T., Dionne, M. A. and Compton, D. A. (1997). Mitotic spindle poles are organized by structural and motor proteins in addition to centrosomes. *J Cell Biol* **138**, 1055-66.

Garcia, M. A., Vardy, L., Koonrugsa, N. and Toda, T. (2001). Fission yeast ch-TOG/XMAP215 homologue Alp14 connects mitotic spindles with the kinetochore and is a component of the Mad2-dependent spindle checkpoint. *Embo J* **20**, 3389-401.

Gard, D. L. and Kirschner, M. W. (1987). A microtubule-associated protein from Xenopus eggs that specifically promotes assembly at the plus-end. *J Cell Biol* **105**, 2203-15.

Gilbreth, M., Yang, P., Bartholomeusz, G., Pimental, R. A., Kansra, S., Gadiraju, R. and Marcus, S. (1998). Negative regulation of mitosis in fission yeast by the shk1 interacting protein skb1 and its human homolog, Skb1Hs. *Proc Natl Acad Sci U S A* **95**, 14781-6.

Gilbreth, M., Yang, P., Wang, D., Frost, J., Polverino, A., Cobb, M. H. and Marcus, S. (1996). The highly conserved *skb1* gene encodes a protein that interacts with Shk1, a fission yeast Ste20/PAK homolog. *Proc. Natl. Acad. Sci. USA* **93**, 13802-13807.

Gill, S. R., Schroer, T. A., Szilak, I., Steuer, E. R., Sheetz, M. P. and Cleveland, D. W. (1991). Dynactin, a conserved, ubiquitously expressed component of an activator of vesicle motility mediated by cytoplasmic dynein. *J Cell Biol* **115**, 1639-50.

Glynn, J. M., Lustig, R. J., Berlin, A. and Chang, F. (2001). Role of bud6p and tea1p in the interaction between actin and microtubules for the establishment of cell polarity in fission yeast. *Curr Biol* **11**, 836-45.

Goldstein, B. and Hird, S. N. (1996). Specification of the anteroposterior axis in Caenorhabditis elegans. *Development* **122**, 1467-74.

Grieco, D., Avvedimento, E. V. and Gottesman, M. E. (1994). A role for cAMP-dependent protein kinase in early embryonic divisions. *Proc Natl Acad Sci U S A* **91**, 9896-900.

Gulli, M. P. and Peter, M. (2001). Temporal and spatial regulation of Rho-type guanine-nucleotide exchange factors: the yeast perspective. *Genes Dev* **15**, 365-79.

Gundersen, G. G. (2002). Evolutionary conservation of microtubule-capture mechanisms. *Nat Rev Mol Cell Biol* **3**, 296-304.

Gutz, H. and Doe, F. J. (1975). On homo- and heterothallism in Schizosaccharomyces pombe. *Mycologia* **67**, 748-59.

Hagan, I. and Yanagida, M. (1995). The product of the spindle formation gene *sad1*$^+$ associates with the fission yeast spindle pole body and is essential for viability. *The Journal of Cell Biology* **129**, 1033-1047.

Hagan, I. M. (1998). The fission yeast microtubule cytoskeleton. *J Cell Sci* **111**, 1603-12.

Hagan, I. M. and Hyams, J. S. (1988). The use of cell division cycle mutants to investigate the control of microtubule distribution in the fission yeast Schizosaccharomyces pombe. *J Cell Sci* **89**, 343-57.

Han, G., Liu, B., Zhang, J., Zuo, W., Morris, N. R. and Xiang, X. (2001). The Aspergillus cytoplasmic dynein heavy chain and NUDF localize to microtubule ends and affect microtubule dynamics. *Curr Biol* **11**, 719-24.

Harada, A., Takei, Y., Kanai, Y., Tanaka, Y., Nonaka, S. and Hirokawa, N. (1998). Golgi vesiculation and lysosome dispersion in cells lacking cytoplasmic dynein. *J Cell Biol* **141**, 51-9.

Hartwell, L. H. (1971). Genetic control of the cell division cycle in yeast. IV. Genes controlling bud emergence and cytokinesis. *Exp Cell Res* **69**, 265-76.

Hayles, J. and Nurse, P. (2001). A journey into space. *Nat Rev Mol Cell Biol* **2**, 647-56.

Hirata, D., Masuda, H., Eddison, M. and Toda, T. (1998). Essential role of tubulin-folding cofactor D in microtubule assembly and its association with microtubules in fission yeast. *Embo J* **17**, 658-66.

Hoffman, C. S. and Welton, R. (2000). Mutagenesis and gene cloning in Schizosaccharomyces pombe using nonhomologous plasmid integration and rescue. *BioTechniques* **28**, 532-6, 538, 540.

Hoffman, C. S. and Winston, F. (1987). A ten-minute DNA preparation from yeast efficiently releases autonomous plasmids for transformation of Escherichia coli. *Gene* **57**, 267-72.

Holleran, E. A., Tokito, M. K., Karki, S. and Holzbaur, E. L. (1996). Centractin (ARP1) associates with spectrin revealing a potential mechanism to link dynactin to intracellular organelles. *J Cell Biol* **135**, 1815-29.

Holzbaur, E. L., Hammarback, J. A., Paschal, B. M., Kravit, N. G., Pfister, K. K. and Vallee, R. B. (1991). Homology of a 150K cytoplasmic dynein-associated polypeptide with the Drosophila gene Glued. *Nature* **351**, 579-83.

Hughes, D., Fukui, A. and Yamamoto, M. (1990). Homologous activators of *ras* in fission and budding yeast. *Nature* **344**, 355-357.

Hughes, D. A. (1995). Control of signal transduction and morphogenesis by Ras. *Semin Cell Biol* **6**, 89-94.

Imai, Y., Miyake, S., Hughes, D. A. and Yamamoto, M. (1991). Identification of a GTPase-activating protein homolog in *Schizosaccharomyces pombe*. *Molecular and Cellular Biology* **11**, 3088-3094.

Imai, Y. and Yamamoto, M. (1992). Schizosaccharomyces pombe sxa1+ and sxa2+ encode putative proteases involved in the mating response. *Mol Cell Biol* **12**, 1827-34.

Imai, Y. and Yamamoto, M. (1994). The fission yeast mating pheromone P-factor: its molecular structure, gene structure, and ability to induce gene expression and G1 arrest in the mating partner. *Genes Dev* **8**, 328-38.

Insall, R. H. and Weiner, O. D. (2001). PIP3, PIP2, and cell movement--similar messages, different meanings? *Dev Cell* **1**, 743-7.

Irvine, K. D. and Rauskolb, C. (2001). Boundaries in development: formation and function. *Annu Rev Cell Dev Biol* **17**, 189-214.

Kamal, A. and Goldstein, L. S. (2002). Principles of cargo attachment to cytoplasmic motor proteins. *Curr Opin Cell Biol* **14**, 63-8.

Karki, S. and Holzbaur, E. L. (1995). Affinity chromatography demonstrates a direct binding between cytoplasmic dynein and the dynactin complex. *J Biol Chem* **270**, 28806-11.

Karki, S. and Holzbaur, E. L. (1999). Cytoplasmic dynein and dynactin in cell division and intracellular transport. *Curr Opin Cell Biol* **11**, 45-53.

Katayama, S., Hirata, D., Arellano, M., Perez, P. and Toda, T. (1999). Fission yeast alpha-glucan synthase Mok1 requires the actin cytoskeleton to localize the sites of growth and plays an essential role in cell morphogenesis downstream of protein kinase C function. *J Cell Biol* **144**, 1173-86.

Kato, J. Y., Matsuoka, M., Polyak, K., Massague, J. and Sherr, C. J. (1994). Cyclic AMP-induced G1 phase arrest mediated by an inhibitor (p27Kip1) of cyclin-dependent kinase 4 activation. *Cell* **79**, 487-96.

Kato, T., Jr., Okazaki, K., Murakami, H., Stettler, S., Fantes, P. A. and Okayama, H. (1996). Stress signal, mediated by a Hog1-like MAP kinase, controls sexual development in fission yeast. *FEBS Lett* **378**, 207-12.

Kawamukai, M., Ferguson, K., Wigler, M. and Young, D. (1991). Genetic and biochemical analysis of the adenylyl cyclase of Schizosaccharomyces pombe. *Cell Regul* **2**, 155-64.

Kim, H. W., Yang, P., Qyang, Y., Lai, H., Du, H., Henkel, J. S., Kumar, K., Bao, S., Liu, M. and Marcus, S. (2001). Genetic and molecular characterization of Skb15, a highly conserved inhibitor of the fission yeast PAK, Shk1. *Mol Cell* **7**, 1095-101.

King, S. J. and Schroer, T. A. (2000). Dynactin increases the processivity of the cytoplasmic dynein motor. *Nat Cell Biol* **2**, 20-4.

King, S. M. (2000). The dynein microtubule motor. *Biochim Biophys Acta* **1496**, 60-75.

Kishimoto, N. and Yamashita, I. (2000). Cyclic AMP regulates cell size of Schizosaccharomyces pombe through Cdc25 mitotic inducer. *Yeast* **16**, 523-9.

Kitamura, K. and Shimoda, C. (1991). The Schizosaccharomyces pombe mam2 gene encodes a putative pheromone receptor which has a significant homology with the Saccharomyces cerevisiae Ste2 protein. *Embo J* **10**, 3743-51.

Kobori, H., Yamada, N., Taki, A. and Osumi, M. (1989). Actin is associated with the formation of the cell wall in reverting protoplasts of the fission yeast *Schizosaccharomyces pombe*. *Journal of Cell Science* **94**, 635-646.

Kohli, J. (1987). Genetic nomenclature and gene list of the fission yeast Schizosaccharomyces pombe. *Curr Genet* **11**, 575-89.

Kumar, S., Lee, I. H. and Plamann, M. (2000). Cytoplasmic dynein ATPase activity is regulated by dynactin-dependent phosphorylation. *J Biol Chem* **275**, 31798-804.

Kunitomo, H., Higuchi, T., Iino, Y. and Yamamoto, M. (2000). A zinc-finger protein, Rst2p, regulates transcription of the fission yeast ste11(+) gene, which encodes a pivotal transcription factor for sexual development. *Mol Biol Cell* **11**, 3205-17.

Laemmli, U. K. (1970). Cleavage of structural proteins during the assembly of the head of bacteriophage T4. *Nature* **227**, 680-685.

Lechler, T., Shevchenko, A. and Li, R. (2000). Direct involvement of yeast type I myosins in Cdc42-dependent actin polymerization. *J Cell Biol* **148**, 363-73.

Lee, I. H., Kumar, S. and Plamann, M. (2001a). Null mutants of the neurospora actin-related protein 1 pointed-end complex show distinct phenotypes. *Mol Biol Cell* **12**, 2195-206.

Lee, M. J., Gergely, F., Jeffers, K., Peak-Chew, S. Y. and Raff, J. W. (2001b). Msps/XMAP215 interacts with the centrosomal protein D-TACC to regulate microtubule behaviour. *Nat Cell Biol* **3**, 643-9.

Lee, W. L., Bezanilla, M. and Pollard, T. D. (2000). Fission yeast myosin-I, Myo1p, stimulates actin assembly by Arp2/3 complex and shares functions with WASp. *J Cell Biol* **151**, 789-800.

Leeuw, T., Fourest-Lieuvin, A., Wu, C., Chenevert, J., Clark, K., Whiteway, M., Thomas, D. Y. and Leberer, E. (1995). Pheromone response in yeast: association of Bem1p with proteins of the MAP kinase cascade and actin. *Science* **270**, 1210-3.

Leupold, U. (1950). Die Verebung von homothallie und heterothallie bei Schizosaccharomyces pombe. *Compt. Rend. Lab. Carlsberg* **24**, 381-475.

Leupold, U. (1987). Sex appeal in fission yeast. *Curr. Genet* **12**, 543-545.

Li, Y. C., Chen, C. R. and Chang, E. C. (2000). Fission yeast Ras1 effector Scd1 interacts with the spindle and affects its proper formation. *Genetics* **156**, 995-1004.

Ligon, L. A., Karki, S., Tokito, M. and Holzbaur, E. L. (2001). Dynein binds to beta-catenin and may tether microtubules at adherens junctions. *Nat Cell Biol* **3**, 913-7.

Loewith, R., Hubberstey, A. and Young, D. (2000). Skh1, the MEK component of the mkh1 signaling pathway in Schizosaccharomyces pombe. *J Cell Sci* **113 (Pt 1)**, 153-60.

Louvet-Vallee, S. (2000). ERM proteins: from cellular architecture to cell signaling. *Biol Cell* **92**, 305-16.

Lye, R. J., Porter, M. E., Scholey, J. M. and McIntosh, J. R. (1987). Identification of a microtubule-based cytoplasmic motor in the nematode C. elegans. *Cell* **51**, 309-18.

Machesky, L. M. and Insall, R. H. (1999). Signaling to actin dynamics. *J Cell Biol* **146**, 267-72.

MacNeill, S. A. and Fantes, P. (1993). Methods for analysis of the fission yeast cell cycle,. In *in "The Cell Cycle", Practical Approach Series, IRL Press at Oxford University Press*, pp. 93-125.

Maddox, P., Chin, E., Mallavarapu, A., Yeh, E., Salmon, E. D. and Bloom, K. (1999). Microtubule dynamics from mating through the first zygotic division in the budding yeast Saccharomyces cerevisiae. *J Cell Biol* **144**, 977-87.

Maeda, T., Mochizuki, N. and Yamamoto, M. (1990). Adenylyl cyclase is dispensable for vegetative cell growth in the fission yeast Schizosaccharomyces pombe. *Proc Natl Acad Sci U S A* **87**, 7814-8.

Maeda, T., Watanabe, Y., Kunitomo, H. and Yamamoto, M. (1994). Cloning of the pka1 gene encoding the catalytic subunit of the cAMP-dependent protein kinase in Schizosaccharomyces pombe. *J Biol Chem* **269**, 9632-7.

Marcus, S., Polverino, A., Chang, E., Robbins, D., Cobb, M. H. and Wigler, M. H. (1995). Shk1, a homolog of the *Saccharomyces cerevisiae* Ste20 and mammalian $p65^{PAK}$ protein kinases, is a component of a Ras/Cdc42 signaling module i the fission yeast *Schizosaccharomyces pombe*. *Proc. Natl. Acad. Sci. USA* **92**, 6180-6184.

Marks, J., Hagan, I. M. and Hyams, J. S. (1986). Growth polarity and cytokinesis in fission yeast: the role of the cytoskeleton. *J Cell Sci Suppl* **5**, 229-41.

Mata, J. and Nurse, P. (1997). tea1 and the microtubular cytoskeleton are important for generating global spatial order within the fission yeast cell. *Cell* **89**, 939-49.

Matsusaka, T., Hirata, D., Yanagida, M. and Toda, T. (1995). A novel protein kinase gene *ssp1*$^+$ is required for alteration of growth polarity and actin localization in fission yeast. *The EMBO Journal* **14**, 3325-3338.

Maundrell, K. (1990). *nmt1* of fission yeast. A highly transcribed gene completely repressed by thiamine. *The Journal of Biological Chemistry* **265**, 10857-10864.

McCollum, D., Feoktistova, A., Morphew, M., Balasubramanian, M. and Gould, K. L. (1996). The *Schizosaccharomyces pombe* actin-related protein, Arp3, is a component of the cortical actin cytoskeleton and interacts with profilin. *EMBO Journal* **15**, 6438-6446.

Merdes, A., Ramyar, K., Vechio, J. D. and Cleveland, D. W. (1996). A complex of NuMA and cytoplasmic dynein is essential for mitotic spindle assembly. *Cell* **87**, 447-58.

Metodiev, M. V., Matheos, D., Rose, M. D. and Stone, D. E. (2002). Regulation of MAPK function by direct interaction with the mating-specific Galpha in yeast. *Science* **296**, 1483-6.

Meyerowitz, E. M. and Kankel, D. R. (1978). A genetic analysis of visual system development in Drosophilia melanogaster. *Dev Biol* **62**, 112-142.

Micklem, D. R., Dasgupta, R., Elliott, H., Gergely, F., Davidson, C., Brand, A., Gonzalez-Reyes, A. and St Johnston, D. (1997). The mago nashi gene is required for the polarisation of the oocyte and the formation of perpendicular axes in Drosophila. *Curr Biol* **7**, 468-78.

Miki, F., Okazaki, K., Shimanuki, M., Yamamoto, A., Hiraoka, Y. and Niwa, O. (2002). The 14-kDa Dynein Light Chain-Family Protein Dlc1 Is Required for Regular Oscillatory Nuclear Movement and Efficient Recombination during Meiotic Prophase in Fission Yeast. *Mol Biol Cell* **13**, 930-46.

Miller, P. J. and Johnson, D. I. (1994). Cdc42p GTPase is involved in controlling polarised cell growth in *Schizosaccharomyces pombe*. *Mol. Cell. Biol.* **14**, 1075-1083.

Minke, P. F., Lee, I. H. and Plamann, M. (1999). Microscopic analysis of Neurospora ropy mutants defective in nuclear distribution. *Fungal Genet Biol* **28**, 55-67.

Minke, P. F., Lee, I. H., Tinsley, J. H. and Plamann, M. (2000). A Neurospora crassa Arp1 mutation affecting cytoplasmic dynein and dynactin localization. *Mol Gen Genet* **264**, 433-40.

Mitchison, J. M. and Nurse, P. (1985). Growth in cell length in the fission yeast Schizosaccharomyces pombe. *J Cell Sci* **75**, 357-76.

Mochizuki, N. and Yamamoto, M. (1992). Reduction in the intracellular cAMP level triggers initiation of sexual development in fission yeast. *Mol Gen Genet* **233**, 17-24.

Moore, S. A. (1983). Comparison of dose-response curves for alpha factor-induced cell division arrest, agglutination, and projection formation of yeast cells. Implication for the mechanism of alpha factor action. *J Biol Chem* **258**, 13849-56.

Moreno, S., Klar, A. and Nurse, P. (1991). Molecular genetic analysis of fission yeast *Schizosaccharomyces pombe*. *Methods Enzymol* **194**, 795-823.

Moreno, S. and Nurse, P. (1994). Regulation of progression through the G1 phase of the cell cycle by the *rum1*$^+$ gene. *Nature* **367**, 236-242.

Morishita, M., Morimoto, F., Kitamura, K., Koga, T., Fukui, Y., Maekawa, H., Yamashita, I. and Shimoda, C. (2002). Phosphatidylinositol 3-phosphate 5-kinase is required for the cellular response to nutritional starvation and mating pheromone signals in Schizosaccharomyces pombe. *Genes Cells* **7**, 199-215.

Morrell, J. L., Morphew, M. and Gould, K. L. (1999). A mutant of Arp2p causes partial disassembly of the Arp2/3 complex and loss of cortical actin function in fission yeast. *Mol Biol Cell* **10**, 4201-15.

Motegi, F., Arai, R. and Mabuchi, I. (2001). Identification of two type V myosins in fission yeast, one of which functions in polarized cell growth and moves rapidly in the cell. *Mol Biol Cell* **12**, 1367-80.

Mulholland, J., Preuss, D., Moon, A., Wong, A., Drubin, D. and Botstein, D. (1994). Ultrastructure of the yeast actin cytoskeleton and its association with the plasma membrane. *The Journal of Cell Biology* **125**, 381-391.

Mullins, R. D. (2000). How WASP-family proteins and the Arp2/3 complex convert intracellular signals into cytoskeletal structures. *Curr Opin Cell Biol* **12**, 91-6.

Murray, J. M. and Johnson, D. I. (2001). The Cdc42p GTPase and its regulators Nrf1p and Scd1p are involved in endocytic trafficking in the fission yeast Schizosaccharomyces pombe. *J Biol Chem* **276**, 3004-9.

Nakano, K., Satoh, K., Morimatsu, A., Ohnuma, M. and Mabuchi, I. (2001). Interactions among a fimbrin, a capping protein, and an actin-depolymerizing factor in organization of the fission yeast actin cytoskeleton. *Mol Biol Cell* **12**, 3515-26.

Nathke, I. S., Adams, C. L., Polakis, P., Sellin, J. H. and Nelson, W. J. (1996). The adenomatous polyposis coli tumor suppressor protein localizes to plasma membrane sites involved in active cell migration. *J Cell Biol* **134**, 165-79.

Nern, A. and Arkowitz, R. A. (2000). Nucleocytoplasmic shuttling of the Cdc42p exchange factor Cdc24p. *J Cell Biol* **148**, 1115-22.

Nielsen, O. and Davey, J. (1995). Pheromone communication in the fission yeast Schizosaccharomyces pombe. *Semin Cell Biol* **6**, 95-104.

Nielsen, O., Davey, J. and Egel, R. (1992). The ras1 function of Schizosaccharomyces pombe mediates pheromone-induced transcription. *Embo J* **11**, 1391-5.

Niwa, O., Shimanuki, M. and Miki, F. (2000). Telomere-led bouquet formation facilitates homologous chromosome pairing and restricts ectopic interaction in fission yeast meiosis. *Embo J* **19**, 3831-40.

Nocero, M., Isshiki, T., Yamamoto, M. and Hoffman, C. S. (1994). Glucose repression of fbp1 transcription of Schizosaccharomyces pombe is partially regulated by adenylate cyclase activation by a G protein alpha subunit encoded by gpa2 (git8). *Genetics* **138**, 39-45.

Novick, P. and Botstein, D. (1985). Phenotypic analysis of temperature-sensitive yeast actin mutants. *Cell* **40**, 405-16.

Nurse, P., Thuriaux, P. and Nasmyth, K. (1976). Genetic control of the cell division cycle in the fission yeast *Schizosaccharomyces pombe. Molecular and General Genetics* **146**, 167-178.

O'Shea, E. K. and Herskowitz, I. (2000). The ins and outs of cell-polarity decisions [news]. *Nat Cell Biol* **2**, E39-41.

Ohi, R., Feoktistova, A. and Gould, K. L. (1996). Construction of vectors and a genomic library for use with *his3*-deficient strains of *Schizosaccharomyces pombe. Gene* **174**, 315-318.

Ohmiya, R., Yamada, H., Nakashima, K., Aiba, H. and Mizuno, T. (1995). Osmoregulation of fission yeast: cloning of two distinct genes encoding glycerol-3-phosphate dehydrogenase, one of which is responsible for osmotolerance for growth. *Mol Microbiol* **18**, 963-73.

Ottilie, S., Miller, P. J., Johnson, D. I., Creasy, C. L., Sells, M. A., Bagrodia, S., Forsburg, S. L. and Chernoff, J. (1995). Fission yeast pak1+ encodes a protein kinase that interacts with Cdc42p and is involved in the control of cell polarity and mating. *Embo J* **14**, 5908-19.

Palazzo, A. F., Joseph, H. L., Chen, Y. J., Dujardin, D. L., Alberts, A. S., Pfister, K. K., Vallee, R. B. and Gundersen, G. G. (2001). Cdc42, dynein, and dynactin regulate MTOC reorientation independent of Rho-regulated microtubule stabilization. *Curr Biol* **11**, 1536-41.

Paluh, J. L., Nogales, E., Oakley, B. R., McDonald, K., Pidoux, A. L. and Cande, W. Z. (2000). A mutation in gamma-tubulin alters microtubule dynamics and organization and is synthetically lethal with the kinesin-like protein pkl1p. *Mol Biol Cell* **11**, 1225-39.

Papadaki, P., Pizon, V., Onken, B. and Chang, E. C. (2002). Two ras pathways in fission yeast are differentially regulated by two ras guanine nucleotide exchange factors. *Mol Cell Biol* **22**, 4598-606.

Paschal, B. M., King, S. M., Moss, A. G., Collins, C. A., Vallee, R. B. and Witman, G. B. (1987). Isolated flagellar outer arm dynein translocates brain microtubules in vitro. *Nature* **330**, 672-4.

Paschal, B. M. and Vallee, R. B. (1987). Retrograde transport by the microtubule-associated protein MAP 1C. *Nature* **330**, 181-3.

Pelham, R. J., Jr. and Chang, F. (2001). Role of actin polymerization and actin cables in actin-patch movement in Schizosaccharomyces pombe. *Nat Cell Biol* **3**, 235-44.

Petersen, J., Heitz, M. J. and Hagan, I. M. (1998). Conjugation in S. pombe: identification of a microtubule-organising centre, a requirement for microtubules and a role for Mad2. *Curr Biol* **8**, 963-6.

Petersen, J., Nielsen, O., Egel, R. and Hagan, I. M. (1998). F-actin distribution and function during sexual differentiation in Schizosaccharomyces pombe. *J Cell Sci* **111**, 867-76.

Petersen, J., Weilguny, D., Egel, R. and Nielsen, O. (1995). Characterization of *fus1* of *Schizosaccharomyces pombe:* a developmentally controlled function needed for conjugation. *Molecular and Cellular Biology* **15**, 3697-3707.

Peterson, J., Zheng, Y., Bender, L., Myers, A., Cerione, R. and Bender, A. (1994). Interactions between the bud emergence proteins Bem1p and Bem2p and rho-type GTPases in yeast. *The Journal of Cell Biology* **127**, 1395-1406.

Quintyne, N. J., Gill, S. R., Eckley, D. M., Crego, C. L., Compton, D. A. and Schroer, T. A. (1999). Dynactin is required for microtubule anchoring at centrosomes. *J Cell Biol* **147**, 321-34.

Qyang, Y., Yang, P., Du, H., Lai, H., Kim, H. and Marcus, S. (2002). The p21-activated kinase, Shk1, is required for proper regulation of microtubule dynamics in the fission yeast, Schizosaccharomyces pombe. *Mol Microbiol* **44**, 325-34.

Radcliffe, P., Hirata, D., Childs, D., Vardy, L. and Toda, T. (1998). Identification of novel temperature-sensitive lethal alleles in essential β–tubulin and nonessential α2-tubulin genes as fission yeast polarity mutants. *Molecular Biology of the Cell* **9**, 1757-1771.

Radcliffe, P. A., Garcia, M. A. and Toda, T. (2000a). The cofactor-dependent pathways for alpha- and beta-tubulins in microtubule biogenesis are functionally different in fission yeast. *Genetics* **156**, 93-103.

Radcliffe, P. A., Hirata, D., Vardy, L. and Toda, T. (1999). Functional dissection and hierarchy of tubulin-folding cofactor homologues in fission yeast. *Mol Biol Cell* **10**, 2987-3001.

Radcliffe, P. A. and Toda, T. (2000). Characterisation of fission yeast alp11 mutants defines three functional domains within tubulin-folding cofactor B. *Mol Gen Genet* **263**, 752-60.

Radcliffe, P. A., Vardy, L. and Toda, T. (2000b). A conserved small GTP-binding protein Alp41 is essential for the cofactor-dependent biogenesis of microtubules in fission yeast. *FEBS Lett* **468**, 84-8.

Ribas, J. C., Diaz, M., Duran, A. and Perez, P. (1991). Isolation and characterization of Schizosaccharomyces pombe mutants defective in cell wall (1-3)beta-D-glucan. *J Bacteriol* **173**, 3456-62.

Rickard, J. E. and Kreis, T. E. (1991). Binding of pp170 to microtubules is regulated by phosphorylation. *J Biol Chem* **266**, 17597-605.

Roberts, C. J., Nelson, B., Marton, M. J., Stoughton, R., Meyer, M. R., Bennett, H. A., He, Y. D., Dai, H., Walker, W. L., Hughes, T. R. et al. (2000). Signaling and circuitry of multiple MAPK pathways revealed by a matrix of global gene expression profiles. *Science* **287**, 873-80.

Rupes, I., Jia, Z. and Young, P. G. (1999). Ssp1 promotes actin depolymerization and is involved in stress response and new end take-off control in fission yeast. *Mol Biol Cell* **10**, 1495-510.

Rupes, I., Jochova, J. and Young, P. G. (1997). Markers of cell polarity during and after nitrogen starvation in *Schizosaccharomyces pombe*. *Biochem. Cell Biol.* **75**, 697-708.

Rupes, I., Webb, B. A., Mak, A. and Young, P. G. (2001). G2/M arrest caused by actin disruption is a manifestation of the cell size checkpoint in fission yeast. *Mol Biol Cell* **12**, 3892-903.

Sambrook, J., Fritsch, E. F. and Maniatis, T. (1989). Molecular Cloning: A Laboratory Manual. Cold Spring Harbor, NY: Cold Spring Harbor Laboratory Press.

Sawin, K. E. and Nurse, P. (1996). Identification of fission yeast nuclear markers using random polypeptide fusions with green fluorescent protein. *Proc Natl Acad Sci U S A* **93**, 15146-51.

Sawin, K. E. and Nurse, P. (1998). Regulation of cell polarity by microtubules in fission yeast. *J Cell Biol* **142**, 457-71.

Sayers, L. G., Katayama, S., Nakano, K., Mellor, H., Mabuchi, I., Toda, T. and Parker, P. J. (2000). Rho-dependence of Schizosaccharomyces pombe Pck2. *Genes Cells* **5**, 17-27.

Sazer, S. and Sherwood, S. W. (1990). Mitochondrial growth and DNA synthesis occur in the absence of nuclear DNA replication in fission yeast. *J. Cell Sci.* **97**, 509-516.

Schaefer, M., Petronczki, M., Dorner, D., Forte, M. and Knoblich, J. A. (2001). Heterotrimeric G proteins direct two modes of asymmetric cell division in the Drosophila nervous system. *Cell* **107**, 183-94.

Schafer, D. A., Gill, S. R., Cooper, J. A., Heuser, J. E. and Schroer, T. A. (1994). Ultrastructural analysis of the dynactin complex: an actin-related protein is a component of a filament that resembles F-actin. *J Cell Biol* **126**, 403-12.

Schrick, K., Garvik, B. and Hartwell, L. H. (1997). Mating in Saccharomyces cerevisiae: the role of the pheromone signal transduction pathway in the chemotropic response to pheromone. *Genetics* **147**, 19-32.

Sells, M. A., Barratt, J. T., Caviston, J., Ottilie, S., Leberer, E. and Chernoff, J. (1998). Characterization of Pak2p, a pleckstrin homology domain-containing, p21-activated protein kinase from fission yeast. *J Biol Chem* **273**, 18490-8.

Shaw, S. L., Yeh, E., Maddox, P., Salmon, E. D. and Bloom, K. (1997). Astral microtubule dynamics in yeast: a microtubule-based searching mechanism for spindle orientation and nuclear migration into the bud. *J Cell Biol* **139**, 985-94.

Shimada, Y., Gulli, M. P. and Peter, M. (2000). Nuclear sequestration of the exchange factor Cdc24 by Far1 regulates cell polarity during yeast mating. *Nat Cell Biol* **2**, 117-24.

Shulman, J. M. and St Johnston, D. (1999). Pattern formation in single cells. *Trends Cell Biol* **9**, M60-4.

Snell, V. and Nurse, P. (1994). Genetic analysis of cell morphogenesis in fission yeast-a role for casein kinase II in the establishment of polarized growth. *EMBO Journal* **13**, 2066-2074.

Spector, I., Shochet, N. R., Kashman, Y. and Groweiss, A. (1983). Latrunculins: novel marine toxins that disrupt microfilament organization in cultured cells. *Science* **219**, 493-5.

Spencer, J. A., Eliazer, S., Ilaria, R. L., Jr., Richardson, J. A. and Olson, E. N. (2000). Regulation of microtubule dynamics and myogenic differentiation by MURF, a striated muscle RING-finger protein. *J Cell Biol* **150**, 771-84.

Starr, D. A., Williams, B. C., Hays, T. S. and Goldberg, M. L. (1998). ZW10 helps recruit dynactin and dynein to the kinetochore. *J Cell Biol* **142**, 763-74.

Stern, B. and Nurse, P. (1997). Fission yeast pheromone blocks S-phase by inhibiting the G1 cyclin B- p34cdc2 kinase. *Embo J* **16**, 534-44.

Stern, B. and Nurse, P. (1998). Cyclin B proteolysis and the cyclin-dependent kinase inhibitor rum1p are required for pheromone-induced G1 arrest in fission yeast. *Mol Biol Cell* **9**, 1309-21.

Svoboda, A., Bähler, J. and Kohli, J. (1995). Microtubule-driven nuclear movements and linear elements as meiosis-specific characteristics of the fission yeasts *Schizosaccharomyces versatilis* and *S. pombe*. *Chromosoma* **104**, 203-214.

Swan, A., Nguyen, T. and Suter, B. (1999). Drosophila Lissencephaly-1 functions with Bic-D and dynein in oocyte determination and nuclear positioning. *Nat Cell Biol* **1**, 444-9.

Swaroop, A., Swaroop, M. and Garen, A. (1987). Sequence analysis of the complete cDNA and encoded polypeptide for the Glued gene of Drosophila melanogaster. *Proc Natl Acad Sci U S A* **84**, 6501-5.

Takegawa, K., DeWald, D. B. and Emr, S. D. (1995). Schizosaccharomyces pombe Vps34p, a phosphatidylinositol-specific PI 3-kinase essential for normal cell growth and vacuole morphology. *J Cell Sci* **108 (Pt 12)**, 3745-56.

Takenawa, T. and Itoh, T. (2001). Phosphoinositides, key molecules for regulation of actin cytoskeletal organization and membrane traffic from the plasma membrane. *Biochim Biophys Acta* **1533**, 190-206.

Tirnauer, J. S. and Bierer, B. E. (2000). EB1 proteins regulate microtubule dynamics, cell polarity, and chromosome stability. *J Cell Biol* **149**, 761-6.

Tran, P. T., Marsh, L., Doye, V., Inoue, S. and Chang, F. (2001). A mechanism for nuclear positioning in fission yeast based on microtubule pushing. *J Cell Biol* **153**, 397-411.

Troxell, C. L., Sweezy, M. A., West, R. R., Reed, K. D., Carson, B. D., Pidoux, A. L., Cande, W. Z. and McIntosh, J. R. (2001). pkl1(+)and klp2(+): Two kinesins of the Kar3 subfamily in fission yeast perform different functions in both mitosis and meiosis. *Mol Biol Cell* **12**, 3476-88.

Tsukita, S. and Yonemura, S. (1999). Cortical actin organization: lessons from ERM (ezrin/radixin/moesin) proteins. *J Biol Chem* **274**, 34507-10.

Tu, H. and Wigler, M. (1999). Genetic evidence for Pak1 autoinhibition and its release by Cdc42. *Mol Cell Biol* **19**, 602-11.

Valetti, C., Wetzel, D. M., Schrader, M., Hasbani, M. J., Gill, S. R., Kreis, T. E. and Schroer, T. A. (1999). Role of dynactin in endocytic traffic: effects of dynamitin overexpression and colocalization with CLIP-170. *Mol Biol Cell* **10**, 4107-20.

van Es, S., Weening, K. E. and Devreotes, P. N. (2001). The protein kinase YakA regulates g-protein-linked signaling responses during growth and development of Dictyostelium. *J Biol Chem* **276**, 30761-5.

Vardy, L. and Toda, T. (2000). The fission yeast gamma-tubulin complex is required in G(1) phase and is a component of the spindle assembly checkpoint. *Embo J* **19**, 6098-111.

Vaughan, K. T., Tynan, S. H., Faulkner, N. E., Echeverri, C. J. and Vallee, R. B. (1999). Colocalization of cytoplasmic dynein with dynactin and CLIP-170 at microtubule distal ends [In Process Citation]. *J Cell Sci* **112**, 1437-47.

Vaughan, K. T. and Vallee, R. B. (1995). Cytoplasmic dynein binds dynactin through a direct interaction between the intermediate chains and p150Glued. *J Cell Biol* **131**, 1507-16.

Verde, F., Mata, J. and Nurse, P. (1995). Fission yeast cell morphogenesis: identification of new genes and analysis of their role during the cell cycle. *J Cell Biol* **131**, 1529-38.

Verde, F., Wiley, D. J. and Nurse, P. (1998). Fission yeast *orb6*, a ser/thr protein kinase related to mammalian rho kinase and myotonic dystrophy kinase, is required for maintenance of cell polarity and coordinates cell morphogenesis with the cell cycle. *Proc. Natl. Acad. Sci. USA* **95**, 7526-7531.

Wang, F., Herzmark, P., Weiner, O. D., Srinivasan, S., Servant, G. and Bourne, H. R. (2002). Lipid products of PI(3)Ks maintain persistent cell polarity and directed motility in neutrophils. *Nat Cell Biol* **4**, 513-8.

Watanabe, Y. and Yamamoto, M. (1994). S. pombe mei2+ encodes an RNA-binding protein essential for premeiotic DNA synthesis and meiosis I, which cooperates with a novel RNA species meiRNA. *Cell* **78**, 487-98.

Waterman-Storer, C. M. and Holzbaur, E. L. (1996). The product of the Drosophila gene, Glued, is the functional homologue of the p150Glued component of the vertebrate dynactin complex. *J Biol Chem* **271**, 1153-9.

Waterman-Storer, C. M., Karki, S. and Holzbaur, E. L. (1995). The p150Glued component of the dynactin complex binds to both microtubules and the actin-related protein centractin (Arp-1). *Proc Natl Acad Sci U S A* **92**, 1634-8.

Weiner, O. D., Neilsen, P. O., Prestwich, G. D., Kirschner, M. W., Cantley, L. C. and Bourne, H. R. (2002). A PtdInsP(3)- and Rho GTPase-mediated positive feedback loop regulates neutrophil polarity. *Nat Cell Biol* **4**, 509-13.

West, R. R., Malmstrom, T., Troxell, C. L. and McIntosh, J. R. (2001). Two related kinesins, klp5+ and klp6+, foster microtubule disassembly and are required for meiosis in fission yeast. *Mol Biol Cell* **12**, 3919-32.

West, R. R., Vaisberg, E. V., Ding, R., Nurse, P. and McIntosh, J. R. (1998). cut11(+): A gene required for cell cycle-dependent spindle pole body anchoring in the nuclear envelope and bipolar spindle formation in Schizosaccharomyces pombe. *Mol Biol Cell* **9**, 2839-55.

Widmann, C., Gibson, S., Jarpe, M. B. and Johnson, G. L. (1999). Mitogen-activated protein kinase: conservation of a three-kinase module from yeast to human. *Physiol Rev* **79**, 143-80.

Won, M., Park, S. K., Hoe, K. L., Jang, Y. J., Chung, K. S., Kim, D. U., Kim, H. B. and Yoo, H. S. (2001). Rkp1/Cpc2, a fission yeast RACK1 homolog, is involved in actin cytoskeleton organization through protein kinase C, Pck2, signaling. *Biochem Biophys Res Commun* **282**, 10-5.

Woods, A., Sherwin, T., Sasse, R., MacRae, T. H., Baines, A. J. and Gull, K. (1989). Definition of individual components within the cytoskeleton of Trypanosoma brucei by a library of monoclonal antibodies. *J Cell Sci* **93**, 491-500.

Wu, J. Q., Bahler, J. and Pringle, J. R. (2001). Roles of a fimbrin and an alpha-actinin-like protein in fission yeast cell polarization and cytokinesis. *Mol Biol Cell* **12**, 1061-77.

Xiang, X., Han, G., Winkelmann, D. A., Zuo, W. and Morris, N. R. (2000). Dynamics of cytoplasmic dynein in living cells and the effect of a mutation in the dynactin complex actin-related protein Arp1. *Curr Biol* **10**, 603-6.

Xiang, X., Roghi, C. and Morris, N. R. (1995). Characterization and localization of the cytoplasmic dynein heavy chain in Aspergillus nidulans. *Proc Natl Acad Sci U S A* **92**, 9890-4.

Yamamoto, A., Tsutsumi, C., Kojima, H., Oiwa, K. and Hiraoka, Y. (2001). Dynamic behavior of microtubules during dynein-dependent nuclear migrations of meiotic prophase in fission yeast. *Mol Biol Cell* **12**, 3933-46.

Yamamoto, A., West, R. R., McIntosh, J. R. and Hiraoka, Y. (1999). A cytoplasmic dynein heavy chain is required for oscillatory nuclear movement of meiotic prophase and efficient meiotic recombination in fission yeast. *J Cell Biol* **145**, 1233-49.

Yamashita, A., Watanabe, Y. and Yamamoto, M. (1997). Microtubule-associated coiled-coil protein Ssm4 is involved in the meiotic development in fission yeast. *Genes Cells* **2**, 155-66.

Yoshida, T., Toda, T. and Yanagida, M. (1994). A calcineurin-like gene *ppb1*$^+$ in fission yeast: mutant defects in cytokinesis, cell polarity, mating and spindle pole body positioning. *Journal of Cell Science* **107**, 1725-1735.

Zhang, Y., Sugiura, R., Lu, Y., Asami, M., Maeda, T., Itoh, T., Takenawa, T., Shuntoh, H. and Kuno, T. (2000). Phosphatidylinositol 4-phosphate 5-kinase Its3 and calcineurin Ppb1 coordinately regulate cytokinesis in fission yeast. *J Biol Chem* **275**, 35600-6.

Zheng, Y., Cerione, R. and Bender, A. (1994). Control of the yeast bud-site assembly GTPase Cdc42. Catalysis of guanine nucleotide exchange by Cdc24 and stimulation of GTPase activity by Bem3. *J Biol Chem* **269**, 2369-72.